frontiers | Research Topics

Novel therapeutic approaches for biliary tract cancer and hepatocellular carcinoma

Edited by
Daniel Neureiter and Maria Lina Tornesello

Coordinated by
Dino Bekric

Published in
Frontiers in Oncology
Frontiers in Cell and Developmental Biology
Frontiers in Pharmacology
Frontiers in Medicine
Frontiers in Immunology

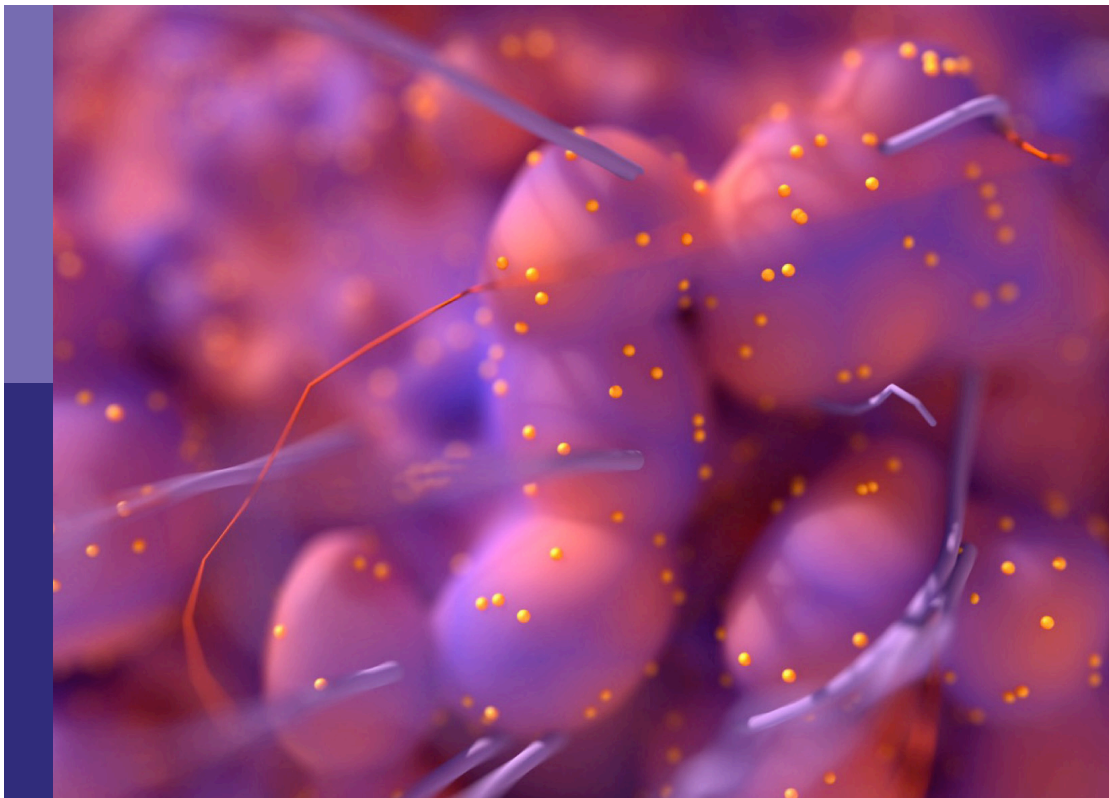

ISSN 1664-8714
ISBN 978-2-8325-3966-8
DOI 10.3389/978-2-8325-3966-8

About Frontiers

Frontiers is more than just an open access publisher of scholarly articles: it is a pioneering approach to the world of academia, radically improving the way scholarly research is managed. The grand vision of Frontiers is a world where all people have an equal opportunity to seek, share and generate knowledge. Frontiers provides immediate and permanent online open access to all its publications, but this alone is not enough to realize our grand goals.

Frontiers journal series

The Frontiers journal series is a multi-tier and interdisciplinary set of open-access, online journals, promising a paradigm shift from the current review, selection and dissemination processes in academic publishing. All Frontiers journals are driven by researchers for researchers; therefore, they constitute a service to the scholarly community. At the same time, the *Frontiers journal series* operates on a revolutionary invention, the tiered publishing system, initially addressing specific communities of scholars, and gradually climbing up to broader public understanding, thus serving the interests of the lay society, too.

Dedication to quality

Each Frontiers article is a landmark of the highest quality, thanks to genuinely collaborative interactions between authors and review editors, who include some of the world's best academicians. Research must be certified by peers before entering a stream of knowledge that may eventually reach the public - and shape society; therefore, Frontiers only applies the most rigorous and unbiased reviews. Frontiers revolutionizes research publishing by freely delivering the most outstanding research, evaluated with no bias from both the academic and social point of view. By applying the most advanced information technologies, Frontiers is catapulting scholarly publishing into a new generation.

What are Frontiers Research Topics?

Frontiers Research Topics are very popular trademarks of the *Frontiers journals series*: they are collections of at least ten articles, all centered on a particular subject. With their unique mix of varied contributions from Original Research to Review Articles, Frontiers Research Topics unify the most influential researchers, the latest key findings and historical advances in a hot research area.

Find out more on how to host your own Frontiers Research Topic or contribute to one as an author by contacting the Frontiers editorial office: frontiersin.org/about/contact

Novel therapeutic approaches for biliary tract cancer and hepatocellular carcinoma

Topic editors
Daniel Neureiter — Salzburger Landeskliniken, Austria
Maria Lina Tornesello — G. Pascale National Cancer Institute Foundation (IRCCS), Italy

Topic Coordinator
Dino Bekric — Paracelsus Medical University, Austria

Citation
Neureiter, D., Tornesello, M. L., Bekric, D., eds. (2023). *Novel therapeutic approaches for biliary tract cancer and hepatocellular carcinoma*. Lausanne: Frontiers Media SA. doi: 10.3389/978-2-8325-3966-8

Table of contents

frontiers | Frontiers in Cell and Developmental Biology

TYPE Editorial
PUBLISHED 03 November 2023
DOI 10.3389/fcell.2023.1320084

OPEN ACCESS

EDITED AND REVIEWED BY
Shyamala Maheswaran,
Massachusetts General Hospital and Harvard Medical School, United States

*CORRESPONDENCE
Dino Bekric,
dino.bekric@pmu.ac.at
Maria Lina Tornesello,
m.tornesello@istitutotumori.na.it

RECEIVED 11 October 2023
ACCEPTED 17 October 2023
PUBLISHED 03 November 2023

CITATION
Bekric D, Tornesello ML, Ocker M, Mayr C, Kiesslich T and Neureiter D (2023), Editorial: Novel therapeutic approaches for biliary tract cancer and hepatocellular carcinoma.
Front. Cell Dev. Biol. 11:1320084.
doi: 10.3389/fcell.2023.1320084

Editorial: Novel therapeutic approaches for biliary tract cancer and hepatocellular carcinoma

Dino Bekric[1,2]*, Maria Lina Tornesello[3]*, Matthias Ocker [4], Christian Mayr[1], Tobias Kiesslich[1] and Daniel Neureiter[2,5]

[1]Center of Physiology, Pathophysiology and Biophysics, Institute of Physiology and Pathophysiology Salzburg, Paracelsus Medical University, Salzburg, Austria, [2]Cancer Cluster Salzburg, Salzburg, Austria, [3]Molecular Biology and Viral Oncology Unit, Istituto Nazionale Tumori IRCCS "Fondazione G. Pascale", Naples, Italy, [4]Medical Department, Division of Hematology, Oncology, and Cancer Immunology, Campus Charité Mitte, Charité University Medicine Berlin, Germany and Tacalyx GmbH, Berlin, Germany, [5]Institute of Pathology, University Clinics Salzburg, Paracelsus Medical University, Salzburg, Austria

KEYWORDS

hepatocellular carcinoma, biliary tract cancer, hepatobiliary cancer, chemoresistance, therapeutic targets, immunotherapy

Editorial on the Research Topic
Novel therapeutic approaches for biliary tract cancer and hepatocellular carcinoma

Background

Hepatocellular carcinoma (HCC) and biliary tract cancers (BTC) represent the two major forms of primary liver cancers. Despite the growing efforts to translate the increasing knowledge on molecular alterations of these cancers into treatment options for patients, the actual clinical outcomes remain unsatisfying (Llovet et al., 2021; Valle et al., 2021).

BTCs are fatal gastrointestinal cancers with very poor 5-year survival rates (Zhu et al., 2010). The incidence rates vary across geographic regions: in the Western World, the incidence ranges from 0.5 to 2 per 100,000 population, while in the Eastern World, the incidence is higher at 60 per 100,000 population (Valle et al., 2021). The molecular background of BTC development and progression is complex and remains only partially understood, although it is clear that besides mutational events and dysregulated signaling pathways, aberrant epigenetics also play a role (Mayr et al., 2015; Mayr et al., 2021; Bekric et al., 2023). Possible explanations for the low survival rates include diagnosis at an advanced stage and the development of resistance to, and ineffectiveness of current therapies as well as not standardized second-line therapies for advanced BTC (Rakic et al., 2014; Moik et al., 2019). Non-specific symptoms such as abdominal pain, unexplained weight loss and painless jaundice can lead to late diagnosis and ineffective clinical management (Nagorney et al., 1993). In addition, current therapies, which include radiotherapy, FGFR inhibitors, immunotherapies, combination chemotherapies such as cisplatin and gemcitabine and palliative care, are not able to significantly improve the low median survival (Valle et al., 2010; Rakic et al., 2014).

HCC is the most common form of liver cancer (Sung et al., 2021). This deadly malignancy was responsible for more than 830,000 deaths around the world in 2020 (Sung et al., 2021). HCC is therefore the second leading cause of cancer related mortality globally (McGlynn et al., 2021). Similar to BTC, patients with HCC are usually diagnosed in mid-to-late stages due to unspecified symptoms such as fatigue, nausea, vomiting and abdominal pain, which make successful surgical treatment difficult (Llovet et al., 2021). Patients with advanced-stage HCC are currently treated with immunotherapy in combination with bevaciuzumab, adjuvant chemotherapy after surgery or multikinase/tyrosinkinase inhibitors such as sorafenib and regorafenib (Llovet et al., 2008; Bruix et al., 2015). Although sorafenib treatment improves survival in HCC patients, recent studies report increasing resistance to this multikinase inhibitor (Chen et al., 2015; Keating, 2017). Therefore, differential combinatorial treatment strategies using signaling, epigenetic and immune targets in HCC will be a promising approach to increase therapeutic success in the future (Neureiter et al., 2019; Ocker et al., 2021).

Due to the ineffectiveness and development of resistance to current therapies, the need to identify and provide alternative therapeutic approaches is of paramount importance to alleviate the suffering of BTC and HCC patients. Therefore, the current Research Topic provided a structural platform to identify mechanisms of resistance, novel relevant therapeutic targets and prognostic/predictive markers as well as to demonstrate promising innovative treatment options. The call for papers attracted an astonishing number of 10 highly interesting publications and over 65 authors contributed to this Research Topic in the form of three structured reviews (Guo et al.; Shen et al.; Yang et al.) and seven original research papers (Liu et al.; Wu et al.; Jansson et al.; Liang et al.; Nagashima et al.; Yang et al.; Tang et al.).

This Research Topic covers a variety of subject areas: promising new survival markers after surgery for BTC patients (Jansson et al.), non-invasive preoperative prediction of angiogenesis related markers in BTC (Liu et al.), optimizing strategies for immunotherapy and the current status of adjuvant therapies in HCC are discussed (Liang et al.; Tang et al.; Shen et al.; Guo et al.), characteristics of extrahepatic cholangiocarcinoma (eCCA) are analyzed (Yang et al.; Nagashima et al.), and novel therapeutic strategies for BTC are demonstrated. (Wu et al.; Yang et al.).

We will discuss the highlights of these published manuscripts in short:

Prognosis and prediction factors in BTC

Improving patient outcomes in BTC requires identifying predictive and prognostic factors.

High levels of vascular endothelial growth factor (VEGF) expression and microvessel density (MVD) correlate with tumor progression and poor prognosis in eCCA patients (Möbius et al., 2007; Thelen et al., 2008; Dongqing et al., 2019). However, current methods for detecting these factors are invasive and challenging to replicate. Liu et al. developed a machine learning tool using regression and classification models for predicting VEGF expression and MVD in eCCA. The MRI-based tool accurately predicted these markers non-invasively in a cohort of 100 BTC patients (Liu et al.).

BTC patients typically experience cancer recurrence within 5 years of surgery, but prognostic factors such as lymph node metastasis and tumor grading can only be observed after tumor resection (Mavros et al., 2014; Koerkamp et al., 2015; Margonis et al., 2016; Bird et al., 2018; Vega et al., 2021). In Jansson et al.'s study, three preoperative immunologic plasma markers were identified - CSF1, TIE2, and TRAIL - that predict survival after surgery in a cohort of 102 BTC patients utilizing high-throughput multiplex immunoassay. CSF1 and TIE2 were found to be negative prognostic factors in BTC, while TRAIL was demonstrated to be a positive prognostic factor (Jansson et al.).

Immunotherapy in HCC

Immunotherapy is a therapeutic option for HCC patients; however, the immune microenvironment of many tumors suppresses the effectiveness of this treatment (Shen et al.).

To address this Research Topic, Shen et al. provide a valuable review article on HDAC inhibitors in HCC. This article demonstrates the ability of HDACs to improve the effectiveness of immunotherapies in cancer treatment. This can be achieved through increased expression of PD-L1 or the recruitment of NK cells and T cells (Shen et al.).

Liang et al. also identified an efficacy enhancement of immunotherapy in HCC by combining anti-PD-1 antibodies with Abrine, an inhibitor of indoleamine 2,3-dioxygenase 1 (IDO1). In their study, Liang et al. showed that IDO1 is upregulated in HCC cells and can lead to tumor immune escape. They found that using Abrine along with anti-PD-1 antibodies can inhibit immune escape and increase $CD8^+$ T cell infiltration, leading to a stronger immune response and anti-tumor effect (Liang et al.).

Taken together, this Research Topic provides insight into the latest efforts to overcome resistance mechanisms of current therapies, discover novel prognostic and predictive markers, and identify alternative anti-BTC/HCC strategies.

We sincerely thank all the authors for their valuable contributions to this Research Topic.

Author contributions

DB: Conceptualization, Writing–original draft. MT: Conceptualization, Writing–original draft. MO: Writing–review

and editing. CM: Writing–review and editing. TK: Writing–review and editing. DN: Conceptualization, Writing–original draft.

Funding

The author(s) declare financial support was received for the research, authorship, and/or publication of this article. This work was funded by the PMU-FFF-stand-alone project (E-20/31/164-MAC).

Acknowledgments

The coordinator and editors of this Research Topic would like to thank all the authors and reviewers for their contribution. We would also like to thank the Frontiers Editorial Team for their helpful support throughout the process.

Conflict of interest

Author MO was employed by company Tacalyx GmbH.

The remaining authors declare that the research was conducted in the absence of any commercial or financial relationships that could be construed as a potential conflict of interest.

The author(s) declared that they were an editorial board member of Frontiers, at the time of submission. This had no impact on the peer review process and the final decision.

Publisher's note

References

Bekric, D., Neureiter, D., Ablinger, C., Dobias, H., Beyreis, M., Ritter, M., et al. (2023). Evaluation of tazemetostat as a therapeutically relevant substance in biliary tract cancer. *Cancers (Basel)* 15 (5), 1569. doi:10.3390/cancers15051569

Bird, N., McKenna, A., Dodd, J., Poston, G., Jones, R., and Malik, H. (2018). Meta-analysis of prognostic factors for overall survival in patients with resected hilar cholangiocarcinoma. *J. Br. Surg.* 105 (11), 1408–1416. doi:10.1002/bjs.10921

Bruix, J., Takayama, T., Mazzaferro, V., Chau, G.-Y., Yang, J., Kudo, M., et al. (2015). Adjuvant sorafenib for hepatocellular carcinoma after resection or ablation (STORM): a phase 3, randomised, double-blind, placebo-controlled trial. *lancet Oncol.* 16 (13), 1344–1354. doi:10.1016/S1470-2045(15)00198-9

Chen, J., Jin, R., Zhao, J., Liu, J., Ying, H., Yan, H., et al. (2015). Potential molecular, cellular and microenvironmental mechanism of sorafenib resistance in hepatocellular carcinoma. *Cancer Lett.* 367 (1), 1–11. doi:10.1016/j.canlet.2015.06.019

Dongqing, X., Jianwen, L., Jiang, F., Kaishuang, C., and Guangxue, R. (2019). The effect and mechanism of vascular endothelial growth factor (VEGF) on tumor angiogenesis in gallbladder carcinoma. *Iran. J. Public Health* 48 (4), 713.

Keating, G. M. (2017). Sorafenib: a review in hepatocellular carcinoma. *Target. Oncol.* 12, 243–253. doi:10.1007/s11523-017-0484-7

Koerkamp, B. G., Wiggers, J. K., Allen, P. J., Besselink, M. G., Blumgart, L. H., Busch, O. R., et al. (2015). Recurrence rate and pattern of perihilar cholangiocarcinoma after curative intent resection. *J. Am. Coll. Surg.* 221 (6), 1041–1049. doi:10.1016/j.jamcollsurg.2015.09.005

Llovet, J. M., Kelley, R. K., Villanueva, A., Singal, A. G., Pikarsky, E., Roayaie, S., et al. (2021). Hepatocellular carcinoma. *Nat. Rev. Dis. Prim.* 7 (1), 6. doi:10.1038/s41572-020-00240-3

Llovet, J. M., Ricci, S., Mazzaferro, V., Hilgard, P., Gane, E., Blanc, J.-F., et al. (2008). Sorafenib in advanced hepatocellular carcinoma. *N. Engl. J. Med.* 359 (4), 378–390. doi:10.1056/NEJMoa0708857

Margonis, G. A., Gani, F., Buettner, S., Amini, N., Sasaki, K., Andreatos, N., et al. (2016). Rates and patterns of recurrence after curative intent resection for gallbladder cancer: a multi-institution analysis from the US Extra-hepatic Biliary Malignancy Consortium. *Hpb* 18 (11), 872–878. doi:10.1016/j.hpb.2016.05.016

Mavros, M. N., Economopoulos, K. P., Alexiou, V. G., and Pawlik, T. M. (2014). Treatment and prognosis for patients with intrahepatic cholangiocarcinoma: systematic review and meta-analysis. *JAMA Surg.* 149 (6), 565–574. doi:10.1001/jamasurg.2013.5137

Mayr, C., Kiesslich, T., Erber, S., Bekric, D., Dobias, H., Beyreis, M., et al. (2021). HDAC screening identifies the HDAC class I inhibitor romidepsin as a promising epigenetic drug for biliary tract cancer. *Cancers (Basel)* 13 (15), 3862. doi:10.3390/cancers13153862

Mayr, C., Neureiter, D., Wagner, A., Pichler, M., and Kiesslich, T. (2015). The role of polycomb repressive complexes in biliary tract cancer. *Expert Opin. Ther. Targets* 19 (3), 363–375. doi:10.1517/14728222.2014.986460

McGlynn, K. A., Petrick, J. L., and El-Serag, H. B. (2021). Epidemiology of hepatocellular carcinoma. *Hepatology* 73, 4–13. doi:10.1002/hep.31288

Möbius, C., Demuth, C., Aigner, T., Wiedmann, M., Wittekind, C., Mössner, J., et al. (2007). Evaluation of VEGF A expression and microvascular density as prognostic factors in extrahepatic cholangiocarcinoma. *Eur. J. Surg. Oncol. (EJSO)* 33 (8), 1025–1029. doi:10.1016/j.ejso.2007.02.020

Moik, F., Riedl, J. M., Winder, T., Terbuch, A., Rossmann, C. H., Szkandera, J., et al. (2019). Benefit of second-line systemic chemotherapy for advanced biliary tract cancer: a propensity score analysis. *Sci. Rep.* 9 (1), 5548. doi:10.1038/s41598-019-42069-1

Nagorney, D. M., Donohue, J. H., Farnell, M. B., Schleck, C. D., and Ilstrup, D. M. (1993). Outcomes after curative resections of cholangiocarcinoma. *Archives Surg.* 128 (8), 871–877. doi:10.1001/archsurg.1993.01420200045008

Neureiter, D., Stintzing, S., Kiesslich, T., and Ocker, M. (2019). Hepatocellular carcinoma: therapeutic advances in signaling, epigenetic and immune targets. *World J. Gastroenterol.* 25 (25), 3136–3150. doi:10.3748/wjg.v25.i25.3136

Ocker, M., Mayr, C., Kiesslich, T., Stintzing, S., and Neureiter, D. (2021). Immunmodulatory treatment strategies of hepatocellular carcinoma: from checkpoint inhibitors now to an integrated approach in the future. *Cancers* 13 (7), 1558. doi:10.3390/cancers13071558

Rakic, M., Patrlj, L., Kopljar, M., Klicek, R., Kolovrat, M., Loncar, B., et al. (2014). Gallbladder cancer. *Hepatobiliary Surg. Nutr.* 3 (5), 221–226. doi:10.3978/j.issn.2304-3881.2014.09.03

Sung, H., Ferlay, J., Siegel, R. L., Laversanne, M., Soerjomataram, I., Jemal, A., et al. (2021). Global cancer statistics 2020: GLOBOCAN estimates of incidence and mortality worldwide for 36 cancers in 185 countries. *CA a cancer J. Clin.* 71 (3), 209–249. doi:10.3322/caac.21660

Thelen, A., Scholz, A., Benckert, C., Schröder, M., Weichert, W., Wiedenmann, B., et al. (2008). Microvessel density correlates with lymph node metastases and prognosis in hilar cholangiocarcinoma. *J. gastroenterology* 43, 959–966. doi:10.1007/s00535-008-2255-9

Valle, J., Wasan, H., Palmer, D. H., Cunningham, D., Anthoney, A., Maraveyas, A., et al. (2010). Cisplatin plus gemcitabine versus gemcitabine for biliary tract cancer. *N. Engl. J. Med.* 362 (14), 1273–1281. doi:10.1056/NEJMoa0908721

Valle, J. W., Kelley, R. K., Nervi, B., Oh, D. Y., and Zhu, A. X. (2021). Biliary tract cancer. *Lancet* 397 (10272), 428–444. doi:10.1016/S0140-6736(21)00153-7

Vega, E. A., Newhook, T. E., Kawaguchi, Y., Qiao, W., De Bellis, M., Okuno, M., et al. (2021). Conditional recurrence-free survival after oncologic extended resection for gallbladder cancer: an international multicenter analysis. *Ann. Surg. Oncol.* 28, 2675–2682. doi:10.1245/s10434-021-09626-3

Zhu, A. X., Hong, T. S., Hezel, A. F., and Kooby, D. A. (2010). Current management of gallbladder carcinoma. *Oncologist* 15 (2), 168–181. doi:10.1634/theoncologist.2009-0302

frontiers | Frontiers in Medicine

TYPE Original Research
PUBLISHED 20 March 2023
DOI 10.3389/fmed.2023.1130692

OPEN ACCESS

EDITED BY
Maria Lina Tornesello,
G. Pascale National Cancer Institute Foundation (IRCCS), Italy

REVIEWED BY
Khaled Obeidat,
Jordan University of Science and Technology, Jordan
Yanwen Jin,
Sichuan University, China

*CORRESPONDENCE
Fu-Nan Qiu
✉ qiufunan72@163.com

†These authors have contributed equally to this work

SPECIALTY SECTION
This article was submitted to Gastroenterology, a section of the journal Frontiers in Medicine

RECEIVED 23 December 2022
ACCEPTED 24 February 2023
PUBLISHED 20 March 2023

CITATION
Wu J-Y, Huang W-T, He W-b, Dai G-F, Lv J-H and Qiu F-N (2023) Long-term outcomes of anatomic vs. non-anatomic resection in intrahepatic cholangiocarcinoma with hepatolithiasis: A multicenter retrospective study. *Front. Med.* 10:1130692. doi: 10.3389/fmed.2023.1130692

Long-term outcomes of anatomic vs. non-anatomic resection in intrahepatic cholangiocarcinoma with hepatolithiasis: A multicenter retrospective study

Jun-Yi Wu[1,2†], Wen-Tao Huang[1,2†], Wen-bin He[1,2], Gao-Fan Dai[3], Jia-Hui Lv[4] and Fu-Nan Qiu[1,2*]

[1]Shengli Clinical Medical College, Fujian Medical University, Fuzhou, China, [2]Department of Hepatobiliary Pancreatic Surgery, Fujian Provincial Hospital, Fuzhou, China, [3]Department of Surgical Intensive Care Unit, First Affiliated Hospital of Fujian Medical University, Fuzhou, China, [4]Department of Hepatobiliary Surgery, Mengchao Hepatobiliary Hospital of Fujian Medical University, Fuzhou, China

Background: The benefits of anatomic resection (AR) vs. non-anatomic resection (NAR) in patients with primary intrahepatic cholangiocarcinoma (ICC) with hepatolithiasis (HICC) are unclear. This study aimed to compare the long-term outcomes of AR vs. NAR in patients with HICC.

Methods: A total of 147 consecutive patients with HICC who underwent R0 hepatectomy were included. Overall survival (OS) and recurrence-free survival (RFS) following AR vs. NARs were compared using a 1:1 propensity score matching (PSM) analysis. A subgroup analysis was also conducted according to whether there are lymph node metastases (LNM).

Results: In a multivariate analysis, CA 19-9 (>39 U/L), microvascular invasion, LNM, and NAR were independent risk factors for poor RFS and OS rates, whereas multiple tumors were independent risk factors for OS. AR had better 1-, 3-, and 5-year RFS and OS rates than NAR (OS: 78.7, 58.9, and 28.5%, respectively, vs. 61.2, 25.4, and 8.8%, respectively; RFS: 59.5, 36.5, and 20.5%, respectively, vs. 38.2, 12.1, and 6.9%, respectively). After PSM, 100 patients were enrolled. The NAR group also had significantly poorer OS and RFS (OS: 0.016; RFS: $p = 0.010$) than the AR group. The subgroup analysis demonstrated that in HICC without LNM, OS and RFS were significantly poorer in the NAR group than the AR group, while no significant differences were observed in HICC with LNM before or after PSM.

Conclusion: Anatomic resection was associated with better long-term survival outcomes than NAR in patients with HICC, except for patients with LNM.

KEYWORDS

intrahepatic cholangiocarcinoma with hepatolithiasis, anatomic resections, overall survival, recurrence-free survival, lymph node metastases (LNM)

Background

Intrahepatic cholangiocarcinoma (ICC) is the second most common primary hepatic malignancy (1, 2). The incidence of ICC has been reported to be increasing worldwide over the past decades (3). Hepatolithiasis is one of the multifactorial etiologies of ICC, which have a high prevalence in Asian countries (4). Several studies have indicated hepatolithiasis as an independent risk factor for patients with ICC, and the total incidence of ICC caused by hepatolithiasis is ∼ 5–13% in Asian populations (5–7).

Liver resection is the first-line therapeutic option for patients with ICC, including those with ICC with hepatolithiasis (HICC), to achieve a possible long-term survival (8). Although many studies have focused on therapy methods for patients with ICC, the prognosis of these patients is dismal owing to high incidences of post-operative recurrence and metastasis (9, 10). Several studies have indicated that the 5-year overall survival (OS) of patients with ICC after curative resection was only 20–35% (9, 10). More importantly, patients with HICC had worse outcomes than those without hepatolithiasis (6, 11).

Anatomic resection (AR) has been recommended to be superior to liver resection in reducing the risk of post-operative intrahepatic recurrence in patients with hepatocellular carcinoma (HCC) (12, 13). However, the number of studies investigating post-hepatectomy OS between AR and non-anatomic resection (NAR) for ICC is limited (14, 15), and the conclusions are still controversial. To the best of our knowledge, no studies have investigated the long-term outcomes of AR and NAR for HICC. In this study, we aimed to compare the clinical outcomes of patients with HICC who underwent AR and NAR using the propensity score matching (PSM) analysis.

Methods

Patients

We retrospectively reviewed the data of patients with HICC who underwent R0 resection between October 2012 and December 2021 at the following three high-volume institutions: Fujian Provincial Hospital (Fuzhou, China), Mengchao Hepatobiliary Hospital of Fujian Medical University (Fuzhou, China), and the First Affiliated Hospital of Fujian Medical University (Fuzhou, China). The diagnosis of HICC was confirmed by two experienced pathologists who were dependent on the post-operative histopathological examination at each participating hospital. R0 resection was defined as complete tumor removal with a free microscopic margin. Data, including standard demographics, perioperative clinicopathological, and post-operative outcomes, were retrospectively collected. This study was approved by the Institutional Ethics Committee of Fujian Provincial Hospital. The ethical license number was K2022-07-011. All the participants provided written informed consent for the use of their data.

The inclusion criteria were as follows: (1) patients with HICC who underwent R0 resection, (2) with primary ICC lesions without contiguous organ invasion or extrahepatic metastasis, and (3) age of 18–75 years with good operative tolerance. The exclusion criteria were as follows: (1) combined with other serious malignant diseases ($n = 3$), (2) Child–Pugh class C liver function ($n = 1$), (3) combined with macrovascular invasion ($n = 16$), (4) receiving pre-operative anticancer treatment ($n = 4$), (5) combined HCC and ICC ($n = 28$), (6) patients who died within 90 days of surgery ($n = 3$), (7) patients who died of other disease-related causes ($n = 2$), (9) non-R0 resection ($n = 14$), and (10) incomplete data ($n = 8$).

Abbreviations: AR, Anatomic resection; NAR, non-anatomic resection; ICC, intrahepatic cholangiocarcinoma; HICC, intrahepatic cholangiocarcinoma with hepatolithiasis; RFS, recurrence-free survival; PSM, propensity score matching; LNM, lymph node metastases; MVI, microvascular invasion; HCC, hepatocellular carcinoma; TBil, total bilirubin; AFP. serum a-fetoprotein; CA19-9, carbohydrate antigen 19-9; CEA, carcinoembryonic antigen; HBsAg, hepatitis B surface antigen.

Liver resection

Patients with obstructive jaundice (total bilirubin (TBil) level >200 μmol/L) or acute cholangitis were treated with percutaneous transhepatic biliary drainage that was placed in their contralateral intrahepatic bile duct to reduce the TBil level pre-operatively. The TBil criteria for surgery after PTCD was TBil level <50 μmol/L or cure for acute cholangitis. It was generally not more than 2 weeks. AR was classified as a liver resection based on the systematic removal of the Couinaud segment(s), which include the tumor together with the tumor-bearing portal vein and hepatic territory, and NAR was classified as all other resections that were not in accordance with the anatomical distribution of the portal vein branches. Regional lymphadenectomy was performed if lymph node metastasis was suspected or diagnosed either pre-operatively or intraoperatively. A choledochoscope was routinely used for exploration in all cases.

Follow-up

Follow-up occurred once every 3 months for the first 2 years after the initial surgery and every 6 months thereafter. At each visit, tests for liver function (TBil, serum albumin, alanine aminotransferase, and aspartate aminotransferase), serum alpha-fetoprotein level (AFP), carbohydrate antigen 19-9 (CA 19-9), and carcinoembryonic antigen (CEA), as well as imaging examinations (contrast-enhanced computed tomography or magnetic resonance imaging) were performed. When recurrence was diagnosed, the treatment was decided based on the pattern of recurrence, liver functional reserve, and general condition of the patient.

The OS rate was calculated from the date of the first liver resection to the date of the patient's death or last follow-up. The recurrence-free survival (RFS) rate was the interval between the date of surgery and the date of diagnosis of the first recurrence or last follow-up.

Statistical analyses

Data were analyzed using the SPSS software (version 17.0; SPSS, Inc., Chicago, IL, USA). Categorical variables were compared using the chi-square test or Fisher's exact test. Continuous variables were compared using the t-test or Mann–Whitney U-test. Univariate and multivariate comparisons of survival distributions were performed using Cox proportional hazard models, and factors with a $p < 0.05$ in the univariate analysis were then incorporated into the multivariate analysis. The OS and RFS rates between AR and NAR were calculated using the Kaplan–Meier method, and the significance of differences between the two groups was compared

using the log-rank test. All *p*-values were two-sided and considered significant at a *p*-value of <0.05.

A PSM analysis was performed to eliminate selection bias. The variables used in the PSM analysis included the following: tumor size, sex, age, hepatitis B surface antigen status (HBsAg), liver cirrhosis, Child–Pugh class, CEA, CA 19-9, tumor size, and tumor number. The PSM was performed *via* 1:1 matching with a caliper width of 0.02 of the standard deviation.

Results

Patient clinicopathological characteristics

Altogether, 147 patients with HICC who underwent R0 hepatectomy without macrovascular invasion, direct invasion to contiguous organs, or extrahepatic metastasis between October 2012 and December 2021 in the three institutions were included in our study. Of these patients, 80 (54.42%) and 67 (45.58%) patients underwent AR and NAR, respectively. The clinicopathological baseline characteristics of the patients with HICC are presented in Table 1. Of the 147 patients, 55 (37.41%) patients had LNM, 99 (67.35%) had tumors >5 cm in diameter, 32 (21.77%) had multiple tumors, and 49 (33.33%) presented with liver cirrhosis. Before PSM, the two groups showed a significant difference in liver cirrhosis. After PSM, there were no significant differences in cirrhosis.

In terms of post-operative characteristics, although the AR group had a slightly longer operative time than the NAR group, there were no significant differences in the operative time (Table 1). Post-operative hospital stay and operative blood loss were also not significantly different between both groups. Meanwhile, the incidence of grades I–II and III–IV surgical complications in the AR and NAR groups was similar (Table 1). More importantly, the AR could significantly reduce the rate of stone recurrence ($P = 0.039$). The long-term outcomes of stone recurrence after PSM ($P = 0.059$) did not significantly differ between the two groups, and this may be because of the small number of cases.

Independent predictors of RFS and OS

Univariate analysis revealed that CA 19-9 (>39 U/L), tumor number (multiple), microvascular invasion (MVI; positive), LNM (positive), and AR (yes) were independent risk factors for OS and RFS rates. Maximum tumor size (>5.0 cm) was independently associated with RFS (Supplementary Table 1). Multivariate analysis revealed that CA 19-9 (>39 U/L), MVI (positive), LNM (positive), and AR (positive) were independent risk factors for OS and RFS rates, whereas tumor number (multiple) was an independent risk factor for OS (Table 2).

Long-term outcomes

Before PSM, the 1-, 3-, and 5-year OS rates for patients with HICC were 78.7, 58.9, and 28.5%, respectively, in the AR group, and 61.2, 25.4, and 8.8%, respectively, in the NAR group ($p < 0.001$) (Figure 1A). The 1-, 3-, and 5-year RFS rates were 59.5, 36.5, and 20.5%, respectively, in the AR group, and 38.2, 12.1, and 6.9%, respectively, in the NAR group ($p < 0.001$) (Figure 1B). After PSM, AR was associated with better 1-, 3-, and 5-year RFS (Figure 1C; 1 year, 49.2 vs. 28.0%; 3 years, 24.7 vs. 11.2%; and 5 years, 16.5 vs. 4.5%; $p = 0.010$) and OS rates (Figure 1D; OS, 65.8 vs. 52.0%; 3 years, 50.1 vs. 16.5%; and 5 years, 22.5 vs. 6.3%; $p = 0.016$) than NAR.

Subgroup analysis of survival according to lymph node metastases

Patients with HICC were sub-categorized according to LNM (Figure 2). Among 92 patients without LNM, the AR group demonstrated better OS and RFS rates than the NAR group before and after PSM. However, no significant difference was observed between both groups among HICC patients with LNM (Figure 3; before PSM, OS: $p = 0.571$, RFS: $p = 0.383$; after PSM, OS: $p = 0.627$, RFS: $p = 0.275$, respectively).

Discussion

To date, a series of studies have indicated that patients with ICC who underwent partial hepatectomy still had a low 5-year OS rate (2, 3). As for those with HICC, their prognosis was poorer than patients with ICC without hepatolithiasis (16, 17). Hepatolithiasis frequently results in the development of atypical epithelium, oncogene activation, and inflammation, leading to the high occurrence of periductal invasion and LNM, which leads to a poor prognosis (18, 19). However, the early symptoms of HICC are not typical and can be easily concealed by intrahepatic bile duct stones and cholangitis. The sensitivity and specificity of laboratory tests and imaging studies for HICC are relatively low, which leads to a delay in diagnosing HICC and the advanced tumor stage (19). In our data, 42 (28.57%) of the patients with HICC were diagnosed by pathological testing after partial hepatectomy. Therefore, surgeons should consider the possibility of co-existing ICC when performing surgery on patients with hepatolithiasis.

Although patients with HICC had a very poor prognosis, curative resection remains the best curative treatment for HICC (20). Previous studies have demonstrated that AR was associated with better survival outcomes than NAR for HCC lesions, with AR considered theoretically effective in reducing intrahepatic recurrence (21, 22). Although both HCC and ICC arise in the hepatic parenchyma, the impact of AR on the prognosis for ICC remains unclear. Moreover, studies on the benefit of AR for ICC are limited, and their conclusions are inconsistent (14, 15). Li et al. concluded that NAR was not inferior to AR in improving the survival outcomes of patients with ICC. In contrast, Si et al. have reported that AR was associated with a better prognosis than NAR in patients with ICC with stage IB or II without vascular invasion. However, no prospective studies have compared the clinical outcomes of patients with HICC who underwent AR and NAR, and the surgical method of operation for patients with HICC has not been extensively researched. Previous studies have reported that AR was effective for treating hepatolithiasis and was associated

TABLE 1 Patient demographics and tumor characteristics.

Variables	Before PSM ($n = 147$)			After PSM ($n = 100$)		
	NAR ($n = 67$)	AR ($n = 80$)	*P*-value	NAR ($n = 50$)	AR ($n = 50$)	*P*-value
Sex			0.278			0.689
Male	30	43		24	26	
Female	37	37		26	24	
Age (years)			0.827			0.373
≤65	48	56		34	38	
>65	19	24		16	12	
HBsAg			0.468			0.517
Yes	23	23		17	14	
No	44	57		33	36	
Anti-HCV			0.510			1.000
Yes	3	2		2	2	
No	64	78		48	48	
Liver cirrhosis			**0.047**			0.826
Yes	28	21		15	14	
No	39	59		35	36	
Tbil			0.324			0.603
≤23 μmol/L	57	63		42	40	
>23 μmol/L	10	17		8	10	
ALB			0.172			0.542
≤40 g/L	30	27		19	22	
>40 g/L	37	53		31	28	
ALT			0.224			0.668
≤40 U/L	49	51		35	33	
>40 U/L	18	29		15	17	
AST			0.797			0.260
≤40 U/L	49	60		39	34	
>40 U/L	18	29		11	16	
ALP			0.429			1.000
≤125 U/L	35	47		28	28	
>125 U/L	32	33		22	22	
GGT			0.787			0.840
≤60 U/L	27	34		21	22	
>60 U/L	49	46		29	28	
AFP			0.535			0.695
≤20 ng/mL	62	76		46	47	
>20 ng/mL	5	4		4	3	

(Continued)

TABLE 1 (Continued)

Variables	Before PSM ($n = 147$)			After PSM ($n = 100$)		
	NAR ($n = 67$)	AR ($n = 80$)	*P*-value	NAR ($n = 50$)	AR ($n = 50$)	*P*-value
CA19-9			0.329			0.529
≤39 U/L	24	35		19	16	
>39 U/L	43	45		31	34	
CEA			0.948			1.000
≤10 μg/L	55	66		40	40	
>10 μg/L	12	14		10	10	
Tumor number			0.539			0.617
Single	50	65		41	39	
Multiple	17	15		9	11	
Tumor diameter			0.244			0.683
≤5	23	35		21	19	
>5	44	45		29	31	
MVI			0.646			1.000
Yes	19	20		16	16	
No	48	60		34	34	
Nodal metastasis			0.508			0.545
Yes	27	28		20	23	
No	40	52		30	27	
Macroscopic type			0.345			0.275
MF	52	67		40	44	
Non-MF	15	13		10	6	
Tumor differentiation			0.771			0.817
Well/moderate	50	58		37	38	
Poor	17	22		13	12	
Operation time, min	206.5 ± 93.0	234.7 ± 82.4	0.053	208.9 ± 91.6	227.1 ± 83.3	0.300
Blood loss, mL median (range)	300 (50–2,450)	300 (50–2,500)	0.505	200 (50–2,450)	300 (100–2,500)	0.763
Post-operative hospital stays, days	13.7 ± 7.7	13.9 ± 7.2	0.913	13.3 ± 7.7	13.1 ± 5.9	0.840
Adjuvant chemoradiotherapy			0.580			0.305
Yes	23	31		17	22	
No	44	49		33	28	
Grade of complications			0.943			1.000
Non	35	44		23	23	
I–II	26	29		22	22	
III–IV	6	7		5	5	
Long-term outcome of stone recurrence			**0.039**			0.059
Yes	9	3		7	1	
No	58	77		43	49	

The bold values indicate $P < 0.05$, which had a significant difference between the two group.

TABLE 2 Multivariate analysis of factors related to the RFS and OS before PSM.

Variables	RFS			OS		
	HR	(95%CI)	*P*-value	HR	(95%CI)	*P*-value
ALP (>125 U/L)	0.899	0.595–1.357	0.612			
CA19-9 (>39 U/L)	1.858	1.210–2.854	**0.005**	1.996	1.249–3.189	**0.004**
Tumor number (multiple)	1.611	0.987–2.628	0.056	2.654	1.591–4.427	**<0.001**
Tumor size (>5 cm)	1.254	0.817–1.925	0.301	1.076	0.689–1.681	0.748
MVI (positive)	2.282	1.484–3.510	**<0.001**	1.874	1.187–2.959	**0.007**
Nodal metastasis (positive)	1.849	1.194–2.863	**0.006**	2.432	1.536–3.852	**<0.001**
AR (yes)	2.008	1.370–2.943	**<0.001**	2.237	1.477–3.390	**<0.001**

The bold values indicate $P < 0.05$, which had a significant difference between the two group.

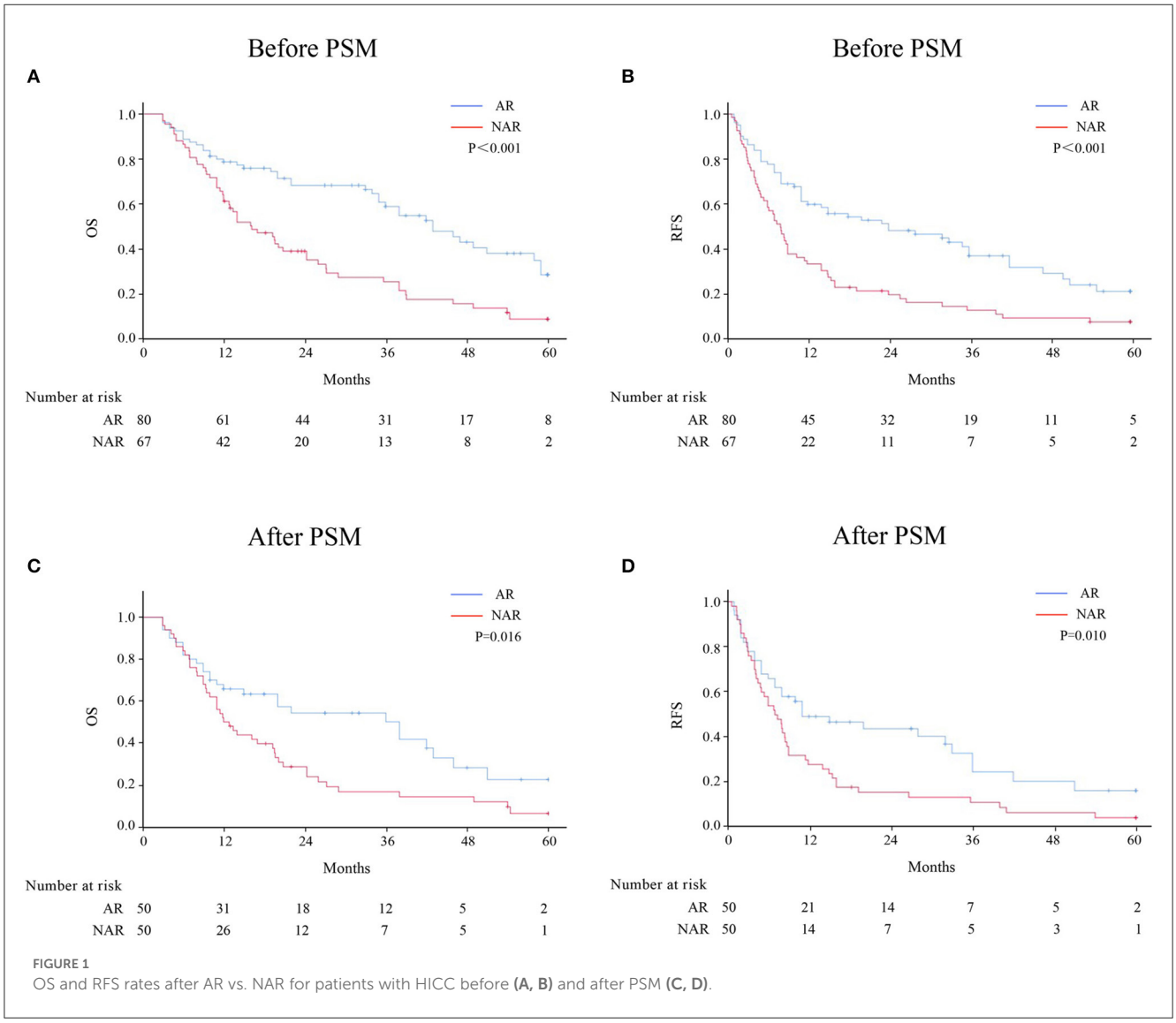

FIGURE 1
OS and RFS rates after AR vs. NAR for patients with HICC before **(A, B)** and after PSM **(C, D)**.

with a low rate of recurrence (23, 24). Thus, patients with HICC may benefit from AR.

In the present study, AR conferred better OS and RFS outcomes than NAR in patients with HICC who underwent R0 hepatectomy without macrovascular invasion, direct invasion to contiguous organs, or extrahepatic metastasis. In addition, AR could significantly reduce the rate of stone recurrence before PSM. Multivariate analyses revealed AR as an independent favorable

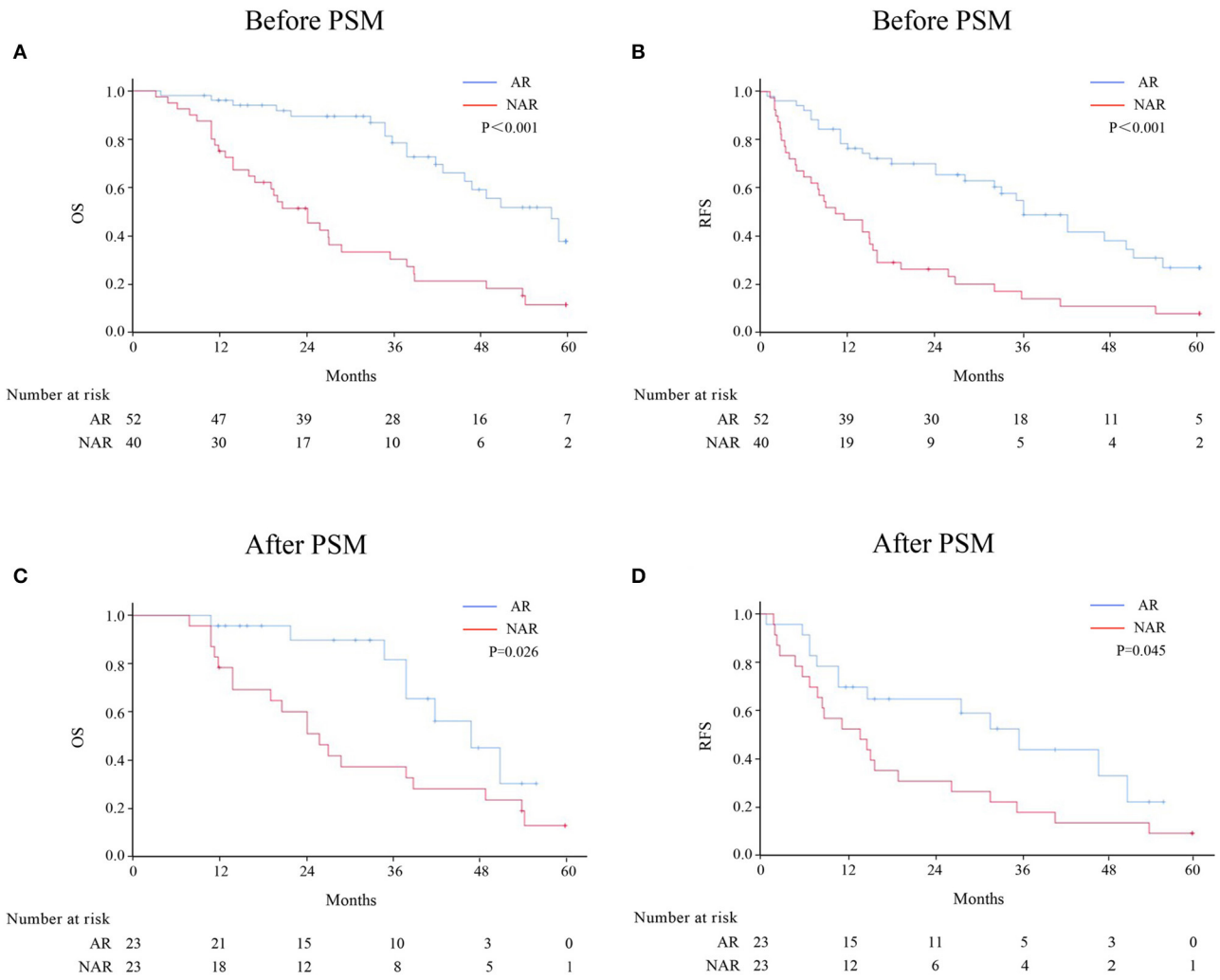

FIGURE 2
OS and RFS rates after AR vs. NAR for HICC patients without LNM before **(A, B)** and after PSM **(C, D)**.

prognostic factor for OS and RFS. Subgroup analyses further demonstrated that HICC patients without LNM would receive more benefits from AR than that from NAR. Meanwhile, no significant difference between AR and NAR was observed in HICC patients with LNM.

Several studies have indicated that NAR is generally suitable for patients with poor liver function or liver cirrhosis (25, 26). Poor liver function and liver cirrhosis are limiting factors for extensive liver resection in patients with ICC. The use of AR in patients with poor liver function or liver cirrhosis should still be assessed carefully to avoid liver failure post-operatively. In our study, the AR group comprised a few patients with liver cirrhosis. The different proportions of liver cirrhosis may be attributable to inconsistent results. Therefore, we used PSM to minimize the selection bias between the two groups. Moreover, our study demonstrated that the intraoperative bleeding, operative time, post-operative hospital stays, and grade of complications did not differ significantly between the AR and NAR groups. This may be due to the technological advances in hepatectomy and the selection of the most appropriate treatment for patients with ICC.

The relationship between LNM and the prognosis of ICC has been indicated in previous studies (27, 28). Nodal metastasis is generally believed to greatly influence the prognosis of patients with ICC compared with other risk factors (27). ICC patients with LNM had a significantly worse prognosis than those without LNM (27, 28). In the present study, the data demonstrated that the LNM of HICC, rather than the resection type, influenced long-term outcomes.

This study has several limitations. First, this was a retrospective study. Although we used PSM, biases in patient selection may still exist. Second, some patients who had normal lymph nodes that were not identified in the pre-operative imaging or surgical exploration did not undergo lymphadenectomy. Nevertheless, all patients with ICC were recommended to undergo lymphadenectomy. Third, the sample size was small. Thus, more

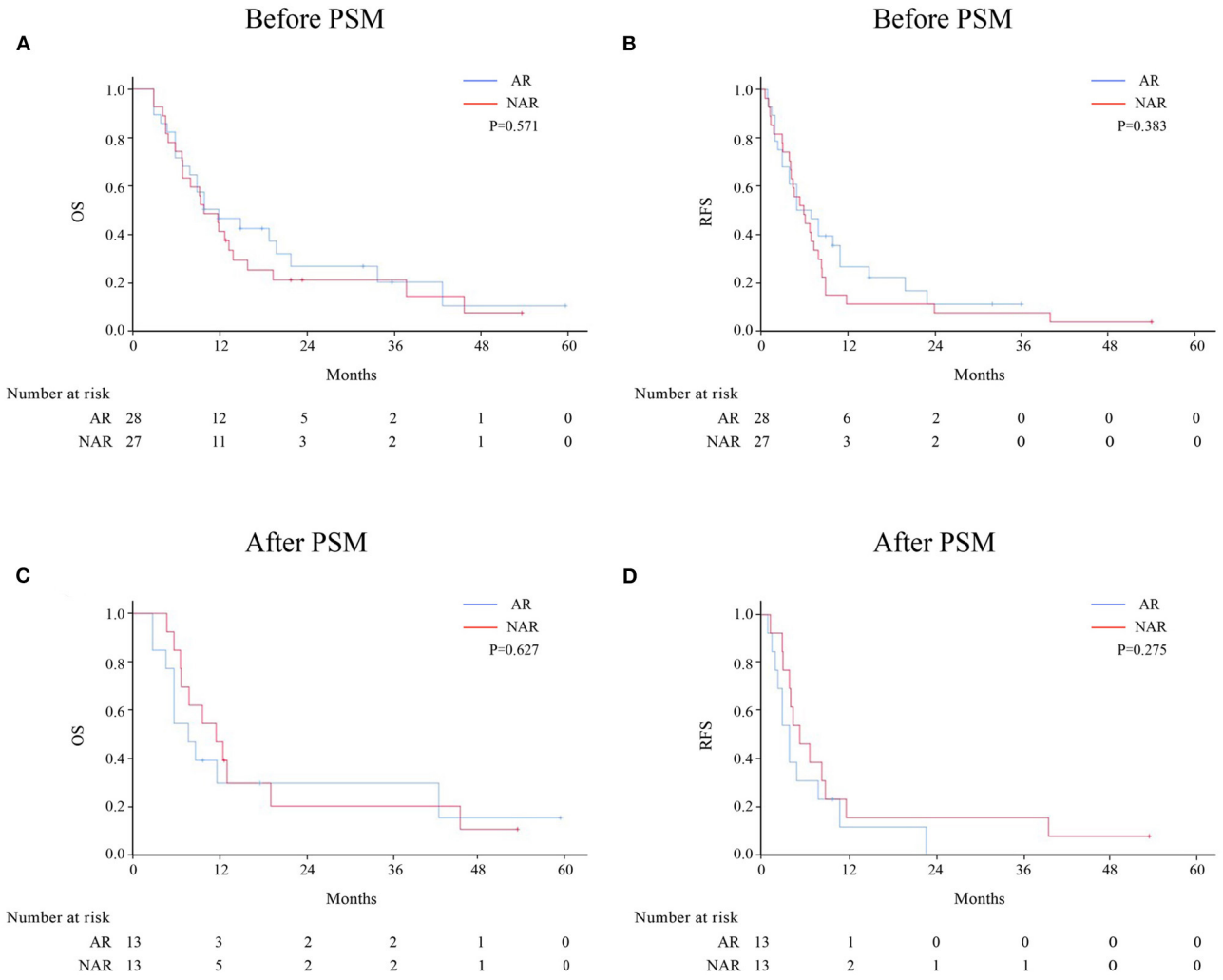

FIGURE 3
OS and RFS rates after AR vs. NAR for HICC patients with LNM before **(A, B)** and after PSM **(C, D)**.

randomized controlled trials with a large sample size are necessary to confirm our results.

Conclusion

In conclusion, our study indicated that AR was associated with better survival outcomes than NAR in HICC patients without LNM.

Data availability statement

The original contributions presented in the study are included in the article/Supplementary material, further inquiries can be directed to the corresponding author.

Ethics statement

The studies involving human participants were reviewed and approved by the Ethics Committee of Fujian Provincial Hospital, Mengchao Hepatobilary Hospital of Fujian Medical University, and The First Affiliated Hospital of Fujian Medical University. All study participants gave their written informed consent. The patients/participants provided their written informed consent to participate in this study.

Author contributions

F-NQ and J-YW: conceived and designed the research and drafted the manuscript. J-YW, W-TH, and W-bH: data acquisition. J-YW, W-TH, J-HL, and G-FD: data analysis. All authors read and approved the final manuscript.

Funding

This research was supported by the Startup Fund for Scientific Research, Fujian Medical University (Grant number: 2018QH1112) and the Natural Science Foundation of Fujian Province, China (Grant number: 2020J05117).

Conflict of interest

The authors declare that the research was conducted in the absence of any commercial or financial relationships that could be construed as a potential conflict of interest.

Publisher's note

Supplementary material

The Supplementary Material for this article can be found online at: https://www.frontiersin.org/articles/10.3389/fmed.2023.1130692/full#supplementary-material

References

1. Zhang H, Yang T, Wu M, Shen F. Intrahepatic cholangiocarcinoma: epidemiology, risk factors, diagnosis and surgical management. *Cancer Lett*. (2016) 379:198–205. doi: 10.1016/j.canlet.2015.09.008

2. Rahnemai-Azar AA, Pandey P, Kamel I, Pawlik TM. Monitoring outcomes in intrahepatic cholangiocarcinoma patients following hepatic resection. *Hepat Oncol*. (2016) 3:223–39. doi: 10.2217/hep-2016-0009

3. Brandi G, Tavolari S. Asbestos and intrahepatic cholangiocarcinoma. *Cells*. (2020) 9:421. doi: 10.3390/cells9020421

4. Gupta A, Dixon E. Epidemiology and risk factors: intrahepatic cholangiocarcinoma. *Hepatobiliary Surg Nutr*. (2017) 6:101–4. doi: 10.21037/hbsn.2017.01.02

5. Tao LY, He XD, Qu Q, Cai L, Liu W, Zhou L, et al. Risk factors for intrahepatic and extrahepatic cholangiocarcinoma: a case-control study in China. *Liver Int*. (2010) 30:215–21. doi: 10.1111/j.1478-3231.2009.02149.x

6. Wang Q, Li J, Lei Z, Wu D, Si A, Wang K, et al. Prognosis of intrahepatic cholangiocarcinomas with HBV infection is better than those with hepatolithiasis after R0 liver resection: a propensity score matching analysis. *Ann Surg Oncol*. (2017) 24:1579–87. doi: 10.1245/s10434-016-5751-9

7. Roy S, Glaser S, Chakraborty S. Inflammation and progression of cholangiocarcinoma: role of angiogenic and lymphangiogenic mechanisms. *Front Med*. (2019) 6:293. doi: 10.3389/fmed.2019.00293

8. Bridgewater J, Galle PR, Khan SA, Llovet JM, Park JW, Patel T, et al. Guidelines for the diagnosis and management of intrahepatic cholangiocarcinoma. *J Hepatol*. (2014) 60:1268–89. doi: 10.1016/j.jhep.2014.01.021

9. Gentile D, Donadon M, Lleo A, Aghemo A, Roncalli M, di Tommaso L, et al. Surgical treatment of hepatocholangiocarcinoma: a systematic review. *Liver Cancer*. (2020) 9:15–27. doi: 10.1159/000503719

10. Zhang XF, Xue F, Dong DH, Weiss M, Popescu I, Marques HP, et al. Number and station of lymph node metastasis after curative-intent resection of intrahepatic cholangiocarcinoma impact prognosis. *Ann Surg*. (2021) 274:e1187–95. doi: 10.1097/SLA.0000000000003788

11. Lin CC, Lin PY, Chen YL. Comparison of concomitant and subsequent cholangiocarcinomas associated with hepatolithiasis: clinical implications. *World J Gastroenterol*. (2013) 19:375–80. doi: 10.3748/wjg.v19.i3.375

12. Tanaka K, Shimada H, Matsumoto C, Matsuo K, Nagano Y, Endo I, et al. Anatomic versus limited nonanatomic resection for solitary hepatocellular carcinoma. *Surgery*. (2008) 143:607–15. doi: 10.1016/j.surg.2008.01.006

13. Jiao S, Li G, Zhang D, Xu Y, Liu J, Li G. Anatomic versus non-anatomic resection for hepatocellular carcinoma, do we have an answer? A meta-analysis. *Int J Surg*. (2020) 80:243–55. doi: 10.1016/j.ijsu.2020.05.008

14. Si A, Li J, Yang Z, Xia Y, Yang T, Lei Z, et al. Impact of anatomical versus non-anatomical liver resection on short- and long-term outcomes for patients with intrahepatic cholangiocarcinoma. *Ann Surg Oncol*. (2019) 26:1841–50. doi: 10.1245/s10434-019-07260-8

15. Li B, Song JL, Aierken Y, Chen Y, Zheng JL, Yang JY. Nonanatomic resection is not inferior to anatomic resection for primary intrahepatic cholangiocarcinoma: a propensity score analysis. *Sci Rep*. (2018) 8:17799. doi: 10.1038/s41598-018-35911-5

16. Deng L, Wang Y, Zhao J, Tong Y, Zhang S, Jin C, et al. The prognostic value of sarcopenia combined with hepatolithiasis in intrahepatic cholangiocarcinoma patients after surgery: a prospective cohort study. *Eur J Surg Oncol*. (2021) 47(3 Pt B):603–12. doi: 10.1016/j.ejso.2020.09.002

17. Suzuki Y, Mori T, Abe N, Sugiyama M, Atomi Y. Predictive factors for cholangiocarcinoma associated with hepatolithiasis determined on the basis of Japanese Multicenter study. *Hepatol Res*. (2012) 42:166–70. doi: 10.1111/j.1872-034X.2011.00908.x

18. Li J, Lu J, Lv S, Sun S, Liu C, Xu F, et al. Linoleic acid pathway disturbance contributing to potential cancerization of intrahepatic bile duct stones into intrahepatic cholangiocarcinoma. *BMC Gastroenterol*. (2022) 22:269. doi: 10.1186/s12876-022-02354-2

19. Su CH, Shyr YM, Lui WY, P'Eng FK. Hepatolithiasis associated with cholangiocarcinoma. *Br J Surg*. (1997) 84:969–73. doi: 10.1002/bjs.1800840717

20. Kim HJ, Kang TU, Swan H, Kang MJ, Kim N, Ahn HS, et al. Incidence and prognosis of subsequent cholangiocarcinoma in patients with hepatic resection for bile duct stones. *Dig Dis Sci*. (2018) 63:3465–73. doi: 10.1007/s10620-018-5262-6

21. Okamura Y, Sugiura T, Ito T, Yamamoto Y, Ashida R, Ohgi K, et al. Anatomical resection is useful for the treatment of primary solitary hepatocellular carcinoma with predicted microscopic vessel invasion and/or intrahepatic metastasis. *Surg Today*. (2021) 51:1429–39. doi: 10.1007/s00595-021-02237-1

22. Wu JY, Sun JX, Bai YN, Huang XX, Wu JY, Wei YG, et al. Long-term outcomes of anatomic versus nonanatomic resection in hepatocellular carcinoma patients with bile duct tumor thrombus: a propensity score matching analysis. *Ann Surg Oncol*. (2021) 28:7686–95. doi: 10.1245/s10434-021-09874-3

23. Jiang H, Wu H, Xu YL, Wang JZ, Zeng Y. An appraisal of anatomical and limited hepatectomy for regional hepatolithiasis. *HPB Surg*. (2010) 2010:791625. doi: 10.1155/2010/791625

24. Jarufe N, Figueroa E, Munoz C, Moisan F, Varas J, Valbuena JR, et al. Anatomic hepatectomy as a definitive treatment for hepatolithiasis: a cohort study. *HPB*. (2012) 14:604–10. doi: 10.1111/j.1477-2574.2012.00488.x

25. Dahiya D, Wu TJ, Lee CF, Chan KM, Lee WC, Chen MF. Minor versus major hepatic resection for small hepatocellular carcinoma (HCC) in cirrhotic patients: a 20-year experience. *Surgery*. (2010) 147:676–85. doi: 10.1016/j.surg.2009.10.043

26. Huang ZY, Chen G, Hao XY, Cai RY, Zhao YF, Chen XP. Outcomes of non-anatomic liver resection for hepatocellular carcinoma in the patients with liver cirrhosis and analysis of prognostic factors. *Langenbecks Arch Surg*. (2011) 396:193–9. doi: 10.1007/s00423-010-0700-8

27. Shimada K, Sano T, Nara S, Esaki M, Sakamoto Y, Kosuge T, et al. Therapeutic value of lymph node dissection during hepatectomy in patients with intrahepatic cholangiocellular carcinoma with negative lymph node involvement. *Surgery*. (2009) 145:411–6. doi: 10.1016/j.surg.2008.11.010

28. Mavros MN, Economopoulos KP, Alexiou VG, Pawlik TM. Treatment and prognosis for patients with intrahepatic cholangiocarcinoma: systematic review and meta-analysis. *JAMA Surg*. (2014) 149:565–74. doi: 10.1001/jamasurg.2013.5137

frontiers | Frontiers in Oncology

TYPE Review
PUBLISHED 17 April 2023
DOI 10.3389/fonc.2023.1098958

OPEN ACCESS

EDITED BY
Maria Lina Tornesello,
G. Pascale National Cancer Institute Foundation (IRCCS), Italy

REVIEWED BY
Dalong Yin,
University of Science and Technology of China, China
Xiu-Ping Zhang,
People's Liberation Army General Hospital, China

*CORRESPONDENCE
Peng Zhu
zhupeng@tjh.tjmu.edu.cn

†These authors have contributed equally to this work and share first authorship

SPECIALTY SECTION
This article was submitted to Gastrointestinal Cancers: Hepato Pancreatic Biliary Cancers, a section of the journal Frontiers in Oncology

RECEIVED 15 November 2022
ACCEPTED 04 April 2023
PUBLISHED 17 April 2023

CITATION
Guo B, Chen Q, Liu Z, Chen X and Zhu P (2023) Adjuvant therapy following curative treatments for hepatocellular carcinoma: current dilemmas and prospects. *Front. Oncol.* 13:1098958. doi: 10.3389/fonc.2023.1098958

Adjuvant therapy following curative treatments for hepatocellular carcinoma: current dilemmas and prospects

Bin Guo[1†], Qian Chen[1,2†], Zhicheng Liu[1], Xiaoping Chen[1] and Peng Zhu[1*]

[1]Hepatic Surgery Center, Tongji Hospital, Tongji Medical College, Huazhong University of Science and Technology, Wuhan, Hubei, China, [2]Hepatobiliary Surgery Department, The First Affiliated Hospital of Shihezi University, Shihezi, Xinjiang, China

Curative surgical treatments, mainly liver resection, are still one of the optimal options for patients with early-, mid-, and even progression-stage hepatocellular carcinoma (HCC). However, the recurrence rate within 5 years after surgery is as high as 70%, especially in patients with high risk factors for recurrence, most of whom experience early recurrence within 2 years. Effective adjuvant therapy may improve prognosis, previous studies found that adjuvant transarterial chemoembolization, antiviral, and traditional Chinese medicine et al. were helpful in preventing HCC recurrence. Nevertheless, due to controversial results or lack of high-level evidence, there is no standardized postoperative management protocol worldwide at present. Continued exploration of effective postoperative adjuvant treatments to improve surgical prognosis is necessary.

KEYWORDS

hepatocellular carcinoma, curative surgery, tumor recurrence, disease-free survival, adjuvant therapy

Abbreviations: HCC, hepatocellular carcinoma; LR, liver resection; LT, liver transplantation; OS, overall survival; BCLC, Barcelona Clinical Liver Cancer; PVTT, portal vein tumor thrombosis; MVI, microvascular invasion; TACE, transarterial chemoembolization; ICIs, immune checkpoint inhibitors; RCT, randomized controlled trials; HBV, hepatitis B virus; HCV, hepatitis C virus; DAAs, direct-acting antivirals; DFS, disease-free survival; PD-1, programmed death protein 1; TKIs, tyrosine kinase inhibitors; TCM, traditional Chinese medicine; THM, traditional herbal medicine; HAIC, hepatic artery infusion chemotherapy; RT, radiotherapy; IMRT, intensity modulated radiotherapy; SBRT, stereotactic body radiotherapy; AEs, adverse effects; CIK, cytokine induced killer cells.

1 Introduction

Hepatocellular carcinoma (HCC) is one of the most common malignancies worldwide, the number of HCC-related death ranking second among all types of cancers (1, 2). Curative surgery is the ideal treatment protocol for patients with HCC (3, 4), and the choice of surgical indications for liver resection (LR) varies between regions based on different administrative medical evidence. According to the recently updated European guidelines for the treatment of HCC (4), only patients with Barcelona Clinical Liver Cancer (BCLC) stage 0-A HCC are suitable for radical surgery including ablation, LR and liver transplantation (LT), and some patients with stage B HCC are appropriate candidates for LT if they meet extended LT criteria. Strict adherence to BCLC guidelines for surgical indications may prevent many patients from undergoing radical surgical treatment. In contrast, some procedures that exceed BCLC guidelines are often performed in the Asia-Pacific region, including some stage B and stage C patients (5, 6), and some studies have confirmed that surgery has more favorable outcomes than other modalities (7–9). However, a wider range of surgical indications also means a higher probability of accompanying high-risk factors for recurrence.

There are two types of postoperative recurrence, one is early recurrence which is thought to be associated with intrahepatic metastasis from the initial tumor within 2 years after the surgery; the other is late recurrence, which usually occurs after two years due to underlying liver disease like cirrhosis or active hepatitis. Previous studies have shown that portal vein tumor thrombosis(PVTT), microvascular invasion (MVI), and multiple tumors et al. are high-risk factors for early recurrence (10–13), while PVTT and MVI are also high-risk factors for late recurrence (14, 15). Patients with high risk factors are more likely to experience early recurrence, which severely affects the overall outcome of surgical treatment and compromises the patient's quality of life.

Regarding the management of postoperative adjuvant therapy, there is no standardized strategies worldwide due to unsatisfactory results, controversial findings or lack of high-level evidence (16, 17). Although there are some regimens that may be helpful in reducing postoperative recurrence, such as sorafenib (18, 19), lenvatinib (20), transarterial chemoembolization (TACE) (21), antiviral for hepatitis B-related HCC (22), and Huaier granule (23). However, more well-designed RCTs are required to validate their value. In recent years, the combination of immune checkpoint inhibitors (ICIs) with systemic agents or locoregional therapy has shown excellent anti-tumor effects in the treatment of advanced HCC. This has also led to more options and directions in the study of postoperative adjuvant therapy for HCC, and some relevant studies have recently been preliminarily reported, with overall encouraging results. Here we summarize the current status and recent advances in postoperative adjuvant therapy for HCC.

2 The current options and recent advances of adjuvant therapy

2.1 Antiviral therapy

2.1.1 Oral antiviral drugs

In Asia, Africa, etc. Hepatitis B virus (HBV) is a major risk factor for the occurrence and progression of HCC. Anti-HBV is an essential basic treatment for HCC, which not only improves liver function and prevents liver fibrosis, but also reduces the recurrence of cured HCC (24). Common oral antiviral drugs include entecavir, tenofovir, adefovir and telbivudine. Huang et al. conducted 2 randomized controlled trials (RCT) confirmed that adjuvant antiviral therapy (telbivudine and adefovir) is helpful in reducing late recurrence for HBV-related HCC after LR, and the OS was also improved (22, 25). Besides, a recent cohort study found that tenofovir maybe a more suitable adjuvant agents for patients received LR than entecavir, which was associated with lower risk of HCC recurrence and better OS (26). For patients with hepatitis C virus (HCV)-associated HCC, the necessity of postoperative adjuvant antiviral therapy remains controversial. A multicenter study which included 47 tertiary care centers in 25 states on the effect of direct-acting antivirals (DAAs) on HCC recurrence did not reach a consistent conclusion (27), 48% responded that DAAs reduce risk, 36% responded that DAAs do not change risk, and 16% responded that DAAs increase risk of HCC recurrence. Similarly, a meta-analysis including 21 studies found no statistically significant difference in the relative risk of DAAs exposure versus no DAAs exposure in preventing HCC recurrence (28). Therefore, postoperative adjuvant antivirals are essential for HBV-related HCC, whereas for HCV-related HCC, there is no high-level evidence to support the necessity of their use.

2.1.2 Interferon

More than a decade ago, many RCTs have explored the value of interferon as an adjuvant therapy due to its antiviral, immunomodulatory, anti-proliferative and anti-angiogenic effects. However, these studies did not obtain consistent conclusions. Two RCTs found adjuvant interferon can't improve the prognosis for hepatitis viral-related HCC after LR (29, 30); while a RCT found adjuvant interferon improved OS for HBV-related HCC (31), and 2 RCTs found adjuvant interferon improved disease-free survival (DFS) for HCV-related HCC (32, 33). A meta-analysis incorporating only RCTs concluded that adjuvant interferon can improved OS for hepatitis viral-related HCC, but the influence of DFS was modest (34). This may explain why interferon is currently used less frequently. Nevertheless, the immunomodulatory effects of interferon have attracted the interest of researchers. Hu et al. (35) found interferon can release the cytotoxic capacity of T cells by reprogramming glucose metabolism in the HCC tumor

microenvironment to enhances the immune response induced by programmed death protein 1 (PD-1) inhibitors. Besides, in a study based on subcutaneous and orthotopic mouse models of HCC, Zhu et al. (36) found a possible synergistic effect of interferon and PD-1inhibitors. The combination of PD-1 inhibitors and interferon is promising both in the treatment of advanced HCC and in adjuvant therapy after radical surgery, and more clinical studies are needed to confirm this conjecture.

2.2 Tyrosine kinase inhibitors

Sorafenib is one of the TKIs, which is the first Food and Drug Administrations-approved anti-angiogenic drug for first-line treatment of advanced HCC (3, 37). STORM trial is a large RCT conducted in multiple countries which evaluated the value of adjuvant sorafenib for patients with HCC following LR or ablation, however, the median DFS was 8.5 months in the sorafenib group which was not significantly improved compared with 8.4 months in the placebo group (38). Some subsequent studies have made different findings. Two small sample studies from China found that adjuvant sorafenib following LR significantly improved DFS and OS for patients with BCLC C stage HCC (18, 39). Another propensity score-matched (PSM) study including 718 patients with MVI from China found that adjuvant sorafenib significantly improved DFS and OS compared to LR alone (The 5-years DFS and OS rate was 39% and 57% vs. 19% and 37%) (19). In addition, a recent meta-analysis of 9 studies also concluded that sorafenib is valuable as adjuvant therapy (40). Lenvatinib is another approved TKIs for advanced HCC, which was proved non-inferior to sorafenib, with comparable OS and longer progression-free survival (41). A retrospective study confirmed a similar adjuvant effect of Lenvatinib following LR for patients with MVI (42), which prolong both DFS and OS. Another retrospective study found adjuvant lenvatinib is helpful in improving the prognosis for patients with high residual alpha-fetoprotein following resection or ablation (20). Expanding the indications for surgical treatment in the Chinese region may be an important factor that could explain the inconsistent results with the STROM trial. Patients with high-risk recurrence factors are more deserving of adjuvant therapy and are more likely to benefit from adjuvant TKIs. Of course, this would need to be confirmed by more regional, well-designed RCTs.

2.3 Traditional Chinese medicine

Mild medicinal properties and well-tolerance is the major advantage of TCM. TCM has a history of thousands of years, but research on the treatment of HCC and adjuvant therapy is scarce. So far, only 2 RCTs have evaluated the adjuvant therapeutic value of Huaier granules and traditional herbal medicine (THM). Huaier granules plays an anti-tumor role by inhibiting cell proliferation, inducing apoptosis and inhibiting tumor angiogenesis (43, 44). A multicenter RCT including 1,044 patients led by our center explored the postoperative adjuvant value of Huaier granules. Patients with BCLC A or B stage HCC who received adjuvant Huaier granules following radical LR had better DFS and OS than those received LR alone (the 96 weeks DFS and OS rates was 62.39% and 95.19% vs. 42.09% and 91.46%), and the extrahepatic recurrence rate was significantly lower in the Huaier granules group (8.6% vs. 13.1%) (23). Wang et al (45). in a cohort study found that adjuvant Huaier granules was also helpful in improving OS for patients with early-stage HCC after thermal ablation compared with no intervention (The median OS was 35 months vs. 31 months). A recent PSM analysis also confirmed that adjuvant Huaier granules after curative resection were helpful in improving prognosis, especially for patients with tumor diameter >3 cm (after PSM, the 5-years DFS was 42.18% vs. 27.14%) (46). Another RCT conducted by Zhai et al. (47, 48) evaluated the effectiveness of adjuvant THM for patients with small HCC, patients' DFS and OS were significantly prolonged when receiving adjuvant THM compared with TACE (the median DFS was 85.83 months vs. 26 months). Many active ingredients and mechanisms of action of TCM for the treatment of malignant tumors are still unclear, limiting its widespread clinical use, and application in countries other than China. Continued in-depth exploration is necessary; besides, it is also worth investigating whether the combination of TCM with TKIs or ICIs will produce better anti-tumor effects.

2.4 Transarterial interventions

2.4.1 TACE

With more than 40 years of development, TACE is a very mature technique and the standard treatment for intermediate stage (BCLC-B) HCC (4). Postoperative angiography allows timely detection of residual lesions and embolization of the blood supply vessels, which determines the value of TACE as an adjunctive therapy. As early as 1994, an RCT evaluated the value of TACE as adjuvant therapy, patients had significantly longer DFS after receiving 1 postoperative TACE compared to no intervention, but no significant difference in OS (49). Five RCTs were subsequently explored in the next 15 years, but the results were controversial. Two studies found that adjuvant TACE significantly improved DFS and OS (50, 51), one study found that TACE only contributed to OS (52), and one study found that TACE had no significant effect on prognosis (53). Research was stalled for nearly a decade due to controversial results, until the last few years, two RCTs have explored TACE adjuvant therapy in depth and have reached consistent conclusions (54). One was conducted by Wei. et al. evaluated the effect of postoperative adjuvant TACE for patients with MVI and tumor diameter ≥ 5cm, patients who received adjuvant TACE had significantly longer DFS and OS (the median DFS and OS was 14.45 months and 44.29months vs. 9.27 months and 22.37 months) (55). The other RCT which including 280 patients conducted by Wang et al. obtained similarly results, adjuvant TACE effectively reduces postoperative recurrence for patients with high-risk factors (tumor diameter ≥5cm with MVI, or multiple tumors) for recurrence, the median DFS was 25.7 months longer than the control group (49.5 months vs. 23.8

months) (21). Based on these results, TACE was included in the recommended postoperative adjuvant regimen in the Chinese liver cancer treatment guidelines (9). A recent meta-analysis involving 40 studies (10 RCTs and 30 non-RCTs) of postoperative adjuvant TACE noted that patients with high-risk factors for recurrence (MVI, multinodular tumors, and tumor diameter ≥5cm) were more likely to benefit from adjuvant TACE, with longer OS and DFS compared with LR alone; conversely, this study found no improvement in OS, and even worse DFS in patients without MVI (56). Studies in recent years have pointed to the possibility that TACE may help reduce early recurrence for patients with high-risk factors for recurrence, and whether those at low risk of recurrence will benefit from adjuvant TACE is debatable.

2.4.2 Hepatic artery infusion chemotherapy

Identification of suspicious lesions by angiography and continuous infusion of chemotherapy is the modus operandi of HAIC. Izumi et al. (49) first evaluated the effect of HAIC as an adjuvant therapy for patients with MVI and/or intrahepatic metastases after LR in an RCT conducted in 1994, and found that HAIC can effectively prevent postoperative recurrence. A small sample RCT from China obtained similar results in 2015, patients who received adjuvant HAIC had significantly better OS and DFS than surgery alone (57). However, two recently published RCT studies did yield inconsistent results. Li et al. (58) found adjuvant HAIC significantly prolonged the DFS and OS compared without any adjuvant therapy for patients with MVI (the 18 months OS and DFS rate was 97.7% and 58.7% vs. 78.5% and 38.6%). Another RCT found that postoperative adjuvant HAIC having little effect on DFS and OS (59), and this RCT did not specifically select patients with high-risk recurrence factors maybe one reason. Hsiao et al. (60) also found that postoperative adjuvant HAIC did not improve OS and DFS compared with LR alone in a recent retrospective study; while in the subgroup analysis, patients with multiple tumors or MVI were more likely benefited from adjuvant HAIC. A recent meta-analysis confirmed that postoperative adjuvant HAIC is effective in improving prognosis and found that patients with MVI and PVTT are more likely to benefit from it (61). Similar to TACE, the available evidence supports that patients with high-risk relapse factors may be better suited to receive this type of adjuvant therapy.

2.5 Radiotherapy

2.5.1 External RT

Narrow pathological margins (< 1 cm), residual tumor tissue/cells or microscopic lesions in the liver that are temporarily undetectable by examination may lead to early recurrence. RT may be helpful in removing these undetectable tumors. In 2014, Yu et al. (62) published the results of the first RCT to assess the effectiveness of postoperative adjuvant RT for patients with narrow margin (< 1 cm), and found that adjuvant RT did not significantly influence the DFS and OS. However, inconsistent conclusions were reached by Gou et al. (63) in a recent retrospective multicenter study that adjuvant RT work a lot in prolonging DFS and OS for patients with narrow or positive surgical margins (the median OS and DFS was 72.5 months and 37.3 months vs. 52.5 months and 24.0 months). With the development of precision RT techniques and the application of new radioisotopes, a variety of external RT modalities have proven to be highly effective for patients with advanced HCC, including intensity modulated RT (IMRT) and stereotactic body RT (SBRT) (64). Recently, Sun et al. (65) found that adjuvant IMRT significantly reduce the postoperative recurrence and prolong the OS for patients with PVTT compared with LR alone (the median DFS and OS was 9.1 months and 18.9 months vs. 4.1 months and 10.8 months). Another single-arm, phase II study also confirmed that postoperative adjuvant IMRT is safe, well tolerated by patients and has a favorable survival prognosis (the 5-year OS and DFS rates were 72.2% and 51.6%) (66). Shi et al. (67) conducted an RCT investigated the prognostic imaging of adjuvant SBRT in patients with MVI who underwent marginal resection, and found that SBRT plays an important role in improving patient's postoperative prognosis (the 5-years DFS and OS rates in the SBRT group were 56.1% and 75% vs. 26.3% and 53.7% in the control group); besides, most patients were well tolerated with no grade 3 or high adverse effects (AEs) occurred.

2.5.2 Internal RT

Localized implantation with radioactive seeds such as iodine-125 and iodine-131 is a form of internal RT. Between 1999 to 2014, a total of 4 RCTs evaluated the value of iodine-125 or iodine-131 as an adjuvant treatment after radical surgery for HCC, however, these studies did not reach consistent conclusions as well. Two studies concluded that adjuvant iodine-125 and iodine-131 was helpful in improving DFS and OS (68–70), one study concluded that adjuvant iodine-131 was effective in preventing postoperative recurrence but did not prolong OS (71), and one concluded that adjuvant iodine-131 did not influence the survival prognosis (72). Because of the controversial results, iodine-125 and iodine-131 have also been used less frequently in recent years, and relevant studies are lacking. Iodine-131-labelled metuximab is a radiolabeled monoclonal antibody block the CD147 antigen which is associated with a greater susceptibility to metastasis and a worse prognosis for patients with HCC. Li et al. (73) explored its role as an adjuvant therapy for patients with CD147 expression after LR, patients who received adjuvant Iodine-131-labelled metuximab had significantly better DFS and OS compared LR alone (the 5-years DFS and OS rates were 43.4% and 61.3% vs. 21.7% and 35.9%). In the subgroup analysis of this study, patients with high-risk recurrence factors (a solitary tumor of any size with microvascular invasion, satellite nodules, poor differentiation, or two to three nodules) had a significantly better survival prognosis in the adjuvant group than in the control group, whereas no difference in survival prognosis was observed in the intermediate-risk group.

2.6 Immunotherapy

Immunotherapies, including lymphocyte infusions, cytokineinduced killer cells (CIK), natural killer cells, tumor

vaccines, and ICIs et al. can recognize and kill immune escape tumor cells by regulating or enhancing autoimmune function (74). Immunotherapy has changed the paradigm of human cancer treatment with potent and durable anti-tumor activity in a subset of patients. Many RCTs have evaluated the effectiveness of adjuvant immunotherapy for HCC following LR. In 2000, the first RCT to evaluate immunotherapy as an adjuvant treatment for postoperative HCC released the results, patients who received adjuvant lymphocyte infusions had significant longer DFS compared with placebo (75). Since then, adjuvant immunotherapy was once a hope. A total of 4 RCTs between 2009 and 2016 explored the effectiveness of CIK as an adjuvant treatment after LR, however, these studies did not reach consistent conclusions. Three studies found that adjuvant CIK was helpful in improving postoperative prognosis (76–78); one study, however, discovered that CIK did not prolong postoperative DFS and OS (79).

In recent years, ICIs have made a breakthrough in the treatment of advanced-stage HCC (80, 81). Theoretically, restoring the body's antitumor cellular immune function is helpful in reducing recurrence after surgery and prolonging the survival time (82). Masatoshi Kudo et al. (83) evaluated the efficacy and safety of adjuvant nivolumab after LR or ablation for HCC in a single-arm study, the median DFS was 26.3 months and the AEs was manageable. And Chen et al. (84) revealed the value of PD-1 inhibitors as adjuvant therapy in a recent cohort study, where patients had significantly better DFS than controls (After PSM, the 2-year DFS was 44.1% vs 21.3%). Similarly, some studies found that adjuvant PD-1 inhibitors also helpful in prolonging DFS for other cancers following surgery such as melanoma, esophageal, and gastroesophageal tumors (85, 86). No relevant RCT study data have been reported on adjuvant PD-1 inhibitors following curative surgery. Besides, the low response rate to PD-1 inhibitors is an important issue to be addressed, and gene sequencing or biomarkers that can predict patient response to PD-1 inhibitors may help identify those patients who are better suited for adjuvant therapy. In addition, there are two issues that should be noted. One is that ICIs may lead to HBV reactivation (87), if ICIs is assisted, regular monitoring for hepatitis B virus and concomitant antiviral treatment is necessary. The other is that ICIs are not commonly used in the perioperative period of LT due to concerns about increased immune rejection. Xie et al. (88) considered that ICIs are not ideal for controlling disease recurrence or *de novo* carcinoma after LT; the immune rejection occurred in 31.9% of patients, with a median OS of only 6.5 months and a mortality rate of 61.7%. In contrast, a meta-analysis of ICIs treatment in solid organ transplant recipients found that approximately 35% of patients faced immune rejection after LT, but this was not the most common cause of death (89). Therefore, adjuvant ICIs after LT should be approached with caution due to the lack of enough evidence.

2.7 Combined adjuvant therapy

Postoperative prophylactic TACE or HAIC through angiography can sometimes detect suspicious residual lesions, but it is often powerless for tumor cells shed by intraoperative manipulation and residual tumor cells in the cut edge or blood vessels. This is the reason for carrying out combined adjuvant therapy. Chen et al. (90) explored the feasibility of TACE plus lenvatinib in a multicenter prospective cohort study that screened patients with high risk factors for recurrence to compared the prognosis of receiving combined adjuvant therapy with TACE alone, and the preliminary results are satisfactory (the median DFS was 17.1 months vs. 9 months). There are several well-designed RCTs underway to explore the effectiveness of TACE combined with anti-angiogenic drugs to prevent tumor recurrence (Table 1).

ICIs is the dawn of malignancy treatment in recent years, but has failed successively in phase III trials in advanced HCC (91, 92). Some recent studies found that anti-angiogenic drugs such as TKIs may have synergistic effects with PD-1 inhibitors. TKIs can not only improve antitumor immune responses by modulating macrophages and myeloid-derived suppressor cells to enhance effector T cell responses, but also help to increase the expression of *PD-1* on T cells, thus promoting the action of PD-1 inhibitors (93, 94). Atezolizumab plus bevacizumab (95), Lenvatinib plus Pembrolizumab (81), and Lenvatinib plus Nivolumab (96) et al. have demonstrated stronger anti-tumor effects than single agents in advanced HCC. Xia et al. conducted a single-arm phase 2 study exploring the efficacy and safety of perioperative adjuvant camrelizumab plus apatinib for resectable HCC (97), the 1-year DFS rate of the enrolled patients was 53.85%. In addition, a small RCT including 32 patients conducted buy Zhao et al. (98) published preliminary results in 2021, which confirmed the superiority of camrelizumab plus apatinib compared with HAIC as adjuvant therapy in patients with high-risk recurrence factors following LR (the median DFS was not reached vs. 10.5 months). There are a number of ongoing trials that will more fully evaluate the feasibility of combined adjuvant therapy, such as IMbrave 050 trial, which evaluate atezolizumab plus bevacizumab as adjuvant therapy for high-risk HCC after curative resection or ablation (Table 1).

3 Discussion

The high early recurrence rate greatly affects the overall outcome of surgical treatment of HCC, forcing scholars from various countries to continuously explore effective adjuvant treatment strategies. Unfortunately, the currently available regimens are either unsatisfactory in terms of efficacy, controversial in terms of study results, or lack of high-grade evidence. There is still no standard adjuvant treatment protocol worldwide. In reviewing published studies on various adjuvant treatment strategies, it is easy to see that people with high-risk recurrence factors may be better suited for adjuvant therapy, and that combined adjuvant therapy may be more effective than monotherapy. Based on the stratification of risk factors for recurrence, we summarized the improvement of prognosis with current adjuvant treatment options and the sources of evidence (Table 2), and a picture was drawn to guide the rapid search for appropriate adjuvant treatment strategies (Figure 1). However, two issues are worth noting, one is what exactly is a "high-risk" recurrence factor, and the other is whether the safety of combined adjuvant therapy is acceptable.

Although many studies have used "high-risk factors" or "intermediate-risk factors" to select appropriate candidates for

TABLE 1 Summary of important ongoing trials on PD-1, and various combination therapies as adjuvant therapy following LR or ablation.

Study ID/Type	Clinicaltrials.gov ID	Eligible patients	Interventions	Primary endpoint
CheckMate9DX (RCT)	NCT03383458	Received LR or ablation and with high-risk factors for recurrence	Nivolumab vs. placebo	DFS
KEYNOTE-937 (RCT)	NCT03867084	Received curative LR or ablation	Pembrolizumab vs. placebo	DFS and OS
JUPITER 04 (RCT)	NCT03859128	Received R0 resection and with high-risk factors for recurrence	Toripalimab vs. placebo	DFS
None (RCT)	NCT05489289	Received LR and with high-risk factors for recurrence	AK104 (anti PD-1/CTLA-4) vs. placebo	DFS
None (RCT)	NCT05240404	Recurrent HCC and received thermal ablation	Toripalimab vs. placebo	DFS
EMERALD-2 (RCT)	NCT03847428	Received curative LR or ablation	Durvalumab + bevacizumab vs. durvalumab + placebo vs. placebo	DFS
IMbrave050 (RCT)	NCT04102098	Received LR or ablation and with high-risk factors for recurrence	Atezolizumab + bevacizumab vs. no intervention	DFS
A-TACE/S-HCC (RCT)	NCT02436902	Received curative LR and with MVI	Sorafenib + TACE vs. no intervention	OS
SOURCE (RCT)	NCT04143191	Received curative LR with resectable advanced HCC	Sorafenib + TACE vs. sorafenib	DFS
DaDaLi (RCT)	NCT04682210	Received curative LR and with high-risk factors for recurrence	Sintilimab + bevacizumab vs. no intervention	DFS
None (RCT)	NCT04639180	Received LR or ablation and with high-risk factors for recurrence	Camrelizumab + apatinib vs. no intervention	DFS
None (RCT)	NCT05367687	Received curative LR or ablation and with high-risk factors for recurrence	Camrelizumab + apatinib vs. camrelizumab	DFS
None (RCT)	NCT05161143	Received LR and with high-risk factors for recurrence	Donafenib + TACE vs. donafenib	DFS
None (RCT)	NCT03839550	Received LR and with high-risk factors for recurrence	Camrelizumab + apatinib vs. HAIC	DFS
None (RCT)	NCT05564338	Received LR and with high-risk factors for recurrence	Sitravatinib + tislelizumab or Placebo + Tislelizumab vs. Placebo	DFS
LANCE (Non-RCT)	NCT03838796	Received LR and with high-risk factors for recurrence	Lenvatinib + TACE vs. TACE	DFS
Y-D202001-0289 (Non-RCT)	NCT05307926	Received curative LR and with high-risk factors for recurrence	Sintilimab + Lenvatinib or sintilimab vs. TACE	DFS
None (Single arm)	NCT04962958	Received LR and with high-risk factors for recurrence	Donafenib + HAIC	DFS
None (Single arm)	NCT05161143	Received LR and with high-risk factors for recurrence	Donafenib + TACE	DFS
ICMJE A (Single arm)	NCT04981665	Received curative LR and with high-risk factors for recurrence	Tislelizumab + TACE	DFS
EMPHASIS (Single arm)	NCT05516628	Received R0 resection and with high-risk factors for recurrence	Atezolizumab + bevacizumab	DFS
CISLD-8 (Single arm)	NCT04418401	Received curative LR and with high-risk factors for recurrence	Donafenib + anti-PD-1 antibody	DFS
ALTER-H006 (Single arm)	NCT05111366	Received R0 resection and with high-risk factors for recurrence	TQB2450(PD L-1) + Anlotinib	DFS
None (Single arm)	NCT05545124	Received R0 resection and with high-risk factors for recurrence	Donafenib + Tislelizumab	DFS
None (Single arm)	NCT05311319	Received curative LR and with high-risk factors for recurrence	Anlotinib + HAIC+ TQB2450	DFS

LR, liver resection; OS, overall survival; DFS, disease-free survival; BCLC, Barcelona Liver Cancer Clinic; PD-1, programmed death protein 1 inhibitors; TACE, transarterial chemoembolization; RCT, randomized controlled trials; HAIC, hepatic artery infusion chemotherapy.

10.3389/fonc.2023.1098958

TABLE 2 Current adjuvant therapy options, improvement in prognosis, and the level of evidence.

Adjuvant therapy options			Eligible patients	Interventions	Improvement of prognosis	Evidence
Antiviral therapy	Oral antiviral drugs	Telbivudine	HBV-related HCC (LR)	Telbivudine vs. no	DFS and OS	RCT (25)
		Adefovir	HBV-related HCC (LR)	Adefovir vs. no	DFS and OS	RCT (22)
		Tenofovir	HBV-related HCC (LR)	Tenofovir vs. entecavir	DFS and OS	R-Cohort (26)
	Interferon	Interferon alpha	HBV-related HCC (LR)	Interferon alpha vs. no	OS	RCT (31)
		Interferon alpha	HCV-related HCC (LR)	Interferon alpha vs. no	DFS	RCTs (32, 33)
Anti-angiogenic drugs		Sorafenib	BCLC-C stage (LR)	Sorafenib vs. no	DFS and OS	R-Cohort (18, 39)
		Sorafenib	MVI-positive (LR)	Sorafenib vs. no	DFS and OS	R-Cohort (19)
		Lenvatinib	HBV-related HCC and MVI-positive (LR)	Lenvatinib vs. no	DFS and OS	R-Cohort (42)
		Lenvatinib	High residual alpha-fetoprotein (LR or ablation)	Lenvatinib vs. TACE vs.no	DFS	R-Cohort (20)
Traditional Chinese medicine		Huaier granules	BCLC stage A or B (LR)	Huaier granules vs. no	DFS and OS	RCT (23)
		Huaier granules	Early-stage HCC (ablation)	Huaier granules vs. no	DFS	R-Cohort (45)
		Huaier granules	BCLC stage A or B (LR)	Huaier granules vs. no	DFS and OS	R-Cohort (46)
		THM	Solitary HCC <5 cm (LR)	THMvs. TACE	DFS and OS	RCT (48)
Locoregional therapy		TACE	MVI and tumor diameter ≥5cm (LR)	TACE vs. no	DFS and OS	RCT (55)
		TACE	Tumor diameter ≥5cm with MVI, or multiple tumors (LR)	TACE vs. no	DFS and OS	RCT (21)
		HAIC	MVI and/or intrahepatic metastases (LR)	HAIC vs. no	DFS	RCT (49)
		HAIC	MVI-positive (LR)	HAIC vs. no	DFS and OS	RCT (58)
Radiotherapy	External RT	RT	Narrow or positive surgical margins (LR)	RT vs. no	DFS and OS	R-Cohort (63)
		IMRT	PVTT (LR)	IMRT vs. no	DFS and OS	RCT (65)
		SBRT	MVI-positive (LR)	SBRT vs.no	DFS and OS	RCT (67)
	Internal RT	Iodine-131	Grades I–III according to Okuda staging system (LR)	Iodine-131 vs. no	DFS and OS	RCT (68, 69)
		Iodine-131	Curative surgery (LR or ablation)	Iodine-131 vs. unlabeled lipiodol	DFS	RCT (71)
		Iodine-125	Without vascular/bile duct invasion, tumor nodules ≤ 3(LR)	Iodine-125 vs. no	DFS and OS	RCT (70)
		Iodine-131-labelled metuximab	No macroscopic vascular invasion or extrahepatic distant metastasis and positive CD147 expression (LR)	Iodine-131-labelled metuximab vs.no	DFS and OS	RCT (73)
Immunotherapy		Lymphocyte infusions	Stage I, II, IIIA, or IVA according to UICC TNM staging system (LR)	lymphocyte infusions vs. no	DFS	RCT (75)
		CIK	Received curative treatment (LR or ablation or percutaneous ethanol injection)	CIK vs. no	DFS and OS	RCT (76)
		CIK	Resection margin >1 cm, no tumor fracture and hemorrhage, and no tumor distant metastases (LR)	CIK vs. no	DFS	RCT (77)

(Continued)

TABLE 2 Continued

Adjuvant therapy options			Eligible patients	Interventions	Improvement of prognosis	Evidence
		CIK	BCLC stage A, B or C (LR)	CIK vs. no	DFS	RCT (78)
		Nivolumab	Received curative treatment (LR or ablation)	Nivolumab	/	Single-arm (83)
		PD-1 inhibitors	MVI, PVTT, satellite nodules, multiple tumors et al. (LR)	PD-1 inhibitors vs. no	DFS and OS	P-Cohort (84)
Combined adjuvant therapy		TACE plus Lenvatinib	With macrovascular or bile duct invasion, or MVI alone with multiple tumors et al. (LR)	TACE plus Lenvatinib vs. TACE	DFS and OS	P-Cohort (90)
		Camrelizumab plus apatinib	With PVTT, MVI, or microsatellites (LR)	Camrelizumab plus apatinib vs. HAIC	DFS and OS	RCT (98)

LR, liver resection; OS, overall survival; DFS, disease-free survival; BCLC, Barcelona Liver Cancer Clinic; MVI, microvascular invasion; TACE, transarterial chemoembolization; RCT, randomized controlled trials; HBV, hepatitis B virus; HCV, hepatitis C virus; THM, traditional herbal medicine; HAIC, hepatic artery infusion chemotherapy; RT, radiotherapy; IMRT, intensity modulated radiotherapy; PVTT, portal vein tumor thrombosis; SBRT, stereotactic body radiotherapy; CIK, cytokine induced killer cells; PD-1, programmed death protein 1 inhibitors; R-Cohort, retrospective cohort study; P-Cohort, prospective cohort study.

adjuvant therapy, there is also a lack of standardized criteria for stratifying the risk of recurrence. The STORM trial incorporated tumor characteristics and pathology reports into the risk level assessment, with high risk recurrence factors including one tumor of any size plus microvascular invasion, satellite tumors, poorly differentiated, or two or three tumors each 3 cm or smaller in size (38). However, many patients with BCLC-stage B or C HCC also underwent radical surgery in some regions, so multiple tumors larger than 3 cm (BCLC-B) and PVTT(BCLC-C) should also been included in high-risk factors. The presence of high-risk recurrence factors means a higher probability of residual tumor in the liver, which is a key factor leading to early recurrence. Effective elimination of residual tumor or prevention of intrahepatic metastasis through postoperative adjuvant therapy will help to reduce early recurrence, which may be one of the reasons why adjuvant therapy is more appropriate for patients with high-risk recurrence factors.

Since the breakthrough of combination therapy in advanced HCC, investigators have not stopped exploring postoperative combined adjuvant therapy. However, the safety of adjuvant therapy cannot be ignored, and whether the remaining liver after LR can withstand the AEs of combined adjuvant therapy also needs to be taken into consideration. In reports of camrelizumab in combination with apatinib for advanced HCC, 77.4% of patients experienced grade ≥ 3 AEs, 28.9% experienced serious AEs, and 2 died (99). In reports of lenvatinib plus pembrolizumab for advanced HCC, 67% of patients experienced grade ≥ 3 AEs, and 3% experienced grade 5 AEs (81). And in the IMbrave 150 study that atezolizumab-bevacizumab caused 56.5% of patients to experience grade 3 or 4 AEs (80). Hypertension and hepatic impairment are the most common AEs. A recent meta-analysis concluded that fatigue, hypertension, and hyperbilirubinemia were more common after combination therapy (100). Triple therapy such as TACE or HAIC combined with TKIs and ICIs has also achieved promising results in

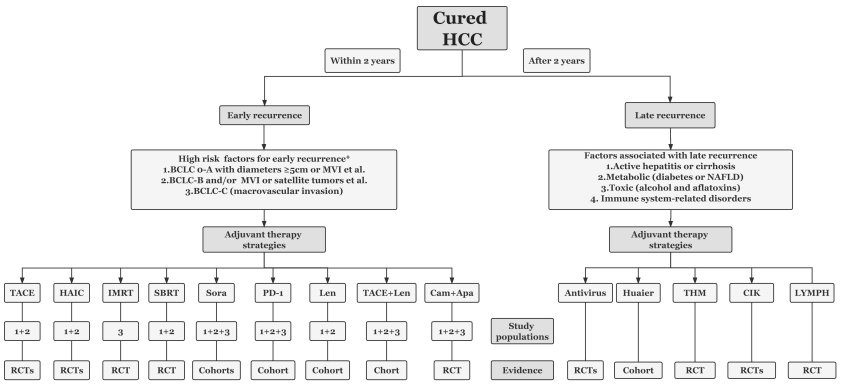

FIGURE 1
A quick overview of available adjuvant treatment strategies for populations with different risk factors for recurrence. *There are no standardized criteria for high-risk recurrence factors which generally determined by tumor characteristics and highly aggressive pathological features, and highly aggressive pathological features generally refer to poor differentiation, satellite lesions, and microvascular invasion. TACE, transarterial chemoembolization; HAIC, hepatic artery infusion chemotherapy; IMRT, intensity modulated radiotherapy; SBRT, stereotactic body radiotherapy; Sora, sorafenib; PD-1, programmed death protein 1 inhibitors; Len, Lenvatinib; Cam, camrelizumab; Apa, apatinib; NAFLD, non-alcoholic fatty liver disease; THM, traditional herbal medicine; Huaier, huaier granules; CIK, cytokine induced killer cells; LYMPH, lymphocyte infusions.

the treatment of advanced HCC, but AEs is a more important issue to be aware of. A recent meata analysis of triple therapy suggests that triple therapy is more likely to cause liver function abnormalities and that some potential AEs cannot be evaluated (101). Patients who have undergone surgical trauma have fragile liver function, especially for patients with severe cirrhosis, postoperative adjuvant therapy should not be used blindly as combination therapy or interventional therapy in pursuit of efficacy alone. Tolerability should be assessed more thoroughly when trying new combination regimens, and more regular follow-up is needed. Low response rate is also an urgent issue to be tackled, it makes sense to look for markers that can differentiate the responding population. Previous studies have found that PD-L1 expression, tumor mutation burden and lymphocyte-neutrophil ratio have potential value in differentiating responding populations (102, 103). In addition, extra attention needs to be paid to the fact that drug abuse may cause drug resistance, and resistance to systemic drugs such as sorafenib is now widespread (104).

Overall, the indications for adjuvant therapy should be strictly grasped, and appropriate adjuvant treatment measures should be taken for those with high-risk factors for recurrence. Reasonable stratification of recurrence factors still requires ongoing exploration, and uniform criteria will help in the management of postoperative adjuvant therapy in different regions. Many important ongoing studies are presented in Table 2, so keep an eye on the results of these studies and look forward to taking postoperative adjuvant therapy to the next level.

Author contributions

BG design of the work, drafting the article. QC design charts, critical revision of the article. ZL critical revision of the article. XC critical revision of the article. PZ design of the work, critical revision of the article, final review of the article. All authors contributed to the article and approved the submitted version.

Acknowledgments

None.

Conflict of interest

The authors declare that the research was conducted in the absence of any commercial or financial relationships that could be construed as a potential conflict of interest.

Publisher's note

References

1. Sung H, Ferlay J, Siegel RL, Laversanne M, Soerjomataram I, Jemal A, et al. Global cancer statistics 2020: GLOBOCAN estimates of incidence and mortality worldwide for 36 cancers in 185 countries. *CA Cancer J Clin* (2021) 71(3):209–49. doi: 10.3322/caac.21660

2. McGlynn KA, Petrick JL, El-Serag HB. Epidemiology of hepatocellular carcinoma. *Hepatology* (2021) 73 Suppl 1(Suppl 1):4–13. doi: 10.1002/hep.31288

3. Marrero JA, Kulik LM, Sirlin CB, Zhu AX, Finn RS, Abecassis MM, et al. Diagnosis, staging, and management of hepatocellular carcinoma: 2018 practice guidance by the American association for the study of liver diseases. *Hepatology* (2018) 68(2):723–50. doi: 10.1002/hep.29913

4. Reig M, Forner A, Rimola J, Ferrer-Fàbrega J, Burrel M, Garcia-Criado Á, et al. BCLC strategy for prognosis prediction and treatment recommendation: the 2022 update. *J Hepatol* (2022) 76(3):681–93. doi: 10.1016/j.jhep.2021.11.018

5. Omata M, Cheng AL, Kokudo N, Kudo M, Lee JM, Jia J, et al. Asia-Pacific clinical practice guidelines on the management of hepatocellular carcinoma: a 2017 update. *Hepatol Int* (2017) 11(4):317–70. doi: 10.1007/s12072-017-9799-9

6. Lu J, Zhang XP, Zhong BY, Lau WY, Madoff DC, Davidson JC, et al. Management of patients with hepatocellular carcinoma and portal vein tumour thrombosis: comparing east and west. *Lancet Gastroenterol Hepatol* (2019) 4(9):721–30. doi: 10.1016/S2468-1253(19)30178-5

7. Yin J, Bo WT, Sun J, Xiang X, Lang JY, Zhong JH, et al. New evidence and perspectives on the management of hepatocellular carcinoma with portal vein tumor thrombus. *J Clin Transl Hepatol* (2017) 5(2):169–76. doi: 10.14218/jcth.2016.00071

8. Wang K, Guo WX, Chen MS, Mao YL, Sun BC, Shi J, et al. Multimodality treatment for hepatocellular carcinoma with portal vein tumor thrombus: a Large-scale, multicenter, propensity mathching score analysis. *Med (Baltimore)* (2016) 95(11): e3015. doi: 10.1097/MD.0000000000003015

9. China NHCotPsRo. Guidelines for the treatment of primary liver cancer (2022 edition). *Chin J Surg* (2022) 60(04):273–309. doi: 10.3760/cma.j.cn112139-2022-02-17-00068

10. Lee KF, Chong CCN, Fong AKW, Fung AKY, Lok HT, Cheung YS, et al. Pattern of disease recurrence and its implications for postoperative surveillance after curative hepatectomy for hepatocellular carcinoma: experience from a single center. *Hepatobil Surg Nutr* (2018) 7(5):320–30. doi: 10.21037/hbsn.2018.03.17

11. Lee S, Kang TW, Song KD, Lee MW, Rhim H, Lim HK, et al. Effect of microvascular invasion risk on early recurrence of hepatocellular carcinoma after surgery and radiofrequency ablation. *Ann Surg* (2021) 273(3):564–71. doi: 10.1097/SLA.0000000000003268

12. Portolani N, Coniglio A, Ghidoni S, Giovanelli M, Benetti A, Tiberio GA, et al. Early and late recurrence after liver resection for hepatocellular carcinoma: prognostic and therapeutic implications. *Ann Surg* (2006) 243(2):229–35. doi: 10.1097/01.sla.0000197706.21803.a1

13. Erstad DJ, Tanabe KK. Prognostic and therapeutic implications of microvascular invasion in hepatocellular carcinoma. *Ann Surg Oncol* (2019) 26 (5):1474–93. doi: 10.1245/s10434-019-07227-9

14. Xu XF, Xing H, Han J, Li ZL, Lau WY, Zhou YH, et al. Risk factors, patterns, and outcomes of late recurrence after liver resection for hepatocellular carcinoma: a multicenter study from China. *JAMA Surg* (2019) 154(3):209–17. doi: 10.1001/jamasurg.2018.4334

15. Chen ZH, Zhang XP, Feng JK, Li LQ, Zhang F, Hu YR, et al. Patterns, treatments, and prognosis of tumor recurrence after resection for hepatocellular carcinoma with microvascular invasion: a multicenter study from china. HPB. *(Oxford)* (2022) 24(7):1063–73. doi: 10.1016/j.hpb.2021.11.016

16. Zhu XD, Li KS, Sun HC. Adjuvant therapies after curative treatments for hepatocellular carcinoma: current status and prospects. *Genes Dis* (2020) 7(3):359–69. doi: 10.1016/j.gendis.2020.02.002

17. Liu Y, Wang Y, Guo X, He Y, Zhou J, Lv Q, et al. Comparative effectiveness of adjuvant treatment for resected hepatocellular carcinoma: a systematic review and network meta-analysis. *Front Oncol* (2021) 11:709278. doi: 10.3389/fonc.2021.709278

18. Xia F, Wu LL, Lau WY, Huan HB, Wen XD, Ma KS, et al. Adjuvant sorafenib after heptectomy for Barcelona clinic liver cancer-stage c hepatocellular carcinoma patients. *World J Gastroenterol* (2016) 22(23):5384–92. doi: 10.3748/wjg.v22.i23.5384

19. Zhang XP, Chai ZT, Gao YZ, Chen ZH, Wang K, Shi J, et al. Postoperative adjuvant sorafenib improves survival outcomes in hepatocellular carcinoma patients with microvascular invasion after R0 liver resection: a propensity score matching analysis. *HPB (Oxford)* (2019) 21(12):1687–96. doi: 10.1016/j.hpb.2019.04.014

20. Cai L, Li H, Guo J, Zhao W, Li Y, Duan Y, et al. Effect of adjuvant lenvatinib (LEN) on tumour recurrence in patients with hepatocellular carcinoma (HCC) and high residual alpha-fetoprotein (AFP) following resection or ablation: a single-center, retrospective study. *Ann Oncol* (2020) 31:S1308–S. doi: 10.1016/j.annonc.2020.10.197

21. Wang Z, Ren Z, Chen Y, Hu J, Yang G, Yu L, et al. Adjuvant transarterial chemoembolization for HBV-related hepatocellular carcinoma after resection: a randomized controlled study. *Clin Cancer Res* (2018) 24(9):2074–81. doi: 10.1158/1078-0432.CCR-17-2899

22. Huang G, Lau WY, Wang ZG, Pan ZY, Yuan SX, Shen F, et al. Antiviral therapy improves postoperative survival in patients with hepatocellular carcinoma: a randomized controlled trial. *Ann Surg* (2015) 261(1):56–66. doi: 10.1097/SLA.0000000000000858

23. Chen Q, Shu C, Laurence AD, Chen Y, Peng BG, Zhen ZJ, et al. Effect of huaier granule on recurrence after curative resection of HCC: a multicentre, randomised clinical trial. *Gut* (2018) 67(11):2006–16. doi: 10.1136/gutjnl-2018-315983

24. Sarin SK, Kumar M, Lau GK, Abbas Z, Chan HL, Chen CJ, et al. Asian-Pacific clinical practice guidelines on the management of hepatitis b: a 2015 update. *Hepatol Int* (2016) 10(1):1–98. doi: 10.1007/s12072-015-9675-4

25. Huang G, Li PP, Lau WY, Pan ZY, Zhao LH, Wang ZG, et al. Antiviral therapy reduces hepatocellular carcinoma recurrence in patients with low HBV-DNA levels: a randomized controlled trial. *Ann Surg* (2018) 268(6):943–54. doi: 10.1097/SLA.0000000000002727

26. Choi J, Jo C, Lim YS. Tenofovir versus entecavir on recurrence of hepatitis b virus-related hepatocellular carcinoma after surgical resection. *Hepatology* (2021) 73(2):661–73. doi: 10.1002/hep.31289

27. Rich NE, Yang JD, Perumalswami PV, Alkhouri N, Jackson W, Parikh ND, et al. Provider attitudes and practice patterns for direct-acting antiviral therapy for patients with hepatocellular carcinoma. *Clin Gastroenterol Hepatol* (2020) 18(4):974–83. doi: 10.1016/j.cgh.2019.07.042

28. Sapena V, Enea M, Torres F, Celsa C, Rios J, Rizzo GEM, et al. Hepatocellular carcinoma recurrence after direct-acting antiviral therapy: an individual patient data meta-analysis. *Gut* (2022) 71(3):593–604. doi: 10.1136/gutjnl-2020-323663

29. Chen LT, Chen MF, Li LA, Lee PH, Jeng LB, Lin DY, et al. Long-term results of a randomized, observation-controlled, phase III trial of adjuvant interferon Alfa-2b in hepatocellular carcinoma after curative resection. *Ann Surg* (2012) 255(1):8–17. doi: 10.1097/SLA.0b013e3182363ff9

30. Lo CM, Liu CL, Chan SC, Lam CM, Poon RT, Ng IO, et al. A randomized, controlled trial of postoperative adjuvant interferon therapy after resection of hepatocellular carcinoma. *Ann Surg* (2007) 245(6):831–42. doi: 10.1097/01.sla.0000245829.00977.45

31. Sun HC, Tang ZY, Wang L, Qin LX, Ma ZC, Ye QH, et al. Postoperative interferon alpha treatment postponed recurrence and improved overall survival in patients after curative resection of HBV-related hepatocellular carcinoma: a randomized clinical trial. *J Cancer Res Clin Oncol* (2006) 132(7):458–65. doi: 10.1007/s00432-006-0091-y

32. Mazzaferro V, Romito R, Schiavo M, Mariani L, Camerini T, Bhoori S, et al. Prevention of hepatocellular carcinoma recurrence with alpha-interferon after liver resection in HCV cirrhosis. *Hepatology* (2006) 44(6):1543–54. doi: 10.1002/hep.21415

33. Kubo S, Nishiguchi S, Hirohashi K, Tanaka H, Shuto T, Yamazaki O, et al. Effects of long-term postoperative interferon-alpha therapy on intrahepatic recurrence after resection of hepatitis c virus-related hepatocellular carcinoma. a randomized, controlled trial. *Ann Intern Med* (2001) 134(10):963–7. doi: 10.7326/0003-4819-134-10-200105150-00010

34. Xu J, Li J, Chen J, Liu ZJ. Effect of adjuvant interferon therapy on hepatitis b/c virus-related hepatocellular carcinoma after curative therapy - meta-analysis. *Adv Clin Exp Med* (2015) 24(2):331–40. doi: 10.17219/acem/29760

35. Hu B, Yu M, Ma X, Sun J, Liu C, Wang C, et al. IFNα potentiates anti-PD-1 efficacy by remodeling glucose metabolism in the hepatocellular carcinoma microenvironment. *Cancer Discovery* (2022) 12(7):1718–41. doi: 10.1158/2159-8290.CD-21-1022

36. Zhu Y, Chen M, Xu D, Li TE, Zhang Z, Li JH, et al. The combination of PD-1 blockade with interferon-α has a synergistic effect on hepatocellular carcinoma. *Cell Mol Immunol* (2022) 19(6):726–37. doi: 10.1038/s41423-022-00848-3

37. Tada T, Kumada T, Hiraoka A, Michitaka K, Atsukawa M, Hirooka M, et al. Safety and efficacy of lenvatinib in elderly patients with unresectable hepatocellular carcinoma: a multicenter analysis with propensity score matching. *Hepatol Res* (2020) 50(1):75–83. doi: 10.1111/hepr.13427

38. Bruix J, Takayama T, Mazzaferro V, Chau G-Y, Yang J, Kudo M, et al. Adjuvant sorafenib for hepatocellular carcinoma after resection or ablation (STORM): a phase 3, randomised, double-blind, placebo-controlled trial. *Lancet Oncol* (2015) 16(13):1344–54. doi: 10.1016/S1470-2045(15)00198-9

39. Li J, Hou Y, Cai XB, Liu B. Sorafenib after resection improves the outcome of BCLC stage c hepatocellular carcinoma. *World J Gastroenterol* (2016) 22(15):4034–40. doi: 10.3748/wjg.v22.i15.4034

40. Li Z, Gao J, Zheng SM, Wang Y, Xiang X, Cheng Q, et al. The efficacy of sorafenib in preventing hepatocellular carcinoma recurrence after resection: a systematic review and meta-analysis. *Rev Esp Enferm Dig* (2020) 112(3):201–10. doi: 10.17235/reed.2020.6458/2019

41. Vogel A, Qin S, Kudo M, Su Y, Hudgens S, Yamashita T, et al. Lenvatinib versus sorafenib for first-line treatment of unresectable hepatocellular carcinoma: patient-reported outcomes from a randomised, open-label, non-inferiority, phase 3 trial. *Lancet Gastroenterol Hepatol* (2021) 6(8):649–58. doi: 10.1016/S2468-1253(21)00110-2

42. Bai S, Hu L, Liu J, Sun M, Sun Y, Xue F. Prognostic nomograms combined adjuvant lenvatinib for hepatitis b virus-related hepatocellular carcinoma with microvascular invasion after radical resection. *Front Oncol* (2022) 12:919824. doi: 10.3389/fonc.2022.919824

43. Li C, Wu X, Zhang H, Yang G, Hao M, Sheng S, et al. A huaier polysaccharide restrains hepatocellular carcinoma growth and metastasis by suppression angiogenesis. *Int J Biol Macromol* (2015) 75:115–20. doi: 10.1016/j.ijbiomac.2015.01.016

44. Shan L, Li Y, Jiang H, Tao Y, Qian Z, Li L, et al. Huaier restrains proliferative and migratory potential of hepatocellular carcinoma cells partially through decreased yes-associated protein 1. *J Cancer* (2017) 8(19):4087–97. doi: 10.7150/jca.21018

45. Wang Z, Yu XL, Zhang J, Cheng ZG, Han ZY, Liu FY, et al. Huaier granule prevents the recurrence of early-stage hepatocellular carcinoma after thermal ablation: a cohort study. *J Ethnopharmacol* (2021) 281:114539. doi: 10.1016/j.jep.2021.114539

46. Luo S, Hu H. Huaier granule prolongs overall survival after curative resection of hepatocarcinoma carcinoma: a propensity score analysis. *J Ethnopharmacol* (2022) 115774. doi: 10.1016/j.jep.2022.115774

47. Zhai XF, Chen Z, Li B, Shen F, Fan J, Zhou WP, et al. Traditional herbal medicine in preventing recurrence after resection of small hepatocellular carcinoma: a multicenter randomized controlled trial. *J Integr Med* (2013) 11(2):90–100. doi: 10.3736/jintegrmed2013021

48. Zhai XF, Liu XL, Shen F, Fan J, Ling CQ. Traditional herbal medicine prevents postoperative recurrence of small hepatocellular carcinoma: a randomized controlled study. *Cancer* (2018) 124(10):2161–8. doi: 10.1002/cncr.30915

49. Izumi R, Shimizu K, Iyobe T, Ii T, Yagi M, Matsui O, et al. Postoperative adjuvant hepatic arterial infusion of lipiodol containing anticancer drugs in patients with hepatocellular carcinoma. *Hepatology* (1994) 20(2):295–301. doi: 10.1002/hep.1840200205

50. Li JQ, Zhang YQ, Zhang WZ, Yuan YF, Li GH. Randomized study of chemoembolization as an adjuvant therapy for primary liver carcinoma after hepatectomy. *J Cancer Res Clin Oncol* (1995) 121(6):364–6. doi: 10.1007/BF01225689

51. Zhong C, Guo RP, Li JQ, Shi M, Wei W, Chen MS, et al. A randomized controlled trial of hepatectomy with adjuvant transcatheter arterial chemoembolization versus hepatectomy alone for stage III a hepatocellular carcinoma. *J Cancer Res Clin Oncol* (2009) 135(10):1437–45. doi: 10.1007/s00432-009-0588-2

52. Peng BG, He Q, Li JP, Zhou F. Adjuvant transcatheter arterial chemoembolization improves efficacy of hepatectomy for patients with hepatocellular carcinoma and portal vein tumor thrombus. *Am J Surg* (2009) 198(3):313–8. doi: 10.1016/j.amjsurg.2008.09.026

53. Li Q, Wang J, Sun Y, Cui YL, Juzi JT, Qian BY, et al. Postoperative transhepatic arterial chemoembolization and portal vein chemotherapy for patients with hepatocellular carcinoma: a randomized study with 131 cases. *Dig Surg* (2006) 23(4):235–40. doi: 10.1159/000095396

54. Zhang W, Zhang B, Chen XP. Adjuvant treatment strategy after curative resection for hepatocellular carcinoma. *Front Med* (2021) 15(2):155–69. doi: 10.1007/s11684-021-0848-3

55. Wei W, Jian PE, Li SH, Guo ZX, Zhang YF, Ling YH, et al. Adjuvant transcatheter arterial chemoembolization after curative resection for hepatocellular carcinoma patients with solitary tumor and microvascular invasion: a randomized clinical trial of efficacy and safety. *Cancer Commun (Lond)* (2018) 38(1):61. doi: 10.1186/s40880-018-0331-y

56. Chen W, Ma T, Zhang J, Zhang X, Chen W, Shen Y, et al. A systematic review and meta-analysis of adjuvant transarterial chemoembolization after curative resection for patients with hepatocellular carcinoma. *HPB (Oxford)* (2020) 22(6):795–808. doi: 10.1016/j.hpb.2019.12.013

57. Huang SX, Wu YL, Tang CW, Feng WM, Xu YQ, Bao Y, et al. Prophylactic hepatic artery infusion chemotherapy improved survival after curative resection in patients with hepatocellular carcinoma. *Hepatogastroenterology* (2015) 62(137):122–5.

58. Li S, Mei J, Wang Q, Guo Z, Lu L, Ling Y, et al. Postoperative adjuvant transarterial infusion chemotherapy with FOLFOX could improve outcomes of hepatocellular carcinoma patients with microvascular invasion: a preliminary report of a phase III, randomized controlled clinical trial. *Ann Surg Oncol* (2020) 27(13):5183–90. doi: 10.1245/s10434-020-08601-8

59. Hirokawa F, Komeda K, Taniguchi K, Asakuma M, Shimizu T, Inoue Y, et al. Is postoperative adjuvant transcatheter arterial infusion therapy effective for patients with hepatocellular carcinoma who underwent hepatectomy? a prospective randomized controlled trial. *Ann Surg Oncol* (2020) 27(11):4143–52. doi: 10.1245/s10434-020-08699-w

60. Hsiao JH, Tsai CC, Liang TJ, Chiang CL, Liang HL, Chen IS, et al. Adjuvant hepatic arterial infusion chemotherapy is beneficial for selective patients with hepatocellular carcinoma undergoing surgical treatment. *Int J Surg* (2017) 45:35–41. doi: 10.1016/j.ijsu.2017.07.071

61. Ke Q, Wang L, Wu W, Huang X, Li L, Liu J, et al. Meta-analysis of postoperative adjuvant hepatic artery infusion chemotherapy versus surgical resection alone for hepatocellular carcinoma. *Front Oncol* (2021) 11:720079. doi: 10.3389/fonc.2021.720079

62. Yu W, Wang W, Rong W, Wang L, Xu Q, Wu F, et al. Adjuvant radiotherapy in centrally located hepatocellular carcinomas after hepatectomy with narrow margin (<1 cm): a prospective randomized study. *J Am Coll Surg* (2014) 218(3):381–92. doi: 10.1016/j.jamcollsurg.2013.11.030

63. Gou XX, Shi HY, Li C, Chen ZL, Ouyang W, Sun LY, et al. Association of adjuvant radiation therapy with long-term overall and recurrence-free survival after hepatectomy for hepatocellular carcinoma: a multicenter propensity-matched study. *Int J Radiat Oncol Biol Phys* (2022) 114(2):238–49. doi: 10.1016/j.ijrobp.2022.05.020

64. Luo F, Li M, Ding J, Zheng S. The progress in the treatment of hepatocellular carcinoma with portal vein tumor thrombus. *Front Oncol* (2021) 11:635731. doi: 10.3389/fonc.2021.635731

65. Sun J, Yang L, Shi J, Liu C, Zhang X, Chai Z, et al. Postoperative adjuvant IMRT for patients with HCC and portal vein tumor thrombus: an open-label randomized controlled trial. *Radiother Oncol* (2019) 140:20–5. doi: 10.1016/j.radonc.2019.05.006

66. Chen B, Wu JX, Cheng SH, Wang LM, Rong WQ, Wu F, et al. Phase 2 study of adjuvant radiotherapy following narrow-margin hepatectomy in patients with HCC. *Hepatology* (2021) 74(5):2595–604. doi: 10.1002/hep.31993

67. Shi C, Li Y, Geng L, Shen W, Sui C, Dai B, et al. Adjuvant stereotactic body radiotherapy after marginal resection for hepatocellular carcinoma with microvascular invasion: a randomised controlled trial. *Eur J Cancer* (2022) 166:176–84. doi: 10.1016/j.ejca.2022.02.012

68. Lau WY, Lai EC, Leung TW, Yu SC. Adjuvant intra-arterial iodine-131-labeled lipiodol for resectable hepatocellular carcinoma: a prospective randomized trial-update on 5-year and 10-year survival. *Ann Surg* (2008) 247(1):43–8. doi: 10.1097/SLA.0b013e3181571047

69. Lau WY, Leung TW, Ho SK, Chan M, Machin D, Lau J, et al. Adjuvant intra-arterial iodine-131-labelled lipiodol for resectable hepatocellular carcinoma: a prospective randomised trial. *Lancet* (1999) 353(9155):797–801. doi: 10.1016/S0140-6736(98)06475-7

70. Chen K, Xia Y, Wang H, Xiao F, Xiang G, Shen F. Adjuvant iodine-125 brachytherapy for hepatocellular carcinoma after complete hepatectomy: a randomized controlled trial. *PloS One* (2013) 8(2):e57397. doi: 10.1371/journal.pone.0057397

71. Dumortier J, Decullier E, Hilleret MN, Bin-Dorel S, Valette PJ, Boillot O, et al. Adjuvant intraarterial lipiodol or ^{131}I-lipiodol after curative treatment of hepatocellular carcinoma: a prospective randomized trial. *J Nucl Med* (2014) 55(6):877–83. doi: 10.2967/jnumed.113.131367

72. Chung AY, Ooi LL, Machin D, Tan SB, Goh BK, Wong JS, et al. Adjuvant hepatic intra-arterial iodine-131-lipiodol following curative resection of hepatocellular carcinoma: a prospective randomized trial. *World J Surg* (2013) 37(6):1356–61. doi: 10.1007/s00268-013-1970-4

73. Li J, Xing J, Yang Y, Liu J, Wang W, Xia Y, et al. Adjuvant (131)I-metuximab for hepatocellular carcinoma after liver resection: a randomised, controlled, multicentre, open-label, phase 2 trial. *Lancet Gastroenterol Hepatol* (2020) 5(6):548–60. doi: 10.1016/S2468-1253(19)30422-4

74. Foerster F, Gairing SJ, Ilyas SI, Galle PR. Emerging immunotherapy for HCC: a guide for hepatologists. *Hepatology* (2022) 75(6):1604–26. doi: 10.1002/hep.32447

75. Takayama T, Sekine T, Makuuchi M, Yamasaki S, Kosuge T, Yamamoto J, et al. Adoptive immunotherapy to lower postsurgical recurrence rates of hepatocellular carcinoma: a randomised trial. *Lancet* (2000) 356(9232):802–7. doi: 10.1016/S0140-6736(00)02654-4

76. Lee JH, Lee JH, Lim YS, Yeon JE, Song TJ, Yu SJ, et al. Sustained efficacy of adjuvant immunotherapy with cytokine-induced killer cells for hepatocellular carcinoma: an extended 5-year follow-up. *Cancer Immunol Immunother* (2019) 68(1):23–32. doi: 10.1007/s00262-018-2247-4

77. Hui D, Qiang L, Jian W, Ti Z, Da-Lu K. A randomized, controlled trial of postoperative adjuvant cytokine-induced killer cells immunotherapy after radical resection of hepatocellular carcinoma. *Dig Liver Dis* (2009) 41(1):36–41. doi: 10.1016/j.dld.2008.04.007

78. Yu X, Zhao H, Liu L, Cao S, Ren B, Zhang N, et al. A randomized phase II study of autologous cytokine-induced killer cells in treatment of hepatocellular carcinoma. *J Clin Immunol* (2014) 34(2):194–203. doi: 10.1007/s10875-013-9976-0

79. Xu L, Wang J, Kim Y, Shuang ZY, Zhang YJ, Lao XM, et al. A randomized controlled trial on patients with or without adjuvant autologous cytokine-induced killer cells after curative resection for hepatocellular carcinoma. *Oncoimmunology* (2016) 5(3):e1083671. doi: 10.1080/2162402X.2015.1083671

80. Finn RS, Qin S, Ikeda M, Galle PR, Ducreux M, Kim TY, et al. Atezolizumab plus bevacizumab in unresectable hepatocellular carcinoma. *N Engl J Med* (2020) 382(20):1894–905. doi: 10.1056/NEJMoa1915745

81. Finn RS, Ikeda M, Zhu AX, Sung MW, Baron AD, Kudo M, et al. Phase ib study of lenvatinib plus pembrolizumab in patients with unresectable hepatocellular carcinoma. *J Clin Oncol* (2020) 38(26):2960–70. doi: 10.1200/JCO.20.00808

82. Brown ZJ, Greten TF, Heinrich B. Adjuvant treatment of hepatocellular carcinoma: prospect of immunotherapy. *Hepatology* (2019) 70(4):1437–42. doi: 10.1002/hep.30633

83. Kudo M, Ueshima K, Nakahira S, Nishida N, Ida H, Minami Y, et al. Final results of adjuvant nivolumab for hepatocellular carcinoma (HCC) after surgical resection (SR) or radiofrequency ablation (RFA) (NIVOLVE): a phase 2 prospective multicenter single-arm trial and exploratory biomarker analysis. *J Clin Oncol* (2022) 40(4). doi: 10.1200/JCO.2022.40.4_suppl.416

84. Chen W, Hu S, Liu Z, Sun Y, Wu J, Shen S, et al. Adjuvant anti-PD-1 antibody for hepatocellular carcinoma with high recurrence risks after hepatectomy. *Hepatol Int* (2023). doi: 10.1007/s12072-022-10478-6

85. Kelly RJ, Ajani JA, Kuzdzal J, Zander T, Van Cutsem E, Piessen G, et al. Adjuvant nivolumab in resected esophageal or gastroesophageal junction cancer. *N Engl J Med* (2021) 384(13):1191–203. doi: 10.1056/NEJMoa2032125

86. Eggermont AMM, Blank CU, Mandala M, Long GV, Atkinson V, Dalle S, et al. Adjuvant pembrolizumab versus placebo in resected stage III melanoma. *N Engl J Med* (2018) 378(19):1789–801. doi: 10.1056/NEJMoa1802357

87. Zhang X, Zhou Y, Chen C, Fang W, Cai X, Zhang X, et al. Hepatitis b virus reactivation in cancer patients with positive hepatitis b surface antigen undergoing PD-1 inhibition. *J Immunother Cancer* (2019) 7(1):322. doi: 10.1186/s40425-019-0808-5

88. Xie M, Dang ZP, Sun XG, Zhang B, Zhang Q, Tian QJ, et al. An analysis report on the application of immune checkpoint inhibitors after liver transplantation. *Ther Adv Chronic Dis* (2022) 13:20406223221099334. doi: 10.1177/20406223221099334

89. Fisher J, Zeitouni N, Fan W, Samie FH. Immune checkpoint inhibitor therapy in solid organ transplant recipients: a patient-centered systematic review. *J Am Acad Dermatol* (2020) 82(6):1490–500. doi: 10.1016/j.jaad.2019.07.005

90. Chen J, Lu L, Wen TF, Lu CD, Zeng YY, Xiang BD, et al. Adjuvant lenvatinib in combination with TACE for hepatocellular carcinoma patients with high risk of postoperative relapse (LANCE): updated results from a multi-center prospective cohort study. *Ann Oncol* (2021) 32:S824–S5. doi: 10.1016/j.annonc.2021.08.165

91. Yau T, Park JW, Finn RS, Cheng AL, Mathurin P, Edeline J, et al. Nivolumab versus sorafenib in advanced hepatocellular carcinoma (CheckMate 459): a randomised, multicentre, open-label, phase 3 trial. *Lancet Oncol* (2022) 23(1):77–90. doi: 10.1016/S1470-2045(21)00604-5

92. Finn RS, Ryoo BY, Merle P, Kudo M, Bouattour M, Lim HY, et al. Pembrolizumab as second-line therapy in patients with advanced hepatocellular carcinoma in KEYNOTE-240: a randomized, double-blind, phase III trial. *J Clin Oncol* (2020) 38(3):193–202. doi: 10.1200/JCO.19.01307

93. Huinen ZR, Huijbers EJM, van Beijnum JR, Nowak-Sliwinska P, Griffioen AW. Anti-angiogenic agents - overcoming tumour endothelial cell anergy and improving immunotherapy outcomes. *Nat Rev Clin Oncol* (2021) 18(8):527–40. doi: 10.1038/s41571-021-00496-y

94. Kato Y, Tabata K, Kimura T, Yachie-Kinoshita A, Ozawa Y, Yamada K, et al. Lenvatinib plus anti-PD-1 antibody combination treatment activates CD8+ T cells through reduction of tumor-associated macrophage and activation of the interferon pathway. *PloS One* (2019) 14(2):e0212513. doi: 10.1371/journal.pone.0212513

95. Cheng AL, Qin S, Ikeda M, Galle PR, Ducreux M, Kim TY, et al. Updated efficacy and safety data from IMbrave150: atezolizumab plus bevacizumab vs. sorafenib for unresectable hepatocellular carcinoma. *J Hepatol* (2022) 76(4):862–73. doi: 10.1016/j.jhep.2021.11.030

96. Wu W-C, Lin T-Y, Chen M-H, Hung Y-P, Liu C-A, Lee R-C, et al. Lenvatinib combined with nivolumab in advanced hepatocellular carcinoma-real-world experience. *Investigational New Drugs* (2022) 40:789–97. doi: 10.1007/s10637-022-01248-0

97. Xia Y, Tang W, Qian X, Li X, Cheng F, Wang K, et al. Efficacy and safety of camrelizumab plus apatinib during the perioperative period in resectable hepatocellular carcinoma: a single-arm, open label, phase II clinical trial. *J Immunother Cancer* (2022) 10(4). doi: 10.1136/jitc-2022-004656

98. Zhao H, Zhao J, Jiang L, Bi X, Qian H, Du S, et al. Anti-PD-1 antibody SHR-1210 combined with apatinib as adjuvant treatment in patients with hepatocellular carcinoma at high risk of recurrence after radical resection: preliminary results from a multicenter, randomized, controlled phase II trial. *J Clin Oncol* (2021) 39(3). doi: 10.1200/JCO.2021.39.3_suppl.285

99. Xu J, Shen J, Gu S, Zhang Y, Wu L, Wu J, et al. Camrelizumab in combination with apatinib in patients with advanced hepatocellular carcinoma (RESCUE): a nonrandomized, open-label, phase II trial. *Clin Cancer Res* (2021) 27(4):1003–11. doi: 10.1158/1078-0432.CCR-20-2571

100. Xian F, Wu C, Zhang G, Xu G. Efficacy and safety of immune checkpoint inhibitors combined anti-angiogenic therapy in patients with unresectable hepatocellular carcinoma: a meta-analysis. *Med (Baltimore)* (2022) 101(44):e31479. doi: 10.1097/MD.0000000000031479

101. Ke Q, Xin F, Fang H, Zeng Y, Wang L, Liu J. The significance of transarterial Chemo(Embolization) combined with tyrosine kinase inhibitors and immune checkpoint inhibitors for unresectable hepatocellular carcinoma in the era of systemic therapy: a systematic review. *Front Immunol* (2022) 13:913464. doi: 10.3389/fimmu.2022.913464

102. Xing R, Gao J, Cui Q, Wang Q. Strategies to improve the antitumor effect of immunotherapy for hepatocellular carcinoma. *Front Immunol* (2021) 12:783236. doi: 10.3389/fimmu.2021.783236

103. Sangro B, Melero I, Wadhawan S, Finn RS, Abou-Alfa GK, Cheng AL, et al. Association of inflammatory biomarkers with clinical outcomes in nivolumab-treated patients with advanced hepatocellular carcinoma. *J Hepatol* (2020) 73(6):1460–9. doi: 10.1016/j.jhep.2020.07.026

104. Tang W, Chen Z, Zhang W, Cheng Y, Zhang B, Wu F, et al. The mechanisms of sorafenib resistance in hepatocellular carcinoma: theoretical basis and therapeutic aspects. *Signal Transduct Target Ther* (2020) 5(1):87. doi: 10.1038/s41392-020-0187-x

frontiers | Frontiers in Oncology

TYPE Review
PUBLISHED 01 May 2023
DOI 10.3389/fonc.2023.1171098

OPEN ACCESS

EDITED BY
Maria Lina Tornesello,
G. Pascale National Cancer Institute Foundation (IRCCS), Italy

REVIEWED BY
Massimiliano Cadamuro,
University of Padua, Italy
Jianfeng Yang,
Hangzhou First People's Hospital, China

*CORRESPONDENCE
Xiaolu Zhang
xiaolu.zhang@sdu.edu.cn

RECEIVED 21 February 2023
ACCEPTED 11 April 2023
PUBLISHED 01 May 2023

CITATION
Yang Y and Zhang X (2023) An overview of extrahepatic cholangiocarcinoma: from here to where?
Front. Oncol. 13:1171098.
doi: 10.3389/fonc.2023.1171098

An overview of extrahepatic cholangiocarcinoma: from here to where?

Yongheng Yang and Xiaolu Zhang*

Department of Physiology and Pathophysiology, School of Basic Medical Sciences, Cheeloo College of Medicine, Shandong University, Jinan, Shandong, China

Extrahepatic cholangiocarcinoma (eCCA) contains perihilar cholangiocarcinoma and distal cholangiocarcinoma both of which can arise at any point of the biliary tree and originate from disparate anatomical sites. Generally, the incidence of eCCA is increasing globally. Though surgical resection is the principal treatment of choice for the early stages of eCCA, optimal survival remains restricted by the high risk of recurrence when most patients are present with unresectable disease or distant metastasis. Furthermore, both intra- and intertumoral heterogeneity make it laborious to determine molecularly targeted therapies. In this review, we mainly focused on current findings in the field of eCCA, mostly including epidemiology, genomic abnormalities, molecular pathogenesis, tumor microenvironment, and other details while a summary of the biological mechanisms driving eCCA may shed light on intricate tumorigenesis and feasible treatment strategies.

KEYWORDS

extrahepatic cholangiocarcinoma, pathogenesis, tumorigenesis, genomics, tumor microenvironment

1 Introduction

Cholangiocarcinoma (CCA) usually refers to a range of invasive adenocarcinomas including intrahepatic cholangiocarcinoma (iCCA), perihilar cholangiocarcinoma (pCCA) and distal cholangiocarcinoma (dCCA) based on dissimilarly anatomical locations while the latter two are also collectively termed as extrahepatic cholangiocarcinoma (eCCA). Anatomically, pCCA and dCCA can be discriminated by whether the tumor originates between the second-order ducts and the insertion of the cystic duct or from epithelium distal to the insertion of the cystic duct whereas dCCA implicates the common bile duct typically (1). Moreover, pCCA and dCCA also diverge in pathogenesis, cells of origin, genome aberrations, molecular profiles, and risk factors. Although distinct from iCCA, eCCA should be cautiously termed to cover pCCA and dCCA due to the ambiguous origins of pCCA (2). Histologically, pCCA and dCCA are mainly common mucin-producing adenocarcinomas or papillary tumors, unlike more heterogeneous iCCA which can be classified into perihilar large duct type and peripheral small duct type with S100P and SPP1 expressed, respectively, in term of the size or level of the bile duct affected by malignant

cells (3–5). Interestingly, the perihilar large duct type of iCCA is more similar to pCCA and dCCA whereas those subtypes can derive from columnar mucin-producing cholangiocytes or peribiliary glands (4). In term of patterns of growth, iCCA tends to be mass-forming while its large duct type and eCCA can be periductal infiltrating or intraductal growing. Besides, several precancerous lesions including mucinous, cystic neoplasm, biliary epithelial neoplasia, intraductal tubulopapillary neoplasm and intraductal papillary neoplasm of the bile duct can be related to iCCA large duct type and eCCA, not iCCA small duct type (4). Furthermore, viral and cirrhosis are usually underlying in iCCA whereas cholangitis and liver flukes are more common in eCCA. Regarding frequent mutations, IDH1 mutations and FGFR2 fusions with targeted drugs are more frequent in iCCA but nearly absent in eCCA which may be inclined to ERBB alterations (4). eCCA is a rare cancer, but its incidence and mortality have been increasing which menace human health severely (6). Regarding the treatment of eCCA, surgical resection with negative margins is the curative and available treatment strategy for patients present with the early-stage or resectable disease when recurrence is still prevalent (7). Moreover, multidisciplinary treatment of advanced eCCA is also crucial. For instance, adjuvant therapy with S-1 encompassing a mixture of tegafu, gimeracil, and oteracil potassium could improve survival among patients with CCA resected according to a phase 3 randomized clinical trial (8). However, effective molecularly targeted therapy for eCCA is still an urgent enigma to be unveiled.

Here, we summarize current advances in the oncogenic mechanisms and treatment strategies of eCCA, mainly concerning epidemiology, genomic abnormalities, molecular pathogenesis, tumor microenvironment, and other pertinent details to provide a comprehensive panorama of eCCA and highlight the importance of personalized and multidisciplinary considerations.

2 Epidemiology and risk factors, past and current

The global Incidence of eCCA increased worldwide during the period 1993-2012 spanning two decades according to the CI5plus database for 33 inclusive countries (9). More accurately, the age-standardized incidence for eCCA indeed increased with geographical variation and most evidently in Thailand and Colombia in the 20 years examined. Mortality rates for eCCA have also increased, but more slowly than iCCA in Western countries (6). Summarizing gallbladder carcinoma and other biliary carcinomas including eCCA, an estimated 12,130 new cases, and 4,400 deaths were reported in the United States, in 2022 with a minute difference by gender (10). However, it was also reported that the age-standardized incidence of eCCA has been descending over the past few decades (11, 12). Of note, these trends need conservative assessment given that International Classification of Diseases (ICD) codes for cholangiocarcinoma have been updated several times. Separate codes for iCCA, pCCA, and dCCA were not available until the new ICD-11 classification came into effect which may influence epidemiological estimation (13). Thus, epidemiological trends reported for eCCA need to be evaluated meticulously whereas data is more reliable when ample and new. In addition, pCCA and dCCA have different prognoses and distinctive epidemiological trends. Surveillance, Epidemiology, and End Results (SEER) database have shown better survival in dCCA when compared with pCCA from 2000 to 2018 (14). Regarding dCCA, a recent Swedish cohort study disclosed that incidence rates elevated principally among those patients aged more than 55 during the consecutive calendar periods. Contrastively, the increase in both intrahepatic and perihilar cholangiocarcinoma was more evident in younger adults (15).

In general, several common risk factors including obesity, alcohol consumption, and cigarette smoking could be linked to eCCA (16). Furthermore, metabolic diseases, such as type 2 diabetes, nonalcoholic fatty liver disease, and hypertension are also risk factors for eCCA which are also shared by iCCA (17, 18). Remarkably, dose-dependent alcohol consumption increased the risk of CCA for patients with prediabetes and diabetes, but not normoglycemic, which indicated a synergistic effect, and alcohol abstinence might humiliate the risk of CCA for those patients (19). A large pan-European cohort showed that pCCA was featured with primary sclerosing cholangitis (PSC) and dCCA with choledocholithiasis (20). Though viral infections including hepatitis B virus and hepatitis C virus have been associated with incremental CCA risk previously, they seem to influence iCCA mainly, not eCCA in Europe while a similar situation could be adequate for primary biliary cholangitis (16, 20). Several studies also evaluated the role of drugs such as statins and aspirin in the prevention of eCCA. Statin usage has been noticed to be associated with a reduced risk for eCCA whose users with dCCA had better overall survival than statin-free patients (HR=0.53) (21). Notably, multiple cohorts have revealed that aspirin was associated with a decreased risk of CCA (22, 23). Even so, low-dose aspirin was not associated with eCCA risk significantly but non-steroidal anti-inflammatory drugs with aspirin excluded could increase the risk of eCCA (HR=1.32) as reported by Marcano-Bonilla L et al. (24). Besides, proton pump inhibitors with extended duration may also increase eCCA risk (25). Those evidence indicated that drug usage should be cautious for patients with eCCA.

Abbreviations: CAFs, Cancer-associated fibroblasts; CCA, cholangiocarcinoma; CfDNA, cell-free DNA; CSCs, cancer stem cells; dCCA, distal cholangiocarcinoma; eCCA, extrahepatic cholangiocarcinoma; EGFR, epidermal growth factor receptor; EMT, epithelial mesenchymal transition; ERCP, endoscopic retrograde cholangiopancreatography; EUS, endoscopic ultrasound; FDA, Food and Drug Administration; FLR, fibrinogen-to-lymphocyte ratio; HR, hazard ratio; iCCA, intrahepatic cholangiocarcinoma; ICD, International Classification of Diseases; LT, liver transplantation; LncRNAs, long non-coding RNAs; MMR, DNA mismatch repair; MRCP, magnetic resonance cholangiopancreatography; MSI, microsatellite instability; NICD1, notch intracellular domain 1; NK, natural killer; pCCA, perihilar cholangiocarcinoma; PSC, primary sclerosing cholangitis; SEER, Surveillance, Epidemiology, and End Results; TANs, tumor-associated neutrophils; TILs, tumor-infiltrating lymphocytes; TME, tumor microenvironment; Tregs, regulatory T cells.

3 Clinical symptoms and diagnosis, early to arise

eCCA can be asymptomatic or non-specific during early stages which makes it tough to diagnose early. The most common symptom of eCCA is obstructive jaundice whereas it is less frequent in iCCA (26). Besides, some constitutional symptoms such as fatigue, anorexia, weight loss, and abdominal pain could be noticed in patients with either benign or malignant diseases (27). Generally, diagnosis of eCCA can benefit from imaging, endoscopy and histology. Imaging techniques including CT and MRI are important for diagnosis and staging of CCA. Owing to direct compression, dCCA shows abrupt biliary tree cutoff from CT scanning while pCCA can be obvious only when dilated segmental bile ducts emerge (28). MRI can delineate the biliary tree with its lesions in detail and allow accurate ducts depicted by magnetic resonance cholangiopancreatography (MRCP) which is critical for the diagnosis, staging, and treatment planning of pCCA (29). MRI illustrates CCA as hypointense lesions and heterogeneously hyperintense lesions on T1-weighted images and T2-weighted images, respectively (30). Remarkably, Endoscopic retrograde cholangiopancreatography (ERCP) is a robust mode for the biliary tree assessment and acquirement of brush cytology and biopsies with high specificity but low sensitivity (31). In addition to the primary modalities including MRCP and ERCP, endoscopic ultrasound (EUS) can be complemental and helpful for the evaluation of biliary strictures and assessment of eCCA or regional lymph nodes (32). It also allows tissue acquisition *via* needle aspiration and may detect small bile duct masses (33). Furthermore, cholangioscopy covering bile duct mucosa and targeted biopsies could enhance the diagnostic accuracy of malignant biliary strictures (34). Recently, Ishii T et al. reported that cholangioscopy enhanced by image systems is very useful for diagnosing eCCA (35). Histologically, eCCA can be flat, nodular sclerosing, or intraductal papillary type whose growth patterns are periductal infiltrating or intraductal growing. eCCA derives from mucous cells and/or columnar cholangiocytes which also concern precancerous lesions including intraductal epithelial neoplasia. Several tissue markers such as MUC5AC, MUC6, S100P, and BAP1 contribute to differentiating eCCA from diverse CCA types (4). In total, early diagnosis is still challenging for eCCA and a combination of clinical, imaging, endoscopy and histologic data is usually necessary.

4 Surgical resection and adjuvant therapy, two rocks and one bird

Surgical resection maintains a momentous tactic for pCCA and dCCA therapy while adequate assessment and preoperative consideration are necessary to be priorly executed which restricts candidates for curative-intent surgical resection therapy (36, 37).

Generally speaking, pancreaticoduodenectomy and lymphadenectomy are involved in surgery for dCCA (Table 1). Achieving a margin negative (R0) resection is crucial for dCCA and pCCA management while negative margin assessment and complete resection may benefit from the intraoperative frozen section (43). Curative and eligible surgical resections for eCCA patients depend on multiple clinical conditions. A study based on a cohort in the Netherlands determined an overall survival predictive model for patients after pancreatoduodenectomy for dCCA. Five independent prognostic factors covering age at diagnosis, pT category, pN category, resection margin status, and tumor differentiation were included in the model which was also robust for inferring prognosis (44). Furthermore, both tumor budding and tumor invasive thickness were associated with adverse postoperative prognosis in eCCA (45, 46). Interestingly, nerve fiber density invaded by tumors could be related to unfavorable outcomes of pCCA patients undergoing curative-intent surgery (47). Regarding preoperative evaluation, preoperative biliary drainage is still debated but needed when obstructive symptoms are present for eCCA patients whereas endoscopic biliary drainage seems to be more suitable for dCCA than percutaneous transhepatic biliary drainage which had lower rates of complications for pCCA (48–50). Moreover, laboratory assessment on peripheral blood revealed that neutrophil count, fibrinogen-to-lymphocyte ratio (FLR), and FLR-neutrophil score could predict the prognosis of patients with resected eCCA (51).

Historically, adjuvant therapy after curative resection of biliary tract cancer is commendatory whose decisions need to be based on adequate and robust data from clinical trials. Previously, no difference was settled between the gemcitabine adjuvant chemotherapy group and the control group in eCCA patients who underwent curative resection from a randomized phase 3 trial (52). Recently, another randomized phase 3 trial confirmed adjuvant therapy with S-1 (a mixture of tegafu, gimeracil, and oteracil) could improve survival among patients with resected eCCA, iCCA, gallbladder carcinoma (GBC), and ampullary carcinoma involved versus surgery alone (8). A prospective study (SWOG 0809) focusing on adjuvant chemotherapy (gemcitabine and capecitabine) followed by chemoradiation in patients with eCCA and GBC showed that adjuvant therapy could benefit patients with lymph node-positive (53). Similarly, adjuvant therapy could improve the long-term survival of patients with perineural invasion and lymph node metastasis after curative-intent resection for dCCA (38). Although phase 3 studies evaluating adjuvant radiotherapy are lacking, there are shreds of evidence that adjuvant radiotherapy should be considered for patients after resection of dCCA (39). To sum up, the role of

TABLE 1 Effective therapeutical procedures for extrahepatic cholangiocarcinoma.

Procedures	Details	Reference
Surgical resection	Pancreaticoduodenectomy, lymphadenectomy	(36, 37)
Adjuvant therapy	Radiotherapy, chemotherapy	(38, 39)
Endoscopy	Radiofrequency ablation, stent	(40)
Targeted therapies	EGFR/ERBB2 inhibitors	(41)
Immunotherapy	Anti-PD1 and/or anti-PD-L1	(42)

neoadjuvant and adjuvant therapies for eCCA should be optimized with more comprehensive investigations (Table 2).

For patients with unresectable disease, the FDA has approved pembrolizumab for patients with unresectable or metastatic microsatellite instability-high or mismatch repair deficient solid tumors (including CCA) (37). However, as shown in results from the KEYNOTE-158 and KEYNOTE-028 studies, pembrolizumab treatment achieved a low objective response rate of 6–13% and an inferior survival of less than 2 months in patients (61). Remarkably, liver transplantation (LT) is a therapeutic option in patients with unresectable malignant tumors including CCA (37). However, early experience showed high recurrence rates with transplant (64). Despite poor outcomes after LT for CCA, recent studies have fluctuated this premise since neoadjuvant therapy including chemotherapy and/or radiotherapy followed by liver transplantation offers a potentially curative strategy for patients with unresectable disease (65). For instance, a recent meta-analysis indicated that LT with neoadjuvant chemoradiation completed achieved higher overall survival rates than LT alone in patients with unresectable pCCA (82.8%, 65.5%, and 65.7% at 1 year, 3 years, and 5 years, respectively, vs. 71.2%, 48%, and 31.6%, respectively; $p < 0.001$) (66). It further supports the curative possibility of neoadjuvant chemoradiation therapy followed by liver transplantation for unresectable CCA patients.

Regarding the management of complications including obstructive jaundice and biliary infection for unresectable eCCA, endoscopic biliary stent placement is effective partially, but limited in improving the overall survival of patients (67). Endoscopic radiofrequency ablation (RFA) has been an accessible technique for alleviating malignant biliary stenosis since first reported (40), although it may be inclined to treat patients without distant metastasis (68, 69) (Table 1). Several randomized controlled trials showed that additional endoscopic RFA could improve the overall survival of patients with unresectable eCCA than those with stent placement alone (54, 55). Furthermore, endoscopic RFA combined with S-1 administered orally for unresectable eCCA patients achieved significantly longer survival (16 months vs. 11 months, $p<0.01$) and stent patency time (6.6 months vs. 5.6 months, $p=0.014$) than RFA sole (56). Evidence from retrospective studies also indicated that patients with locally advanced eCCA could benefit from the combination of endobiliary RFA and gemcitabine plus cisplatin treatments (70, 71).

5 Tumor microenvironment of eCCA, no cell is alone

The tumor microenvironment (TME) is composed of diverse cellular types and extracellular components, supporting and maintaining tumor progression while deciphering the complexity of TME is more feasible in the single-cell era (72).

Among innate immune cells, activated M2 macrophages induce tumor progression with anti-inflammatory and immunosuppressive effects which could stimulate the canonical Wnt/b-catenin pathway driving CCA growth (73). A high density of tumor-associated macrophages was associated with incremental recurrence of pCCA in a retrospective study (74). Furthermore, elevated PD-L1+ M2 tumor-associated macrophages (CD45+ CSF1R+ CD68+ CD163+) also correlated with inferior outcomes in dCCA and higher expression of IL6, IL10, and ARG1, contributing to effector T cell suppression (Figure 1) (75). Though natural killer (NK) cells may comprise a considerable proportion across immune ingredients of eCCA and seem to be lower in tumors compared to para-tumor tissues and peripheral blood (76), they were insufficiently studied in eCCA. A previous study reported that a mouse xenograft model induced by HuCCT-1 cells, an iCCA cell line, and then infused with *ex vivo* expanded human NK cells showed significant tumor inhibition (77). Tumor-associated neutrophils (TANs, CD66b+) could predict poor prognosis in eCCA patients (78). Similarly, the systemic immune-inflammation index calculated by neutrophil, platelet, and lymphocyte counts from serum was an independent prognostic factor for patients under resection of eCCA (79). Interestingly, neutrophils recruited by

TABLE 2 Robust clinical trials of extrahepatic cholangiocarcinoma.

Approach	Sample size	Agents	Clinical trial ID	Reference
Adjuvant chemotherapy	225	Gemcitabine	UMIN 000000820	(52)
Adjuvant chemotherapy	69	Gemcitabine and Capecitabine	SWOG 0809	(53)
Endoscopic radiofrequency ablation	65	NA	NCT02592538	(54)
Endoscopic radiofrequency ablation	174	NA	NCT01844245	(55)
Endoscopic radiofrequency ablation	75	S-1	NCT02592538	(56)
Chemotherapy plus targeted therapy	133	Gemcitabine and Oxaliplatin plus Erlotinib	NCT01149122	(57)
Chemotherapy plus targeted therapy	122	Gemcitabine and Oxaliplatin plus Cetuximab	NCT01267344	(58)
Chemotherapy plus targeted therapy	90	Cisplatin and Gemcitabine plus Panitumumab	NCT01320254	(59)
Chemotherapy plus targeted therapy	85	Gemcitabine and Oxaliplatin plus Panitumumab	NCT01389414	(60)
Immunotherapy	104	Pembrolizumab	NCT02628067	(61)
Immunotherapy	54	Nivolumab	NCT02829918	(62)
Immunotherapy	77	Atezolizumab plus Cobimetinib	NCT03201458	(63)

tumor-cell-derived microvesicles loading methotrexate and subsequent macrophage repolarization could alleviate biliary obstructions of patients with eCCA and execute tumor cells with reactive oxygen species and nitric oxide levels elevated, displaying an antitumor N1 phenotype (80). However, neutrophils heterogeneity in eCCA is still poorly understood. Remarkably, immunosuppressive functions including recruiting macrophages and suppressing T cell cytotoxicity of TANs have been elucidated adequately in liver cancer at the single cell resolution recently (81).

Regarding the adaptive immune system, tumor-infiltrating lymphocytes (TILs) mainly include CD4+ T lymphocytes and CD8 + T lymphocytes which consist of diverse subsets in eCCA (82). FOXP3+ regulatory T cells (Tregs) characterized by TGF-β and IL-10 secretion are noticed to infiltrate into the tumors with an immunosuppressive profile. Several studies have elevated Tregs in eCCA based on immunohistochemical results for FOXP3 while increased Tregs are significantly associated with worse OS in patients with p/dCCA (78, 83, 84). Experiments *in vitro* showed that FOXP3+ Tregs could be recruited by FOXM1 which bound to the FOXP3 promoter region and thus promoted its transcription in pCCA cell lines (85). Similarly, single-cell RNA sequencing on tissues derived from patients with dCCA also revealed that tumor infiltrating Tregs were abundant in dCCA tumors with immunosuppressive genes such as TIGIT, CTLA4, and TNFRSF18 highly expressed (Figure 1) (86). Furthermore, several genes related to immunotherapy including ACP5, MAGEH1, TNFRSF9, and CCR8 could be specially expressed in tumor infiltrating Tregs in eCCA as shown in the single-cell landscape from another research (76). For CD8+ T cells, some studies concluded that higher numbers of them were associated with better OS for eCCA (78, 82) while heterogeneity of CD8+ T cells may be neglected. As reported recently, cytotoxic CD8+ T cells could function as effectors in dCCA while exhausted CD8+ T cells were also enriched with PDCD1, CTLA4, LAG3, and HAVCR2 expressed (76, 86). Notably, mucosal-associated invariant T cells possessing cytotoxicity and innateness were absent in the pCCA tumor microenvironment (87). Histologically, canonical tertiary lymphoid structures were associated with favorable survival in pCCA (88).

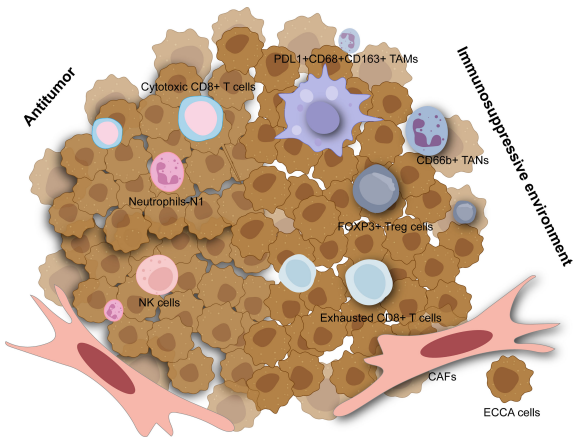

FIGURE 1
The tumor microenvironment in extrahepatic cholangiocarcinoma. The immunosuppressive environment is mainly composed of tumor-associated macrophage (TAMs), tumor-associated neutrophils (TANs), regulatory T cells (Tregs), exhausted CD8+ T cells and cancer-associated fibroblasts (CAFs) which are all associated with worse outcomes. Cytotoxic CD8+ T cells, neutrophils with N1 phenotype, and natural killer (NK) cells can have antitumor effects in extrahepatic cholangiocarcinoma.

Cancer-associated fibroblasts (CAFs) are a heterogeneous cell population of fibroblasts and myofibroblast-like cells and constitute CCA stroma chiefly with typical phenotypic markers such as α-SMA, PDGFRβ, FAP, and so on (89). In CCA, CAFs likely derive from a variety of cell types including hepatic stellate cells, portal fibroblasts, fibrocytes, or epithelial mesenchymal transition (EMT) (90). CAFs can mediate crosstalk with CCA cells or TME which pave the road for tumorigenesis. Extrahepatic TFK-1 cells co-cultured with CAFs showed incremental activation of STAT3, JNK, ERK, and AKT pathways (91). Admittedly, recent studies focused on CAFs and iCCA more while some evidence was also not special for eCCA (92, 93).

6 Genomic landscape of eCCA, common and maverick

Molecular heterogeneity across eCCA has been unveiled at the genomic level whereas pCCA and dCCA do bear dissimilar genomic alterations (94). DNA mismatch repair (MMR) deficiency could be found in about 5% of pCCA and dCCA, lower than iCCA as reported previously (95). Conventional mutations in TP53, KRAS, ARID1A, SMAD4, and GNAS were commonly shared in eCCA whereas CCA subtypes do carry diverse genomic profiles (96, 97). PRKACA and PRKACB fusions and ELF3 mutations could be inclined to occur in pCCA/dCCA (98). According to Simbolo M et al, KRAS mutations may be more prevalent in dCCA when compared to pCCA (99). Paradoxically, KRAS mutations were more common in pCCA than dCCA in another cohort (94). Furthermore, ERBB2 amplifications could occur more frequently in eCCA (100). ERBB2 mutations or amplifications were also linked to a proliferation class of eCCA where patients with dCCA predominate (96). Several driver genes involved in post-transcriptional modification such as RBM10 and METTL14 mutation were more enriched in pCCA than iCCA. Conversely, both tumor mutation burden and copy number alteration burden of pCCA were lower than iCCA (101). Intriguingly, aristolochic acid exposure which could induce TP53 mutation in iCCA was superior to eCCA in a Chinese cohort where high mutational frequencies of THAP9, SEC24B, and CAND1 were noticed in eCCA (102). Actually, canonical FGFR2 fusion events were nearly absent in eCCA whereas AXL-HNRNPUL1 gene fusions could be detected in a few cases with eCCA (98, 100). Of note, cell-free DNA (cfDNA) analysis excels at shedding light on tumor heterogeneity and provides an unbiased genomic profiling for patients. cfDNA analysis on advanced cholangiocarcinoma (both iCCA and eCAA, subtype was not specified) revealed that three targetable alterations including FGFR2 fusion, IDH1 mutations, and BRAF V600E were clonal in the generality of the cohort. Besides, discordance and concordance between cfDNA and

tissue for mutation detection could be noticed in the former one and the latter two, respectively (103). The high heterogeneity of eCCA can be likely attributed to genomics aberrations, highlighting the demand for characterizing the molecular basis of sensitivity and resistance to available treatments (Figure 2).

7 Pathogenesis of eCCA, classical but complex

To elaborate pathogenesis of eCCA is insurmountable while it is challenging to catch the "Achilles' Heel" of eCCA which can be related to signaling pathways to some extent. According to bulk transcriptomic profiles, 'metabolic', 'proliferation', 'mesenchymal', and 'immune' subtypes of eCCA were previously identified with disparate oncogenic pathways activated respectively (96). Indeed, several developmental pathways can be linked to eCCA (Figure 3). The Notch signaling pathway counts on ligands attaching to Notch receptors and subsequent release of Notch intracellular domain 1 (NICD1) which is then shifted to the nucleus where target genes regulating cell proliferation, migration, and invasion are activated (2). Although recent research mainly focused on the mechanism of the Notch pathway and iCCA (104), the Notch receptors were indeed overexpressed in pCCA and dCCA (105). The Wnt/β-catenin pathway is commonly activated in CCA and partially mutated in dCCA (73, 106). The Wnt/β-catenin pathway could be inhibited through ClC-5 inhibition in eCCA cells (107). TTYH3 could facilitate cell proliferation, migration, and invasion *via* the Wnt/β-catenin pathway in the QBC939 cell line (108). lncRNA PCAT1 was also involved in the positive regulation of pCCA and dCCA progression through miR-122 (109). Remarkably, SOX17 which is the WNT/β-catenin pathway promoter inhibitor was hypermethylated and thus repressed in patients with CCA (110). Apart from its seeming tumor suppression effect, SOX17 could sensitize tumors to chemotherapy with MRP3 suppressed in EGI-1 and TFK-1 cell lines (111). Alteration of classic oncogenic pathways is also involved in the pathogenesis of eCCA with genomic instability (96). For instance, transcription factor HOXA5 could augment MXD1 expression by binding to its promoter region directly which then activated the p53 signaling pathway, thus inhibiting eCCA cell proliferation (112). Notably, the MYC-oncogene pathways can drive tumorigenesis and be related to immune evasion in cancer (Figure 3) (113). HMGA1 inducing TRIP13 expression which suppressed FBXW7 transcription could stabilize c-Myc which expedited their transcription in a positive feedback, thus promoting EMT and stemness of pCCA (114). TCF7 inducing c-Myc transcription could impel pCCA progression (115). Besides, WDR5 could boost HIF-1α accumulation and then drive EMT and metastasis of eCCA in a Myc-dependent way (116). Interestingly, the depletion of glutamine could offset hypoxia-induced chemoresistance in eCCA cells with c-Myc restraint (117). Regarding metabolism pathways, lipid metabolism, and fatty acid oxidation were strikingly enhanced in the EGI1 cell line with intracellular lipids accumulation and increased cell stemness (118). Compared with iCCA, FABP5 functioning as a fatty acid transport protein is highly expressed and associated with poor

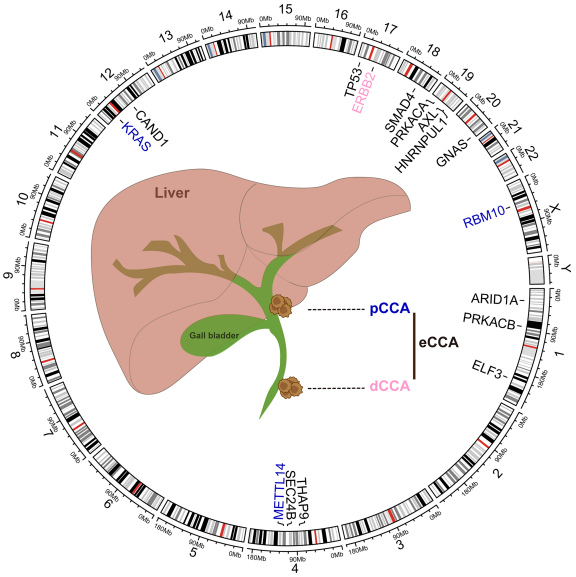

FIGURE 2
Common genomic alterations in extrahepatic cholangiocarcinoma. The genetic alterations and locations in human chromosomes (hg38) were depicted in the circos plot executed by R language package criclize.

survival in eCCA (119). Moreover, JNK/c-Jun pathways could also be associated with both iCCA and eCCA (120, 121). Proinflammatory cytokines, such as IL-6, IL-8. can be involved in augmenting tumorigenesis of eCCA. IL-6 in serum was a prognostic factor in eCCA patients (122). Likewise, the Genetic variant of CXCR1 (also termed IL-8RA) could predict inferior outcomes for pCCA patients (123). Angiogenesis is also essential for eCCA. High levels of VEGF have been noticed in eCCA cell lines and tissues previously (124). Recently, Li T et al. reported that VEGF was regulated by Gab1 *via* SHP2/ERK1/2 which could be inhibited by apatinibin in pCCA cells (125).

Cancer stem cells (CSCs) are a characteristic subpopulation of tumor cells and harbor the ability to maintain renewal which can be involved in recurrence, metastasis, and drug resistance (126). As shown in accumulative shreds of evidence, CSCs are interrelated with EMT intimately (4). Not only does TGFβ contribute to EMT, but it also facilitates stemness in extrahepatic TFK-1 cells *in vitro* (127). Besides, CSCs from iCCA and eCCA can be identified with ALDH expressed (127). Remarkably, though cell proliferation and invasion were more increased in iCCA than in eCCA cell lines, stem cell surface markers (CD13, CD24, CD44, CD90, and EPCAM) were similarly expressed for both sides (128).

8 Biomarkers of eCCA, novel or clinical

Non-invasive and robust biomarkers of eCCA with diagnostic and prognostic significance have been urgent for execution. Novel biomarkers of eCCA have been emerging with advanced test tools and abundant specimens available (Figure 4). Squamous cell carcinoma

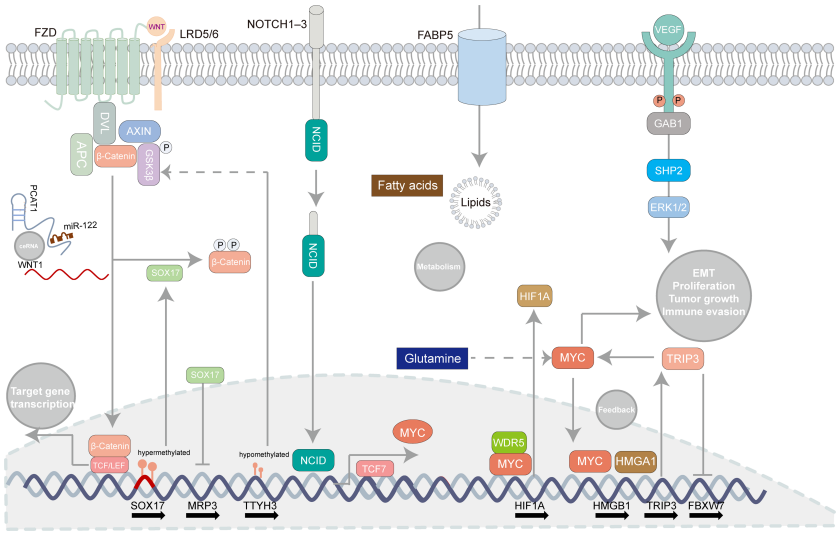

FIGURE 3
Oncogenic pathways involved in extrahepatic cholangiocarcinoma. Some canonical pathways can be related to tumorigenesis in extrahepatic cholangiocarcinoma such as the Notch signaling pathway, the WNT/β-catenin pathway, the MYC-oncogene pathways, lipid metabolism, and angiogenesis. Several regulatory mechanisms concerning those pathways are recapitulated in the illustrator.

antigen (SCCA) detected in bile samples was found to be increased in patients with eCCA and could be a special biomarker for eCCA (129). Similarly, microRNA (miR-31-5p, miR-378d, miR-182-5p, and miR-92a-3p) derived from bile cytologic samples were also increased in eCCA cases compared with control cases (130). Anti-apoptotic protein Bcl-x_L encoded by BCL2L1 was identified as a prognostic marker in cholangiocarcinoma depending on anatomical subtypes when it indicated beneficial prognosis, especially for pCCA (131). The preoperative serum is also an accessible and robust source for biomarkers in biofluids. Preoperative serum carbohydrate antigen 19-9 could be related to regional lymph node metastases and the prognosis of both pCCA and dCCA with a cutoff of 37 U/ml (132–134). A recent study reported that elevated serum CA242 (>20 IU/ml) was associated with vascular invasion and lymph node metastasis of pCCA (135). Furthermore, inflammatory markers including neutrophils, fibrinogen-to-prealbumin ratio, and fibrinogen-to-lymphocyte-to-neutrophil ratio from preoperative peripheral blood were all independent factors for overall survival of eCCA according to the recent multivariate Cox analyses (51).

Moreover, long non-coding RNAs (lncRNAs) are characterized as non-coding RNAs whose transcripts are longer than 200 nucleotides lacking the ability to code for proteins but influencing tumorigenesis, which are also implicated in the molecular biomarkers of CCA (136, 137). For instance, lncRNA PCAT1 was

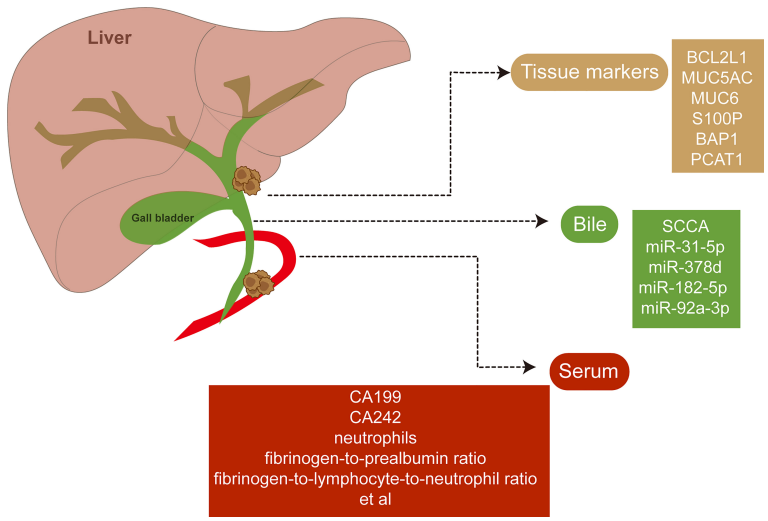

FIGURE 4
Potential biomarkers of extrahepatic cholangiocarcinoma. Novel biomarkers of extrahepatic cholangiocarcinoma have been discovered with abundant specimens including tissues, bile, and serum available.

remarkably upregulated in both eCCA tissues and cell lines (109). MALAT1 could be involved in the pathogenesis of pCCA and predict poor overall survival (138). Some studies have also evaluated the role of lncRNAs in eCCA cell lines. AFAP1-AS1 was relevant to cell growth and metastasis in TFK-1 cell line (139). LINC00184 increased cell growth in QBC939 cell line (140). However, effective tissue markers related to lncRNA for identify eCCA are yet to be discovered.

9 Rare histological subtypes related to eCCA, less is more

Histologically, pCCA and dCCA mainly cover mucinous adenocarcinomas or papillary tumors beyond which several additional histological subtypes could be also noticed in eCCA, rarely but factually (141). Adenosquamous carcinoma featured with concomitant adenocarcinoma and squamous carcinoma accounts for 2% of eCCA as previously reported (142). Though it occurs predominantly among the rare subtypes of eCCA, adenosquamous carcinoma can carry different molecular profiles (143). A recent case report showed that an adenosquamous carcinoma patient with distant lymph node metastases carried Her-2 amplification and preserved a stable state after receiving several lines of trastuzumab treatment combined with chemotherapy and radiotherapy (144). Besides, another rare type related to eCCA is signet ring cell carcinoma. Signet ring cell carcinoma is characterized by abundant mucus in the cytoplasm extruding nucleus from center to margin of cell. Generally, a few cases with signet ring cell carcinoma of eCCA were reported up to now (145). Previous studies also described two separable types containing intestinal type and pancreatobiliary type with CK7 negative plus CK20/MUC2 positive and CK7 positive plus CK20/MUC2 negative, respectively (146, 147). That signet ring cell carcinoma of eCCA with distant lymph node metastasis has also been noticed recently (145). Distant metastases always lead to a poor prognosis in eCCA patients. A SEER-based study reported that the liver and distant lymph were the most common sites for metastases and multiple sites (at least two) occurred in some cases (148). Particularly, patients with unresectable advanced eCCA and liver metastases may benefit from chemotherapy combining gemcitabine and cisplatin or pembrolizumab and nab-paclitaxel (149, 150). About the gastrointestinal tracts, several studies also reported colonic metastasis of eCCA (151, 152). Rarely, distal skeletal muscle metastasis could appear in a few eCCA patients as reported (153). Those evidence suggested that adequate follow-up periods should be considered for eCCA since sporadic metastasis could occur.

10 Targeted therapies and immunotherapy

Molecularly in-depth understanding of CCA contributes to confirming achievable drug targets. Although IDH1 mutations and FGFR2 fusions do provide new treatment tactics, they are more frequent in iCCA and nearly absent in eCCA (100, 154, 155). Moreover, several randomized controlled trials concerning the epidermal growth factor receptor (EGFR) inhibitors (erlotinib, cetuximab, lapatinib, or panitumumab) did not achieve effective outcomes in advanced CCA (57–60, 156) (Table 2). A previous meta-analysis has also shown that first-line chemotherapy with the addition of anti-EGFR monoclonal antibodies does not improve the overall and progression-free survival of patients with advanced CCA (157). Alternatively, targeting abnormal ERBB2 which is more common in eCCA may be a favorable approach. A case report suggested a combination of Trastuzumab and pertuzumab was curative for the patient with ERBB2-amplified eCCA (41). Immune checkpoint blockade can reinforce antitumor immunity by hindering intrinsic suppressors (e.g. CTLA4, PD1, or PDL1) from the immunosuppressive microenvironment where the tumor locates while several checkpoint inhibitors have been approved for clinical application (158). Regarding eCCA, four novel transcriptome-based subtypes have been suggested (96). Tumors in the “immune” class not only overexpressed PD-1/PD-L1 but also had a higher lymphocyte infiltration which implies a better response to immune checkpoint inhibitors. Furthermore, the ratio of PD1 positive to CD8 + TILs could be linked to worse outcomes for eCCA patients (159). A subset of CD8+RORγt+ T cells with PD1 expressed lowly was noticed to be associated with reduced survival in dCCA as reported previously (160). Actually, pembrolizumab seems to be more effective in CCA patients with microsatellite instability (MSI) or mismatch repair deficiency (dMMR) whose incidence is low in CCA while it is also reported that the number of ECC patients with PDL1 positive could be small (161, 162). Indeed, the TOPAZ-1 trial has improved our understanding of CCA and immunotherapy (42).

Several immunotherapy agents such as Pembrolizumab, Nivolumab and Atezolizumab have shown low response rates in patients with advanced stages of CCA (61–63).

Up to now, more clinical trials are still requisite for eCCA.

11 Conclusion

CCA is heterogeneous and comprised of diverse subtypes. Not only do those subtypes arise from different locations, but iCCA and eCCA also carry disparate risk factors, diverse cells of origin, and individual genome aberrations. Sophisticated interactions between eCCA cells or CSCs, and the TME make it laborious to elaborate the biological mechanisms underpinning tumorigenesis where high-resolution single cell multi-omics may shed light on. Now, there is still a lack of therapeutic approaches for eCCA since not all patients with eCCA can benefit from accessible treatments including surgery, adjuvant therapy, targeted therapies, and immunotherapy, emphasizing the importance of personalized and multidisciplinary considerations. However, improved understanding of the specific TME and pathogenesis in eCCA, along with accumulating data from single cell resolution will indisputably bring more efficient therapeutic options for patients in the future. Furthermore, considering that several benign diseases are risk factors of eCCA, it is also crucial for patients with

eCCA to prevent early, diagnose accurately, and treat timely. That is, better to batten down the hatches before the storm comes.

Author contributions

YY: Visualization, data curation, writing - original draft. XZ: Project administration, supervision, writing - review & editing. Both authors contributed to the article and approved the submitted version.

Funding

This work was supported by grants from the National Natural Science Foundation of China (no. 8210100902) to XZ.

Conflict of interest

The authors declare that the research was conducted in the absence of any commercial or financial relationships that could be construed as a potential conflict of interest.

Publisher's note

References

1. Valle JW, Kelley RK, Nervi B, Oh DY, Zhu AX. Biliary tract cancer. *Lancet* (2021) 397(10272):428–44. doi: 10.1016/S0140-6736(21)00153-7

2. Rodrigues PM, Olaizola P, Paiva NA, Olaizola I, Agirre-Lizaso A, Landa A, et al. Pathogenesis of cholangiocarcinoma. *Annu Rev Pathol* (2021) 16:433–63. doi: 10.1146/annurev-pathol-030220-020455

3. Kendall T, Verheij J, Gaudio E, Evert M, Guido M, Goeppert B, et al. Anatomical, histomorphological and molecular classification of cholangiocarcinoma. *Liver Int* (2019) 39 Suppl 1:7–18. doi: 10.1111/liv.14093

4. Banales JM, Marin JJG, Lamarca A, Rodrigues PM, Khan SA, Roberts LR, et al. Cholangiocarcinoma 2020: the next horizon in mechanisms and management. *Nat Rev Gastroenterol Hepatol* (2020) 17(9):557–88. doi: 10.1038/s41575-020-0310-z

5. Song G, Shi Y, Meng L, Ma J, Huang S, Zhang J, et al. Single-cell transcriptomic analysis suggests two molecularly subtypes of intrahepatic cholangiocarcinoma. *Nat Commun* (2022) 13(1):1642. doi: 10.1038/s41467-022-29164-0

6. Vithayathil M, Khan SA. Current epidemiology of cholangiocarcinoma in Western countries. *J Hepatol* (2022) 77(6):1690–8. doi: 10.1016/j.jhep.2022.07.022

7. Komaya K, Ebata T, Shirai K, Ohira S, Morofuji N, Akutagawa A, et al. Recurrence after resection with curative intent for distal cholangiocarcinoma. *Br J Surg* (2017) 104(4):426–33. doi: 10.1002/bjs.10452

8. Nakachi K, Ikeda M, Konishi M, Nomura S, Katayama H, Kataoka T, et al. Adjuvant s-1 compared with observation in resected biliary tract cancer (Jcog1202, ascot): a multicentre, open-label, randomised, controlled, phase 3 trial. *Lancet* (2023) 401(10372):195–203. doi: 10.1016/S0140-6736(22)02038-4

9. Florio AA, Ferlay J, Znaor A, Ruggieri D, Alvarez CS, Laversanne M, et al. Global trends in intrahepatic and extrahepatic cholangiocarcinoma incidence from 1993 to 2012. *Cancer* (2020) 126(11):2666–78. doi: 10.1002/cncr.32803

10. Siegel RL, Miller KD, Fuchs HE, Jemal A. Cancer statistics, 2022. *CA Cancer J Clin* (2022) 72(1):7–33. doi: 10.3322/caac.21708

11. Rizvi S, Khan SA, Hallemeier CL, Kelley RK, Gores GJ. Cholangiocarcinoma - evolving concepts and therapeutic strategies. *Nat Rev Clin Oncol* (2018) 15(2):95–111. doi: 10.1038/nrclinonc.2017.157

12. Khan SA, Tavolari S, Brandi G. Cholangiocarcinoma: epidemiology and risk factors. *Liver Int* (2019) 39 Suppl 1:19–31. doi: 10.1111/liv.14095

13. Piegari G. The who's global clinical practice network and the icd-11 implementation. *World Psychiatry* (2021) 20(2):313–4. doi: 10.1002/wps.20866

14. Ali H, Zweigle J, Patel P, Tedder B, Khan R, Agrawal S. Survival analysis of extrahepatic cholangiocarcinoma based on surveillance, epidemiology, and end results database. *Ann Hepatobiliary Pancreat Surg* (2023). doi: 10.14701/ahbps.22-090

15. Rahman R, Ludvigsson JF, von Seth E, Lagergren J, Bergquist A, Radkiewicz C. Age trends in biliary tract cancer incidence by anatomical subtype: a Swedish cohort study. *Eur J Cancer* (2022) 175:291–8. doi: 10.1016/j.ejca.2022.08.032

16. Clements O, Eliahoo J, Kim JU, Taylor-Robinson SD, Khan SA. Risk factors for intrahepatic and extrahepatic cholangiocarcinoma: a systematic review and meta-analysis. *J Hepatol* (2020) 72(1):95–103. doi: 10.1016/j.jhep.2019.09.007

17. Park JH, Hong JY, Park YS, Kang G, Han K, Park JO. Association of prediabetes, diabetes, and diabetes duration with biliary tract cancer risk: a nationwide cohort study. *Metabolism* (2021) 123:154848. doi: 10.1016/j.metabol.2021.154848

18. Park JH, Hong JY, Kwon M, Lee J, Han K, Han IW, et al. Association between non-alcoholic fatty liver disease and the risk of biliary tract cancers: a south Korean nationwide cohort study. *Eur J Cancer* (2021) 150:73–82. doi: 10.1016/j.ejca.2021.03.024

19. Park JH, Hong JY, Han K, Park YS, Park JO. Light-to-Moderate alcohol consumption increases the risk of biliary tract cancer in prediabetes and diabetes, but not in normoglycemic status: a nationwide cohort study. *J Clin Oncol* (2022) 40 (31):3623–32. doi: 10.1200/JCO.22.00145

20. Izquierdo-Sanchez L, Lamarca A, La Casta A, Buettner S, Utpatel K, Klumpen HJ, et al. Cholangiocarcinoma landscape in Europe: diagnostic, prognostic and therapeutic insights from the enscca registry. *J Hepatol* (2022) 76(5):1109–21. doi: 10.1016/j.jhep.2021.12.010

21. Lavu S, Therneau TM, Harmsen WS, Mara KC, Wongjarupong N, Hassan M, et al. Effect of statins on the risk of extrahepatic cholangiocarcinoma. *Hepatology* (2020) 72(4):1298–309. doi: 10.1002/hep.31146

22. Liao SF, Koshiol J, Huang YH, Jackson SS, Huang YH, Chan C, et al. Postdiagnosis aspirin use associated with decreased biliary tract cancer-specific mortality in a Large nationwide cohort. *Hepatology* (2021) 74(4):1994–2006. doi: 10.1002/hep.31879

23. Kim MH, Park SM, Chang J, Hwang IC. Association between aspirin and cholangiocarcinoma in a Large Asian cohort. *JAMA Oncol* (2020) 6(12):1974–6. doi: 10.1001/jamaoncol.2020.5018

24. Marcano-Bonilla L, Schleck CD, Harmsen WS, Sadr-Azodi O, Borad MJ, Patel T, et al. Aspirin, statins, non-aspirin nsaids, metformin, and the risk of biliary cancer: a Swedish population-based cohort study. *Cancer Epidemiol Biomarkers Prev* (2022) 31 (4):804–10. doi: 10.1158/1055-9965.EPI-20-1322

25. Kamal H, Sadr-Azodi O, Engstrand L, Brusselaers N. Association between proton pump inhibitor use and biliary tract cancer risk: a Swedish population-based cohort study. *Hepatology* (2021) 74(4):2021–31. doi: 10.1002/hep.31914

26. Bowlus CL, Olson KA, Gershwin ME. Evaluation of indeterminate biliary strictures. *Nat Rev Gastroenterol Hepatol* (2017) 14(12):749. doi: 10.1038/nrgastro.2017.154

27. Blechacz B, Komuta M, Roskams T, Gores GJ. Clinical diagnosis and staging of cholangiocarcinoma. *Nat Rev Gastroenterol Hepatol* (2011) 8(9):512–22. doi: 10.1038/nrgastro.2011.131

28. Joo I, Lee JM, Yoon JH. Imaging diagnosis of intrahepatic and perihilar cholangiocarcinoma: recent advances and challenges. *Radiology* (2018) 288(1):7–13. doi: 10.1148/radiol.2018171187

29. Beyer G, Kasprowicz F, Hannemann A, Aghdassi A, Thamm P, Volzke H, et al. Definition of age-dependent reference values for the diameter of the common bile duct and pancreatic duct on mrcp: a population-based, cross-sectional cohort study. *Gut* (2023). doi: 10.1136/gutjnl-2021-326106

30. Cadamuro M, Al-Taee A, Gonda TA. Advanced endoscopy meets molecular diagnosis of cholangiocarcinoma. *J Hepatol* (2023). doi: 10.1016/j.jhep.2023.01.027

31. Park MS, Kim TK, Kim KW, Park SW, Lee JK, Kim JS, et al. Differentiation of extrahepatic bile duct cholangiocarcinoma from benign stricture: findings at mrcp versus ercp. *Radiology* (2004) 233(1):234–40. doi: 10.1148/radiol.2331031446

32. Coronel M, Lee JH, Coronel E. Endoscopic ultrasound for the diagnosis and staging of biliary malignancy. *Clin Liver Dis* (2022) 26(1):115–25. doi: 10.1016/j.cld.2021.08.010

33. Sadeghi A, Mohamadnejad M, Islami F, Keshtkar A, Biglari M, Malekzadeh R, et al. Diagnostic yield of eus-guided fna for malignant biliary stricture: a systematic

review and meta-analysis. *Gastrointest Endosc* (2016) 83(2):290–8 e1. doi: 10.1016/j.gie.2015.09.024

34. Draganov PV, Chauhan S, Wagh MS, Gupte AR, Lin T, Hou W, et al. Diagnostic accuracy of conventional and cholangioscopy-guided sampling of indeterminate biliary lesions at the time of ercp: a prospective, long-term follow-up study. *Gastrointest Endosc* (2012) 75(2):347–53. doi: 10.1016/j.gie.2011.09.020

35. Ishii T, Kaneko T, Murakami A, Ueda M, Sugimori K, Kawana I, et al. New image-enhanced cholangioscopy for the diagnosis of cholangiocarcinoma. *Endoscopy* (2023) 55(S 01):E139–E40. doi: 10.1055/a-1956-0967

36. Gorji L, Beal EW. Surgical treatment of distal cholangiocarcinoma. *Curr Oncol* (2022) 29(9):6674–87. doi: 10.3390/curroncol29090524

37. Hewitt DB, Brown ZJ, Pawlik TM. Current perspectives on the surgical management of perihilar cholangiocarcinoma. *Cancers (Basel)* (2022) 14(9):2208. doi: 10.3390/cancers14092208

38. Hou JJ, Maithel SK, Weber SM, Poultsides G, Wolfgang CL, Fields RC, et al. Impact of adjuvant therapy on outcomes after curative-intent resection for distal cholangiocarcinoma. *J Surg Oncol* (2023) 127(4):607–15. doi: 10.1002/jso.27146

39. Kamarajah SK, Bednar F, Cho CS, Nathan H. Survival benefit with adjuvant radiotherapy after resection of distal cholangiocarcinoma: a propensity-matched national cancer database analysis. *Cancer* (2021) 127(8):1266–74. doi: 10.1002/cncr.33356

40. Steel AW, Postgate AJ, Khorsandi S, Nicholls J, Jiao L, Vlavianos P, et al. Endoscopically applied radiofrequency ablation appears to be safe in the treatment of malignant biliary obstruction. *Gastrointest Endosc* (2011) 73(1):149–53. doi: 10.1016/j.gie.2010.09.031

41. Yarlagadda B, Kamatham V, Ritter A, Shahjehan F, Kasi PM. Trastuzumab and pertuzumab in circulating tumor DNA Erbb2-amplified Her2-positive refractory cholangiocarcinoma. *NPJ Precis Oncol* (2019) 3:19. doi: 10.1038/s41698-019-0091-4

42. Greten TF, Schwabe R, Bardeesy N, Ma L, Goyal L, Kelley RK, et al. Immunology and immunotherapy of cholangiocarcinoma. *Nat Rev Gastroenterol Hepatol* (2023). doi: 10.1038/s41575-022-00741-4

43. Chen Z, Yu B, Bai J, Li Q, Xu B, Dong Z, et al. The impact of intraoperative frozen section on resection margin status and survival of patients underwent pancreatoduodenectomy for distal cholangiocarcinoma. *Front Oncol* (2021) 11:650585. doi: 10.3389/fonc.2021.650585

44. Belkouz A, Van Roessel S, Strijker M, van Dam JL, Daamen L, van der Geest LG, et al. Development and external validation of a prediction model for overall survival after resection of distal cholangiocarcinoma. *Br J Cancer* (2022) 126(9):1280–8. doi: 10.1038/s41416-021-01687-1

45. Ogino M, Nakanishi Y, Mitsuhashi T, Hatanaka Y, Amano T, Marukawa K, et al. Impact of tumour budding grade in 310 patients who underwent surgical resection for extrahepatic cholangiocarcinoma. *Histopathology* (2019) 74(6):861–72. doi: 10.1111/his.13827

46. Zhao Y, Nakanishi Y, Ogino M, Oba M, Okamura K, Tsuchikawa T, et al. Validation study of tumor invasive thickness for postoperative prognosis in 110 patients who underwent pancreatoduodenectomy for distal cholangiocarcinoma at a single institution. *Am J Surg Pathol* (2019) 43(5):717–23. doi: 10.1097/PAS.0000000000001244

47. Bednarsch J, Kather J, Tan X, Sivakumar S, Cacchi C, Wiltberger G, et al. Nerve fibers in the tumor microenvironment as a novel biomarker for oncological outcome in patients undergoing surgery for perihilar cholangiocarcinoma. *Liver Cancer* (2021) 10(3):260–74. doi: 10.1159/000515303

48. Mori S, Aoki T, Park KH, Shiraki T, Sakuraoka Y, Iso Y, et al. Impact of preoperative percutaneous transhepatic biliary drainage on post-operative survival in patients with distal cholangiocarcinoma. *ANZ J Surg* (2019) 89(9):E363–E7. doi: 10.1111/ans.15329

49. Coelen RJS, Roos E, Wiggers JK, Besselink MG, Buis CI, Busch ORC, et al. Endoscopic versus percutaneous biliary drainage in patients with resectable perihilar cholangiocarcinoma: a multicentre, randomised controlled trial. *Lancet Gastroenterol Hepatol* (2018) 3(10):681–90. doi: 10.1016/S2468-1253(18)30234-6

50. Al Mahjoub A, Menahem B, Fohlen A, Dupont B, Alves A, Launoy G, et al. Preoperative biliary drainage in patients with resectable perihilar cholangiocarcinoma: is percutaneous transhepatic biliary drainage safer and more effective than endoscopic biliary drainage? a meta-analysis. *J Vasc Interv Radiol* (2017) 28(4):576–82. doi: 10.1016/j.jvir.2016.12.1218

51. Li S, Zhang X, Lou C, Gu Y, Zhao J. Preoperative peripheral blood inflammatory markers especially the fibrinogen-to-Lymphocyte ratio and novel flr-n score predict the prognosis of patients with early-stage resectable extrahepatic cholangiocarcinoma. *Front Oncol* (2022) 12:1003845. doi: 10.3389/fonc.2022.1003845

52. Ebata T, Hirano S, Konishi M, Uesaka K, Tsuchiya Y, Ohtsuka M, et al. Randomized clinical trial of adjuvant gemcitabine chemotherapy versus observation in resected bile duct cancer. *Br J Surg* (2018) 105(3):192–202. doi: 10.1002/bjs.10776

53. Gholami S, Colby S, Horowitz DP, Guthrie KA, Ben-Josef E, El-Khoueiry AB, et al. Adjuvant chemoradiation in patients with lymph node-positive biliary tract cancers: secondary analysis of a single-arm clinical trial (Swog 0809). *Ann Surg Oncol* (2023) 30(3):1354–63. doi: 10.1245/s10434-022-12863-9

54. Yang J, Wang J, Zhou H, Zhou Y, Wang Y, Jin H, et al. Efficacy and safety of endoscopic radiofrequency ablation for unresectable extrahepatic cholangiocarcinoma: a randomized trial. *Endoscopy* (2018) 50(8):751–60. doi: 10.1055/s-0043-124870

55. Gao DJ, Yang JF, Ma SR, Wu J, Wang TT, Jin HB, et al. Endoscopic radiofrequency ablation plus plastic stent placement versus stent placement alone for unresectable extrahepatic biliary cancer: a multicenter randomized controlled trial. *Gastrointest Endosc* (2021) 94(1):91–100 e2. doi: 10.1016/j.gie.2020.12.016

56. Yang J, Wang J, Zhou H, Wang Y, Huang H, Jin H, et al. Endoscopic radiofrequency ablation plus a novel oral 5-fluorouracil compound versus radiofrequency ablation alone for unresectable extrahepatic cholangiocarcinoma. *Gastrointest Endosc* (2020) 92(6):1204–12 e1. doi: 10.1016/j.gie.2020.04.075

57. Lee J, Park SH, Chang HM, Kim JS, Choi HJ, Lee MA, et al. Gemcitabine and oxaliplatin with or without erlotinib in advanced biliary-tract cancer: a multicentre, open-label, randomised, phase 3 study. *Lancet Oncol* (2012) 13(2):181–8. doi: 10.1016/S1470-2045(11)70301-1

58. Chen JS, Hsu C, Chiang NJ, Tsai CS, Tsou HH, Huang SF, et al. A kras mutation status-stratified randomized phase ii trial of gemcitabine and oxaliplatin alone or in combination with cetuximab in advanced biliary tract cancer. *Ann Oncol* (2015) 26(5):943–9. doi: 10.1093/annonc/mdv035

59. Vogel A, Kasper S, Bitzer M, Block A, Sinn M, Schulze-Bergkamen H, et al. Picca study: panitumumab in combination with Cisplatin/Gemcitabine chemotherapy in kras wild-type patients with biliary cancer-a randomised biomarker-driven clinical phase ii aio study. *Eur J Cancer* (2018) 92:11–9. doi: 10.1016/j.ejca.2017.12.028

60. Leone F, Marino D, Cereda S, Filippi R, Belli C, Spadi R, et al. Panitumumab in combination with gemcitabine and oxaliplatin does not prolong survival in wild-type kras advanced biliary tract cancer: a randomized phase 2 trial (Vecti-bil study). *Cancer* (2016) 122(4):574–81. doi: 10.1002/cncr.29778

61. Piha-Paul SA, Oh DY, Ueno M, Malka D, Chung HC, Nagrial A, et al. Efficacy and safety of pembrolizumab for the treatment of advanced biliary cancer: results from the keynote-158 and keynote-028 studies. *Int J Cancer* (2020) 147(8):2190–8. doi: 10.1002/ijc.33013

62. Kim RD, Chung V, Alese OB, El-Rayes BF, Li D, Al-Toubah TE, et al. A phase 2 multi-institutional study of nivolumab for patients with advanced refractory biliary tract cancer. *JAMA Oncol* (2020) 6(6):888–94. doi: 10.1001/jamaoncol.2020.0930

63. Yarchoan M, Cope L, Ruggieri AN, Anders RA, Noonan AM, Goff LW, et al. Multicenter randomized phase ii trial of atezolizumab with or without cobimetinib in biliary tract cancers. *J Clin Invest* (2021) 131(24). doi: 10.1172/JCI152670

64. Meyer CG, Penn I, James L. Liver transplantation for cholangiocarcinoma: results in 207 patients. *Transplantation* (2000) 69(8):1633–7. doi: 10.1097/00007890-200004270-00019

65. Rizzo A, Brandi G. Neoadjuvant therapy for cholangiocarcinoma: a comprehensive literature review. *Cancer Treat Res Commun* (2021) 27:100354. doi: 10.1016/j.ctarc.2021.100354

66. Cambridge WA, Fairfield C, Powell JJ, Harrison EM, Soreide K, Wigmore SJ, et al. Meta-analysis and meta-regression of survival after liver transplantation for unresectable perihilar cholangiocarcinoma. *Ann Surg* (2021) 273(2):240–50. doi: 10.1097/SLA.0000000000003801

67. Xia MX, Cai XB, Pan YL, Wu J, Gao DJ, Ye X, et al. Optimal stent placement strategy for malignant hilar biliary obstruction: a Large multicenter parallel study. *Gastrointest Endosc* (2020) 91(5):1117–28 e9. doi: 10.1016/j.gie.2019.12.023

68. Xia MX, Wang SP, Yuan JG, Gao DJ, Ye X, Wang TT, et al. Effect of endoscopic radiofrequency ablation on the survival of patients with inoperable malignant biliary strictures: a Large cohort study. *J Hepatobiliary Pancreat Sci* (2022) 29(6):693–702. doi: 10.1002/jhbp.960

69. Xia M, Qin W, Hu B. Endobiliary radiofrequency ablation for unresectable malignant biliary strictures: a survival benefit perspective. *Dig Endosc* (2023). doi: 10.1111/den.14542

70. Inoue T, Naitoh I, Kitano R, Ibusuki M, Kobayashi Y, Sumida Y, et al. Endobiliary radiofrequency ablation combined with gemcitabine and cisplatin in patients with unresectable extrahepatic cholangiocarcinoma. *Curr Oncol* (2022) 29(4):2240–51. doi: 10.3390/curroncol29040182

71. Gonzalez-Carmona MA, Mohring C, Mahn R, Zhou T, Bartels A, Sadeghlar F, et al. Impact of regular additional endobiliary radiofrequency ablation on survival of patients with advanced extrahepatic cholangiocarcinoma under systemic chemotherapy. *Sci Rep* (2022) 12(1):1011. doi: 10.1038/s41598-021-04297-2

72. Kang B, Camps J, Fan B, Jiang H, Ibrahim MM, Hu X, et al. Parallel single-cell and bulk transcriptome analyses reveal key features of the gastric tumor microenvironment. *Genome Biol* (2022) 23(1):265. doi: 10.1186/s13059-022-02828-2

73. Boulter L, Guest RV, Kendall TJ, Wilson DH, Wojtacha D, Robson AJ, et al. Wnt signaling drives cholangiocarcinoma growth and can be pharmacologically inhibited. *J Clin Invest* (2015) 125(3):1269–85. doi: 10.1172/JCI76452

74. Atanasov G, Hau HM, Dietel C, Benzing C, Krenzien F, Brandl A, et al. Prognostic significance of macrophage invasion in hilar cholangiocarcinoma. *BMC Cancer* (2015) 15:790. doi: 10.1186/s12885-015-1795-7

75. Xia T, Li K, Niu N, Shao Y, Ding D, Thomas DL, et al. Immune cell atlas of cholangiocarcinomas reveals distinct tumor microenvironments and associated prognoses. *J Hematol Oncol* (2022) 15(1):37. doi: 10.1186/s13045-022-01253-z

76. Xu L, Lu Y, Deng Z, Li X, Shi Y, Zhao K, et al. Single-cell landscape of immunocytes in patients with extrahepatic cholangiocarcinoma. *J Transl Med* (2022) 20(1):210. doi: 10.1186/s12967-022-03424-5

77. Jung IH, Kim DH, Yoo DK, Baek SY, Jeong SH, Jung DE, et al. *In Vivo* Study of natural killer (Nk) cell cytotoxicity against cholangiocarcinoma in a nude mouse model. *In Vivo* (2018) 32(4):771–81. doi: 10.21873/invivo.11307

78. Kitano Y, Okabe H, Yamashita YI, Nakagawa S, Saito Y, Umezaki N, et al. Tumour-infiltrating inflammatory and immune cells in patients with extrahepatic cholangiocarcinoma. *Br J Cancer* (2018) 118(2):171–80. doi: 10.1038/bjc.2017.401

79. Toyoda J, Sahara K, Maithel SK, Abbott DE, Poultsides GA, Wolfgang C, et al. Prognostic utility of systemic immune-inflammation index after resection of extrahepatic cholangiocarcinoma: results from the U.S. extrahepatic biliary malignancy consortium. *Ann Surg Oncol* (2022) 29(12):7605–14. doi: 10.1245/s10434-022-12058-2

80. Gao Y, Zhang H, Zhou N, Xu P, Wang J, Gao Y, et al. Methotrexate-loaded tumour-Cell-Derived microvesicles can relieve biliary obstruction in patients with extrahepatic cholangiocarcinoma. *Nat BioMed Eng* (2020) 4(7):743–53. doi: 10.1038/s41551-020-0583-0

81. Xue R, Zhang Q, Cao Q, Kong R, Xiang X, Liu H, et al. Liver tumour immune microenvironment subtypes and neutrophil heterogeneity. *Nature* (2022) 612 (7938):141–7. doi: 10.1038/s41586-022-05400-x

82. Liu D, Heij LR, Czigany Z, Dahl E, Lang SA, Ulmer TF, et al. The role of tumor-infiltrating lymphocytes in cholangiocarcinoma. *J Exp Clin Cancer Res* (2022) 41 (1):127. doi: 10.1186/s13046-022-02340-2

83. Goeppert B, Frauenschuh L, Zucknick M, Stenzinger A, Andrulis M, Klauschen F, et al. Prognostic impact of tumour-infiltrating immune cells on biliary tract cancer. *Br J Cancer* (2013) 109(10):2665–74. doi: 10.1038/bjc.2013.610

84. Ueno T, Tsuchikawa T, Hatanaka KC, Hatanaka Y, Mitsuhashi T, Nakanishi Y, et al. Prognostic impact of programmed cell death ligand 1 (Pd-L1) expression and its association with epithelial-mesenchymal transition in extrahepatic cholangiocarcinoma. *Oncotarget* (2018) 9(28):20034–47. doi: 10.18632/oncotarget.25050

85. Ma K, Sun Z, Li X, Guo J, Wang Q, Teng M. Forkhead box M1 recruits Foxp3(+) treg cells to induce immune escape in hilar cholangiocarcinoma. *Immun Inflammation Dis* (2022) 10(11):e727. doi: 10.1002/iid3.727

86. Li H, Qu L, Yang Y, Zhang H, Li X, Zhang X. Single-cell transcriptomic architecture unraveling the complexity of tumor heterogeneity in distal cholangiocarcinoma. *Cell Mol Gastroenterol Hepatol* (2022) 13(5):1592–609 e9. doi: 10.1016/j.jcmgh.2022.02.014

87. Zimmer CL, Filipovic I, Cornillet M, O'Rourke CJ, Berglin L, Jansson H, et al. Mucosal-associated invariant T-cell tumor infiltration predicts long-term survival in cholangiocarcinoma. *Hepatology* (2022) 75(5):1154–68. doi: 10.1002/hep.32222

88. Zhang FP, Zhu K, Zhu TF, Liu CQ, Zhang HH, Xu LB, et al. Intra-tumoral secondary follicle-like tertiary lymphoid structures are associated with a superior prognosis of overall survival of perihilar cholangiocarcinoma. *Cancers (Basel)* (2022) 14(24):6107. doi: 10.3390/cancers14246107

89. Montori M, Scorzoni C, Argenziano ME, Balducci D, De Blasio F, Martini F, et al. Cancer-associated fibroblasts in cholangiocarcinoma: current knowledge and possible implications for therapy. *J Clin Med* (2022) 11(21):6498. doi: 10.3390/jcm11216498

90. Ying F, Man Chan MS, Wah Lee TK. Cancer-associated fibroblasts in hepatocellular carcinoma and cholangiocarcinoma. *Cell Mol Gastroenterol Hepatol* (2023) 15(4):985–99. doi: 10.1016/j.jcmgh.2023.01.006

91. Gundlach JP, Kerber J, Hendricks A, Bernsmeier A, Halske C, Roder C, et al. Paracrine interaction of cholangiocellular carcinoma with cancer-associated fibroblasts and schwann cells impact cell migration. *J Clin Med* (2022) 11(10):2785. doi: 10.3390/jcm11102785

92. Sun L, Wang Y, Wang X, Navarro-Corcuera A, Ilyas S, Jalan-Sakrikar N, et al. Pd-L1 promotes myofibroblastic activation of hepatic stellate cells by distinct mechanisms selective for tgf-beta receptor I versus ii. *Cell Rep* (2022) 38(6):110349. doi: 10.1016/j.celrep.2022.110349

93. Olaizola P, Lee-Law PY, Fernandez-Barrena MG, Alvarez L, Cadamuro M, Azkargorta M, et al. Targeting Nae1-mediated protein hyper-neddylation halts cholangiocarcinogenesis and impacts on tumor-stroma crosstalk in experimental models. *J Hepatol* (2022) 77(1):177–90. doi: 10.1016/j.jhep.2022.02.007

94. Simbolo M, Bersani S, Vicentini C, Taormina SV, Ciaparrone C, Bagante F, et al. Molecular characterization of extrahepatic cholangiocarcinoma: perihilar and distal tumors display divergent genomic and transcriptomic profiles. *Expert Opin Ther Targets* (2021) 25(12):1095–105. doi: 10.1080/14728222.2021.2013801

95. Silva VW, Askan G, Daniel TD, Lowery M, Klimstra DS, Abou-Alfa GK, et al. Biliary carcinomas: pathology and the role of DNA mismatch repair deficiency. *Chin Clin Oncol* (2016) 5(5):62. doi: 10.21037/cco.2016.10.04

96. Montal R, Sia D, Montironi C, Leow WQ, Esteban-Fabro R, Pinyol R, et al. Molecular classification and therapeutic targets in extrahepatic cholangiocarcinoma. *J Hepatol* (2020) 73(2):315–27. doi: 10.1016/j.jhep.2020.03.008

97. Lowery MA, Ptashkin R, Jordan E, Berger MF, Zehir A, Capanu M, et al. Comprehensive molecular profiling of intrahepatic and extrahepatic cholangiocarcinomas: potential targets for intervention. *Clin Cancer Res* (2018) 24 (17):4154–61. doi: 10.1158/1078-0432.CCR-18-0078

98. Nakamura H, Arai Y, Totoki Y, Shirota T, Elzawahry A, Kato M, et al. Genomic spectra of biliary tract cancer. *Nat Genet* (2015) 47(9):1003–10. doi: 10.1038/ng.3375

99. Simbolo M, Fassan M, Ruzzenente A, Mafficini A, Wood LD, Corbo V, et al. Multigene mutational profiling of cholangiocarcinomas identifies actionable molecular subgroups. *Oncotarget* (2014) 5(9):2839–52. doi: 10.18632/oncotarget.1943

100. Rizzato M, Brignola S, Munari G, Gatti M, Dadduzio V, Borga C, et al. Prognostic impact of Fgfr2/3 alterations in patients with biliary tract cancers receiving systemic chemotherapy: the bitcoin study. *Eur J Cancer* (2022) 166:165–75. doi: 10.1016/j.ejca.2022.02.013

101. Zhang Y, Ma Z, Li C, Wang C, Jiang W, Chang J, et al. The genomic landscape of cholangiocarcinoma reveals the disruption of post-transcriptional modifiers. *Nat Commun* (2022) 13(1):3061. doi: 10.1038/s41467-022-30708-7

102. Deng M, Ran P, Chen L, Wang Y, Yu Z, Cai K, et al. Proteogenomic characterization of cholangiocarcinoma. *Hepatology* (2023) 77(2):411–29. doi: 10.1002/hep.32624

103. Berchuck JE, Facchinetti F, DiToro DF, Baiev I, Majeed U, Reyes S, et al. The clinical landscape of cell-free DNA alterations in 1671 patients with advanced biliary tract cancer. *Ann Oncol* (2022) 33(12):1269–83. doi: 10.1016/j.annonc.2022.09.150

104. Hu S, Molina L, Tao J, Liu S, Hassan M, Singh S, et al. Notch-Yap1/Tead-Dnmt1 axis drives hepatocyte reprogramming into intrahepatic cholangiocarcinoma. *Gastroenterology* (2022) 163(2):449–65. doi: 10.1053/j.gastro.2022.05.007

105. Aoki S, Mizuma M, Takahashi Y, Haji Y, Okada R, Abe T, et al. Aberrant activation of notch signaling in extrahepatic cholangiocarcinoma: clinicopathological features and therapeutic potential for cancer stem cell-like properties. *BMC Cancer* (2016) 16(1):854. doi: 10.1186/s12885-016-2919-4

106. Gingras MC, Covington KR, Chang DK, Donehower LA, Gill AJ, Ittmann MM, et al. Ampullary cancers harbor Elf3 tumor suppressor gene mutations and exhibit frequent wnt dysregulation. *Cell Rep* (2016) 14(4):907–19. doi: 10.1016/j.celrep.2015.12.005

107. Shi Z, Zhou L, Zhou Y, Jia X, Yu X, An X, et al. Inhibition of clc-5 suppresses proliferation and induces apoptosis in cholangiocarcinoma cells through the Wnt/Beta-catenin signaling pathway. *BMB Rep* (2022) 55(6):299–304. doi: 10.5483/BMBRep.2022.55.6.044

108. Xue W, Dong B, Zhao Y, Wang Y, Yang C, Xie Y, et al. Upregulation of Ttyh3 promotes epithelial-to-Mesenchymal transition through Wnt/Beta-catenin signaling and inhibits apoptosis in cholangiocarcinoma. *Cell Oncol (Dordr)* (2021) 44(6):1351–61. doi: 10.1007/s13402-021-00642-9

109. Zhang F, Wan M, Xu Y, Li Z, Leng K, Kang P, et al. Long noncoding rna Pcat1 regulates extrahepatic cholangiocarcinoma progression *Via* the Wnt/Beta-Catenin-Signaling pathway. *BioMed Pharmacother* (2017) 94:55–62. doi: 10.1016/j.biopha.2017.07.025

110. Merino-Azpitarte M, Lozano E, Perugorria MJ, Esparza-Baquer A, Erice O, Santos-Laso A, et al. Sox17 regulates cholangiocyte differentiation and acts as a tumor suppressor in cholangiocarcinoma. *J Hepatol* (2017) 67(1):72–83. doi: 10.1016/j.jhep.2017.02.017

111. Lozano E, Asensio M, Perez-Silva L, Banales JM, Briz O, Marin JJG. Mrp3-mediated chemoresistance in cholangiocarcinoma: target for chemosensitization through restoring Sox17 expression. *Hepatology* (2020) 72(3):949–64. doi: 10.1002/hep.31088

112. Xiong F, Liu W, Wang X, Wu G, Wang Q, Guo T, et al. Hoxa5 inhibits the proliferation of extrahepatic cholangiocarcinoma cells by enhancing Mxd1 expression and activating the P53 pathway. *Cell Death Dis* (2022) 13(9):829. doi: 10.1038/s41419-022-05279-6

113. Dhanasekaran R, Deutzmann A, Mahauad-Fernandez WD, Hansen AS, Gouw AM, Felsher DW. The myc oncogene - the grand orchestrator of cancer growth and immune evasion. *Nat Rev Clin Oncol* (2022) 19(1):23–36. doi: 10.1038/s41571-021-00549-2

114. Li Z, Liu J, Chen T, Sun R, Liu Z, Qiu B, et al. Hmga1-Trip13 axis promotes stemness and epithelial mesenchymal transition of perihilar cholangiocarcinoma in a positive feedback loop dependent on c-myc. *J Exp Clin Cancer Res* (2021) 40(1):86. doi: 10.1186/s13046-021-01890-1

115. Liu Z, Sun R, Zhang X, Qiu B, Chen T, Li Z, et al. Transcription factor 7 promotes the progression of perihilar cholangiocarcinoma by inducing the transcription of c-myc and fos-like antigen 1. *EBioMedicine* (2019) 45:181–91. doi: 10.1016/j.ebiom.2019.06.023

116. Chen T, Li K, Liu Z, Liu J, Wang Y, Sun R, et al. Wdr5 facilitates emt and metastasis of cca by increasing hif-1alpha accumulation in myc-dependent and independent pathways. *Mol Ther* (2021) 29(6):2134–50. doi: 10.1016/j.ymthe.2021.02.017

117. Wappler J, Arts M, Roth A, Heeren RMA, Peter Neumann U, Olde Damink SW, et al. Glutamine deprivation counteracts hypoxia-induced chemoresistance. *Neoplasia* (2020) 22(1):22–32. doi: 10.1016/j.neo.2019.10.004

118. Ruiz de Gauna M, Biancaniello F, Gonzalez-Romero F, Rodrigues PM, Lapitz A, Gomez-Santos B, et al. Cholangiocarcinoma progression depends on the uptake and metabolization of extracellular lipids. *Hepatology* (2022) 76(6):1617–33. doi: 10.1002/hep.32344

119. Nakagawa R, Hiep NC, Ouchi H, Sato Y, Harada K. Expression of fatty-Acid-Binding protein 5 in intrahepatic and extrahepatic cholangiocarcinoma: the possibility of different energy metabolisms in anatomical location. *Med Mol Morphol* (2020) 53 (1):42–9. doi: 10.1007/s00795-019-00230-9

120. Jiao CY, Feng QC, Li CX, Wang D, Han S, Zhang YD, et al. Bub1b promotes extrahepatic cholangiocarcinoma progression *Via* Jnk/C-jun pathways. *Cell Death Dis* (2021) 12(1):63. doi: 10.1038/s41419-020-03234-x

121. Chen XX, Yin Y, Cheng JW, Huang A, Hu B, Zhang X, et al. Bap1 acts as a tumor suppressor in intrahepatic cholangiocarcinoma by modulating the Erk1/2 and Jnk/C-jun pathways. *Cell Death Dis* (2018) 9(10):1036. doi: 10.1038/s41419-018-1087-7

122. Shimura T, Shibata M, Gonda K, Kofunato Y, Okada R, Ishigame T, et al. Clinical significance of soluble intercellular adhesion molecule-1 and interleukin-6 in patients with extrahepatic cholangiocarcinoma. *J Invest Surg* (2018) 31(6):475–82. doi: 10.1080/08941939.2017.1358310

123. Lurje I, Czigany Z, Bednarsch J, Gaisa NT, Dahl E, Knuchel R, et al. Genetic variant of Cxcr1 (Rs2234671) associates with clinical outcome in perihilar cholangiocarcinoma. *Liver Cancer* (2022) 11(2):162–73. doi: 10.1159/000521613

124. Yoshikawa D, Ojima H, Iwasaki M, Hiraoka N, Kosuge T, Kasai S, et al. Clinicopathological and prognostic significance of egfr, vegf, and Her2 expression in cholangiocarcinoma. *Br J Cancer* (2008) 98(2):418–25. doi: 10.1038/sj.bjc.6604129

125. Li T, Tian Y, Ren W, Chen P, Luo M, Sang H. Gab1 regulates invadopodia and autocrine vegf through Shp2/Erk1/2 in hilar cholangiocarcinoma cells. *Am J Transl Res* (2022) 14(12):8934–46.

126. Batlle E, Clevers H. Cancer stem cells revisited. *Nat Med* (2017) 23(10):1124–34. doi: 10.1038/nm.4409

127. Shuang ZY, Wu WC, Xu J, Lin G, Liu YC, Lao XM, et al. Transforming growth factor-Beta1-Induced epithelial-mesenchymal transition generates aldh-positive cells with stem cell properties in cholangiocarcinoma. *Cancer Lett* (2014) 354(2):320–8. doi: 10.1016/j.canlet.2014.08.030

128. Yang J, Sontag DP, Burczynski FJ, Xi S, Gong Y, Minuk GY. Comparison of growth features and cancer stem cell prevalence in intrahepatic and extrahepatic cholangiocarcinoma cell lines. *Clin Exp Hepatol* (2022) 8(1):60–9. doi: 10.5114/ceh.2022.114192

129. Gringeri E, Biasiolo A, Di Giunta M, Mescoli C, Guzzardo V, Sartori A, et al. Bile detection of squamous cell carcinoma antigen (Scca) in extrahepatic cholangiocarcinoma. *Dig Liver Dis* (2022) 55(4):534–40. doi: 10.1016/j.dld.2022.10.010

130. Uchihata Y, Arihiro K, Kaneko Y, Shimizu T, Marubashi Y, Aoki C, et al. Analysis of microrna in bile cytologic samples is useful for detection and diagnosis of extrahepatic cholangiocarcinoma. *Am J Clin Pathol* (2022) 158(1):122–31. doi: 10.1093/ajcp/aqac015

131. Hoffmeister-Wittmann P, Mock A, Nichetti F, Korell F, Heilig CE, Scherr AL, et al. Bcl-X(L) as prognostic marker and potential therapeutic target in cholangiocarcinoma. *Liver Int* (2022) 42(12):2855–70. doi: 10.1111/liv.15392

132. Yamamoto R, Sugiura T, Ashida R, Ohgi K, Yamada M, Otsuka S, et al. Prognostic value of carbohydrate antigen 19-9 and the surgical margin in extrahepatic cholangiocarcinoma. *Ann Gastroenterol Surg* (2022) 6(2):307–15. doi: 10.1002/ags3.12525

133. Bolm L, Petrova E, Weitz J, Ruckert F, Wittel UA, Makowiec F, et al. Prognostic relevance of preoperative bilirubin-adjusted serum carbohydrate antigen 19-9 in a multicenter subset analysis of 179 patients with distal cholangiocarcinoma. *HPB (Oxford)* (2019) 21(11):1513–9. doi: 10.1016/j.hpb.2019.03.363

134. Lee JW, Lee JH, Park Y, Kwon J, Lee W, Song KB, et al. Prognostic impact of perioperative Ca19-9 levels in patients with resected perihilar cholangiocarcinoma. *J Clin Med* (2021) 10(7):1345. doi: 10.3390/jcm10071345

135. Heng G, Huang B, Shen Y, Wang D, Lan Z, Yao Y, et al. Vascular invasion and lymph node metastasis mediate the effect of Ca242 on prognosis in hilar cholangiocarcinoma patients after radical resection. *Front Oncol* (2022) 12:1071439. doi: 10.3389/fonc.2022.1071439

136. Ghafouri-Fard S, Safarzadeh A, Hussen BM, Taheri M, Samsami M. A review on the role of ncrnas in the pathogenesis of cholangiocarcinoma. *Int J Biol Macromol* (2023) 225:809–21. doi: 10.1016/j.ijbiomac.2022.11.144

137. Wu Y, Hayat K, Hu Y, Yang J. Long non-coding rnas as molecular biomarkers in cholangiocarcinoma. *Front Cell Dev Biol* (2022) 10:890605. doi: 10.3389/fcell.2022.890605

138. Tan X, Huang Z, Li X. Long non-coding rna Malat1 interacts with mir-204 to modulate human hilar cholangiocarcinoma proliferation, migration, and invasion by targeting Cxcr4. *J Cell Biochem* (2017) 118(11):3643–53. doi: 10.1002/jcb.25862

139. Shi X, Zhang H, Wang M, Xu X, Zhao Y, He R, et al. Lncrna Afap1-As1 promotes growth and metastasis of cholangiocarcinoma cells. *Oncotarget* (2017) 8 (35):58394–404. doi: 10.18632/oncotarget.16880

140. Sun HB, Zhang GC, Liu J, Nie CS. Long noncoding rna Linc00184 facilitates the proliferation, metastasis, and adenine metabolism of cholangiocarcinoma *Via* modulating hsa-Mir-23b-3p/Anxa2 axis. *Environ Toxicol* (2021) 36(8):1576–90. doi: 10.1002/tox.23154

141. Sapuppo E, Brunetti O, Tessitore D, Brandi G, Di Giovanni N, Fadda G, et al. Rare histotypes of epithelial biliary tract tumors: a literature review. *Crit Rev Oncol Hematol* (2023) 181:103892. doi: 10.1016/j.critrevonc.2022.103892

142. Hoshimoto S, Hoshi S, Hishinuma S, Tomikawa M, Shirakawa H, Ozawa I, et al. Adenosquamous carcinoma in the biliary tract: association of the proliferative ability of the squamous component with its proportion and tumor progression. *Scand J Gastroenterol* (2017) 52(4):425–30. doi: 10.1080/00365521.2016.1273383

143. Kanagasabapathy S, Subasinghe D, Sivaganesh S, Wijesinghe H. Adenosquamous carcinoma of the distal common bile duct: a case of a rare type of cholangiocarcinoma. *Clin Pathol* (2022) 15:2632010X221099884. doi: 10.1177/2632010X221099884

144. Hong Y, Li X, Cao D. Case report: trastuzumab treatment in adenosquamous carcinoma of the extrahepatic biliary tract with her-2 amplification. *Front Oncol* (2021) 11:538328. doi: 10.3389/fonc.2021.538328

145. Xie CB, Wu Y, Li F, Zhao KF, Shi RS, Huang Q, et al. Primary signet-ring cell carcinoma of the extrahepatic bile duct: a case report. *World J Gastrointest Oncol* (2022) 14(7):1356–62. doi: 10.4251/wjgo.v14.i7.1356

146. Kita E, Tsujimoto A, Nakamura K, Sudo K, Hara T, Kainuma O, et al. Signet ring cell carcinoma of the extrahepatic bile duct diagnosed by preoperative biopsy: a case report. *Case Rep Gastroenterol* (2014) 8(3):353–7. doi: 10.1159/000369249

147. Fischer HP, Zhou H. Pathogenesis of carcinoma of the papilla of vater. *J Hepatobiliary Pancreat Surg* (2004) 11(5):301–9. doi: 10.1007/s00534-004-0898-3

148. Wang X, Yu GY, Chen M, Wei R, Chen J, Wang Z. Pattern of distant metastases in primary extrahepatic bile-duct cancer: a seer-based study. *Cancer Med* (2018) 7(10):5006–14. doi: 10.1002/cam4.1772

149. Adachi K, Okuwaki K, Nishiyama R, Kida M, Imaizumi H, Iwai T, et al. A case of extrahepatic bile duct cancer with distant metastases showing pathological complete response to treatment combining gemcitabine and cisplatin. *Clin J Gastroenterol* (2019) 12(5):466–72. doi: 10.1007/s12328-019-00972-0

150. Tan S, Yu J, Huang Q, Zhou N, Xiong X, Gou H. Durable response to the combination of pembrolizumab and nab-paclitaxel in a metastatic extrahepatic cholangiocarcinoma: a case report and literature review. *Front Pharmacol* (2022) 13:1037646. doi: 10.3389/fphar.2022.1037646

151. Zheng X, Zhang WT, Hu J, Chen XF. A colonic metastasis from extrahepatic cholangiocarcinoma after removal of primary tumor: a case report and literature review. *Chin Clin Oncol* (2020) 9(2):21. doi: 10.21037/cco.2020.01.08

152. Vabi BW, Carter J, Rong R, Wang M, Corasanti JG, Gibbs JF. Metastatic colon cancer from extrahepatic cholangiocarcinoma presenting as painless jaundice: case report and literature review. *J Gastrointest Oncol* (2016) 7(2):E25–30. doi: 10.3978/j.issn.2078-6891.2015.119

153. Qian H, Huang Z, Sun X, Ren P. Skeletal muscle metastasis from extrahepatic cholangiocarcinoma: a case report and literature review. *Front Surg* (2022) 9:922834. doi: 10.3389/fsurg.2022.922834

154. Boscoe AN, Rolland C, Kelley RK. Frequency and prognostic significance of isocitrate dehydrogenase 1 mutations in cholangiocarcinoma: a systematic literature review. *J Gastrointest Oncol* (2019) 10(4):751–65. doi: 10.21037/jgo.2019.03.10

155. Javle M, Bekaii-Saab T, Jain A, Wang Y, Kelley RK, Wang K, et al. Biliary cancer: utility of next-generation sequencing for clinical management. *Cancer* (2016) 122(24):3838–47. doi: 10.1002/cncr.30254

156. Peck J, Wei L, Zalupski M, O'Neil B, Villalona Calero M, Bekaii-Saab T. Her2/Neu may not be an interesting target in biliary cancers: results of an early phase ii study with lapatinib. *Oncology* (2012) 82(3):175–9. doi: 10.1159/000336488

157. Rizzo A, Frega G, Ricci AD, Palloni A, Abbati F, DEL S, et al. Anti-egfr monoclonal antibodies in advanced biliary tract cancer: a systematic review and meta-analysis. *In Vivo* (2020) 34(2):479–88. doi: 10.21873/invivo.11798

158. Morad G, Helmink BA, Sharma P, Wargo JA. Hallmarks of response, resistance, and toxicity to immune checkpoint blockade. *Cell* (2022) 185(3):576. doi: 10.1016/j.cell.2022.01.008

159. Lim YJ, Koh J, Kim K, Chie EK, Kim B, Lee KB, et al. High ratio of programmed cell death protein 1 (Pd-1)(+)/Cd8(+) tumor-infiltrating lymphocytes identifies a poor prognostic subset of extrahepatic bile duct cancer undergoing surgery plus adjuvant chemoradiotherapy. *Radiother Oncol* (2015) 117(1):165–70. doi: 10.1016/j.radonc.2015.07.003

160. Chellappa S, Hugenschmidt H, Hagness M, Subramani S, Melum E, Line PD, et al. Cd8+ T cells that coexpress rorgammat and T-bet are functionally impaired and expand in patients with distal bile duct cancer. *J Immunol* (2017) 198(4):1729–39. doi: 10.4049/jimmunol.1600061

161. O'Rourke CJ, Munoz-Garrido P, Andersen JB. Molecular targets in cholangiocarcinoma. *Hepatology* (2021) 73 (Suppl 1):62–74. doi: 10.1002/hep.31278

162. Vatankhah F, Salimi N, Khalaji A, Baradaran B. Immune checkpoints and their promising prospect in cholangiocarcinoma treatment in combination with other therapeutic approaches. *Int Immunopharmacol* (2023) 114:109526. doi: 10.1016/j.intimp.2022.109526

frontiers | Frontiers in Oncology

TYPE Original Research
PUBLISHED 18 May 2023
DOI 10.3389/fonc.2023.1048311

OPEN ACCESS

EDITED BY
Daniel Neureiter,
Salzburger Landeskliniken, Austria

REVIEWED BY
Zhiyu Xiao,
Sun Yat-Sen University, China
Tian-wu Chen,
Affiliated Hospital of North Sichuan Medical College, China

*CORRESPONDENCE
Jian Shu
shujiannc@163.com

†These authors have contributed equally to this work

RECEIVED 19 September 2022
ACCEPTED 28 April 2023
PUBLISHED 18 May 2023

CITATION
Liu J, Liu M, Gong Y, Su S, Li M and Shu J (2023) Prediction of angiogenesis in extrahepatic cholangiocarcinoma using MRI-based machine learning. *Front. Oncol.* 13:1048311. doi: 10.3389/fonc.2023.1048311

Prediction of angiogenesis in extrahepatic cholangiocarcinoma using MRI-based machine learning

Jiong Liu[1,2†], Mali Liu[1,2†], Yaolin Gong[1,2], Song Su[3], Man Li[4] and Jian Shu[1,2*]

[1]Department of Radiology, The Affiliated Hospital of Southwest Medical University, Luzhou, Sichuan, China, [2]Nuclear Medicine and Molecular Imaging Key Laboratory of Sichuan Province, Luzhou, Sichuan, China, [3]Department of Hepatobiliary Surgery, The Affiliated Hospital of Southwest Medical University, Luzhou, China, [4]Department of Research and Development, Shanghai United Imaging Intelligence Co., Shanghai, China

Purpose: Reliable noninvasive method to preoperative prediction of extrahepatic cholangiocarcinoma (eCCA) angiogenesis are needed. This study aims to develop and validate machine learning models based on magnetic resonance imaging (MRI) for predicting vascular endothelial growth factor (VEGF) expression and the microvessel density (MVD) of eCCA.

Materials and methods: In this retrospective study from August 2011 to May 2020, eCCA patients with pathological confirmation were selected. Features were extracted from T1-weighted, T2-weighted, and diffusion-weighted images using the MaZda software. After reliability testing and feature screening, retained features were used to establish classification models for predicting VEGF expression and regression models for predicting MVD. The performance of both models was evaluated respectively using area under the curve (AUC) and Adjusted R-Squared (Adjusted R^2).

Results: The machine learning models were developed in 100 patients. A total of 900 features were extracted and 77 features with intraclass correlation coefficient (ICC) < 0.75 were eliminated. Among all the combinations of data preprocessing methods and classification algorithms, Z-score standardization + logistic regression exhibited excellent ability both in the training cohort (average AUC = 0.912) and the testing cohort (average AUC = 0.884). For regression model, Z-score standardization + stochastic gradient descent-based linear regression performed well in the training cohort (average Adjusted R^2 = 0.975), and was also better than the mean model in the test cohort (average Adjusted R^2 = 0.781).

Conclusion: Two machine learning models based on MRI can accurately predict VEGF expression and the MVD of eCCA respectively.

KEYWORDS

cholangiocarcinoma, magnetic resonance imaging, machine learning, vascular endothelial growth factor, microvessel density

1 Introduction

Cholangiocarcinoma (CCA) is a group of highly heterogeneous malignancies. CCA can be divided into three subtypes: intrahepatic cholangiocarcinoma (iCCA), perihilar cholangiocarcinoma (pCCA) and distal cholangiocarcinoma (dCCA). pCCA and dCCA are collectively referred to as extrahepatic cholangiocarcinoma (eCCA), accounting for 80–90% of all types of CCA (1). Improvements in diagnosis and treatment have stabilized or decreased the morbidity and mortality of eCCA in most areas (1, 2). Although surgery has played an essential role, more oncologists have emphasized the necessity for neoadjuvant therapy, including vascular-targeted therapy.

CCA is traditionally regarded as a lymphovascular tumor with a rich polymorphic tumor microenvironment, and the overexpression of microvessels has a strong correlation with tumors (3). Vascular-targeted therapy mainly inhibits tumor-associated angiogenesis through drugs (e.g. bevacizumab). Angiogenesis is an important factor for maintain the rapid growth and metastasis of malignant tumors, providing necessary oxygen and nutrients to tumor cells (4, 5). Vascular endothelial growth factor (VEGF), a kind of homodimeric heparin-binding protein, can enhance the division capability of vascular endothelial cells and promote tumor-associated angiogenesis (6). Poor T cell infiltration and high M2-TAM in eCCA are correlated with elevated VEGF levels (7). In addition, the 5-year survival rate of eCCA patients with high microvessel density MVD (2.2%) was significantly worse than low MVD patients (42.1%) (8, 9). It is undeniable that VEGF and MVD are indeed related to the prognosis and progression of almost all tumors, and this is also true in eCCA (10), and about 59% of eCCA patients overexpress VEGF (11). Currently, immunohistochemical stains and microarray analysis are most commonly used to detect VEGF expression and MVD. However, this method is invasive and difficult to repeat.

Magnetic resonance imaging (MRI) can clearly visualize various biliary diseases (12). However, naked-eye evaluation of the tumor VEGF level and MVD still remains extremely challenging. Machine learning, which can deeply mine images and analyze them objectively and quantitatively, has become a commonly used method in clinical oncology research (13–15). One study showed that six pathological features of iCCA, including VEGF, can be evaluated accurately by machine learning of ultrasound images before operation. The area under the curve (AUC) for the VEGF group was 0.86 (16). However, carcinogenesis, diagnosis, and treatment markedly differ between iCCA and eCCA (1, 17). Additionally, the ultrasound has great variability according to the level of the operators. Additionally, MVD belongs to continuous numerical data, and there is no exact cut-off value. Thus, most related studies use the mean or median value of MVD as cut-off (1, 8). However, this method is controversial for the clinical interpretation of different patient samples. In this study, we constructed a classification model for prediction of VEGF expression and a regression model for quantitative prediction of MVD based on multi-sequence MR images, using machine learning for objective and non-invasive preoperative evaluation of VEGF expression and MVD of eCCA.

2 Materials and methods

2.1 Patients' enrollment

This retrospective study was approved by the institutional review board, and the human-related procedures followed the "Helsinki Declaration". Since the study was retrospective, written informed consent of patients was not required. We collected patients treated in our hospital from January 2011 to December 2020 and met the following inclusion and exclusion criteria. Inclusion criteria included: (I) had complete medical records; (II) had complete preoperative multiparametric MR images; (III) pathologically confirmed eCCA. Exclusion criteria included: (I) the patient had received any treatment before MR scan, such as surgery, and targeted treatment; (II) the image quality was too poor or the focus was too small (< 5 mm) to outline the focus target area. The flow diagram of patient enrollment is displayed in Figure 1.

2.2 Pathological specimen processing

All enrolled patients underwent surgical resection. Tumor specimens obtained during surgery were used for pathological analysis to determine VEGF expression and MVD count. Immunohistochemical staining and microarray analysis of VEGF and MVD were performed according to relevant standard methods by a pathologist with more than 10 years of clinical experience.

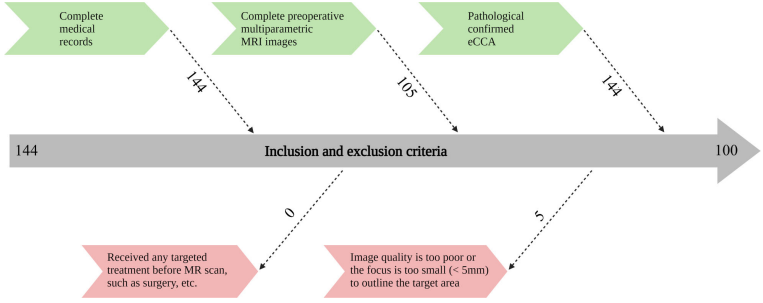

FIGURE 1
Flow chart of inclusion and exclusion criteria of patients. MRI, magnetic resonance imaging; eCCA, extrahepatic cholangiocarcinoma.

2.3 MR image acquisition

Preoperative evaluation included standard upper abdominal scanning with 3.0T MRI scanner (Achieva, Philips, Netherlands) and 16-channel trunk coil. MRI acquisition sequence included but was not limited to transverse T1-weighted imaging (T1WI), T2-weighted imaging (T2WI), and diffusion-weighted imaging (DWI). The parameters of these three acquisition sequences are detailed in Table 1. All MR images were retrieved and analyzed by the Picture Archiving and Communication Systems. In addition, all MR images applied voxel size normalization and voxel intensity normalization.

2.4 Image segmentation and features extraction

Region of interest (ROI) segmentation and feature extraction were performed by an experienced radiologist using the software MaZda (version 4.6, http://www.eletel.p.lodz.pl/programy/mazda/) (18–20). The ROI margins were strictly defined to always be 1–2 mm from the tumor margin. In addition, the "± 3 sigma" option in the MaZda software was selected for image standardization.

2.5 Intra-observer and inter-observer agreement

To assess the stability of features, two radiologists jointly selected T1WI, T2WI, and DWI images of 20 patients at random for repeated segmentation. One radiologist re-outlined the ROI twice at different times of the week. Another radiologist independently outlined the ROI once. The extracted features were used for ICC calculation using Python programming language (version 3.7, https://www.python.org) to evaluate the intra-observer and inter-observer agreement of each feature. ICC > 0.75 indicated good reliability, and this feature was retained.

TABLE 1 MRI sequences and parameters.

Parameter	T1WI	T2WI	DWI
TR (msec)	3.1	1610	934
TE (msec)	1.44	70	52
Section thickness (mm)	3	7	7
Section gap (mm)	1.5	1	1
FOV (mm^2)	280 × 305	280 × 305	280 × 305
Matrix size	244 × 186	176 × 201	100 × 124
Flip angle (°)	10	90	90
b values (s/mm2)	–	–	0 and 800

MRI, magnetic resonance imaging; T1WI, T1-weighted imaging; T2WI, T2-weighted imaging; DWI, diffusion-weighted imaging; TR, repetition time; TE, echo time; FOV, field of view.

2.6 Feature processing and model building

Feature processing and model building were performed with the uAI Research Portal (United Imaging Intelligence, China). First, 80% of the samples were randomly selected as the training cohort and the other 20% as the test cohort. Then, Z-score standardization was used to eliminate errors caused by different dimensions. The least absolute shrinkage and selection operator (Lasso) regression method was used for feature selection. When constructing both models, eight data preprocessing methods were tried: Box-cox transform, L1-norm regularization, L2-norm regularization, max abs normalization, min-max normalization, Quantile transform, YeoJohnson transform, and Z-score standardization. Finally, when constructing the classification model for predicting VEGF expression, nine machine learning algorithms were tried: Gaussian process regression, K-nearest neighbors, logistic regression, partial least squares-discriminant analysis, quadratic discriminant analysis, random forest, stochastic gradient descent based linear regression, support vector machine, and XGboost. In addition to logistic regression, partial least squares-discriminant analysis, quadratic discriminant analysis, the other six algorithms were also used to construct the regression model for predicting MVD. The above steps were repeated 20 times to ensure good reliability of the models. An overview of the machine learning workflow is shown in Figure 2.

AUC of the subject ROC and the Adjusted R-Squared (Adjusted R^2) were used to evaluate the effectiveness of the classification model and the regression model, respectively. Other auxiliary evaluation indices including F1 score, recall, precision, sensitivity, specificity, accuracy, mean square error (MSE), mean absolute error (MAE), and Pearson correlation coefficient (PCC) were also calculated. Finally, the bias and variance of both models were calculated to evaluate their fitting and generalization. The models with the highest average AUC or Adjusted R^2 in the test cohort were identified as the best models for classification or regression.

2.7 Statistical analysis

Statistical analysis of the data on clinical and pathological characteristics of patients was performed using Statistical Product and Service Solutions (SPSS, version 25.0, IBM). Continuous variables were expressed as mean ± standard deviation (SD) when they followed a normal distribution, and median value was used for non-normally distributed data. The correlation between VEGF expression and age, gender, tumor location, and MVD was evaluated using binary multivariate logistic regression. The evaluation indices of both machine learning models were calculated using the uAI Research Portal. All statistical tests were two-sided, and P values < 0.05 were considered significant.

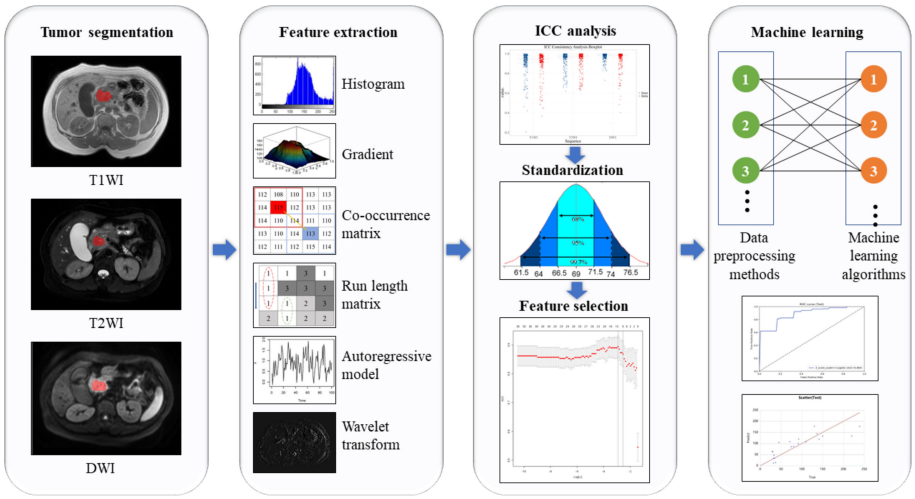

FIGURE 2
Workflow of machine learning process in the current study.

3 Results

3.1 Patient characteristics

There are 105 patients were in accordance with the inclusive criteria. No patients were excluded as the reason that they received any treatment before MRI. However, 5 patients were excluded because the image quality was too poor or the lesion was too small. Finally, we identified 100 eligible patients based on the inclusion and exclusion criteria. The mean age of all eCCA patients was 57.38 years. The ratio of male to female and pCCA patients to dCCA patients was close to 50%. Additionally, there were more patients with positive VEGF expression than negative. The detailed results are shown in Table 2.

In addition, in the multivariable logistic regression analysis of the related factors of VEGF expression, age ($P = 0.125$, OR = 0.461), gender ($P = 0.059$, OR = 0.952), and tumor ($P = 0.583$, OR = 0.764) location did not affect the expression of VEGF, while there was a significant positive relationship ($P = 0.008$, OR = 1.014) between MVD and VEGF expression. Likelihood ratio test (χ^2 (4) = 16.670, $P = 0.002$) and Hosmer–Lemeshow test (χ^2 (8) = 13.278, p = 0.103) showed the validity and goodness of fit of the multivariable logistical regression analysis model.

TABLE 2 Clinical and histologic characteristics of all eCCA patients.

Variable	Whole (n = 100)
Age, mean ± SD, years	57.38 ± 10.06
Gender	
Female, n Male, n	46 54
Localization	
pCCA, n dCCA, n	47 53
MVD, mean ± SD	101.16 ± 58.11
VEGF	
Positive, n Negative, n	71 29

SD, standard deviation; pCCA, perihilar cholangiocarcinoma; dCCA, distal cholangiocarcinoma; VEGF, vascular endothelial growth factor; MVD, microvessel density. *, $P < 0.05$.

3.2 Features extraction

More than 300 image features were extracted from each ROI using MaZda. Then, the features with missing values were deleted. Finally, each sequence image uniformly retained 300 features. These features were classified into six feature families including histogram (12), gradient (6), co-occurrence matrix (20), run length matrix (240), autoregressive model (6), and wavelet (16). Finally, the features extracted from T1WI, T2WI, and DWI images of each patient were mixed, and a total of 900 features were obtained.

3.3 Intra-observer and inter-observer agreement

Through ICC consistency analysis, 823 features with both intra- and inter-observer ICC values greater than 0.75 were identified among the 900 features. The removed features included 30 T1WI image features, 29 T2WI image features, and 18 DWI image features. Figure 3 shows the results of the ICC consistency analysis for each feature.

3.4 Feature selection and models construction

In the classification model for predicting VEGF expression, the nine best features were obtained by selection using Lasso with an

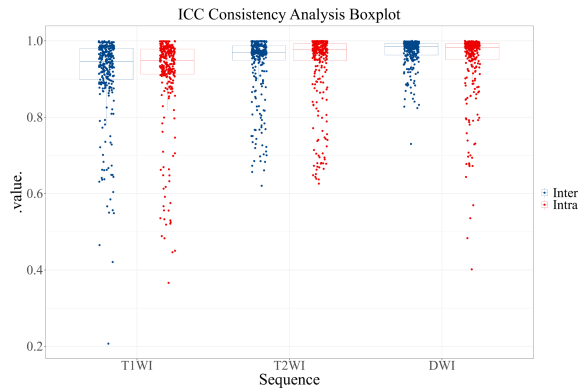

FIGURE 3
ICC consistency analysis boxplot. Blue represents inter-observer agreement, and red represents intra-observer agreement.

alpha value of 0.075. Five of them were DWI image features, namely DWI-sigma, DWI-s(3_0)sumofsqs, DWI-s(3_0)sumvarnc, DWI-s(5_-5)invdfmom, and DWI-wavenll_s-2. The other four features were T1WI-s(3_0)difentrp, T1WI-wavenll_s-3, T2WI-s(5_-5)sumofsqs, and T2WI-kurtosis (Figure 4A). Based on the nine features, 72 different combinations of machine learning classification models were constructed. Finally, the combination with the highest average AUC value in the test cohort was the Z-score standardization + logistic regression. The average AUCs of the training and test cohorts were 0.912 (range, 0.876–0.963) and 0.884 (range, 0.631–1), respectively (Figures 4B, C). The average accuracy and sensitivity of the model in the test cohort were also excellent, 0.84 (range, 0.65–0.952) and 0.926 (range, 0.786–1), respectively. The average specificity in the test cohort was relatively poor, at only 0.633 (range, 0.333–0.833).

In the regression model for predicting MVD, 66 features were retained using Lasso with an alpha value of 1.000. Of these, the number of T1WI, T2WI, and DWI image features were 22, 25, and 19, respectively (Figure 5A). Using these 66 features, 48 machine learning regression models were constructed. Lastly, the model of the Z-score standardization + stochastic gradient descent based linear regression showed good performance and was chosen as the best model. The average Adjusted R^2 of its training and test cohorts were 0.975 (range, 0.964–0.984) and 0.781 (range, 0.233–0.896), respectively. The results of the average Adjusted R^2 in both the training and test cohorts were acceptable, and their values were greater than the mean model. The scatter plots (Figures 5B, C) and prediction curves (Figures 5D, E) display the prediction results and trends for each sample. Table 3 shows the results of all evaluation indices for the two models predicting VEGF expression and MVD.

4 Discussion

In this study, we established two machine learning models based on MR images to predict VEGF expression and MVD in eCCA. When constructing the machine learning model for predicting MVD, we used the regression model, which is rarely used in medical research machine learning, and obtained satisfactory results. The classification model successfully predicted the expression of VEGF in eCCA. The regression model for predicting MVD also exhibited excellent performance. This demonstrates that machine learning is promising for the clinical evaluation of tumor-associated angiogenesis in eCCA.

Recent studies have shown that VEGF overexpression and MVD are related to tumor progression, metastasis, and prognosis in eCCA (8, 9, 21). For unresectable middle and advanced eCCA patients, the

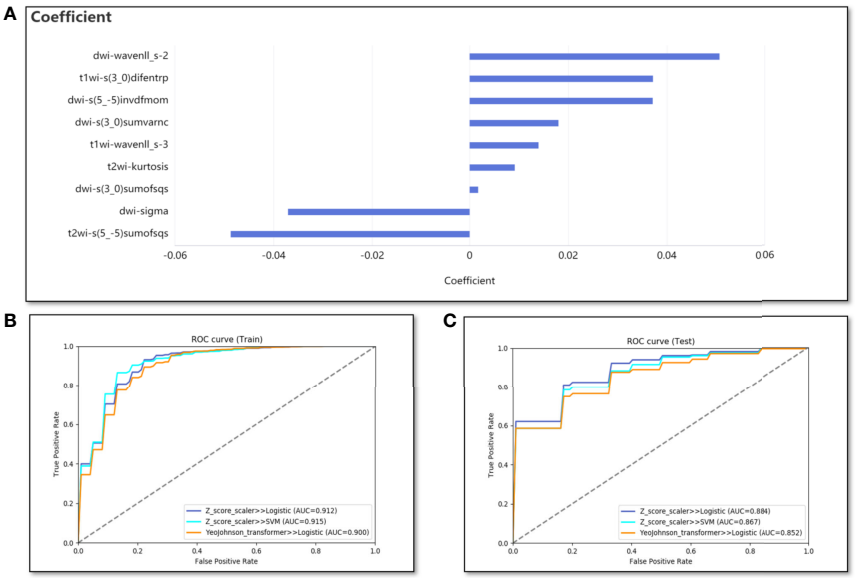

FIGURE 4
The performance of the classification model. **(A)** The bar graph shows the weight coefficient of each predictive feature in the model of Z-score standardization + logistic regression. **(B, C)** The ROC curves for training and test cohorts of different combinations (Three combinations with the best results are listed).

10.3389/fonc.2023.1048311

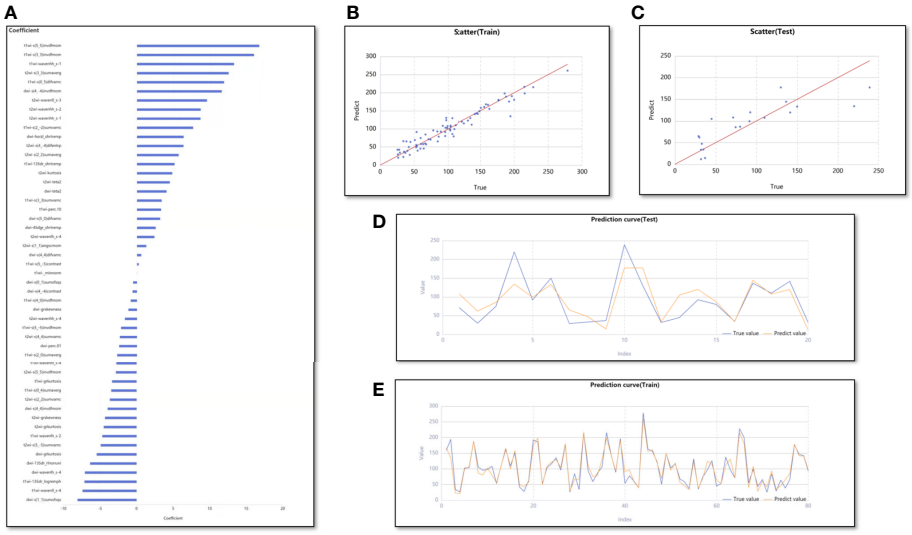

FIGURE 5
The performance of the Z-score standardization + stochastic gradient descent based linear regression. **(A)** The bar graph shows the weight coefficient of top 50 predictive feature. **(B, C)** The scatter plots for training and test cohorts. **(D, E)** The prediction curves for training and test cohorts.

TABLE 3 Performance evaluation of two models for predicting VEGF expression and MVD.

Evaluation metrics	Classification model		Regression model	
	Training cohorts (80 patients)	Testing cohorts (20 patients)	Training cohorts (80 patients)	Testing cohorts (20 patients)
AUC	0.912	0.884		
F1-score	0.923	0.891		
Precision	0.887	0.864		
Sensitivity	0.961	0.926		
Specificity	0.701	0.633		
Accuracy	0.886	0.84		
R^2			0.927	0.434
MAE			11.409	34.374
MSE			245	1891.407
PCC			0.963	0.725
Bias	0.129		2327.009	
Variance	0.062		2902.103	

VEGF, vascular endothelial growth factor; MVD, microvessel density; AUC, area under the curve; R^2, coefficient of determination; MAE, mean absolute error; MSE, mean square error; PCC, Pearson correlation coefficient.

effect of conventional chemotherapy is not satisfactory (22, 23). Therefore, researchers are exploring new treatment protocols for the molecular pathways (such as tumor-associated angiogenesis) in the occurrence and development of CCA. Currently, the application of purely vascular targeted therapies in CCA patients is limited. However, studies have shown that combining vascular targeted therapies with immunotherapies will bring significant benefits to patients (24–26). In addition, in clinical practice, invasive histopathological examinations for monitoring angiogenesis within tumors still presents many problems and inconvenience. Some scholars have used conventional imaging methods to study the angiogenesis of CCA. Park et al. retrospectively analyzed the CT images of 147 patients with iCCA. They found that high blood supply on CT images was related to higher relapse-free survival and better prognosis, and the vascular distribution on CT images could be used as a non-invasive prognostic index for iCCA (27). Furthermore,

Yugawa et al. confirmed that MVD in CCA tumors was closely related to radiological characteristics of the hepatic arterial phase on enhanced CT, which may be a potential prognostic indicator (28).

In the research studied to date, the number of molecular or pathological studies of CCA using machine learning is still relatively rare, and most of the research subjects are iCCA. Studies by Sadot et al. indicated that quantitative imaging phenotypes in CT images correlated with the expression of specific hypoxic markers in iCCA, including VEGF (29). Recently, Zhou and his team established a machine learning model based on dynamic contrast-enhanced MR images whose features can be used to preoperatively predict microvascular invasion in patients with mass-forming iCCA (30). Prior studies have shown, the pathological features of eCCA (including pathological grading, lymph node metastasis, T stage, perineural infiltration, and microvascular infiltration) can also be predicted by several machine learning models with excellent results (31, 32).

In the present work, our machine learning models, based on MR images and used to predict the VEGF expression and MVD of eCCA, further enriched the knowledge in the field of eCCA machine learning and provides credible aid for the treatment and prognosis of patients with eCCA. In addition, our exploration of regression-based machine learning for continuous variables in which optimal cut-off values are not clinically available was effective. More interestingly, we found that the DWI image features accounted for a relatively large number (5/9) of the classification model features, while the number of T2WI image features was larger (25/66) in the regression model. The reasons for this result may be varied, such as correlation between different types of images and predicted objects or systematic error caused by inconsistent algorithms in the process of machine learning. In addition, in both the classification and regression models, the feature with the largest weight coefficient was the wavelet transform feature in the DWI image. This is in agreement with the previous research results of several other scholars (30, 33, 34), indicating that wavelet transform features may be able to characterize tumor biology on multiple scales.

There are scenarios in which the present studies fall short. First, this is a retrospective case-control study with a small sample size and all patients were from a single institution, so selection bias may be present. To increase the universality of the model application, it is necessary to carry out prospective multicenter studies with larger samples. Second, this study only included conventional non-enhanced MRI sequences and did not include enhancement sequences and other special sequences. On the one hand, almost all patients underwent conventional sequence scans, which is conducive to increasing the applicability of the model. On the other hand, adding sequence types would further reduce the number of patient samples included in the study. Last but not least, radiomics mines the deep feature information hidden in the image, which can not be recognized by the naked eye, and may be related to the disease itself, regardless of whether it is enhanced or not. Some studies have shown that enhanced images may not significantly improve the efficiency of radiomics models compared with non-enhanced images (35). Third, tumors smaller than 5 mm were excluded during this study, making it difficult for the machine learning models to predict tumors of smaller size. Finally, the number of features in the regression model was relatively large. In future work, we will test further methods and algorithms to obtain the minimum number of features and the best model efficiency.

In this study, we constructed and internally validated MRI-based machine learning models to predict VEGF expression and MVD in eCCA. Both models provide powerful guidance for monitoring eCCA angiogenesis, may assist in clinical decision-making, and ultimately improve the prognosis of patients.

Data availability statement

The raw data supporting the conclusions of this article will be made available by the authors, without undue reservation.

Author contributions

JS and JL contributed to conception and design. JL, MLL and YLG contributed to the collection and arrangement of data. JL and ML contributed to data analysis and manuscript writing. JS and SS edited the manuscript. All authors contributed to the article and approved the submitted version.

Funding

This study is supported by the National Natural Science Foundation of China, 82272077; Central Government Funds of Guiding Local Scientific and Technological Development for Sichuan Province of China, 2021ZYD0075; Key projects of Science and Technology Department of Sichuan Province, 2022YFS0070; Key Research and Development Project of Science & Technology Department of Sichuan Province, 2020YFS0324.

Acknowledgments

We thank LetPub (www.letpub.com) for its linguistic assistance during the preparation of this manuscript.

Conflict of interest

Author ML was employed by Shanghai United Imaging Intelligence Co.

The remaining authors declare that the research was conducted in the absence of any commercial or financial relationships that could be construed as a potential conflict of interest.

Publisher's note

References

1. Banales JM, Marin JJG, Lamarca A, Rodrigues PM, Khan SA, Roberts LR, et al. Cholangiocarcinoma 2020: the next horizon in mechanisms and management. *Nat Rev Gastroenterol Hepatol* (2020) 17(9):557–88. doi: 10.1038/s41575-020-0310-z

2. Bertuccio P, Malvezzi M, Carioli G, Hashim D, Boffetta P, El-Serag HB, et al. Global trends in mortality from intrahepatic and extrahepatic cholangiocarcinoma. *J Hepatol* (2019) 71(1):104–14. doi: 10.1016/j.jhep.2019.03.013

3. Mariotti V, Fiorotto R, Cadamuro M, Fabris L, Strazzabosco M. New insights on the role of vascular endothelial growth factor in biliary pathophysiology. *JHEP Rep* (2021) 3(3):100251. doi: 10.1016/j.jhepr.2021.100251

4. Jayson GC, Kerbel R, Ellis LM, Harris AL. Antiangiogenic therapy in oncology: current status and future directions. *Lancet* (2016) 388(10043):518–29. doi: 10.1016/S0140-6736(15)01088-0

5. Butler JM, Kobayashi H, Rafii S. Instructive role of the vascular niche in promoting tumour growth and tissue repair by angiocrine factors. *Nat Rev Cancer* (2010) 10(2):138–46. doi: 10.1038/nrc2791

6. Ellis LM, Hicklin DJ. VEGF-targeted therapy: mechanisms of anti-tumour activity. *Nat Rev Cancer* (2008) 8(8):579–91. doi: 10.1038/nrc2403

7. King G, Javle M. FGFR inhibitors: clinical activity and development in the treatment of cholangiocarcinoma. *Curr Oncol Rep* (2021) 23(9):108. doi: 10.1007/s11912-021-01100-3

8. Möbius C, Demuth C, Aigner T, Wiedmann M, Wittekind C, Mössner J, et al. Evaluation of VEGF a expression and microvascular density as prognostic factors in extrahepatic cholangiocarcinoma. *Eur J Surg Oncol* (2007) 33(8):1025–9. doi: 10.1016/j.ejso.2007.02.020

9. Thelen A, Scholz A, Benckert C, Schröder M, Weichert W, Wiedenmann B, et al. Microvessel density correlates with lymph node metastases and prognosis in hilar cholangiocarcinoma. *J Gastroenterol* (2008) 43(12):959–66. doi: 10.1007/s00535-008-2255-9

10. Calastri MCJ, Ferreira RF, Tenani GD, Spinola LP, Vieira GF, Rabaça Roque Botelho MF, et al. Investigating VEGF. miR-145-3p, and miR-101-3p expression in patients with cholangiocarcinoma. *Asian Pac J Cancer Prev* (2022) 23(7):2233–41. doi: 10.31557/APJCP.2022.23.7.2233

11. Wang M, Chen Z, Guo P, Wang Y, Chen G. Therapy for advanced cholangiocarcinoma: current knowledge and future potential. *J Cell Mol Med* (2021) 25(2):618–28. doi: 10.1111/jcmm.16151

12. Ringe KI, Wacker F. Radiological diagnosis in cholangiocarcinoma: application of computed tomography, magnetic resonance imaging, and positron emission tomography. *Best Pract Res Clin Gastroenterol* (2015) 29(2):253–65. doi: 10.1016/j.bpg.2015.02.004

13. Liu Z, Wang S, Dong D, Wei J, Fang C, Zhou X, et al. The applications of radiomics in precision diagnosis and treatment of oncology: opportunities and challenges. *Theranostics* (2019) 9(5):1303–22. doi: 10.7150/thno.30309

14. Lambin P, Leijenaar RTH, Deist TM, Peerlings J, de Jong EEC, van Timmeren J, et al. Radiomics: the bridge between medical imaging and personalized medicine. *Nat Rev Clin Oncol* (2017) 14(12):749–62. doi: 10.1038/nrclinonc.2017.141

15. Tsilimigras DI, Mehta R, Moris D, Sahara K, Bagante F, Paredes AZ, et al. A machine-based approach to preoperatively identify patients with the most and least benefit associated with resection for intrahepatic cholangiocarcinoma: an international multi-institutional analysis of 1146 patients. *Ann Surg Oncol* (2020) 27(4):1110–9. doi: 10.1245/s10434-019-08067-3

16. Peng YT, Zhou CY, Lin P, Wen DY, Wang XD, Zhong XZ, et al. Preoperative ultrasound radiomics signatures for noninvasive evaluation of biological characteristics of intrahepatic cholangiocarcinoma. *Acad Radiol* (2020) 27(6):785–97. doi: 10.1016/j.acra.2019.07.029

17. Rizvi S, Gores GJ. Pathogenesis, diagnosis, and management of cholangiocarcinoma. *Gastroenterology* (2013) 145(6):1215–29. doi: 10.1053/j.gastro.2013.10.013

18. Strzelecki M, Szczypinski P, Materka A, Klepaczko A. A software tool for automatic classification and segmentation of 2D/3D medical images. *Nucl Instruments Methods Phys Res Section A: Accelerators Spectrometers Detectors Associated Equipment* (2013) 702:137–40. doi: 10.1016/j.nima.2012.09.006

19. Szczypiński PM, Strzelecki M, Materka A, Klepaczko A. MaZda–a software package for image texture analysis. *Comput Methods Programs Biomed* (2009) 94 (1):66–76. doi: 10.1016/j.cmpb.2008.08.005

20. Szczypinski PM, Strzelecki M, Materka A. Mazda-A software for texture analysis, in: *2007 international symposium on information technology convergence (ISITC 2007).* (2007) 245–9.

21. Xu D, Li J, Jiang F, Cai K, Ren G. The effect and mechanism of vascular endothelial growth factor (VEGF) on tumor angiogenesis in gallbladder carcinoma. *Iran J Public Health* (2019) 48(4):713–21.

22. Neuzillet C, Casadei-Gardini A, Brieau B, Vivaldi C, Brandi G, Tougeron D, et al. Fluropyrimidine single agent or doublet chemotherapy as second line treatment in advanced biliary tract cancer. *Int J Cancer* (2020) 147(11):3177–88. doi: 10.1002/ijc.33146

23. Fornaro L, Vivaldi C, Cereda S, Leone F, Aprile G, Lonardi S, et al. Second-line chemotherapy in advanced biliary cancer progressed to first-line platinum-gemcitabine combination: a multicenter survey and pooled analysis with published data. *J Exp Clin Cancer Res* (2015) 34:156. doi: 10.1186/s13046-015-0267-x

24. Ma Z, Li H, Liu L. Combining PD-1 inhibitor with VEGF/VEGFR2 inhibitor in chemotherapy: report of a patient with end-stage cholangiocarcinoma and review of literature. *Recent Pat Anticancer Drug Discov* (2021) 16(1):101–7. doi: 10.2174/1574892815999201231215311

25. Hack SP, Verret W, Mulla S, Liu B, Wang Y, Macarulla T, et al. IMbrave 151: a randomized phase II trial of atezolizumab combined with bevacizumab and chemotherapy in patients with advanced biliary tract cancer. *Ther Adv Med Oncol* (2021) 13:17588359211036544. doi: 10.1177/17588359211036544

26. Yuan M, Zhu Z, Mao W, Wang H, Qian H, Wu J, et al. Anlotinib combined with anti-PD-1 antibodies therapy in patients with advanced refractory solid tumors: a single-center, observational, prospective study. *Front Oncol* (2021) 11:683502. doi: 10.3389/fonc.2021.683502

27. Park HM, Jang HY, Lee DE, Kang MJ, Han SS, Kim SW, et al. Prognostic impact of tumor vascularity on CT in resectable intrahepatic cholangiocarcinoma. *HPB (Oxford)* (2022) 24(3):359–69. doi: 10.1016/j.hpb.2021.06.424

28. Yugawa K, Itoh S, Yoshizumi T, Iseda N, Tomiyama T, Toshima T, et al. Prognostic impact of tumor microvessels in intrahepatic cholangiocarcinoma: association with tumor-infiltrating lymphocytes. *Mod Pathol* (2021) 34(4):798–807. doi: 10.1038/s41379-020-00702-9

29. Sadot E, Simpson AL, Do RK, Gonen M, Shia J, Allen PJ, et al. Cholangiocarcinoma: correlation between molecular profiling and imaging phenotypes. *PloS One* (2015) 10(7):e0132953. doi: 10.1371/journal.pone.0132953

30. Zhou Y, Zhou G, Zhang J, Xu C, Wang X, Xu P. Radiomics signature on dynamic contrast-enhanced MR images: a potential imaging biomarker for prediction of microvascular invasion in mass-forming intrahepatic cholangiocarcinoma. *Eur Radiol* (2021) 31(9):6846–55. doi: 10.1007/s00330-021-07793-1

31. Yang C, Huang M, Li S, Chen J, Yang Y, Qin N, et al. Radiomics model of magnetic resonance imaging for predicting pathological grading and lymph node metastases of extrahepatic cholangiocarcinoma. *Cancer Lett* (2020) 470:1–7. doi: 10.1016/j.canlet.2019.11.036

32. Huang X, Shu J, Yan Y, Chen X, Yang C, Zhou T, et al. Feasibility of magnetic resonance imaging-based radiomics features for preoperative prediction of extrahepatic cholangiocarcinoma stage. *Eur J Cancer* (2021) 155:227–35. doi: 10.1016/j.ejca.2021.06.053

33. Xu X, Zhang HL, Liu QP, Sun SW, Zhang J, Zhu FP, et al. Radiomic analysis of contrast-enhanced CT predicts microvascular invasion and outcome in hepatocellular carcinoma. *J Hepatol* (2019) 70(6):1133–44. doi: 10.1016/j.jhep.2019.02.023

34. Liang W, Xu L, Yang P, Zhang L, Wan D, Huang Q, et al. Novel nomogram for preoperative prediction of early recurrence in intrahepatic cholangiocarcinoma. *Front Oncol* (2018) 8:360. doi: 10.3389/fonc.2018.00360

35. Dong J, Li S, Li L, Liang S, Zhang B, Meng Y, et al. Differentiation of paediatric posterior fossa tumours by the multiregional and multiparametric MRI radiomics approach: a study on the selection of optimal multiple sequences and multiregions. *Br J Radiol* (2022) 95(1129):20201302. doi: 10.1259/bjr.20201302

frontiers | Frontiers in Immunology

TYPE Original Research
PUBLISHED 24 May 2023
DOI 10.3389/fimmu.2023.1185985

OPEN ACCESS

EDITED BY
Daniel Neureiter,
Salzburger Landeskliniken, Austria

REVIEWED BY
Guan-Jun Yang,
Ningbo University, China
Shengpeng Wang,
University of Macau, China
JingJing Li,
Hong Kong Polytechnic University, Hong Kong SAR, China

*CORRESPONDENCE
Renyikun Yuan
yryk0808@163.com
Chun Yao
yaochun111111@163.com

†These authors have contributed equally to this work

RECEIVED 15 March 2023
ACCEPTED 16 May 2023
PUBLISHED 24 May 2023

CITATION
Liang X, Gao H, Xiao J, Han S, He J, Yuan R, Yang S and Yao C (2023) Abrine, an IDO1 inhibitor, suppresses the immune escape and enhances the immunotherapy of anti-PD-1 antibody in hepatocellular carcinoma.
Front. Immunol. 14:1185985.
doi: 10.3389/fimmu.2023.1185985

Abrine, an IDO1 inhibitor, suppresses the immune escape and enhances the immunotherapy of anti-PD-1 antibody in hepatocellular carcinoma

Xiaowei Liang[1,2†], Hongwei Gao[1,2†], Jian Xiao[2], Shan Han[1,2], Jia He[1,2], Renyikun Yuan[1,2*], Shilin Yang[1,2] and Chun Yao[2*]

[1]College of Pharmacy, Guangxi University of Chinese Medicine, Nanning, China, [2]Engineering Research Center in Ministry of Education for Innovative Drugs of Traditional Chinese Medicine and Zhuang Yao Medicine, Nanning, China

Background: Indoleamine-2,3-dioxygenase 1 (IDO1) is responsible for tumor immune escape by regulating T cell-associated immune responses and promoting the activation of immunosuppressive. Given the vital role of IDO1 in immune response, further investigation on the regulation of IDO1 in tumors is needed.

Methods: Herein, we used ELISA kit to detect the interferon-gamma (IFN-γ), Tryptophan (Trp), and kynurenic acid (Kyn) levels; western blot, Flow cytometry, and immunofluorescence assays detected the expression of the proteins; Molecular docking assay, SPR assay and Cellular Thermal Shift Assay (CETSA) were used to detect the interaction between IDO1 and Abrine; nano live label-free system was used to detect the phagocytosis activity; tumor xenografts animal experiments were used to explore the anti-tumor effect of Abrine; flow cytometry detected the immune cells changes.

Results: The important immune and inflammatory response cytokine interferon-gamma (IFN-γ) up-regulated the IDO1 expression in cancer cells through the methylation of 6-methyladenosine (m6A) m6A modification of RNA, metabolism of Trp into Kyn, and JAK1/STAT1 signaling pathway, which could be inhibited by IDO1 inhibitor Abrine. CD47 is IFN-γ-stimulated genes (ISGs) and prevents the phagocytosis of macrophages, leading to the cancer immune escape, and this effect could be inhibited by Abrine both in vivo and in vitro. The PD-1/PD-L1 axis is an important immune checkpoint in regulating immune response, overexpression of PD-1 or PD-L1 promotes immune suppression, while in this study Abrine could inhibit the expression of PD-L1 in cancer cells or tumor tissue. The combination treatment of Abrine and anti-PD-1 antibody has a synergistic effect on suppressing the tumor growth through up-regulating $CD4^+$ or $CD8^+$ T

cells, down-regulating the Foxp3$^+$ Treg cells, and inhibiting the expression of IDO1, CD47, and PD-L1.

Conclusion: Overall, this study reveals that Abrine as an IDO1 inhibitor has an inhibition effect on immune escape and has a synergistic effect with the anti-PD-1 antibody on the treatment of HCC.

KEYWORDS

IDO1, Abrine, CD47, PD-L1, m^{6}A RNA modification, immune escape, hepatocellular carcinoma

1 Introduction

Epigenetics is the stable inheritance that changes gene expression or function by regulating the interaction between the genome and the environment without changing the basic sequence of DNA, mainly including DNA methylation, histone modification, chromatin reorganization, and RNA modification (1). The methylation of 6-methyladenosine (m^{6}A) is the most abundant epitranscriptomic modification in eukaryotic mRNA, which plays an important role in affecting oncogenic and tumor suppressor networks and regulating tumor immunogenicity (2).

Primary liver cancer is a high-incidence and malignant tumor in the world and the second leading cause of cancer deaths worldwide (3). Hepatocellular carcinoma (HCC) is the most common type of primary liver cancer and most commonly occurs in patients with chronic liver disease, such as cirrhosis caused by hepatitis B or C infection (4). The updates of HCC treatment methods mainly include surgical resection, liver transplantation, local ablative therapy, systemic therapy, etc (5). Indoleamine-2,3-dioxygenase 1 (IDO1) is an intracellular enzyme expressed by HCC and is the rate-limiting enzyme that catalyzes the metabolism of Tryptophan (Trp) along the kynurenic acid (Kyn) pathway, which leads to the inhibition of T cells and is responsible for tumor cells to escape monitoring and clearance of the immune system (6). IDO1 could be up-regulated by some cytokines and immune checkpoint molecules, such as interferon-γ (IFN-γ), Toll-like receptor (TLR) 3, TLR4, immune checkpoint (including PD-1, CTLA4, CD47) to escape the immunosuppressive environment through the Janus kinase1/signal transducers and activators of transcription1 (JAK1/STAT1) pathway (7, 8). IFN-γ is one of the most essential cytokines in regulating the immune system, through up-regulating inhibitory immune checkpoints such as PD-L1 and CD47 (9). CD47 is a transmembrane protein of the immunoglobulin (Ig) superfamily and is overexpressed in several cancers, which could directly bind with SIRPα to deliver the "don't eat me" signal that exerts anti-phagocytosis function (10, 11). Studies have shown that IFN-γ-induced CD47 upregulation is a common phenomenon in human cancers, and the JAK1-STAT1 axis is the main pathway (12).

Abrine is the dominant alkaloid extracted from *Abrus cantoniensis* and *Abrus precatorius* Linn with significant functions of protecting the liver and is a specific IDO inhibitor (13). In this study, we evaluated the effect of Abrine on anti-HCC and immune response and determined that Abrine as an IDO1 inhibitor could inhibit IFN-γ, PBMCs, or IDO1-induced IDO1-JAK1-STAT1 signaling pathway, enhanced the phagocytosis of macrophages through inhibiting CD47 expression, and decreased the PD-L1 expression in HCC cells. In the HCC xenograft mice model, Abrine suppressed the tumor growth, and promote the anti-HCC effect of anti-PD-1 antibody through increasing the infiltration of CD8$^+$ T cells, decreasing Treg cells, and inhibiting PD-L1, and CD47 expression. In addition, we found that Abrine could significantly decrease the m^{6}A RNA methylation in IFN-γ-induced HepG2 cells, which meant that m^{6}A RNA methylation may play a role in Abrine suppression HCC.

2 Materials and methods

2.1 Cell culture

HepG2 (Human liver cancer) cells were from American Type Culture Collection (ATCC, USA), and were cultured in DMEM (Gibco, USA) medium complemented with 10% fetal bovine serum (FBS) (Gibco, USA) and 1% penicillin/streptomycin (Gibco, USA). Human peripheral blood mononuclear cells (PBMCs) were isolated from whole blood through Human Peripheral Blood Mononuclear Cell Isolation Kit (Solarbio, China) and cultured in RPMI-1640 with 15% FBS and 1% penicillin/streptomycin. The mentioned cells were maintained in 37°C incubator filled with 5% CO2. PBMC was cultured in 10% human serum RPMI-1640. The PBMC was extracted from healthy volunteers, which was approved by the Ethics Committee of Guangxi University of Chinese Medicine.

Abbreviations: Indoleamine-2,3-dioxygenase 1, IDO1; Interferon-gamma, IFN-γ; Methylation of 6-methyladenosine, m^{6}A; Tryptophan, Trp; kynurenic acid, Kyn; IFN-γ-stimulated genes, ISGs; immunoglobulin, Ig; Toll-like receptor, TLR; immunoglobulin, Ig; Suppressors of cytokine signaling, SOCS; Methyltransferase-like 3, METTL3; Immune checkpoint inhibitors, ICIs; Natural killer, NK; Hepatocellular carcinoma, HCC; Effector T cells, Teff; Memory T cells, Tm; Regulatory T lymphocytes, Treg; Exhausted T cells, Tex; Cellular Thermal Shift Assay, CESTA; Hematoxylin and Eosin, HE; Multiplex immunofluorescence, mIHC.

2.2 Cell viability assay

The cell viability was detected by MTT assay. HepG2 cells were seeded into 96-well plates and cultured over 16 hours. Then, Abrine (Chengdu Pufei De Biotech Co., Ltd, China, the purity is over 98%) at different concentrations from 5 to 40 μM was added to the HepG2 cells for 24 hours. After which 100 μL 1mg/mL MTT (Solarbio, China) reagent was added and incubated for another 4 hours at 37°C. After incubation, cells were treated with DMSO for 15 minutes at room temperature. Absorbance was measured at OD = 490 nm by a MicroplateReader (BioTeK, USA).

2.3 Enzyme-linked immunosorbent assay

HepG2 Cells were plated into 6 cm dishes overnight. Consequently, cells were pretreated with Abrine (0, 10, 20, and 40 μM) for 1 h, following co-incubation with IFN-γ (20 ng/mL), PBMC, or IDO1(30 ng/mL) for 24 h. The medium was collected for the determination of IFN-γ or Kyn by the ELISA Kits (Fankew, China) following the manufacturer's instructions.

2.4 m^6A modification of mRNA analysis

Buffer, S1 nuclease (Takara, Japan), phosphodiesterase (Sigma-Aldrich, USA), and alkaline phosphatase (Takara, Japan) were added into 1 μg of total RNA to completely digest RNA into nucleic acid at 37°C, then extracted with chloroform (Sinopharm Chemical Reagent co., Ltd. China) and took the upper layer water sample for subsequent LC-ESI-MS/MS analysis. The liquid phase conditions are as follows: Chromatographic column: Waters ACQUITY UPLC HSS T3 C18 column (1.8 μm, 100 mm × 2.1 mm i.d.); gradient elution program: 0 min A/B is 95:5 (V/V), 1.0 min A/B is 95:5 (V/V), 9.0 min A/B is 5:95 (V/V), 11.0 min A/B is 95:5 (V/V), 11.1 min A/B is 95:5 (V/V), 14.0 min A/B is 95:5 (V/V) (phase A is ultrapure water (2mM ammonium bicarbonate), phase B is methanol (2mM ammonium bicarbonate); flow rate was at 0.3 mL/min; column temperature is 40°C; the injection volume is 10 μL. Then the MS/MS analysis conditions are as follows: Electrospray Ionization (ESI) temperature is 550°C, mass spectrometer voltage is 5500v under the positive ion mode, and Curtain Gas (CUR) is 35 psi. In Q-Trap 6500+ (SCIEX, USA), each ion pair is scanned according to optimized Declustering Potential (DP) and Collision Energy (CE). Finally, build an MWDB (Metware Database) database based on the standard, and perform qualitative analysis on the data detected by mass spectrometry.

2.5 Western blot

The process of western blot was described before (14). Antibodies for GAPDH (#8884), IDO1 (#86630S), PD-L1 (#13684T), p-STAT1 (#9167S), STAT1 (# 14994S), JAK1 (#3332S) and the secondary antibodies including horseradish peroxidase (HRP)-conjugated goat anti-rabbit IgG (#7074) were purchased from Cell Signaling Technology (Beverly, MA, USA). CD47 (#ab284132) was obtained from Abcam (Cambridge, MA, USA).

2.6 Fluorescence assay

HepG2 cells were pretreated with or without 20 μM Abrine followed by IFN-γ (20 ng/mL), PBMCs or IDO1 treatment for 24 h. Then cells were washed with PBS for 2 times and fixed with 4% PFA for 20 min at room temperature. Cells were permeabilized with 0.5% Triton X-100 and subsequently blocked with 5% BSA for 30 min. After that, the cell samples were incubated with the primary antibody against IDO1, PD-L1, STAT1, or CD47 (1:100 dilution, 100 μL) at 4 °C overnight. Cells were then incubated with the Coralite 488 Goat Anti-Rabbit lgG (1:200 dilution, 100 μL) (SA00013-2, proteintech, China) or Coralite594 Goat Anti-Rabbit lgG (SA0001d-4, proteintech, China) for 2 h at room temperature. Immunofluorescence images were captured by the confocal laser scanning microscope (Leica TCS SP8, Solms, Germany) after staining with Hoechst 33342 for 5 min.

2.7 Flow cytometry

The HepG2 cells were collected after Abrine and IFN-γ, PBMC, or IDO1 treatment for 24 h. Resuspend cells (5×10^5) in 100 μL of diluted primary antibody including IDO1, PD-L1, and CD47 respectively incubated for 0.5 h on ice and protect from light. Afterward, cells were washed with PBS and resuspended cells in 200-500 μL of PBS and analyzed by FACSMelody™ Cell Sorter (BD bioscience, USA).

2.8 Cellular thermal shift assay

The HEK293T cells were lysed with RIPA Lysis Buffer (1% PMSF and 1% cocktail). The respective cell lysates were co-incubated with vehicle control (DMSO) or Abrine (20 μM) for 0.5 h on ice and then centrifuged at 15,000 rpm for 20 minutes at 4° C. After which the supernatant was divided into 6 parts on average and heated respectively at different temperatures (44, 48, 52, 56, 60, and 64 °C) for 3 minutes followed by cooling for 30 s at room temperature, then detected by western blot assay (15).

2.9 Molecular Docking

The 2D structure of Abrine in sdf format was obtained from the PubChem database and transformed into a three-dimensional structure using ChemBio3D energy minimization saved as mol2 format. Next, the PDB number of IDO was got from the RCSB PDB database, download the 3D structure of IDO and use PyMol software to delete the water molecule and the original ligand. Hereafter, Using IDO protein as receptor and Abrine molecule as ligand, the active sites of molecular docking were determined according to the coordinates of the ligands in the target protein

complex, and AutoDock Vina was used for molecular docking, then PyMol was used for correlation mapping.

2.10 Molecular interaction analysis

Biacore X100 (Cytiva, United States) was used for the measurement of the interaction of Abrine with IDO1. Using HBS-EP buffer (Cytiva, United States) as the working buffer, dilute the IDO recombinant protein (Sino Biological, China) to a final concentration of 20 μg/ml. Next, The surface of the CM5 chip was activated with a mixture of 0.2 mol/L EDC and 50 mmol/L NHS at a ratio of 1:1 injected continuously at a flow rate of 10 μl/min for 7 minutes, and then injected 20 ug/mL IDO recombinant protein to be coupled to CM5 chip by amino coupling method, after which 1 mol/L ethanolamine hydrochloride (pH 8.5) blocking solution was injected for 7 min to block the activated chip surface. What's more, Abrine was diluted with HBS-EP buffer to 100, 50, 25, 12.5, 6.25, 3.125, and 1.5625 nmol/L, kinetic experiments were performed using the kinetic and affinity methods in the template of the Kinetic Analysis Wizard to analyze the interaction between the ligand and the receptor. The obtained data were fitted according to the analysis software, with time as the abscissa and the response value as the ordinate to calculate the binding kinetics between Abrine and IDO1.

2.11 Phagocytosis assay

The macrophages were labeled with Calcein-AM (5 μM) and incubated at 37°C in the dark for 20 min, then co-cultured with HepG2 cells labeled with pHrodo Red (120 ng/mL) at the ratio of 1:2, then added 20 μM Abrine and incubated at 37°C in the dark for 2 h. The phagocytosis of macrophages was detected by fluorescence microscope. HepG2 cells were co-cultured with macrophage cells at a ratio of 1:2 (HepG2: macrophages) and treated with or without Abrine. After 2 h, the nanolive label-free system was used to in real time observe the effect of Abrine on macrophage cells engulfing tumor cells. The videos were processed with image J.

2.12 Gene expression profiling

To further reveal the role of IFN-γ in hepatic carcinoma, the correlations between IFN-γ and CD47, IDO1, and PD-L1 were analyzed by calculating Pearson correlation coefficients through The Cancer Genome Atlas (TCGA) database, the cBioPortal website (https://www.cbioportal.org/) and UCSC Xena (https://xena.ucsc.edu/) website. The correlation between IFN-γ and CD47, IDO1, and PD-L1 was analyzed by calculating Pearson correlation coefficients in GraphPad Prism 9.

2.13 Tumor xenografts animal experiments

Animal experiments were approved by the Ethics Committee on Laboratory Animal Management of Guangxi University of Chinese Medicine (Approval Document No. SYXK-2019–0001). Healthy C57BL/6J mice (SPF degree, 6-8 weeks old, male, weight 18-22 g) were purchased from Vital River Laboratory (Guangdong, China, animal license #: SCXK-2022-0063). All animals were housed under specific pathogen-free (SPF) conditions at 25°C with 50% humidity and free access to food and water. After three days of adaptive feeding, Hepa1-6 cells in 0.1 mL basic DMEM were inoculated in the right hind leg of the mice at a density of 1×10^6 cells/mice apart from those in the control group (16, 17). After 7 days, the tumor volume reached almost 100 mm^3 in mice. The tumor-bearing mice were randomly divided into 4 groups (n = 6 for each group): the model group, the anti-PD-1 Ab group, the Abrine group (15 mg/kg) (18), and the combination of Abrine and anti-PD-1 Ab group. The unvaccinated mice served as a control group (n=6). On day 7, Abrine was dissolved with saline and administered into mice by intraperitoneal injection (i.p.) for 14 days, once a day. At the same time, anti-PD-1 Ab (Purity>95%, InVivoMab anti-mouse PD-1 (CD279), BioXCell, USA) was freshly prepared by PBS and intraperitoneally injected into mice (200 μg/mice), once every 3 days (19). Besides, the mice in the control and model groups were injected with an equal volume of saline. The mice's tumor volume was measured every two days. On day 21, the blood, tumor, and organ tissues of mice were collected after the mice were anesthetized with isoflurane and sacrificed.

2.14 Flow cytometry of tumor tissues

The single cell suspension from tumor tissues was filtered after subsequently resuspended for counting and concentration adjustment, labeled with biomarkers CD45-PerCP-Cy™5.5 rat anti-mouse (#550994, BD Biosciences, USA), CD3-BV510 hamster anti-mouse (#740113, BD Biosciences, USA), CD4-PE-Cy™7 rat anti-mouse (#552775, BD Biosciences, USA) and CD8a-BV786 rat anti-mouse (#563332, BD Biosciences, USA) for subsequent flow cytometry detection.

2.15 Hematoxylin and eosin staining, single- and multiplex immunofluorescence

After the mice were anesthetized, the heart, liver, spleen, lung, kidney, brain tissue, and part of tumor tissue specimens were isolated, and fixed in 4% Paraformaldehyde Fix Solution for HE staining, single- and multiplex immunofluorescence for CD47, IDO1, CD8, PD-L1, and Foxp3. The rest of the tumor was frozen in liquid nitrogen for other studies.

2.16 Statistics

Student's unpaired t-test and one-way ANOVA in GraphPad Prism were used for statistical analysis in GraphPad Prism 9 (GraphPad Software, USA). $P < 0.05$ were considered statistically significant.

3 Results

3.1 Abrine inhibits m^{6}A RNA methylation and IDO1/JAK1/STAT1 signal pathway in IFN-γ-induced HepG2 cells

Abrine is a natural product extracted from Traditional Chinese Medicine (Figure 1A). To explore the relationship between IFN-γ and the expression of immune checkpoints, the correlation between IFN-γ and CD47, IDO1, and PD-L1 was detected from the TCGA database, and it was found that IFN-γ had positive correlation responses with all of them in HCC (Figures 1B–D). The m^{6}A RNA methylation modification plays an important role in the occurrence and progression of cancers, in this study, we found that IFN-γ treatment increased the m^{6}A RNA methylation in HepG2 cells, while Abrine inhibits IFN-γ-induced RNA m^{6}A methylation (Figure 1E). At the same time, Abrine at 5, 10, 20, and 40 μM has no cytotoxic in HepG2 cells. (Figure 1F). In addition, Abrine inhibited Kynurenine (Kyn) level, which was produced by the metabolism of tryptophan through the activation of the key metabolic enzyme IDO1 (Figure 1G). Abrine decreased the protein expression of IDO1, JAK1, p-STAT1, and STAT1 (Figures 1H, I, L) in IFN-γ-induced HepG2 cells. Moreover, Abrine inhibited the translocation of STAT1 from the cytoplasm into nuclear (Figures 1J, K, M). These data indicated that Abrine has an epigenetic regulatory role and inhibits IDO1/JAK1/STAT1 signaling pathway in IFN-γ-induced HepG2 cells.

3.2 Abrine inhibits IDO-1/JAK1/STAT1 signal pathway in PBMC-induced HepG2 cells

The co-culture model of immune cells and tumor cells is the most widely used model of tumor immunity research *in vitro*. In this study, PBMCs were co-cultured with HepG2 cells to imitate the interaction between immune cells and tumor cells, and to better explore the effectiveness and internal mechanism of tumor immunity research strategies (Figure 2A). As shown in Figures 2B, C, PBMCs treatment increased the IFN-γ and Kyn level, which was suppressed by Abrine. What's more, the expression of IDO1, JAK1, p-STAT1, and STAT1 was determined by western blot. The results showed that the expressions of IDO-1, JAK1, p-STAT1, and STAT1 proteins were increased in PBMCs co-cultured HepG2 cells, while Abrine inhibited the protein expression (Figures 2D–F). Besides, Abrine suppressed the STAT1 translocation from the cytoplasm into the nuclear (Figure 2G), these data indicated that PBMC increased the IFN-γ and Kyn level in HepG2 cells, therefore increasing the IDO1/JAK1/STAT1 signaling pathway proteins expression, which was suppressed by Abrine.

3.3 Abrine targets on IDO1 to inhibit IDO1/JAK1/STAT1 signaling pathway

IDO1, the first rate-limiting enzyme of tryptophan catabolism, is continuously highly expressed in a variety of solid tumor tissues and is closely related to poor prognosis. The inhibition of IDO1 can promote the efficacy of immunization and chemotherapy (20). Therefore, IDO1 inhibitors have a prospect for development as potential drugs for tumor immunotherapy. Abrine has been reported to be a specific IDO1 inhibitor. In the present study, Abrine suppressed the increased IFN-γ and Kyn levels in IDO1 recombinant protein-treated HepG2 cells (Figures 3A, B), and increased the expression of IDO1, JAK1, p-STAT1, and STAT1 in HepG2 cells, while all of which were decreased by Abrine (Figures 3C, D). What's more, flow cytometry results further indicated that increased IDO1 expression was inhibited by Abrine in IDO1-induced HepG2 cells (Figures 3E, F). Afterward, the molecular docking assay was used to examine the interaction between Abrine and IDO1. The results showed that Abrine interacts with IDO1 at the sites of SER:167, VAL:170, PHE:214, LEU:342, VAL:269, PHE:270, and ARG:343 (Figures 3H, I). Biacore X100 SPR assay was used to detect the Kinetics/Affinity of Abrine and IDO1, results showed that the K_D value was 64.5 μM, which indicated that Abrine has a strong interaction ability with IDO1 (Figures 3J, K). CETSA assay further confirmed that IDO1 protein was more stable under the action of Abrine at a series of temperatures (Figure 3G). These data indicated that Abrine interacts with IDO1 and as an inhibitor of IDO1 to inhibit IDO1/JAK1/STAT1 signaling pathway in IDO-1-induced HepG2 cells.

3.4 Abrine inhibits CD47 and promotes the phagocytosis of macrophages

CD47 is an important anti-phagocytosis signal, which can prevent the phagocytosis of tumor cells by macrophages *via* binding to ligand signal regulatory protein α (SIRPα) on macrophages (21). We found a positive correlation between interferon-γ (IFN-γ) and CD47 in HCC cells (Figure 1B), IFN-γ, PBMCs, and IDO1 could increase the expression of CD47 in HepG2 cells, while Abrine decreased the expression of CD47 (Figures 4A–C). The CD47 expression was further detected by flow cytometry and immunofluorescence, results indicated that Abrine could decrease the expression of CD47 in IFN-γ, PBMCs, and IDO1-induced cells (Figures 4D–I). Then, Calcein-AM-labeled macrophages derived from PBMC, and pHrodo Red-labeled HepG2 cells were co-cultured to detect the phagocytosis of macrophages to tumor cells. Results showed that Abrine treatment in either HepG2 or macrophages both increased the phagocytosis effect of macrophages on HepG2 cells and could recruit more macrophages to the cancer cells (Figures 4J, K and Video1, 2). Collectively, these data suggested that Abrine could promote the phagocytosis of tumor cells by macrophages and prevent the immune escape of tumor cells by inhibiting the expression of CD47.

3.5 Abrine inhibits PD-L1 in IDO1 overexpression HepG2 cells

PD-L1/PD-1 axis is an important immune checkpoint, which can promote the tumor cell escape from immune monitoring, and the PD-L1/PD-1 inhibitors as ICIs are widely used in clinical for the

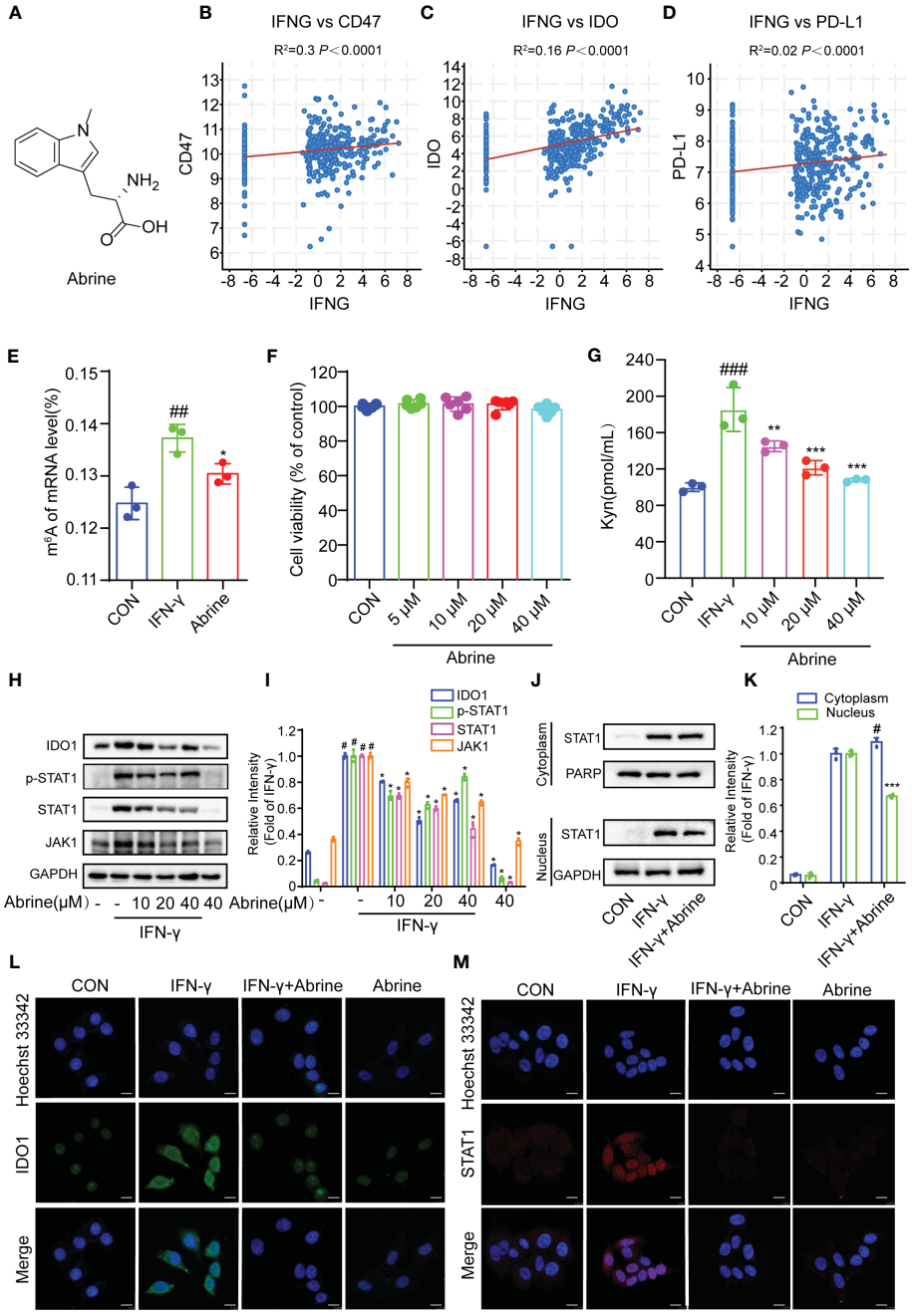

FIGURE 1
Abrine inhibits m^{6}A RNA methylation and IDO1/JAK1/STAT1 signal pathway in IFN-γ-induced HepG2 cells. **(A)** The structure of Abrine; **(B–E)** The correlations between IFN-γ and CD47, IDO, and PD-L1 in HCC cells were analyzed by calculating the Pearson correlation coefficient; **(E)** The RNA m6A methylation analysis based on LC-MS/MS, $^{\#\#}p < 0.01$ versus the control group; $^{*}p < 0.05$ versus the IFN-γ group; **(F)** HepG2 cells were treated with the Abrine for 24 **h** The cytotoxicity was determined by MTT assay; **(G)** The effect of Abrine on the Kyn levels in IFN-γ-induced HepG2 cells by ELISA assay, $^{\#\#\#}p < 0.001$ versus the control group; $^{**}p < 0.01$, $^{***}p < 0.001$ versus the IFN-γ group; **(H, I)** Western blot analysis detects the effect of Abrine on the expression of the proteins including IDO1, p-STAT1, STAT1, and JAK1. The relative protein band intensities were counted, $^{\#}p < 0.001$ versus the control group; $^{*}p < 0.001$ versus the IFN-γ group; **(J, K)** The localization of STAT1 in the cytoplasm and nucleus of HepG2 cells was detected by western blotting, $^{\#}p < 0.05$ versus the control group; $^{***}p < 0.001$ versus the IFN-γ group; **(L, M)** The immunofluorescence detected the effect of Abrine on the expression of IDO1 and STAT1 translocation in IFN-γ-induced HepG2 cells (Scale bar = 20 μm).

treatment of varieties of cancers (22). In this study, we found a positive correlation between interferon-γ (IFN-γ) and PD-L1 in HCC cells (Figure 1B), and this study found that Abrine could decrease the PD-L1 expression in IFN-γ, PBMCs, and IDO1-induced IDO1 overexpression HepG2 cells (Figures 5A–C). The flow cytometry results indicated that IDO1 increased the expression of PD-L1, Abrine could decrease the expression of PD-L1 (Figures 5D, E). The immunofluorescence results showed that PBMC or IFN-γ increased the expression of PD-L1, and Abrine suppressed its expression (Figures 5F, G). These data indicated that

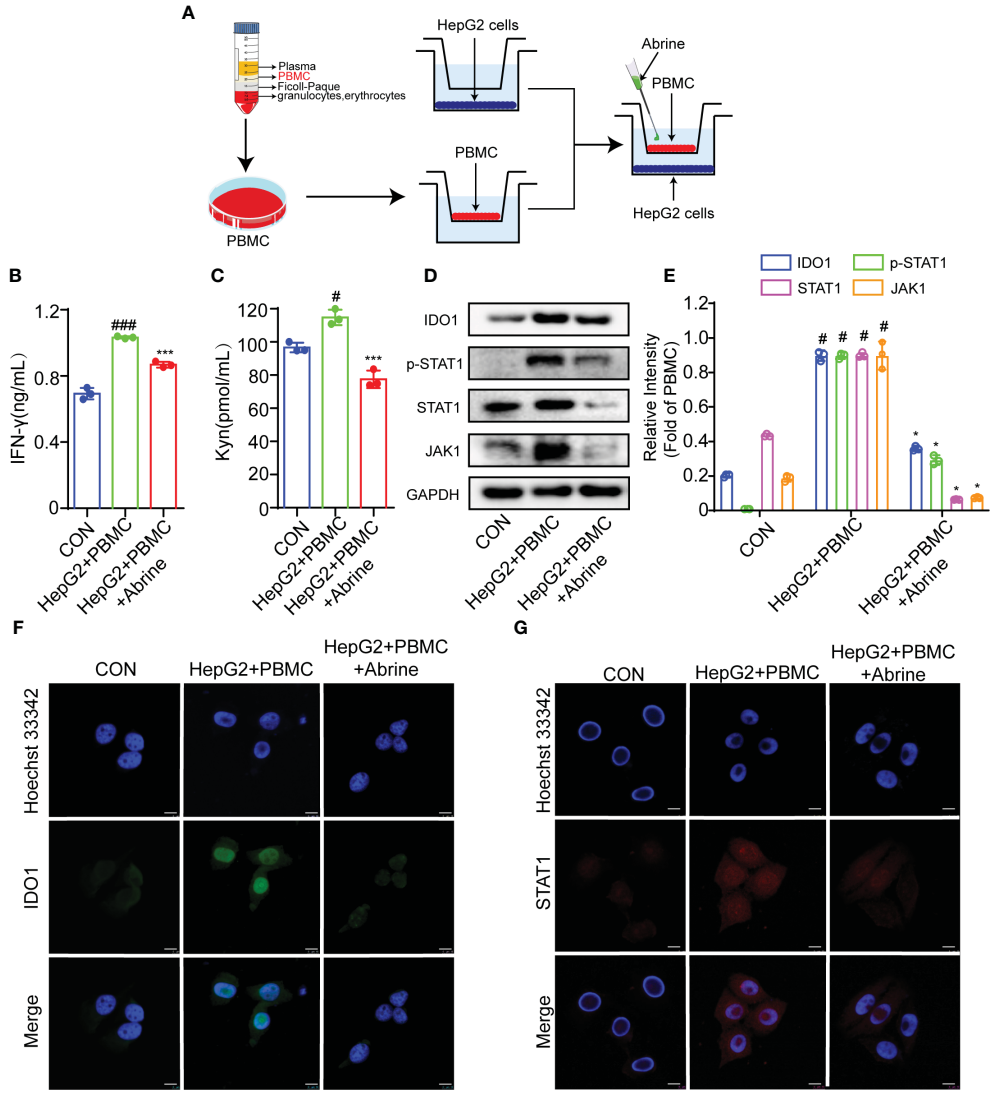

FIGURE 2
Abrine inhibits IDO-1/JAK1/STAT1 signal pathway in PBMC-induced HepG2 cells. **(A)** The schedule of PBMC co-culture with HepG2 cells; **(B, C)** The effect of Abrine on the level of IFN-γ and Kyn in PBMC-induced HepG2 cells; $^{\#}p < 0.05$, $^{\#\#\#}p < 0.001$ versus the control group; $^{***}p < 0.001$ versus the HepG2+PBMC group; **(D, E)** The effect of Abrine on the proteins expressions in PBMC-induced HepG2 cells as indicated; $^{\#}p < 0.001$ versus the control group; $^{*}p < 0.001$ versus the HepG2+PBMC group; **(F, G)** Immunofluorescence detected the effect of Abrine on the expression of IDO1 and STAT1 in PBMC-induced HepG2 cells (Scale bar = 20 μm).

IDO1 overexpression may lead to the increased expression of PD-L1, which could be inhibited by the IDO1 inhibitor Abrine.

3.6 Abrine and anti-PD-1 antibody treatment has a synergistic effect on Hepa1-6 xenograft mice model

Although anti-PD-1 immunotherapy has great progress in tumor treatment, there are still problems such as low response rate and adverse reactions in the treatment of many solid tumors. The high expression of IDO1 is also the main cause of resistance to PD-1/PD-L1 inhibitors. Based on this, we combined Abrine with anti-PD-1 antibody to treat the Hepa1-6 xenograft mice model. Results showed that Abrine, anti-PD-1 antibody, and the combination treatment groups could suppress the tumor growth and tumor volume, and Abrine co-treated with anti-PD-1 antibody has a synergistic effect on inhibiting the tumor growth than Abrine or anti-PD-1 antibody-treated groups (Figures 6A–D). And HE staining of the heart, liver, spleen, lung, kidney, and brain showed the safety of Abrine (Figure 6E). Flow cytometry detected the $CD3^{+}CD4^{+}$ T cells and $CD3^{+}CD8^{+}$ T cells, results indicated that Abrine co-treated with anti-PD-1 antibody increased the $CD3^{+}CD8^{+}$ T cells obviously than Abrine or anti-PD-1 antibody-treated groups, which means that the infiltration of $CD8^{+}$T cells was increased in tumor cells and promotes immune responses (Figures 7A, B). As shown in Figure 7C, CD47 expression increased in model mice, while Abrine, anti-PD-1 antibody, and the combination treatment groups could suppress the expression of CD47, and the combination treatment groups has a better

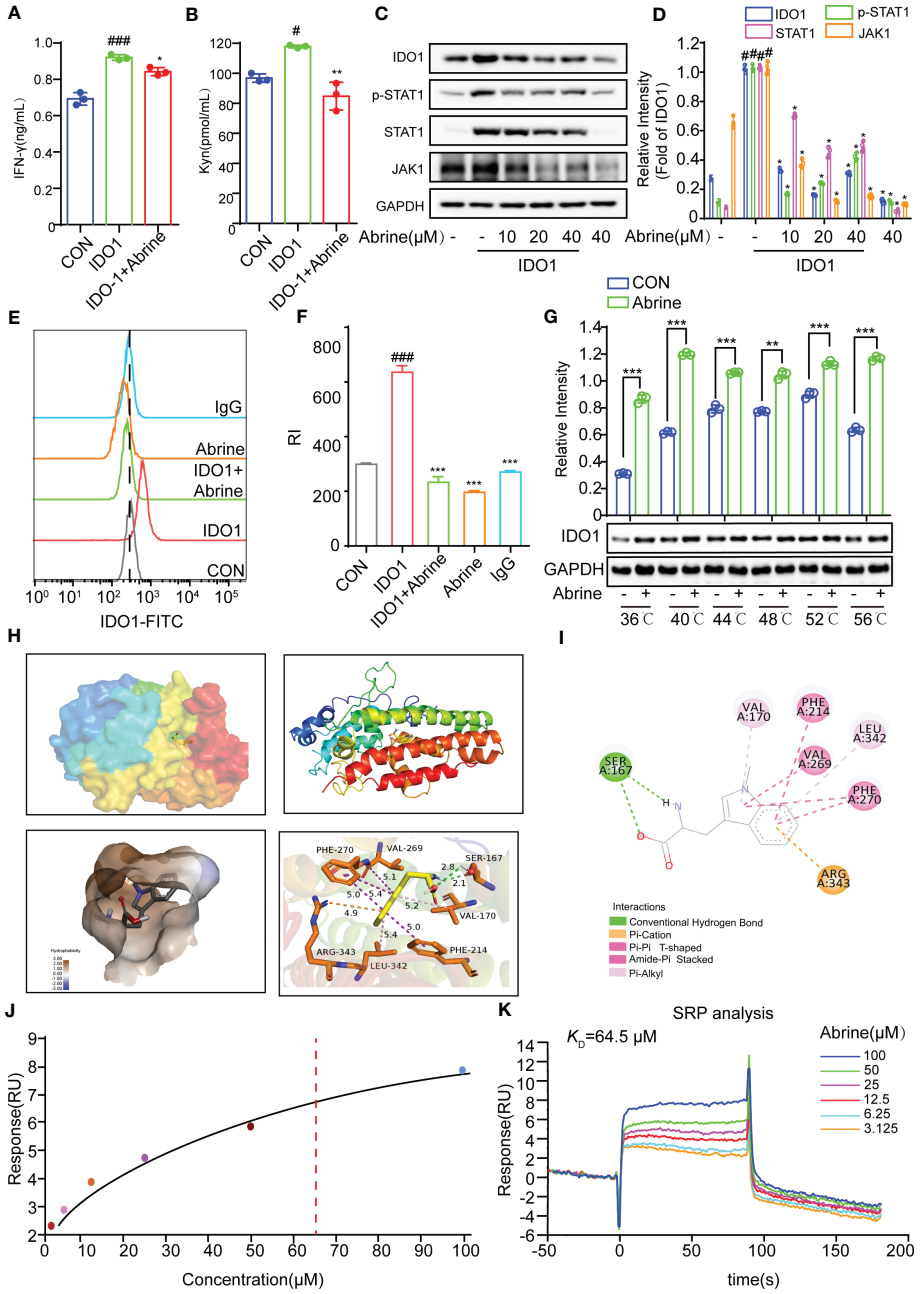

FIGURE 3
Abrine targets on IDO1 to inhibit IDO1/JAK1/STAT1 signaling pathway. **(A, B)** The effect of Abrine on the level of IFN-γ and Kyn in IDO1-induced HepG2 cells, $^{\#}p < 0.05$, $^{\#\#\#}p < 0.001$ versus the control, $^{*}p < 0.05$, $^{**}p < 0.01$versus the IDO1 group; **(C, D)** The effect of Abrine on the expression of the proteins in IDO1-induced HepG2 cells as indicated, $^{\#}p < 0.001$ versus the control, $^{*}p < 0.001$ versus the IDO1 group; **(E, F)** Flow cytometry detected the level of IDO-1 in IDO-1-induced HepG2 cells, $^{\#\#\#}p < 0.001$ versus the control, $^{***}p < 0.001$ versus the IDO1 group; **(G)** CETSA detected the interaction of Abrine with IDO1; **(H, I)** Molecular docking results of Abrine with IDO1, $^{**}p < 0.01$, $^{***}p < 0.001$; **(J, K)** Biacore X100 detected the kinetics/Affinity of Abrine with IDO-1.

suppression effect than Abrine or anti-PD-1 antibody-treated groups. mIHC results showed that Abrine co-treated with anti-PD-1 antibody increased $CD8^+$ cytotoxic T cells infiltration in tumor cells, decreased $Foxp3^+$ Treg cells, and inhibited IDO1 and PD-L1 expression (Figure 7D). These data indicated that Abrine has a synergistic effect with the anti-PD-1 antibody on the treatment of HCC through regulating immune responses.

4 Discussion

Due to the complex pathogenesis, high molecular heterogeneity and immune tolerance microenvironment, the systemic treatment of advanced liver cancer has always been a difficult research point (23–25). In recent years, immunotherapy especially immune checkpoint inhibitors (ICIs) have brought a new opportunity to

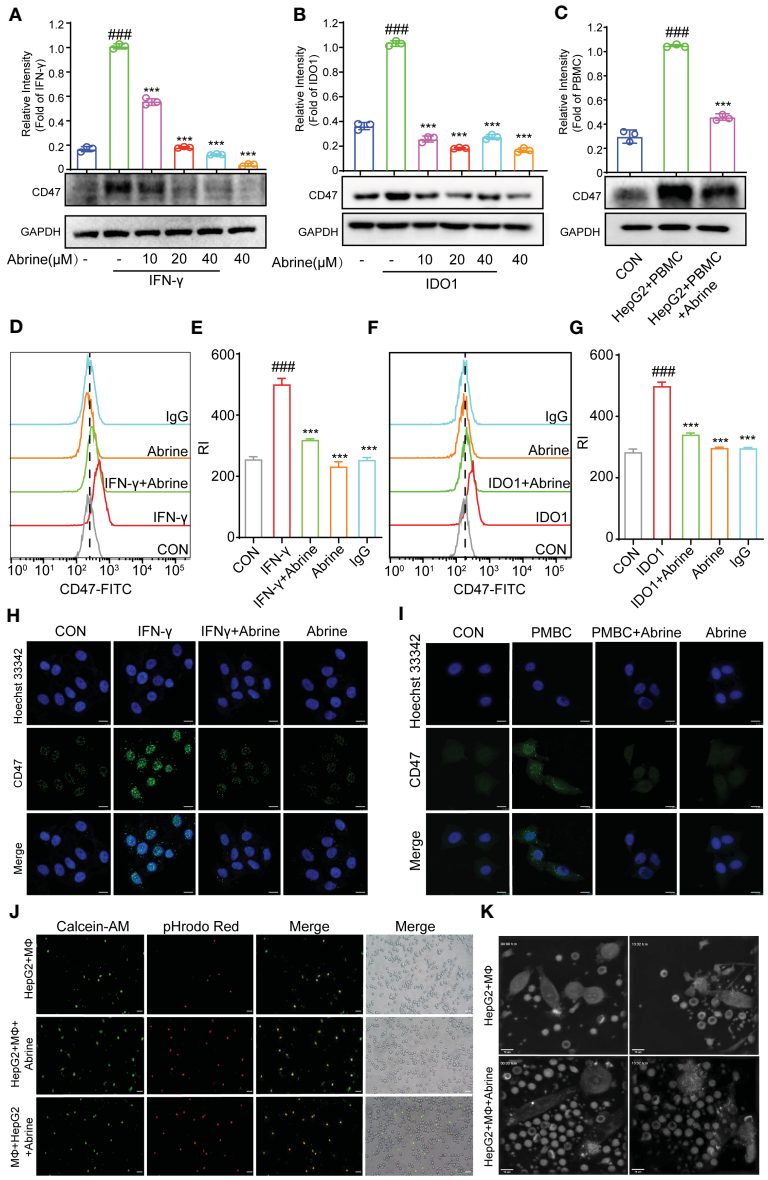

FIGURE 4
Abrine inhibits CD47 and promotes the phagocytosis of macrophages. **(A–C)** Western blot detected the expression of CD47 in IFN-γ, IDO1, and PBMC-induced HepG2 cells; **(D–G)** Flow cytometry detected the level of CD47 in IFN-γ and IDO1-induced HepG2 cells; **(H, I)** Immunofluorescence detected the expression of CD47 in IFN-γ and PBMC-induced HepG2 cells (Scale bar = 20 μm); **(J)** The phagocytosis effect of Abrine on macrophages engulf the HepG2 cells (Scale bar = 20 μm). **(K)** Images from Video 1 and 2, HepG2 cells were co-cultured with macrophages at a ratio of 1:2, and the phagocytosis effect of Abrine on macrophages engulf the HepG2 cells after co-culture 2 h was detected by the nanolive label-free system (Scale bar = 10 μm). $^{###}p < 0.001$ versus the control, $^{***}p < 0.005$ versus the model group.

improve the survival rate of patients with advanced liver cancer (26). However, the related therapeutic drugs and mechanisms still need more research. In this study, we found that Abrine as an IDO1 inhibitor has an inhibition effect on immune escape, and its combination therapy with immune checkpoint inhibitor anti-PD-1 antibody exerted a better anti-tumor effect.

IDO1 expression is present not only in tumor cells but also in endothelial cells, fibroblasts, and immune cells that infiltrate the TME (27). The main function of IDO1 is to decompose Trp into Kyn and its downstream metabolites, which are responsible for tumor immune escape by regulating T cell-associated immune responses and promoting the activation of immunosuppressive cells (28). Studies have shown that most tumor cells are positive for IDO1, and the strong expression of IDO1 in tumor tissue has also been identified as an independent negative prognostic factor for many cancers (29–32). IDO1 expression of tumor cells correlates with tumor-infiltrating $Foxp3^+$ Tregs and other immunosuppressive molecules such as PD-1 and its ligand PD-L1 (33). IFN-γ is widely considered to be the major inducer of IDO1. As HepG2 cells hardly express IDO1, co-cultured with IFN-γ or PBMCs could be upregulated (34). Our data showed that Abrine significantly reduced the expression of IDO1 and Kyn level in IFN-γ, PBMCs, or exogenous IDO1-induced HepG2 cells.

IFN-γ is one of the most important cytokines in inflammatory and immune responses, mainly produced by natural killer (NK)

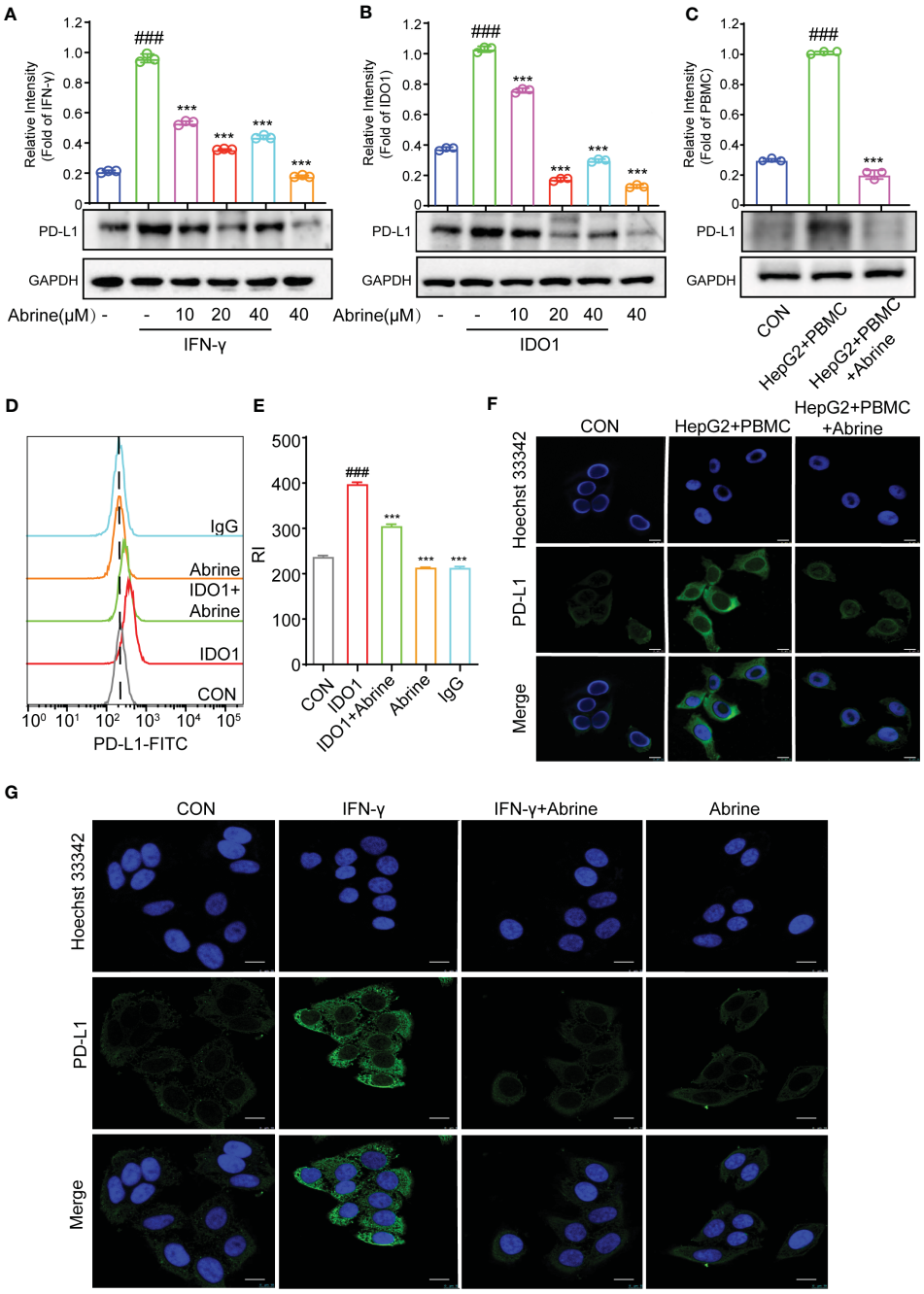

FIGURE 5
Abrine inhibits PD-L1 in IDO1 overexpression HepG2 cells. **(A–C)** Western blot detected the expression of PD-L1 in IFN-γ, IDO1, and PBMC-induced HepG2 cells; **(D, E)** Flow cytometry detected the level of PD-L1 in IDO1-induced HepG2 cells; **(F, G)** Immunofluorescence detected the expression of PD-L1 in PBMC and IFN-γ-induced HepG2 cells (Scale bar = 20 μm). $^{###}p < 0.001$ versus the control, $^{***}p < 0.005$ versus the model group.

cells in the innate immune system and T cells in the adaptive immune system, which plays an important role in immunopathology and immune response (35). The JAKs/STAT1 pathway is critical for IFN-γ to generate signal transduction. Binding of IFN-γ to its receptor IFNGR activates JAKs, which subsequently lead to phosphorylation, activation, and dimerization of the transcription factor STAT1. The newly formed STAT1 homodimers subsequently translocate to the nucleus where they initiate the transcription of some IFN-γ-stimulated genes (ISGs) (36, 37). Our data showed that Abrine could reduce the level of IFN-γ elevated by PBMCs or IDO1, significantly decrease the expression of JAK1 and the phosphorylation of STAT1, besides, prevent IFN-γ or PBMCs-induced nuclear translocation of STAT1.

IFN-γ regulates immune escape correlated with the overexpression of immune checkpoint receptors including PD-L1 and IDO1, which eliminates T cell activity in tumor tissues (38, 39). The combination of highly expressed PD-L1 on tumor cells and the receptor PD-1 on T cells transmit negative regulatory signals,

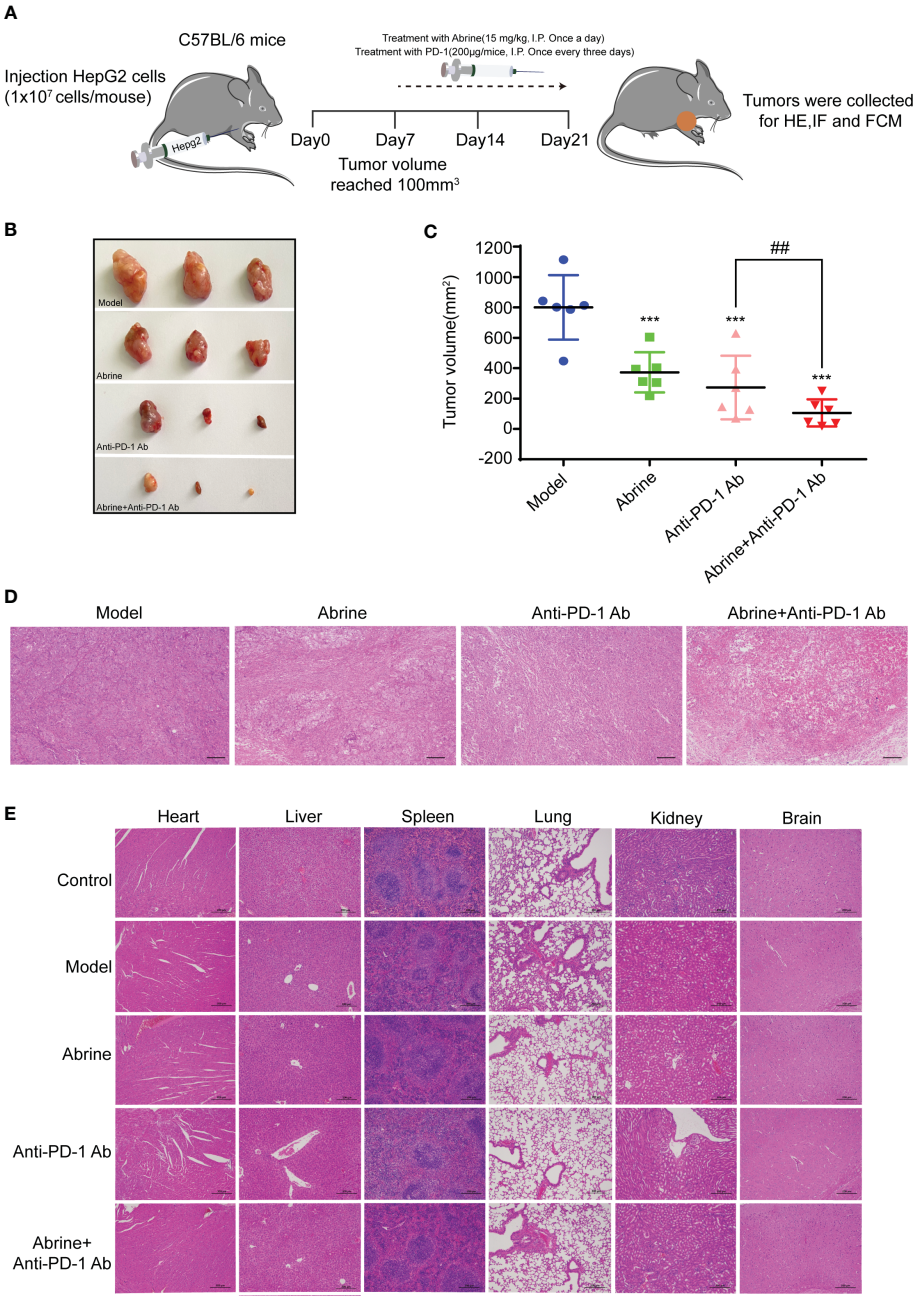

FIGURE 6
Abrine and anti-PD-1 antibody treatment has a synergistic effect on Hepa1-6 xenograft mice model. **(A–C)** The effect of Abrine, anti-PD-1 antibody, and Abrine co-culture with anti-PD-1 antibody on tumor size, tumor volume, and pathological changes; **(D)** The HE staining of tumor tissues (Scale bar = 20 μm). **(E)** The HE staining of heart, liver, spleen, lung, kidney, and brain (Scale bar = 20 μm). ***$p < 0.005$ versus the model group, $^{\#\#}p < 0.01$ versus the anti-PD-1 Ab group.

induce T cell apoptosis, or lead to immune incompetence, therefore, tumor cells can escape from the immune monitoring and killing (40). At the same time, the activation of the PD-1/PD-L1 axis can also change the differentiation of T cells, impair the differentiation of effector T cells (Teff), memory T cells (Tm), regulatory T lymphocytes (Treg) and exhausted T cells (Tex), thereby significantly inhibiting T cell immune effects (41, 42). In addition, Ye et al. found that IFN-γ-induced increased CD47 expression through the JAK1-STAT1 axis might be a common phenomenon in cancer, which would increase the affinity between CD47 and SIRPα, amplify the "don't eat me" signal, reduce the phagocytosis ability of macrophages, and mediate immune escape (43). TCGA database statistic results showed that IFN-γ was positively correlated with both CD47 and PD-L1 in HCC. Our further experiments found that IFN-γ or PBMCs up-regulated the levels of PD-L1 and CD47 in HepG2 cells obviously, which could be inhibited by Abrine. Moreover, the Abrine treatment also promoted the phagocytosis of HepG2 cells by macrophages, which might be related to the inhibitory effect of Abrine on CD47. However, the effect of Abrine on CD47-SIRPα signal needs further study.

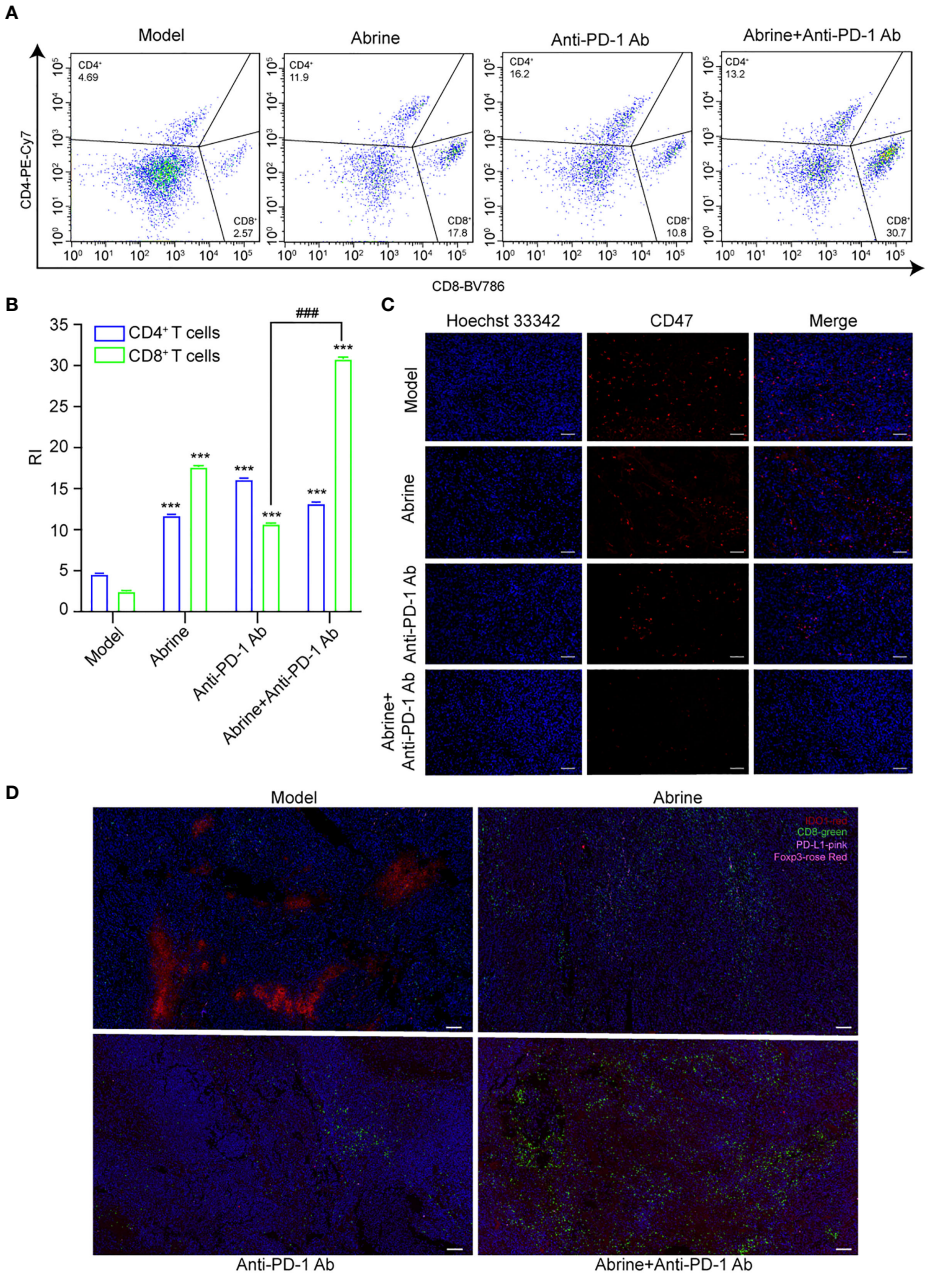

FIGURE 7
Abrine and anti-PD-1 antibody treatment has a synergistic effect on Hepa1-6 xenograft mice model. **(A, B)** Flow cytometry detected the effect of Abrine, amti-PD-1 antibody, and Abrine co-culture with anti-PD-1 antibody on $CD4^+$ T cells and $CD8^+$ T cells; **(C)** The IHC staining of CD47 expression (Scale bar = 20 μm); **(D)** The mIHC staining detect the expression of CD8+ T cells, PD-L1, IDO1, Foxp3 expression in tumor tissues (Scale bar = 10 μm). ***$p < 0.005$ versus the model group, $^{###}p < 0.001$ versus anti-PD-1 Ab group.

PD-1/PD-L1 monoclonal antibodies have made breakthroughs in the treatment of many cancers in clinical, but there are still problems such as a high incidence of adverse reactions and a large range of treatment tolerance (44, 45). Previous studies found that the high expression of IDO1 is the main cause of resistance to PD-1/PD-L1 inhibitors (46). Therefore, IDO1 inhibitors not only exert anti-tumor activity but also may enhance the therapeutic effect of PD-1/PD-L1 inhibitors when combined with PD-1/PD-L1 inhibitors. In this study, Abrine and anti-PD-1 antibody were used to treat Hepa1-6 xenograft mice, results showed that both inhibited the expression of CD47 and PD-L1 in tumor tissues of mice, increased the levels of $CD4^+$ and $CD8^+$ T cells, decreased the level of $Foxp3^+$ Treg cells. The combination of Abrine and anti-PD-1 antibody obtained a better tumor inhibitory effect than the two used alone, indicating that there is a synergistic effect of Abrine with anti-PD-1 antibody on the treatment of HCC.

m6A modification is an RNA-associated epigenetic regulation similar to DNA and histone modifications. Among which, m6A methylation is the most abundant epitranscriptomic modification in eukaryotic mRNA, participates in the complex and fine biological

regulation of important functional genes in many cellular activities, and may promote carcinogenesis by up-regulating or down-regulating important components of cell signal transduction in the occurrence and development of cancer (47–50). Studies have shown that JAKs-STAT1 signaling pathway may be regulated by m6A at the transcriptional level, resulting in aberrant signaling in cancer progression. Suppressors of cytokine signaling (SOCS) are negative regulators of the JAKs-STAT1 signaling pathway, inhibiting the activation of this pathway under normal physiological conditions (51, 52). In HCC, SOCS is recognized and degraded as a target of m6A writer methyltransferase-like 3 (METTL3)-mediated m6A modification, thereby abrogating its inhibitory effect on the JAKs-STAT1 pathway (53, 54). These findings show that m6A methylation modification has a regulatory effect on the JAKs-STAT1 pathway in HCC progression. In the study, we found that IFN-γ can induce the increase of m6A modification in HepG2 cells, and this increased m6A methylation level was significantly inhibited by Abrine, indicating that abrine has a role in regulating abnormal m6A modification in tumor cells, therefore affecting the JAK1/STAT1 signal pathway.

Collectively, we found that Abrine has an anti-tumor immune escape and promote immune response effect by inhibiting IDO1. Abrine targets IDO1 to down-regulate the level of IFN-γ and the accumulation of metabolite Kyn, inhibiting the expression of PD-L1 and CD47 through the JAK1-STAT1 signaling pathway. In addition, Abrine synergizes with immune checkpoint inhibitor anti-PD-1 antibody to enhance tumor suppression, increases the infiltration of $CD8^+$ T cells in the tumor cells, decreases the expression of CD47 and PD-L1 in tumor tissues, and down-regulate the $Foxp3^+$ Treg cells to exert anti-tumor immune escape.

Data availability statement

The original contributions presented in the study are included in the article/Supplementary Material. Further inquiries can be directed to the corresponding authors.

Ethics statement

The studies involving human participants were reviewed and approved by the Ethics Committee of Guangxi University of Chinese Medicine. The patients/participants provided their written informed consent to participate in this study. The animal study was reviewed and approved by Ethics Committee on Laboratory Animal Management of Guangxi University of Chinese Medicine.

Author contributions

HG and JX designed the research. XL, SH, and JH conducted experiments in vitro. XL and RY conducted experiments in vivo. RY and XL wrote the manuscript. C. Yao and SY revised the manuscript. All authors reviewed the manuscript.

Acknowledgments

We would like to appreciate the Guangxi Science and Technology Major Project (GUIKEAA22096029, 2022JBGS042), the Doctoral Foundation of Guangxi University of Chinese Medicine (2022BS008), the 2023 Young and middle-aged teachers in colleges and universities in Guangxi Scientific research basic ability improvement project (2023KY0303), the project of Guangxi overseas “100 persons’ plan” high-level expert, the Innovation Project of Guangxi Graduate Education (YCSW2019176, China), and Qihuang High-level Talent Team Cultivation Project of Guangxi University of Chinese Medicine (2021002).

Conflict of interest

The authors declare that the research was conducted in the absence of any commercial or financial relationships that could be construed as a potential conflict of interest.

Publisher’s note

Supplementary material

The Supplementary Material for this article can be found online at: https://www.frontiersin.org/articles/10.3389/fimmu.2023.1185985/full#supplementary-material

References

1. Feinberg AP, Levchenko A. Epigenetics as a mediator of plasticity in cancer. *Sci (New York N.Y.)* (2023) 379(6632). doi: 10.1126/science.aaw3835

2. Li X, Ma S, Deng Y, Yi P, Yu J. Targeting the RNA m(6)A modification for cancer immunotherapy. *Mol Cancer* (2022) 21(1):76. doi: 10.1186/s12943-022-01558-0

3. Li X, Ramadori P, Pfister D, Seehawer M, Zender L, Heikenwalder M. The immunological and metabolic landscape in primary and metastatic liver cancer, nature reviews. *Cancer* (2021) 21(9):541–57. doi: 10.1038/s41568-021-00383-9

4. Craig AJ, von Felden J, Garcia-Lezana T, Sarcognato S, Villanueva A. Tumour evolution in hepatocellular carcinoma, nature reviews. *Gastroenterol Hepatol* (2020) 17 (3):139–52. doi: 10.1038/s41575-019-0229-4

5. Ferrante ND, Pillai A, Singal AG. Update on the diagnosis and treatment of hepatocellular carcinoma. *Gastroenterol Hepatol (N Y)* (2020) 16(10):506–16.

6. Tang K, Wu YH, Song Y, Yu B. Indoleamine 2,3-dioxygenase 1 (IDO1) inhibitors in clinical trials for cancer immunotherapy. *J Hematol Oncol* (2021) 14(1):68. doi: 10.1186/s13045-021-01080-8

7. Zhai L, Ladomersky E, Lenzen A, Nguyen B, Patel R, Lauing KL, et al. IDO1 in cancer: a Gemini of immune checkpoints. *Cell Mol Immunol* (2018) 15(5):447–57. doi: 10.1038/cmi.2017.143

8. Shao J, Hou L, Liu J, Liu Y, Ning J, Zhao Q, et al. Indoleamine 2,3-dioxygenase 1 inhibitor-loaded nanosheets enhance CAR-T cell function in esophageal squamous cell carcinoma. *Frontiers in Immunology* (2021) 12:. doi: 10.3389/fimmu.2021.661357

9. Burke JD, Young HA. IFN-γ: a cytokine at the right time, is in the right place. *Semin Immunol* (2019) 43:101280. doi: 10.1016/j.smim.2019.05.002

10. Feng M, Jiang W, Kim BYS, Zhang CC, Fu YX, Weissman IL. Phagocytosis checkpoints as new targets for cancer immunotherapy, nature reviews. *Cancer* (2019) 19(10):568–86. doi: 10.1038/s41568-019-0183-z

11. Zhang W, Huang Q, Xiao W, Zhao Y, Pi J, Xu H, et al. Advances in anti-tumor treatments targeting the CD47/SIRPα axis. *Frontiers in Immunology* (2020) 11:. doi: 10.3389/fimmu.2020.00018

12. Qu S, Jiao Z, Lu G, Xu J, Yao B, Wang T, et al. Human lung adenocarcinoma CD47 is upregulated by interferon-γ and promotes tumor metastasis. *Mol Ther oncolytics* (2022) 25:276–87. doi: 10.1016/j.omto.2022.04.011

13. Yang M, Al Zaharna M, Chen YS, Li L, Cheung HY. *In vitro* antioxidant activities and anti-proliferative properties of the functional herb abrus cantoniensis and its main alkaloid abrine. *Food Funct* (2014) 5(9):2268–77. doi: 10.1039/c4fo00217b

14. Yuan R, Zhao W, Wang QQ, He J, Han S, Gao H, et al. Cucurbitacin b inhibits non-small cell lung cancer in vivo and in vitro by triggering TLR4/NLRP3/GSDMD-dependent pyroptosis. *Pharmacol Res* (2021) 170. doi: 10.1016/j.phrs.2021.105748

15. Jafari R, Almqvist H, Axelsson H, Ignatushchenko M, Lundbäck T, Nordlund P, et al. The cellular thermal shift assay for evaluating drug target interactions in cells. *Nat Protoc* (2014) 9(9):2100–22. doi: 10.1038/nprot.2014.138

16. Shin S-W, Yang K, Lee M, Moon J, Son A, Kim Y, et al. Manganese ferrite nanoparticles enhance the sensitivity of Hepa1-6 hepatocellular carcinoma to radiation by remodeling tumor microenvironments. *Int J Mol Sci* (2021) 22(5):2637. doi: 10.3390/ijms22052637

17. Kimura T, Kato Y, Ozawa Y, Kodama K, Ito J, Ichikawa K, et al. Immunomodulatory activity of lenvatinib contributes to antitumor activity in the Hepa1-6 hepatocellular carcinoma model. *Cancer Sci* (2018) 109(12):3993–4002. doi: 10.1111/cas.13806

18. Zhang S. Abrine elicits liver carcinoma immunity and enhances antitumor efficacy of immune checkpoint blockade by modulating PD-L1 signaling. *J Oncol* (2022) 2022:7609676. doi: 10.1155/2022/7609676

19. Mall C, Sckisel GD, Proia DA, Mirsoian A, Grossenbacher SK, Pai CS, et al. Repeated PD-1/PD-L1 monoclonal antibody administration induces fatal xenogeneic hypersensitivity reactions in a murine model of breast cancer. *Oncoimmunology* (2016) 5(2):e1075114. doi: 10.1080/2162402x.2015.1075114

20. Li K, Shi H, Zhang B, Ou X, Ma Q, Chen Y, et al. Myeloid-derived suppressor cells as immunosuppressive regulators and therapeutic targets in cancer. *Signal Transduction Targeted Ther* (2021) 6(1):362. doi: 10.1038/s41392-021-00670-9

21. Hu J, Xiao Q, Dong M, Guo D, Wu X, Wang B. Glioblastoma immunotherapy targeting the innate immune checkpoint CD47-SIRPα axis. *Front Immunol* (2020) 11:593219. doi: 10.3389/fimmu.2020.593219

22. Hack SP, Zhu AX, Wang Y. Augmenting anticancer immunity through combined targeting of angiogenic and PD-1/PD-L1 pathways: challenges and opportunities. *Front Immunol* (2020) 11:598877. doi: 10.3389/fimmu.2020.598877

23. Lindblad KE, Ruiz de Galarreta M, Lujambio A. Tumor-intrinsic mechanisms regulating immune exclusion in liver cancers. *Frontiers in Immunology* (2021) 12:. doi: 10.3389/fimmu.2021.642958

24. Sia D, Villanueva A, Friedman SL, Llovet JM. Liver cancer cell of origin, molecular class, and effects on patient prognosis. *Gastroenterology* (2017) 152 (4):745–61. doi: 10.1053/j.gastro.2016.11.048

25. Xu X, Li R, Dong R, Yang Y, Wang H, Cheng J, et al. *In vitro* characterization and cellular uptake profiles of TAMs-targeted lipid calcium carbonate nanoparticles for cancer immunotherapy. *Acta Materia Med* (2022) 1(3):400–10. doi: 10.15212/amm-2022-0030

26. Dall'Olio FG, Marabelle A, Caramella C, Garcia C, Aldea M, Chaput N, et al. Tumour burden and efficacy of immune-checkpoint inhibitors, nature reviews. *Clin Oncol* (2022) 19(2):75–90. doi: 10.1038/s41571-021-00564-3

27. Kim M, Lee JS, Kim W, Lee JH, Jun BH, Kim KS, et al. Aptamer-conjugated nano-liposome for immunogenic chemotherapy with reversal of immunosuppression. *J Controlled release* (2022) 348:893–910. doi: 10.1016/j.jconrel.2022.06.039

28. Triplett TA, Garrison KC, Marshall N, Donkor M, Blazeck J, Lamb C, et al. Reversal of indoleamine 2,3-dioxygenase-mediated cancer immune suppression by systemic kynurenine depletion with a therapeutic enzyme. *Nat Biotechnol* (2018) 36 (8):758–64. doi: 10.1038/nbt.4180

29. Cheong JE, Sun L. Targeting the IDO1/TDO2-KYN-AhR pathway for cancer immunotherapy - challenges and opportunities. *Trends Pharmacol Sci* (2018) 39 (3):307–25. doi: 10.1016/j.tips.2017.11.007

30. Zhou QH, Han H, Lu JB, Liu TY, Huang KB, Deng CZ, et al. Up-regulation of indoleamine 2,3-dioxygenase 1 (IDO1) expression and catalytic activity is associated with immunosuppression and poor prognosis in penile squamous cell carcinoma patients. *Cancer Commun (London England)* (2020) 40(1):3–15. doi: 10.1002/cac2.12001

31. Kiyozumi Y, Baba Y, Okadome K, Yagi T, Ishimoto T, Iwatsuki M, et al. IDO1 expression is associated with immune tolerance and poor prognosis in patients with surgically resected esophageal cancer. *Ann Surg* (2019) 269(6):1101–8. doi: 10.1097/sla.0000000000002754

32. Song X, Si Q, Qi R, Liu W, Li M, Guo M, et al. Indoleamine 2,3-dioxygenase 1: a promising therapeutic target in malignant tumor. *Frontiers in Immunology* (2021) 12:. doi: 10.3389/fimmu.2021.800630

33. Carvajal-Hausdorf DE, Mani N, Velcheti V, Schalper KA, Rimm DL. Objective measurement and clinical significance of IDO1 protein in hormone receptor-positive breast cancer. *J immunother Cancer* (2017) 5(1):81. doi: 10.1186/s40425-017-0285-7

34. Chinnadurai R, Porter AP, Patel M, Lipat AJ, Forsberg MH, Rajan D, et al. Hepatocellular carcinoma cells are protected from immunolysis by mesenchymal stromal cells through indoleamine 2,3 dioxygenase. *Front Cell Dev Biol* (2021) 9:715905. doi: 10.3389/fcell.2021.715905

35. Jorgovanovic D, Song M, Wang L, Zhang Y. Roles of IFN-γ in tumor progression and regression: a review. *biomark Res* (2020) 8:49. doi: 10.1186/s40364-020-00228-x

36. Dufour A, Bellac CL, Eckhard U, Solis N, Klein T, Kappelhoff R, et al. C-terminal truncation of IFN-γ inhibits proinflammatory macrophage responses and is deficient in autoimmune disease. *Nat Commun* (2018) 9(1):2416. doi: 10.1038/s41467-018-04717-4

37. Kim DS, Jang IK, Lee MW, Ko YJ, Lee DH, Lee JW, et al. Enhanced immunosuppressive properties of human mesenchymal stem cells primed by interferon-γ. *EBioMedicine* (2018) 28:261–73. doi: 10.1016/j.ebiom.2018.01.002

38. Mulder K, Patel AA, Kong WT, Piot C, Halitzki E, Dunsmore G, et al. Cross-tissue single-cell landscape of human monocytes and macrophages in health and disease. *Immunity* (2021) 54(8):1883–1900.e5. doi: 10.1016/j.immuni.2021.07.007

39. Liu Y, Liang X, Yin X, Lv J, Tang K, Ma J, et al. Blockade of IDO-kynurenine-AhR metabolic circuitry abrogates IFN-γ-induced immunologic dormancy of tumor-repopulating cells. *Nat Commun* (2017) 8:15207. doi: 10.1038/ncomms15207

40. Yi M, Zheng X, Niu M, Zhu S, Ge H, Wu K. Combination strategies with PD-1/PD-L1 blockade: current advances and future directions. *Mol Cancer* (2022) 21(1):28. doi: 10.1186/s12943-021-01489-2

41. Huang Q, Wu X, Wang Z, Chen X, Wang L, Lu Y, et al. The primordial differentiation of tumor-specific memory CD8(+) T cells as bona fide responders to PD-1/PD-L1 blockade in draining lymph nodes. *Cell* (2022) 185(22):4049–4066.e25. doi: 10.1016/j.cell.2022.09.020

42. Shi J, Hou S, Fang Q, Liu X, Liu X, Qi H. PD-1 controls follicular T helper cell positioning and function. *Immunity* (2018) 49(2):264–274.e4. doi: 10.1016/j.immuni.2018.06.012

43. Ye ZH, Jiang XM, Huang MY, Xu YL, Chen YC, Yuan LW, et al. Regulation of CD47 expression by interferon-gamma in cancer cells. *Trans Oncol* (2021) 14(9). doi: 10.1016/j.tranon.2021.101162

44. Chen G, Huang AC, Zhang W, Zhang G, Wu M, Xu W, et al. Exosomal PD-L1 contributes to immunosuppression and is associated with anti-PD-1 response. *Nature* (2018) 560(7718):382–6. doi: 10.1038/s41586-018-0392-8

45. Zhou X, Yao Z, Bai H, Duan J, Wang Z, Wang X, et al. Treatment-related adverse events of PD-1 and PD-L1 inhibitor-based combination therapies in clinical trials: a systematic review and meta-analysis, the lancet. *Oncology* (2021) 22(9):1265–74. doi: 10.1016/s1470-2045(21)00333-8

46. Li A, Barsoumian HB, Schoenhals JE, Cushman TR, Caetano MS, Wang X, et al. Indoleamine 2,3-dioxygenase 1 inhibition targets anti-PD1-resistant lung tumors by blocking myeloid-derived suppressor cells. *Cancer Lett* (2018) 431:54–63. doi: 10.1016/j.canlet.2018.05.005

47. Wang T, Kong S, Tao M, Ju S. The potential role of RNA N6-methyladenosine in cancer progression. *Mol Cancer* (2020) 19(1):88. doi: 10.1186/s12943-020-01204-7

48. Sendinc E, Shi Y. RNA m6A methylation across the transcriptome. *Mol Cell* (2023) 83(3):428–41. doi: 10.1016/j.molcel.2023.01.006

49. Quan C, Belaydi O, Hu J, Li H, Yu A, Liu P, et al. N6-methyladenosine in cancer immunotherapy: an undervalued therapeutic target. *Frontiers in Immunology* (2021) 12:. doi: 10.3389/fimmu.2021.697026

50. Zhang X, Shen L, Cai R, Yu X, Yang J, Wu X, et al. Comprehensive analysis of the immune-oncology targets and immune infiltrates of n (6)-Methyladenosine-Related long noncoding RNA regulators in breast cancer. *Front Cell Dev Biol* (2021) 9:686675. doi: 10.3389/fcell.2021.686675

51. Zhou Z, Lv J, Yu H, Han J, Yang X, Feng D, et al. Mechanism of RNA modification N6-methyladenosine in human cancer. *Mol Cancer* (2020) 19(1):104. doi: 10.1186/s12943-020-01216-3

52. Liu Z, He J, Han J, Yang J, Liao W, Chen N. m6A regulators mediated methylation modification patterns and tumor microenvironment infiltration characterization in nasopharyngeal carcinoma. *Frontiers in Immunology* (2022) 12:. doi: 10.3389/fimmu.2021.762243

53. Shi B, Liu WW, Yang K, Jiang GM, Wang H. The role, mechanism, and application of RNA methyltransferase METTL14 in gastrointestinal cancer. *Mol Cancer* (2022) 21(1):163. doi: 10.1186/s12943-022-01634-5

54. Yue B, Song C, Yang L, Cui R, Cheng X, Zhang Z, et al. METTL3-mediated N6-methyladenosine modification is critical for epithelial-mesenchymal transition and metastasis of gastric cancer. *Mol Cancer* (2019) 18(1):142. doi: 10.1186/s12943-019-1065-4

frontiers | Frontiers in Immunology

TYPE Review
PUBLISHED 26 May 2023
DOI 10.3389/fimmu.2023.1170207

OPEN ACCESS

EDITED BY
Maria Lina Tornesello,
G. Pascale National Cancer Institute Foundation (IRCCS), Italy

REVIEWED BY
Zhuo Yu,
Shanghai University of Traditional Chinese Medicine, China
Elena Di Gennaro,
G. Pascale National Cancer Institute Foundation (IRCCS), Italy

*CORRESPONDENCE
Yao Luo
luoyao@scu.edu.cn
Yinan Zhang
yinan_zhang@tongji.edu.cn

†These authors have contributed equally to this work and share first authorship

RECEIVED 21 February 2023
ACCEPTED 18 May 2023
PUBLISHED 26 May 2023

CITATION
Shen C, Li M, Duan Y, Jiang X, Hou X, Xue F, Zhang Y and Luo Y (2023) HDAC inhibitors enhance the anti-tumor effect of immunotherapies in hepatocellular carcinoma.
Front. Immunol. 14:1170207.
doi: 10.3389/fimmu.2023.1170207

HDAC inhibitors enhance the anti-tumor effect of immunotherapies in hepatocellular carcinoma

Chen Shen[1†], Mei Li[1†], Yujuan Duan[2,3†], Xin Jiang[1], Xiaoming Hou[1], Fulai Xue[1], Yinan Zhang[2*] and Yao Luo[1*]

[1]Department of Laboratory Medicine, Medical Equipment Innovation Research Center/Medical Device Regulatory Research and Evaluation Center, West China Hospital, Sichuan University, Chengdu, China, [2]School of Chemical Science and Engineering, Tongji University, Shanghai, China, [3]School of Chemistry and Chemical Engineering, Shanghai Jiao Tong University, Shanghai, China

Hepatocellular carcinoma (HCC), the most common liver malignancy with a poor prognosis and increasing incidence, remains a serious health problem worldwide. Immunotherapy has been described as one of the ideal ways to treat HCC and is transforming patient management. However, the occurrence of immunotherapy resistance still prevents some patients from benefiting from current immunotherapies. Recent studies have shown that histone deacetylase inhibitors (HDACis) can enhance the efficacy of immunotherapy in a variety of tumors, including HCC. In this review, we present current knowledge and recent advances in immunotherapy-based and HDACi-based therapies for HCC. We highlight the fundamental dynamics of synergies between immunotherapies and HDACis, further detailing current efforts to translate this knowledge into clinical benefits. In addition, we explored the possibility of nano-based drug delivery system (NDDS) as a novel strategy to enhance HCC treatment.

KEYWORDS

hepatocellular carcinoma, tumor immune microenvironment, immunotherapy, immune checkpoint inhibitors, HDAC inhibitors, nano-based drug delivery system

1 Introduction

Primary liver cancer is currently the sixth most commonly diagnosed cancer and the third leading cause of cancer-related death worldwide, hepatocellular carcinoma (HCC) accounts for approximately 75%-85% of liver cancer cases (1, 2). Due to the tumor heterogeneity, tumor metastasis, and resistance to traditional chemotherapeutic agents, current treatment options such as surgical resection, radiofrequency ablation, neoadjuvant chemoradiotherapy, and liver transplantation for HCC will only benefit a few percentages of patients, novel therapeutic modalities are urgently needed for patients with advanced or unresectable HCC (3).

The crucial role of the immune system in suppressing the growth, proliferation, and progression of tumors is widely accepted (4). The immunotherapy of tumors mainly utilizes the host immune system to fight the tumor by regulating the host's own immune function or enhancing the immunogenicity of the tumors (5). HCC is considered to be inflammation-induced cancer, showing good sensitivity to immunotherapies (6). Immunotherapy strategies for HCC mainly include immune checkpoint inhibitors (ICIs), cell-based therapies, and tumor immune vaccines. Cytokines such as interferon also show certain anti-HCC effects (7). Checkpoint inhibitors are typically monoclonal antibodies that target programmed cell death protein 1 (PD-1), programmed death-ligand 1 (PD-L1) or cytotoxic T lymphocyte-associated antigen 4 (CTLA-4). PD-1 is a surface receptor highly expressed by activated T cells, B cells, dendritic cells (DC), and natural killer cells (NK) which provides inhibitory signals to the immune system to modulate the activity of immune cells in peripheral tissues and keep T-cells from attacking normal cells in the body. The interaction between PD-L1 expressed on cancer cells and PD-1 is a key mediator of cancer immune escape, which leads to the suppression of anticancer immunity and the promotion of tumor progression (8). Immune checkpoints blockade with anti-PD-1/PD-L1 antibodies have been successfully utilized in the treatment of various cancers such as melanoma (9), non–small cell lung cancer (10), bladder carcinoma (11), Hodgkin's lymphoma (12), and Merkel cell carcinoma (13). CTLA-4, another important ICIs target, competitively inhibits the binding of the B7 ligand to the costimulatory receptor CD28, resulting in decreased peripheral T-cell activity. Specific blocking of CTLA-4 can increase the T-cell infiltration of tumors and enhance the killing effect of the immune system on tumors (14, 15). In addition, chimeric antigen receptor T cells (CAR-T) and other cell therapies as well as HCC tumor immune vaccines also show good effects and application prospects. However, the unique inhibitory tumor microenvironment (TME) of HCC and the genetic differences of the host make existing immunotherapies challenges. Compared to unprecedented and durable responses in these T cell-inflamed cancers, the objective response rates (ORRs) of PD-1 and PD-L1 blockade in HCC remain relatively low (16–18). It was proved that TME, specific receptors, and signaling pathways can affect the clinical outcome of PD-1/PD-L1 treatment (19), Combining different immunotherapies or combining immunotherapies with other modalities may provide synergistic effects and facilitate the development of the treatment of HCC (20).

Regulated by related histone-modifying enzymes (HMEs), various post-translational modifications (PTMs) of histone substrates, such as acetylation, methylation, phosphorylation, ubiquitination, and ADP ribosylation, play a crucial role in chromatin dynamics, relative gene regulation and many other biological functions (21). Increasing evidence indicates that abnormal epigenetic regulation of gene transcription associated with histone modifications plays a crucial role in cancer initiation, progression, and metastasis (22). In contrast to direct mutations or deletions in the main DNA sequence, aberrant epigenetic modifications are potentially reversible by epigenetic therapies (23). Several small-molecule inhibitors of HME, such as histone methylation inhibitors, histone demethylation inhibitors, histone deacetylation inhibitors, and DNA methylation inhibitors, can lead to the programmed death of tumor cells by affecting the cell cycle, angiogenesis, proliferation, and migration (24–26). To date, histone deacetylation inhibitors (HDACis) including vorinostat, romidepsin, belinostat, and panobinostat have been approved by FDA for the treatment of hematological malignancies such as cutaneous T-cell lymphoma (CTCL) and multiple myeloma (27–29). Despite promising results in the treatment of blood cancers, the therapeutic efficacy of several HDACis as a single therapeutic agent in solid tumors such as HCC has been unsatisfactory, and the prevalence of drug-induced side effects was relatively high (30). Till now, numerous combination therapies involving HDACis in synergy with chemotherapy, radiotherapy, phototherapy, targeted therapy, and immunotherapy have been efficiently developed to enhance therapeutic efficacy (31).

HDACis can regulate gene expression by regulating host epigenetic modification, thereby overcoming the tolerance of HCC patients to immunotherapy and enhancing the therapeutic effect. HDACis have been shown to promote immunotherapies in a variety of tumors (32). This effect is mainly achieved by enhancing the immunogenicity of the tumor and regulating the tumor immune microenvironment. Studies have shown that HDACis can increase the expression of PD-1/PD-L1, thereby increasing the sensitivity of tumors to ICIs treatment (33). In some tumors, HDACis also increase the expression of MHC molecules that assist the host immune system in recognizing tumor antigens (34). The regulation of HDACis on TME can promote the recruitment of T cells and NK cells and exert the function of tumor inhibition by increasing the expression of chemokines, cytokines and NK cell-related receptors. Similar mechanisms were also found in HCC. Moreover, these mechanisms work together to promote the effect of immunotherapies. The effect of HDACis on immunotherapy also allows these drugs to work without high doses. This reduces the possible cytotoxicity and adverse reactions of immune drugs, and also creates chances for wider research and application (35).

In the past few years, the rapid development of nanotechnology and its application in many fields have had a profound impact on the development of biomedicine (36). Nano-based drug delivery system (NDDS) constructed on the basis of nanomaterials provides an effective and powerful new strategy for enhancing the efficacy of immunotherapy drugs for HCC (37). NDDS specifically targets tumor cells through advanced delivery systems, overcoming inhibitory TME while effectively reducing the damage to normal cells. Currently, a large number of nanomedicine-based therapies are being developed for HCC (38).

Combined multidrug approaches for cancer treatment could overcome the limitations of single therapies, increase antitumor effects, and reduce drug resistance. In this review, we describe immunotherapies and HDACis in detail, explain the mechanism of their therapeutic effects in HCC respectively, and discuss current progress in the combination of novel immunotherapies with HDACis. In addition, concerned that the nano-based drug delivery system (NDDS) exhibits outstanding properties such as targeted delivery, TME response, and site-specific release in the

delivery of multi-drug combination, we further discuss the potential clinical applications of NDDS in dual-therapy for HCC briefly.

2 Immunotherapy for HCC

2.1 The immune microenvironment of HCC

The TME is the environment around a tumor mass that consists not only of a heterogeneous population of cancer cells but also of stromal cells, neovessels, immune cells, and extracellular matrix (ECM). Considering the close relationship and constant interaction between tumors and their surrounding microenvironment, it is becoming increasingly apparent that TME has a significant impact on tumorigenesis, immune evasion, recurrence, as well as drug resistance (39).

The immunosuppressive microenvironment in HCC is thought to be counterbalanced by cells that generate antitumor immune responses and/or clear tumor cells. Liver cells are normally exposed to a significant number of bacterial antigens from portal circulation, leading to constant immune stimulation and antigen exposure. As a result, the liver has developed intrinsic tolerogenic mechanisms in the innate and adaptive immune responses to prevent autoimmune responses and unnecessary tissue damage, which makes it considered an immune-tolerant tissue (40). The immune microenvironment in the liver is dominated by immunosuppressive cells and signals. The key immune suppressor cells implicated in HCC immune escape comprise tissue-resident macrophages (mostly Kupffer cells), regulatory T (T_{reg}) cells, and myeloid suppressor cells (MDSCs) (41, 42). Known as specialized macrophages located in the liver, Kupffer cells remove bacteria and produce immunosuppressive cytokines, such as IL-10 and prostaglandins. Additionally, they are capable of negatively regulating immune response by expressing the inhibitory immune checkpoint ligand PD-L1, recruiting T_{reg} cells, and IL-17-expressing $CD4^+$ T helper 17 (TH17) cells, as well as downregulating major histocompatibility complex class II (MHC II) and costimulatory molecules (41–43). T_{reg} cells and monocyte-derived tumor-associated macrophages (TAMs) can suppress innate and adaptive immunity against HCC through the cooperation with dysfunctional DCs, dysfunctional $CD8^+PD\text{-}1^+$ T cells, neutrophils, and regulatory B (B_{reg}) cells (43–45). The high numbers of MDSCs in the liver produce vascular endothelial growth factor (VEGF), transforming growth factor-β (TGF-β), and arginase, which also suppress T cell activation (41). There is a higher abundance of T_{reg} cells and MDSCs in peripheral blood among HCC patients than in normal individuals (46, 47).

The deepening of research and the development of technology have improved our understanding of the complexity and heterogeneity of the tumor immune microenvironment and its components, and their effects on response to tumor immunotherapy. Tumor immunotherapy is considered to be a novel and promising therapy for tumors and it has recently become a hot research topic.

2.2 Immunotherapies and immune checkpoint inhibitors for HCC

HCC is usually developed from chronic liver disease, such as chronic hepatitis B, and is therefore considered to be inflammatory cancer. This inflammation promotes the transformation of liver cells and contributes to cancer (48). As inflammatory cancer, patients with high lymphocyte density in HCC tumors tend to have a better prognosis (6). Therefore, immunotherapies are considered as ideal treatment for HCC. Existing treatment options for HCC, such as surgery, adjuvant chemoradiotherapy, liver transplantation and radiofrequency ablation, do not benefit all patients, and a more comprehensive approach is needed. Immunotherapies have been shown to be effective and safe in the treatment of a large number of solid tumors (e.g., malignant melanoma and non-small cell lung cancer), extending the overall survival (OS) and providing tolerable toxicity, which are revolutionizing the management of cancer (49). Existing HCC immunotherapy strategies include ICIs, cytokine-based therapies, cell-based therapies, and tumor vaccines (Figure 1). However, due to the low tumor mutation load (TML) and the special immunosuppressive microenvironment, the application of HCC immunotherapies is facing challenges and further optimization strategies are needed (50).

2.2.1 Immune checkpoint inhibitors

ICIs are monoclonal antibodies that block immune checkpoint molecules that inhibit the anti-tumor immune response. Immune checkpoint molecules are key modulators of anti-tumor T cell responses and can be expressed not only by T cells, but also by antigen-presenting cells (such as DC and macrophages) and tumor cells. Major inhibitory immune checkpoint receptors naturally inhibit T cell activity and play a critical role in maintaining self-tolerance, also mediating immune-escape of cancer cells (7). Currently, the targeted therapies of PD-1, its ligand PD-L1 and CTLA-4 have been fully studied and have become the pillar of immunotherapy for solid tumors (51).

The interaction between PD-L1 and PD-1 leads to widespread dephosphorylation of T-cell-activated kinases, resulting in T-cell inactivation. This effect mediates the immune tolerance of tumors (52). Studies have shown that PD-L1 is expressed in 82% of HCC samples, and the expression rate in HBV-positive patients is higher than that in HBV-negative patients (53). Therefore, blocking PD-1 or PD-L1 can restore the function of $CD8^+$ T cells and exert anti-tumor function in HCC patients. Currently, the clinical value of PD-1 or PD-L1 inhibitors has been widely demonstrated and approved for use in several countries. Existing drugs include nivolumab, pembrolizumab and atezolizumab. Nivolumab is a human anti-PD-1 IgG4 monoclonal antibody that blocks PD-1 and was approved by the FDA in 2017 for second-line advanced HCC patients with sorafenib progression. Clinical studies have shown that nivolumab has a manageable safety profile and shows sustained antitumor activity in patients with advanced HCC (17). In a study of 743 HCC patients, first-line nivolumab and sorafenib-treated patients had comparable overall survival (15.2 *vs* 13.4

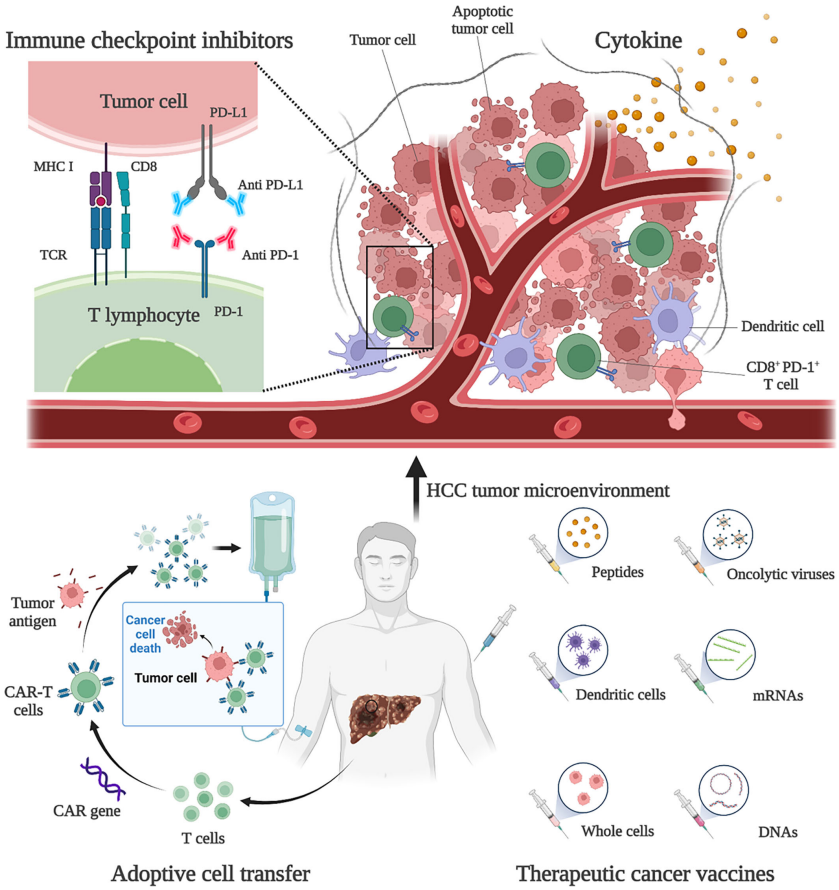

FIGURE 1
Immunotherapies for HCC. Current HCC immunotherapy strategies include immune checkpoint inhibitors (ICIs), cytokine-based therapies, adoptive cell transfer (ACT), and therapeutic vaccines. Anti-PD-1 and anti-PD-L1 treatments are examples of ICIs therapy. By blocking PD-1 and PD-L1, the anti-tumor activity of $CD8^+$ T cells can be restored. An example of ACT therapy is CAR-T therapy. CAR-T therapy is derived from immune cells extracted from patients' peripheral blood and genetically engineered to express chimeric antigen receptors (CARs). These CARs can recognize specific cancer antigens and stimulate the immune destruction of tumor cells. Therapeutic vaccines include peptides, DCs, whole-cell vaccines, oncolytic viruses, mRNAs, and DNA preparations to increase or achieve a specific immune response to tumor antigens.

months) and showed a good safety profile (54). An Asian cohort study showed a response rate of 15% for nivolumab in HCC patients who had already been treated with sorafenib (55). Nivolumab combined with ipilimumab (an antibody against CTLA-4) showed better efficacy and safety in the treatment of advanced HCC patients. The objective response rate was 32% (95% CI, 20%-47%) in 148 subjects using a combination regimen (4 doses of nivolumab 1 mg/kg + ipilimumab 3 mg/kg every 3 weeks, then nivolumab 240 mg every 2 weeks) (56). In addition, atezolizumab, an IgG1 monoclonal antibody targeting PD-L1, and the anti-VEGFA antibody bevacizumab have produced better outcomes in advanced HCC patients than sorafenib and have become the new standard treatment for patients with unresectable HCC. Atezolizumab in combination with bevacizumab (AtezoBev) has been shown to be repeatable safe and effective in routine clinical practice (57). In a phase Ib trial, of 104 unresectable HCC patients treated with atezolizumab in combination with bevacizumab, 37 (36%; 95% CI 26%-46%) patients achieved a confirmed objective response (58). In a comparative trial, atezolizumab combined with bevacizumab showed better 12-month survival (67.2% *vs* 54.6%) and progression-free survival (6.8 *vs* 4.3 months) than sorafenib (59). Further molecular mechanism studies have also confirmed that anti-VEGF can act synergically with anti-PD-L1 to target angiogenesis, T_{reg} proliferation and myeloid cell inflammation (60). Pembrolizumab, an anti-PD-1 IgG4 monoclonal antibody, also demonstrated high efficacy and tolerability in patients with advanced HCC. In a Phase III study, pembrolizumab had a median OS of 13.9 months for advanced HCC (61). In 2020, atezolizumab plus bevacizumab became the standard first-line systemic therapy for advanced HCC, and the monotherapies pembrolizumab and nivolumab plus ipilimumab are currently approved as second-line therapy for patients with disease progression in first-line tyrosine kinase inhibitors (TKI) (49). It is important to note that some experimental and clinical studies of solid tumors seem to favor anti-PD-1 over anti-PD-L1 therapy. A meta-analysis of 19 randomized clinical trials showed that anti-PD-1 therapy resulted in better survival outcomes than anti-PD-L1 treatment (62). This finding may be partly attributed to the poor pharmacokinetic properties of anti-PD-L1 antibodies and the additional blocking effect of anti-PD-1 antibodies on PD-L2 (62).

CTLA-4 competitively inhibits the binding of the B7 ligand to the costimulatory receptor CD28, resulting in decreased peripheral T-cell activity. Inhibition of CTLA-4 can promote the increased activation of infantile $CD4^+$ and $CD8^+$ T cells, as well as the rebalancing of endogenous effector and regulatory regions in the TME (15). Anti-CTLA-4 treatment can activate and increase the abundance of $CD4^+$ and $CD8^+$ T cells, and reduce the clonability of peripheral T cells in HCC patients (63). Studies have shown that the expression of CTLA-4 in $CD8^+$ and $CD4^+$ T cells isolated from HCC tissues is significantly higher than that in tumor-free tissues or blood (64). Therefore, inhibition of CTLA-4 can play an antitumor role by enhancing T-cell activity in HCC patients. Ipilimumab, a CTLA-4 inhibitor, has been shown to be effective in combination with nivolumab for advanced HCC. This strategy has been approved in many countries for second-line advanced HCC patients with sorafenib progression (49). Tremelimumab is a fully human IgG2 monoclonal antibody that binds to CTLA-4 on the surface of activated T cells, thereby blocking its binding to CD28 (65). Current studies have proved that Tremelimumab combined with tumor ablation is feasible in the treatment of advanced HCC patients, with a partial response rate of 26.3%. This combination therapy resulted in the accumulation of $CD8^+$ T cells in the tumor and decreased viral load in HCV patients (66). Although CTLA-4 inhibitors have achieved promising results in clinical trials to date, researches on the mechanisms of CTLA-4 blocking from HCC preclinical models are limited, and further studies are needed (15).

In addition to PD-1/PD-L1 and CTLA-4, blocking other co-inhibitory checkpoints such as LAG-3 or TIM-3 is also currently the focus of extensive clinical research. T_{reg} and $CD8^+$ T cells isolated from HCC TME expressed more PD-1, LAG-3 and TIM-3 than those isolated from non-tumor microenvironment (NTME) by proteomics and transcriptomic analysis, and showed T cell inhibition (67). Lymphocyte activation gene 3 (LAG-3) is a membrane protein closely related to CD4. It is expressed by a variety of T cells, such as $CD4^+$, $CD8^+$, and T_{reg}, as well as NK cells, DCs, and B cells. LAG-3 binds to MHC II of APC and prevents recognition of T cell receptors (TCRs), thereby inhibiting T-cell-mediated immune responses (50, 68). The density of LAG-3 positive cells increased significantly in HCC tumor tissues. Increased density of $LAG\text{-}3^+$ cells and decreased level of $CD8^+$ T cells were associated with poor prognosis (69). Studies have demonstrated the potential predictive and prognostic effects of LAG-3 as a serum biomarker in HCC patients undergoing transarterial chemoembolization (TACE) therapy. High LAG-3 levels before TACE are associated with poor disease outcomes and reduce overall survival (70). The expression of LAG-3 in tumor tissues is usually accompanied by an increased level of PD-L1 (71). Therefore, the development of LAG-3 inhibitors and their combination with anti-PD-1/PD-L1 may have significant synergistic clinical benefits. However, there are few clinical trials using these targets for HCC, and their efficacy has yet to be proven. T-cell immunoglobulin and mucin domain 3 (TIM-3) is an immunomodulatory receptor that binds to ligands on tumor cells and the microenvironment and inhibits antitumor immunity in a variety of cancers, including HCC. TIM-3 is one of the main inhibitory receptors on NK cells, which can mediate the reduction of anti-tumor ability (72, 73). At present, there are relatively few studies on how TIM-3 inhibits NK cells in HCC. This may be related to an endogenous ligand called phosphatidylserine (PtdSer). PtdSer is involved in promoting the phosphorylation of TIM-3, which then competes with PI3K p110 to bind p85 and inhibit the downstream Akt/mTORC1 signaling pathway, leading to NK cell dysfunction. Gene ablation, antibody-based functional blocking and lentivirus-mediated TIM-3 inhibition can inhibit HCC growth by restoring cytokine secretion and cytotoxicity of NK cells (74).

Overall, ICIs have several advantages over other types of immunotherapies, such as cell-based therapies, in terms of commercial availability, suitability, and not being limited by human leukocyte antigen (HLA) status. Although many trials showed promising results with ICIs in patients with advanced HCC, more trials are needed to show efficacy as a first-line treatment and in combination with other immunotoxic or cytotoxic therapies. Moreover, some new immune checkpoint inhibition therapeutic strategies need further mechanism studies and clinical validation (65).

2.2.2 Vaccine therapy and cell-based therapy

Measurable T-cell responses to tumor-associated antigens expressed by HCC cells, such as AFP, GCP3, and MUC1, have guided the development of antigen-specific therapeutic vaccines and cell therapies (75). These strategies play a therapeutic role by activating or enhancing tumor immunity in HCC patients through the introduction of tumor antigens or tumor-associated antigen (TAA) sensitive immune cells *in vitro*. HCC vaccine therapy utilizes similar immune recognition principles and promotes an adaptive immune response to specific antigens. This method can not only be used for cancer prevention, but also for cancer treatment (49). Classical tumor vaccines involve exogenous antigens or antigen pulsed DCs. One strategy is to transfect DCs with a pulse of tumor cell lysate or with a TAA-expressing vector. Adoptive transfer of these modified DCs into patients was used to optimize the immunogenicity of secreted cancer antigens (including AFP) in response to weakened natural immune responses or functional abnormalities in HCC patients (76). Therapeutic vaccines include peptides, DCs, whole-cell vaccines, oncolytic viruses, mRNAs and DNA preparations to increase or achieve a specific immune response to tumor antigens (77). The key to vaccine therapy is that tumor antigens should provide sufficient immunogenicity to break the tolerance imposed by the many self-molecules expressed by tumor cells. At the same time, the antigen should confer specificity on tumor cells and avoid unnecessary recognition of non-tumor cells. So, screening for the right antigens is challenging. Due to the special immunosuppressive environment of HCC, it is also unknown whether antigen input can induce a strong enough immune response (78). Combination therapy and new vaccine synthesis strategies can overcome these challenges. For example, the combination of ICIs and tumor vaccine treatment can enhance the activity of T cells by blocking immunosuppressive factors, thus enhancing the function of the vaccine (79). The development of new tumor vaccines using nanotechnology has also contributed to the

advancement of this therapeutic approach (80). For example, one study tried to use DC-derived exosomes (DEX) as a non-cellular vaccine for tumor immunotherapy. By anchoring HCC targeting peptide p47 (P) and an alpha-fetal protein epitope (AFP212-A2) to DEX, the researchers produced a novel vaccine, DEXP&A2&N. DEXP&A2&N achieves tumor-targeted delivery of high-mobility group nucleosome binding protein 1 (HMGN1; N1ND-N) and promotes N1ND-mediated endogenous DC recruitment and activation in tumors in the presence of HCC antigens. To achieve cross-presentation of tumor antigens and induce tumor-specific T-cell responses (81).

Another strategy for immune regulation of antitumor responses is adoptive cell transfer (ACT). ACT is a highly personalized form of cancer immunotherapy involving the metastasis of host-derived amplified immune cells (82). ACT therapy for HCC includes tumor infiltrating lymphocytes (TILs), cytokine induced killer cells (CIKs), and CAR-T (50). Adoptive metastasis of TIL has been shown to produce complete and lasting tumor regression in patients with metastatic melanoma, and its efficacy in HCC remains to be demonstrated (83). Another ACT strategy tried in adjuvant therapy for HCC is the use of CIK. CIK cells are autologous cells amplified *in vitro* from peripheral blood mononuclear cells of patients cultured with cytokine cocktails and anti-CD3 antibodies. CIK cells consist of a variety of subpopulations: CD3+/CD56+ cells, CD3−/CD56+ NK cells, and CD3+/CD56− cytotoxic T cells. Therefore, CIK cells have the dual function of T cells and NK cells, with a strong anti-tumor effect (84). Current studies have proved that CIK is an effective adjunctive therapy in early HCC. For advanced HCC, CIK can also show a good therapeutic effect by targeting MDSCs to reduce their immunosuppressive function (85). CAR-T therapy, as a new ACT, has made considerable progress in the treatment of HCC. CAR-T therapy takes immune cells from patients' peripheral blood and genetically engineers them to express chimeric antigen receptors (CARs). These cell membrane proteins bind to specific cancer antigens and stimulate the immune destruction of tumor cells (86, 87). It was shown that CAR-T therapy inhibited tumors through multiple mechanisms. For example, a CAR-T therapy targeting Glypican 3 (GPC3) has been shown to be effective against HCC in mice. The mechanisms involved include inducing perforin and granulozyme-mediated apoptosis and reducing the level of active β-catenin in HCC cells. This is because GPC3 is a cancerous fetal antigen involved in Wnt-dependent cell proliferation (88).

2.2.3 Cytokine-based therapy

For patients with HCC, cytokine-based therapies have met limited benefits. The use of interferon (IFN) seems to be a reasonable first choice for HCC treatment, which may have both antiviral and antitumor functions. It has been demonstrated that the combination of IFN-α and IL-24 can inhibit HCC by promoting tumor apoptosis and reducing angiogenesis (89). However, patients with cirrhosis and HCC have poor tolerance to IFN therapy, resulting in nearly half of the patients discontinuing treatment due to intolerance or adverse events (90).

2.3 Resistance to immunotherapies

Due to the microenvironmental specificity of the liver, the TME in HCC exhibits high immunosuppression and drug resistance, resulting in excessive or insufficient responses to immunotherapies (91). Recent studies have revealed the underlying mechanisms of immunotherapy resistance, which can be divided into primary resistance and adaptive or acquired resistance. Primary resistance is characterized by tumor failure to respond to immunotherapy, which may be due to T cells' lack of tumor antigen recognition. When the patient's immune system is able to recognize tumor antigens, the tumor can also protect itself from immune attack through adaptive or acquired resistance. The occurrence of drug resistance may be due to intrinsic characteristics of the tumor, such as low tumor mutation load and high PD-L1 expression, or extrinsic characteristics of the tumor, such as the absence of T cells with antigen-specific TCRs and high immunosuppressive TME (92). Specific to each type of immunotherapy, their resistance mechanisms are very complex and involve many factors. Take ICIs, for example. Although some ICIs (such as anti-PD-1 antibodies and anti-CTLA-4 antibodies) have been approved for first-line or second-line treatment of HCC in some countries, some advanced HCC patients do not respond to therapy, and the overall response rate remains low (93). This may be related to immune-regulatory metabolite production in HCC TME. In one HCC model, the use of ICIs led to an increase in IFN-γ-dependent expression of indoleamine 2, 3-dioxygenase (IDO) in tumor cells. Among them, an increase in tumor-derived IDO1 promotes resistance to ICIs therapy. The combination of IDO inhibitors can enhance the efficacy of ICIs (94). Another potential cause of ICIs resistance is the production of anti-drug antibodies (ADAs), which can alter the clearance of these drugs or neutralize their activity. It is not clear whether ADAs cause resistance to HCC. However, ADAs were detected in up to 36% of Non-small cell lung cancer (NSCLC) patients treated with atezolizumab, which has a negative impact on systemic exposure to the drug and has detrimental effects on anti-tumor efficacy (7). In addition to the effects of TME, genetic and epigenetic defects in patients themselves can induce immune evasion of tumor cells, further affecting the response to ICIs. For example, genetic and epigenetic aberrations that lead to defective antigen presentation can promote primary and acquired resistance to ICIs (95). Some studies have also demonstrated the role of signal-related mutations in tumor resistance to ICIs. For example, some mutations can activate the Wnt/β-catenin pathway, thus leading to changes in tumor PD-L1 and triggering the occurrence of ICIs resistance (96).

Although some resistance mechanisms have not been demonstrated in HCC, further optimization of HCC immunotherapy strategies is imperative. New directions have been opened for the development of immunotherapy by combining different treatments or by using new technologies to synthesize new immunotherapy drugs. Recent studies have shown the value of combination immunotherapy and epigenetic therapy. Among them, HDACis combined with immunotherapy has achieved better results in HCC treatment. Moreover, nano-based

drug delivery systems (NNDS) built using nanotechnology further optimize existing treatment options.

3 HDACs and HDACis treatment for HCC

3.1 Histone deacetylation modification and HDAC inhibitors

The nucleosome is the basic unit of chromatin and is made up of DNA and histones. Histones are a group of small, positively charged proteins that include H1, H2A, H2B, H3 and H4. Histones are essential in packaging DNA into cells, chromatin and chromosomes. The histone core octamer is composed of H2A, H2B, H3, and H4. They are wrapped in a 147-base pair DNA band and linked by H1 (97). Covalent modifications of histones are central to the regulation of chromatin dynamics which comprise methylation, phosphorylation, acetylation, ubiquitylation, sumoylation, glycosylation, and ADP-ribosylation (98). Many biological processes involving chromatin, such as transcription, DNA repair, replication, and genome stability, are regulated by chromatin and its modifications. N^{ϵ}-acetylation of lysine residues is a major histone modification involved in transcription, chromatin structure and DNA repair. Acetylation neutralizes the positive charge of lysine and weakens the electrostatic interaction between histones and negatively charged DNA. Thus, histone acetylation is often associated with a more "open" chromatin conformation (99). Acetylation is highly dynamic and regulated by the competitive activity of two enzyme families, histone acetyltransferases (HATs) and histone deacetylases (HDACs). These two enzymes alter the state of chromatin, which in turn affects gene transcription and genome stability. Abnormalities in the functioning of these two enzymes have also been shown to play a role in the development of cancer. In contrast to DNA mutations, epigenetic changes represent reversible changes that offer the possibility of truly "restorative" therapeutic interventions. Great progress has been made in the therapeutic strategies targeting HDACs (100).

HDACs reverse lysine acetylation and restore positive the charge on the side chain, causing chromatin to contract. HDACs consist of 18 enzymes from two families and can be divided into 4 groups based on their sequence homology and domain organization. Class I HDACs (HDAC-1, HDAC-2, HDAC-3, HDAC-8) are located in the nucleus, widely expressed in various tissues and involved in gene expression. Class II HDACs are divided into two subgroups, Class IIa (HDAC-4, HDAC-5, HDAC-7, and HDAC-9) and Class IIb (HDAC-6 and HDAC-10), which are involved in cell differentiation. Class IIa HDACs shuttle between cytoplasm and nucleus. Class IIb HDACs are located in the cytoplasm. Class I HDACs and Class II HDACs represent the HDACs most closely associated with yeast *sc*Rpd3 and *sc*Hda1, respectively. Class IV HDACs include only one enzyme, HDAC-11. Class I, II, and IV HDACs share related catalytic mechanisms that require Zn^{+} but do not involve the use of cofactors. In contrast, Class III HDACs (sirtuin 1-7) are homologous to yeast *sc*Sir2 and employ a unique NAD^{+}-dependent catalytic mechanism (99, 101, 102). In addition, HDACs are known to regulate a variety of non-histone targets, such as tubulin, heat shock protein 90 (HSP-90), and *p53*, thereby affecting cell growth, apoptosis, invasion, and angiogenesis (103). It has been found that HDAC-6 is involved in α-tubulin deacetylation, affecting mitosis and other processes dependent on microtubule network acetylation patterns (104).

Abnormal HDACs are involved in the occurrence and development of many tumors, including cell proliferation, cell migration, cell death, and angiogenesis. HDACs shrink chromatin through deacetylation, resulting in transcriptional silencing of tumor suppressor and apoptosis genes, disrupting the balance between oncogenes and oncosuppressor genes. Many non-histone transcription factors, such as HSP-90 and tubulin, are also substrates for HDACs (101). Chimeric fusion proteins in leukemia, such as PML-RARα, PLZF-RARα, and AML1-ETO, have been shown to recruit HDACs to mediate abnormal gene silencing, which contributes to the development of leukemia (105). HDACs have also been found to be overexpressed or overactive in various solid tumors and inhibit the expression of tumor suppressor genes, leading to uncontrolled proliferation and inhibiting cell repair and apoptosis (102). Studies have shown that HDAC-5 can directly interact with T-box3 (a transcriptional suppressor) to jointly inhibit the expression of E-cadherin and promote the metastasis of tumor cells (106). Therefore, HDACs may be promising drug targets for cancer treatment. Currently, HDACis have been shown to be powerful in the treatment of cancer (107, 108).

HDACi reverses some abnormal gene inhibition in malignant tumors and induces growth arrest, differentiation, and apoptosis of cancer cells (Table 1). There are currently four HDACis approved by the FDA for cancers (99). The first approved HDACi is suberoylanilide hydroxamic acid (SAHA) or vorinostat for the treatment of refractory CTCL. The second is romidepsin for CTCL and peripheral T-cell lymphoma (PTCL). The third drug approved as an HDACi was panobinostat for oral use, in combination with bortezomib and dexamethasone for the treatment of relapsed multiple myeloma. The fourth, belinostat, is used for the treatment of PTCL. In addition, another HDACi chidamide was approved in China for the treatment of hematologic malignancies (101, 109). These drugs have produced impressive clinical data. In a Phase II trial, chidamide showed significant single-agent activity and controlled toxicity in relapsed or refractory PTCL. 79 patients with PTCL histology who received chidamide had an overall survival of 21.4 months. Patients with vascular immunoblastic T-cell lymphoma (AITL) had a higher ORR (50%) and a 40% complete response/unconfirmed complete response (CR/CRu) on chidamide, as well as a more durable response (110). Microarray experiments show that < 10% of the genome showed significant changes in expression after HDACis treatment. In cancer cells, these perturbations appear to disrupt their metastases and lead cells to non-proliferative destinies, including differentiation, immune regulation, chromatin instability, reduced DNA damage repair, reactive oxygen species production, cell cycle arrest, apoptosis, autophagy, and reduced angiogenesis and cell migration. For example, HDACis can restore

TABLE 1 HDAC inhibitors for tumors.

HDAC inhibitors	HDAC specificity	Tumors
Vorinostat	Class I, II, IV	CTCL
Romidepsin	Class I	CTCL, PTCL
Panobinostat	Class I, II, IV	MM
Belinostat	Class I, II, IV	PTCL, HCC
Chidamide	Class I, IIb	Hematologic malignancy
Trichostatin A	Class I, II, IV	Broad cancers
Givinostat	Class I, II, IV	Leukemia
Entinostat	Class I	Hematologic malignancy, breast cancer
Mocetinostat	Class I, IV (HDAC-1, HDAC-2, HDAC-3, HDAC-11)	Hematologic malignancy, lung cancer
Rocilinostat	Class IIb (HDAC-6)	MM, lymphoma, lung cancer, breast cancer
Nicotinamide	Class III (SIRT-3)	Skin cancer
Cambinol	Class III (SIRT-1, SIRT-2)	Lymphoma, breast cancer
Quisinostat	Class I, II, IV (HDAC-1, HDAC-2, HDAC-4, HDAC-10, HDAC-11)	MM, multiple solid tumors
Purinostat Mesylate	Class I, IIb	CML
Thailandepsin A	Class I (HDAC-1, HDAC-2, HDAC-3)	Breast cancer

HDAC, histone deacetylase; SIRT, sirtuin; CTCL, cutaneous T-cell lymphoma; PTCL, peripheral T cell lymphoma; HCC, Hepatocellular carcinoma; MM, multiple myeloma; CML, Chronic myelogenous leukemia.

p53 protein transcription and thus induce apoptosis of drug-resistant cancer cells (30, 109, 111). Some of the newer HDACis are now being shown to work in a wide range of tumors. For example, one study demonstrated the ability of a modified novel highly selective HDAC I/IIb inhibitor, Purinostat Mesylate (PMF), to treat chronic myelogenous leukemia (CML). PMF can significantly prevent the progression of BCR-ABL(T315I) induced CML by inhibiting leukemia stem cells (LSCs). This may provide a new treatment strategy for TKI-resistant CML patients in the future (112). Thailandepsin A (TDP-A) is another novel HDACi with extensive anti-proliferative activity. It has been proved that TDP-A can inhibit proliferation and induce apoptosis of breast cancer cells at low nanomolar concentrations. Furthermore, TDP-A has strong selective inhibition on Class I HDACs, such as HDAC-1, HDAC-2 and HDAC-3, and weak inhibitory activity on HDAC-4 and HDAC-8. This selectivity makes TDP-A a promising epigenetic drug for cancer treatment (113).

However, HDACis also face some challenges in treating cancer. One concern is the multipotency of drugs and their targets. Currently used HDACis are mostly non-selective pan-HDACis, whose relatively low specificity may alter the expression of thousands of important genes, leading to adverse consequences and hindering the wide clinical application of HDACis (99, 114). It is also challenging to determine the dosage of HDACis. Doctors need to find a treatment window that allows higher doses to be administered to more aggressive cancers, taking into account patients' tolerance (105). HDACis resistance is another challenge. Studies have shown that tumor cells can develop resistance through compensatory changes in HAT/HDAC expression levels, induction of p21 and thioredoxin, and drug effluence by ATP-binding cassette transporters (109). Combining HDACis with other drugs is a credible way to address these challenges. However, combination therapy still faces many problems, such as different drug solubility, resulting in physical incompatibility, which leads to formula precipitation or drug inactivation, requiring reformulation. In addition, there is an increased risk of drug-drug interactions and an increased tendency for adverse reactions (101). Chimeric HDACis synthesized by molecular hybridization (MH) strategy is a new development direction of HDACis. By combining drugs with different therapeutic effects, such as TKI and HDACi, in a single molecule, new drugs with better affinity and efficacy can be created. A highly effective dual inhibitor targeting bromodomain and extra-terminal (BET) and HDACs for pancreatic cancer has been reported. The antitumor activity of this dual inhibitor was higher *in vivo* and *in vitro* than that of BET inhibitor and HDACis alone or in combination (115).

3.2 HDAC inhibitors for HCC treatment

The dysregulation of HDACs and their roles in HCC development are being actively studied (Table 2). At present, there have been many reports indicating that HDACs are over-expressed or over-activated in HCC patients. Some of these studies have demonstrated the relationship between the overexpression of Class I HDACs such as HDAC-1 and HDAC-2 in HCC tissues and the increased mortality and poor prognosis of patients (124). Currently, many molecular classifications and prognostic gene markers for HCC patients have been established based on

TABLE 2 HDAC inhibitors for HCC treatment.

Treatment strategies	HDAC specificity	Mechanisms	References
Trichostatin A	Class I, II, IV	• Decrease the expression of oncogene *c-Met* and increase the level of MicroRNA-449	(116)
Trichostatine A + curcumin	Class I, II, IV	• Inhibition of NF-κB signaling pathway • sensitize resistant tumor cells to the curcumin treatment.	(117)
Belinostat	Class I, II, IV	• Inhibit histone deacetylase and reverse the up-regulation of oncogenes	(118)
Resminostat + sorafenib	Class I, IIb (HDAC-1, HDAC-3, HDAC-6, HDAC-8)	• Inhibition of histone acetylation associated with sensitivity and tolerance to sorafenib	(119)
TMP269 + lenvatinib	Class IIa	• Down-regulate FGFR4 and block FGFR signaling in FGFR4-positive HCC cell lines	(120)
Panobinostat + radiotherapy	Class I, II, IV	• Inhibit nuclear translocation and dissociate the HDAC4/Ubc9/Rad51 complex to impair DNA repair	(121)
AR42 + telomerase-specific oncolytic adenoviral therapy	Class I, II, IV	• Decrease telomerase-induced phosphorylated Akt activation and enhance telomerase-induced apoptosis	(122)
SAHA+ FOXO1 inhibitor AS1842856	Class I, II, IV	• Inhibition of autophagy mediated by AMPK-FOXO1-ULK1 signaling axis • Preventing EMT induced cancer cells metastasis	(123)

HDAC, histone deacetylase; FGFR, fibroblast growth factor receptor 4; Ubc9, ubiquitin-conjugating enzyme 9; SAHA, suberoylanilide hydroxamic acid, vorinostat; AMPK, AMP-activated protein kinase; FOXO1, forkhead box o1; ULK1, Unc-51-like kinase 1; EMT, epithelial-mesenchymal transition.

genome-wide gene expression profiles. A recent study systematically assessed the effect of these genetic characteristics on prognosis and identified valuable prognostic biomarkers by integrating these genetic characteristics. Tissue microarray analysis of 60 HCC patients showed that the expression level of HDAC-2 was negatively correlated with OS in HCC patients. The expression level of HDAC-2 in tumor tissues is significantly higher than that in adjacent normal tissues, and is associated with poor survival in HCC patients (125). Class II and III HDACs, such as HDAC-4, HDAC-5, SIRT-1, SIRT-2, and SIRT-7, have also been found to be up-regulated in HCC, and their correlation with tumor progression has been demonstrated in some cases (126). A large number of mechanism studies have shown that HDACs are involved in the pathogenesis of HCC. When overexpressed, these epigenetic modification factors exhibit various cancer-promoting effects, including inhibiting the expression of tumor suppressor genes, activating cell cycle progression, escaping apoptosis, adapting to hypoxia, and metabolic reprogramming. The interactions between HDACs and other carcinogenic molecules are also quite complex (125). In contrast, some HDACs appear to play a role in tumor inhibition in HCC. For example, HDAC-6 is a unique tumor suppressor in HCC. Inhibition or inactivation of HDAC-6 can promote the development of the tumor (127). The discovery of these mechanisms not only explains the role of HDACs in HCC, but also provides targets for targeted therapy. For example, existing studies have demonstrated that HDAC-2 is associated with poor prognosis in HCC, suggesting that inhibiting HDAC-2 may be a potential strategy to improve prognosis in HCC patients. In fact, in HCC cells, inhibition of HDAC-2 disrupts the G1/S phase of the cell cycle and ultimately leads to apoptosis by upregulating total *p21*, *p27* and acetylated *p53* and reducing the expression levels of some oncogenes (125, 128). These results are consistent with the above conjecture.

The role of HDACs in the development of HCC is related to the regulation of acetylation of oncogenes (e.g., *c-Met* and *c-Myc*) and oncosuppressor genes (e.g., *p53*). Trichostatin A has previously been shown to effectively inhibit *c-Met* expression and promote apoptosis of HCC tumor cells (116). A recent study found that HDAC-3 and tumor necrosis factor receptor-associated factor 6 (TRAF6), an E3 ubiquitin ligase, are jointly involved in significant upregulation of the oncogene *c-Myc* in HCC, thereby promoting malignant transformation and progression of tumors. TRAF6 disrupts the binding of HDAC-3 and *c-Myc* promoters, resulting in histone acetylation and epigenetic enhancement of *c-Myc* mRNA expression. This process also ultimately leads to increased stability of the *c-Myc* protein (129). In addition, a long non-coding RNA (lncRNA) that can be trans-activated by the *p53* gene, lnc-Ip53, can block *p53* acetylation by inhibiting the degradation of HDAC-1. This mechanism can lead to the loss of *p53* activity and the subsequent generation of tumor cell proliferation and apoptosis resistance (130).

Recent studies have also indicated the effects of HDACs on HCC cancer stem cells (CSCs), including maintaining cancer cell dryness and promoting self-renewal and proliferation. CSCs can cause tumor recurrence and metastasis, and play an important role in the generation of multi-drug resistant cancers (131). The promotion of HDACs on CSCs is achieved by affecting multiple signaling pathways. Recent studies have pointed to the key role of HDAC-11 in maintaining the dryness of HCC CSCs, while inhibition of HDAC-11 can promote apoptosis of cancer cells. HDAC-11 overexpression also reduced the sensitivity of HCC to sorafenib. This may be related to the regulation of HDAC-11 on the enhancement of glycolysis of HCC CSCs. CSCs require glycolysis and lipid metabolism for energy, and give priority to glycolysis for homeostasis (132). Further studies have shown that knockout of HDAC-11 in mice can promote histone acetylation of liver kinase

B1 (LKB1) promoter region to increase LKB1 transcription, thus activating adenosine 5'-monophosphate (AMP)-activated protein kinase (AMPK) signaling pathway and inhibiting glycolysis pathway, thus inhibiting cancer dryness and HCC progression (133). In addition, HDAC-2 also promotes the proliferation and renewal of HCC CSCs by activating the Hedgehog (Hh) pathway. In this process, HDAC-2 and lnHDAC -2 (a lncRNA highly expressed in HCC and related to HDAC-2) co-inhibit the expression of patched 1 (PTCH1), thus activating Hedgehog signaling pathway and maintenance of hepatic CSCs dryness (134). The discovery of the mechanism of HDACs on CSCs provides a new target for combination therapy to overcome drug resistance in HCC tumors. For example, a recent study found that combined with Class I/II HDACis trichostatine can effectively improve the efficacy of inhibitor of kappa B kinase (IKK) in the treatment of drug-resistant HCC. Curcumin inhibits class I and II HDACs by inhibiting the NF-kB signaling pathway, which is enhanced by trichostatine combination therapy, sensitizing resistant tumor cells to curcumin therapy (117).

Currently, the mechanism of HDACis monotherapy for HCC is still in the stage of exploration, and its clinical effect remains to be proved. A Phase II trial previously demonstrated tolerable cytotoxicity of belinostat in HCC (118). Further pharmacokinetic studies demonstrated that belinostat was mainly metabolized through the glucoaldehyde pathway (135). In addition, HDACis have demonstrated excellent adjunctive therapeutic capabilities to enhance the efficacy of multiple HCC therapies. In terms of chemotherapy, HDACis have shown better adjuvant effect in many studies. HDACis can improve the efficacy of some traditional chemotherapy drugs (e.g., Fluoropyrimidines) against HCC and overcome resistance by targeting specific genes or proteins (35, 136). A phase I/II trial validated the combination of resminostat and sorafenib in the treatment of HCC. The results showed better safety and early signs of efficacy (119). Additionally, a new study has demonstrated that a selective class IIa HDACi (TMP269) enhances the efficacy of lenvatinib in fibroblast growth factor receptor 4 (FGFR4) positive HCC in mice (120, 135). Notably, the synergistic effect of HDACis allows these chemotherapeutic agents to exert their antitumor power without the need to reach very high doses. This effect greatly reduces the cytotoxicity of chemotherapy drugs, enabling them to be more widely used in the treatment of HCC, bringing a new development direction for the development of traditional drugs (35). For radiotherapy, it has shown that the use of HDAC-4 inhibitors can effectively enhance the killing efficiency of radiation on HCC tumor cells. Interruption of the HDAC-4 signaling pathway enhanced the radiation-induced mortality of cancer cells (121). In addition to traditional treatments, HDACis and several new treatments have shown good synergies. For example, Lin et al. demonstrated a synergistic therapeutic effect of pan-HDACi AR42 and telomerase-specific oncolytic adenovirus therapy. AR42 significantly enhanced telomerase-induced apoptosis in HCC tumor cells (122). These studies all showed the strong potential of HDACis in the field of HCC therapy.

Combination therapy can also overcome the occurrence of HDACi resistance and reduce the risk of drug use. Recently, studies have demonstrated that HDACis therapy can promote the epithelial-mesenchymal transition (EMT) of HCC through autophagy mediated by the AMPK-FOXO1-ULK1 signaling axis (123). EMT is a key step in tumor invasion and metastasis (137). This mechanism increases the risk of HDACis therapy, which leads to a limited therapeutic role in epithelial cell-derived cancers, including HCC. The combination of HDACis and FOXO1 inhibitors can effectively reduce this risk and increase the efficacy of treatment (123). Another example of combination therapy for HCC is the use of HDACis to enhance the efficacy of immunotherapy, which will be discussed in detail below. In general, HDACs play an important role in the development of HCC and provide new targets for more accurate treatment. HDACis have shown great value in the treatment and adjuvant therapy of HCC.

4 HDACis enhance the efficacy of HCC immunotherapy

4.1 HDACis enhance tumor immunotherapy

Immunotherapy has been successfully used in preclinical models or clinical settings to treat a variety of tumors, including HCC. However, the emergence of immunotherapy resistance is currently a major challenge. Although immunotherapy, such as immune checkpoint suppression therapy, has shown impressive clinical results, only some patients have achieved a lasting response (92). To overcome this problem, combination therapy strategies have been sought to achieve better efficacy. One strategy is to combine immunotherapy with HDACis. HDACis can potentially increase tumor immunogenicity, promote anti-tumor immune responses, or reverse immunosuppressive TME. Recently, HDACis combined immunotherapy has attracted much attention in cancer treatment (32) (Table 3).

HDACis increase the expression of PD-L1 and other immune checkpoints in tumor cells, which is an important mechanism to enhance the immunogenicity of tumor cells, and can improve the applicability and efficacy of ICIs. Abnormal expression of PD-L1 observed on the surface of human cancer cells mediates the inactivation of anti-tumor T cells and tumor immune escape (147). This mechanism also provides a target for PD-1/PD-L1 blockers to treat tumors. Studies have shown that the high expression of PD-L1 in tumors is one of the biomarkers to improve the sensitivity to PD-1/PD-L1 block (148). HDACis have been shown to increase PD-L1 expression in several tumors, including breast cancer, melanoma, HCC, soft tissue sarcoma, and B-cell lymphoma, thereby improving the efficacy of immunotherapy (33, 149, 150). Pan-HDACis, such as vorinostat and panobinostat, induce PD-L1 expression in B-cell lymphoma (33). Selective HDAC-3 inhibitors have also been shown to up-regulate the expression of PD-L1 in B-cell lymphoma, suggesting that HDAC-3 may be one of the key inhibitors mediating PD-L1 transcription in B-cell lymphoma (138). A similar mechanism has

TABLE 3 HDACi enhances the efficacy of immunotherapy.

HDAC inhibitors	HDAC specificity	Mechanisms	References
Vorinostat	Class I, II, IV	• Increase immunogenicity of tumor cells by increasing the expression of PD-1/PD-L1	(33)
Panobinostat	Class I, II, IV		(33)
OKI-179	Class I (HDAC-3)		(138)
Chidamide	Class I, IIb		(139)
Zabadinostat (CXD101)	Class I (HDAC-1, HDAC-2, HDAC3)	• Increase immunogenicity of tumor cells by increasing the expression of MHC molecule	(140)
Romidepsin	Class I	• Modulate the tumor microenvironment by increasing chemokine expression • Enhance the expression of NKG2D ligands and enhance the tumor killing ability	(141, 142)
PCI-34051 (for HCC)	Class I (HDAC-8)	• Reactivate the production of T-cell chemokines • Increase tumor infiltrating $CD8^+$ T cells and enhance anti-PD-L1 therapy	(143)
HDAC-10 inhibitor (for HCC)	Class IIb (HDAC-10)	• Modulate the tumor microenvironment by increasing chemokine (CXCL10) expression	(144)
Tubacin (for HCC)	Class IIb (HDAC-6)	• Increase IL-17A in the tumor microenvironment • Increasing the expression of PD-1	(145)
Sodium valproate	Class I (HDAC-1, HDAC-2)	• Increase the expression of NKG2D ligand MICB by down-regulating miR-889	(146)

HDAC, histone deacetylase; PD-1/PD-L1, programmed death receptor-1/programmed death receptor-ligand 1; MHC, major histocompatibility complex; NKG2D, natural killer group 2D; CXCL10, C-X-C motif chemokine 10; IL-17A, interleukin-17A; MICB, major histocompatibility complex class I chain-related gene B; miR-889, microRNA 889.

been found in soft tissue sarcomas (STS). Recent studies have shown that class I HDACi chidamide can increase histone acetylation of PD-L1 gene promoter in STS cancer cells and stimulate PD-L1 expression through activation of transcription factor STAT1. Further studies also demonstrated better efficacy of chidamide in combination with the anti-PD-1 antibody toripalimab in patients with advanced and metastatic sarcoma. Combination therapy also reduced the number of MDSCs in the TME, a key immunosuppressive cell population that mediates resistance to ICIs (139). HDACis' increased PD-L1 expression and increased PD-1 blocking efficiency may be related to more drug therapeutic targets. Recently, it has been found in breast cancer that the highly expressed membrane PD-L1 can translocate into the nucleus mediated by HDAC-2, thereby regulating tumor gene expression. The effects of this mechanism are multiple (151). On the one hand, nuclear PD-L1 can regulate the expression of pro-inflammatory and immune response-related genes, promoting immune inflammation in the local TME and thus making tumors more sensitive to immunotherapy. On the other hand, this gene regulation also promotes distant metastasis of cancer and enhances tumor aggressiveness. In addition, nuclear PD-L1 also triggers the expression of other immune checkpoint molecules, leading to possible acquired immunotherapy resistance. Blocking nuclear translocation of PD-L1 using HDAC-2 inhibitors can reduce transcription of these immune checkpoint genes, leading to increased infiltration of $CD8^+$ T cells and decreased levels of TNF-α in tumors (151, 152).

HDACis have also been shown to enhance tumor immunogenicity by promoting tumor antigen processing and presentation. The expression of MHC I in cancer is usually decreased due to epigenetic mechanisms, and HDACis can up-regulate the expression of MHC I in various types of cancer (34). Histone deacetylation usually induces chromatin shutdown of MHC II promoters, leading to MHC II downregulation in tumors, and HDACis can reverse this process (153). The effect of HDACis on tumor antigen processing and presentation enhances immunotherapy efficacy. Recently, a Class I HDACi CXD101 with selective activity was shown to enhance the efficacy of anti-PD-1 ICI in colorectal cancer. CXD101 induces the expression of molecules associated with antigen presentation, including MHC I, which increases antigen presentation and helps improve cytotoxic T cell conjugation and tumor cell killing. Anti-PD-1 antibodies release T cells by inhibiting immune checkpoints, which can then bind to MHC I with increased expression levels on tumor cells *via* T cell receptors, leading to increased cytotoxicity and tumor cell killing levels (140).

The regulation of the TME by HDACis is another important mechanism that enhances the efficacy of antitumor immunotherapy. Insufficient infiltration or abnormal function of anti-tumor immune cells, such as T cells and NK cells, is an important mechanism that causes tumor immune escape. HDACis can overcome this mechanism by recruiting more T and NK cells and enhancing their antitumor activity. HDACis enhance tumor immunogenicity essentially by activating more T cells to enhance the immune system's ability to recognize and kill tumor cells. In addition, HDACi can also play an immune-enhancing role by inducing chemokine production and regulating the expression of activation or apoptosis-related ligands. Increased expression of T cell chemokines (e.g. CXCL10, CXCL10 and CCL5) in tumors is associated with better response to immunotherapy and improved patient outcomes (154, 155). In a mouse model, HDACi romidepsin significantly increased CXCL10 expression in lung cancer and induced a strong T-cell-dependent antitumor response (141). HDACis can induce tumor regression or rejection in various lung

tumor models by promoting T cell recruitment and enhancing T cell function in combination with anti-PD-1 therapy. However, treatment with HDACis alone can lead to the overexpression of PD-L1 in tumor cells and the restriction of T cell function (150). Combined anti-PD-1 therapy can overcome this limitation by releasing IFN-γ and increasing the sensitivity of tumor cells to immunotherapy (141). This suggests that HDACis combined immunotherapy is a mutually reinforcing process that ultimately leads to a stronger synergistic therapeutic effect.

In addition to anti-tumor T cells, NK cells are also important immune components in the fight against tumors. HDACis can significantly enhance the expression of natural killer group 2D (NKG2D) ligands and activate NKG2D expressed in NK cells, thus enhancing the killing function of NK cells on tumors (142). Mechanistically, HDACis may enhance the expression of major histocompatibility complex class I-related chain A and B (MICA and MICB) and UL16 binding protein (ULBp) in tumor cells, which are key NKG2D ligands (156–158). This mechanism activates endogenous NK cells and enhances the toxicity of chimeric antigen receptor NK cell therapy (CAR-NK) to tumor cells. CAR-NK therapy refers to adding a chimeric antibody that can recognize tumor antigens and activate NK cells at the same time to enhance the anti-tumor ability of NK cells through genetic engineering (159). CAR-NK cells possess the dual intrinsic ability of natural receptors to recognize and target tumor cells. HDACis can increase the expression of NKG2D ligands to enhance the ability of CAR-NK cells to recognize tumors through natural receptors (32). Although many studies have demonstrated that HDACis enhance the anti-tumor response of NK cells by upregulating NKG2D, the results of a recent study suggest that HDACis may down-regulate another activating ligand, B7-H6, thereby inhibiting NK cell-mediated tumor cell recognition (160). This finding was confirmed in primary lymphoma and HCC samples and was associated with the inhibition of HDAC-3 (160). This suggests that combining HDACis with immunotherapy requires a rational strategy design, and that using non-selective HDACis may lead to unpredictable outcomes.

4.2 HDAC is combined with immunotherapy for HCC

HCC is a tumor with insufficient T-cell infiltration, which limits the effectiveness of immunotherapy in some patients (143). Therefore, additional mechanisms are needed to overcome HCC-induced immune tolerance and enhance the effectiveness of existing immunotherapy strategies. At present, many studies have shown that the combination of immunotherapies (such as ICIs) and HDACis may have a better therapeutic effect on HCC. For example, Belinostat has recently been shown to improve the efficacy of anti-CTLA-4 monotherapy and anti-CTLA-4 combined with anti-PD-1/PD-L1 in HCC patients, leading to complete tumor rejection (161). Mechanically, HDACis also improves the efficacy of immunotherapy by enhancing the immunogenicity of HCC cancer cells and regulating the TME. Specific mechanisms include up-regulation of PD-L1 expression, induction of chemokines, recruitment of T cells and NK cells, and enhancement of the anti-tumor function of immune cells (Figure 2) (143–146).

Zeste homolog 2 enhancer (EZH2) inhibition is one of the important mechanisms of HDACis enhancing HCC immunotherapy. EZH2, a histone H3 lysine methyltransferase,

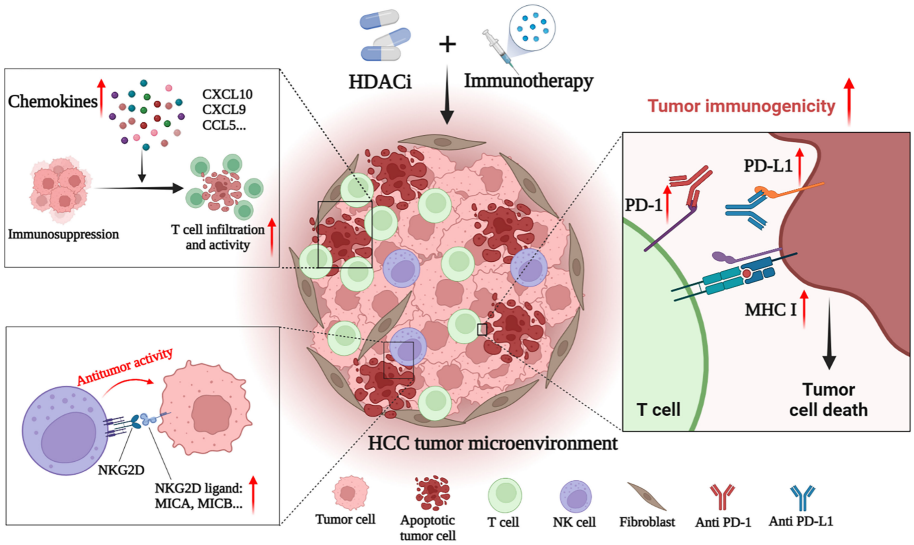

FIGURE 2
HDACi enhances the anti-tumor effect of immunotherapies in HCC. HDACi can enhance the efficacy of immunotherapy by enhancing the immunogenicity of tumor cells and modulating the tumor immune microenvironment. HDACi can increase the expression of PD-1 and PD-L1, thereby enhancing the sensitivity of HCC to ICIs. HDACi also facilitates the processing and presentation of tumor antigens by increasing the expression of MHC I and MHC II. HDACi can induce the expression of chemokines (CXCL10, CXCL9 and CCL5) in the microenvironment, increase the infiltration of T cells and enhance their antitumor activity. In addition, HDACi can increase the expression of NKG2D ligands in tumor cells, and activate and enhance the anti-tumor activity of NK cells.

is a proven oncogene (162). HDAC-10 can induce EZH2 recruitment at the CXCL10 promoter of the chemokine and ultimately inhibit CXCL10 transcription (144). HDAC-10 is necessary for this process to occur and provides a target for treatment. By inhibiting the recruitment of EZH2 on the CXCL10 promoter, knockdown of HDAC-10 can promote the increase of CXCL10 expression in HCC, inducing the recruitment of T cells and NK cells, and regulating and controlling the anti-tumor response in the TME (144). In addition to inhibiting the expression of CXCL10, EZH2 has also been shown to inhibit the expression of PD-L1 and reduce the effect of anti-CTLA-4 therapy (163, 164). HDAC-8 inhibition has also recently been shown to promote chemokine production. Down-regulation of HDAC-8 increases global acetylation and enhancer acetylation of histone H3 lysine 27 (H3K27), thereby reactivating the production of HCC T cell chemokines and alleviating tumor T cell rejection. In the preclinical model of HCC, selective inhibition of HDAC-8 increased tumor inhibition of $CD8^+$ T cells, and enhanced eradication of HCC by anti-PD-L1 therapy, with good safety (143). Additionally, recent have shown that HDAC-6 inhibits helper T 17 cells (Th17) that produce interleukin-17 (IL-17), thereby inhibiting the antitumor immune response. Adoptive transfer of HDAC-6-deficient Th17 cells can increase IL-17A in the HCC TME, thereby enhancing the anti-tumor response mediated by $CD8^+$ T cells. This suggests that HDAC-6 inhibitors can enhance the effect of immunotherapy in an IL-17A-dependent manner. Interestingly, this process also increased the expression of PD-1, making advanced HCC sensitive to ICIs and showing a strong synergistic effect (145). In addition to cytokines, microRNAs (miRNAs) are also important regulatory factors in the HCC microenvironment. It has been mentioned that HDACis may activate NK cells by increasing the expression of NKG2D ligand MICB and exerting antitumor effects. Recent studies have shown that HDACis also facilitates this process in HCC by inhibiting a miRNA called miR-889. miR-889 is considered to be a new MICB-targeting miRNA. Overexpression of miR-889 can significantly inhibit the mRNA and protein expression of MICB in HCC cells, and reduce the cytotoxicity mediated by NK cells. After the use of sodium valproate to inhibit HDACs, HCC cells showed down-regulation of miR-889 and increased sensitivity to NK cells (146).

Most HDACi drugs are approved for the treatment of hematologic tumors, such as PTCL, with a low mutation rate. HCC has been described as having a higher mutation load than most hematological malignancies, suggesting that HDACis have great potential to overcome the immune evasion of HCC. Given the significant obstacles to the development of novel anti-tumor drugs, combining HDACis with immunotherapy is an excellent option to enhance the effectiveness of existing treatment strategies. HDACis can regulate the immunogenicity and TME of HCC tumor cells in a variety of ways, and cope with tumor heterogeneity. Moreover, the effects of HDACis on immunotherapy result in a lower dose, which reduces cytotoxicity and adverse drug reactions (35). Generally, the use of HDACis to synergistically enhance HCC immunotherapy is a multi-mechanism strategy with good application prospects.

5 The potential applications of nano-based drug delivery system in HCC

Extensive research has been carried out to find mechanisms involved in the pathogenesis of HCC to develop novel strategies for diagnostic and therapeutic for the past few years. Nanotechnology has significantly affected the medical field by applying nanostructure to achieve specific therapeutic functions and improve medical limitations (165, 166). In this respect, nanotechnology provides huge opportunities in the diagnosis and treatment of HCC, which can target selectivity and specificity, and effectively achieve sufficient dosage in targeted tumor areas without adverse effects or minimal damage to normal cells (167). HCC has the characteristics of hypoxia, vascular leakage, specific receptors and acidic micro-environment, which can be recruited as targeting agents or by designing controlled delivery systems (168). Nanomedicine-based therapeutics have shown the potential to tackle the dilemma of the side effects of conventional chemotherapeutics, and a large number of nanomedicine-based therapeutics are under development for the treatment of HCC (38).

Generally, the therapeutic agent and a delivery system containing nano-carriers, targeting moiety, and stimuli-responsive units are the key components of designing a novel therapeutic (169, 170). As nano-carriers, organic nanoparticles (NPs) like dendrimers, polymeric NPs, Lipid-based NPs, Nanogels, and inorganic NPs such as hollow copper sulfide NPs, AgNPs, Bi2S3 NPs, quantum dots (QDs), carbon nanotubes, graphene-based nanomaterials have been proved to be feasible in HCC treatment (168). In the drug delivery system, molecularly targeted strategies for nano-drug mainly comprise passive targeting and active targeting. Passive targeting generally contributes to the EPR effect which allows the NPs to selectively accumulate in the tumor. While, active targeting enables therapeutic agents to be delivered to tumors in a highly specific and efficient manner using different targeting moieties. It mainly works based on recognition between the targeting agent immobilized on the NP surface and the over-expressed targeting agent receptor on the tumor cell's surface. Large amounts of targeting agents such as small molecule targeting ligands (glycyrrhetinic acid (171), folate, etc.), proteins (transferrin, GPC3 (172), etc.), antibodies (anti-GPC3 antibody, anti-VEGFR antibody, etc.), aptamers (TLS 9a aptamer, EpCAM-specific aptamer, etc.) and peptides (SP94 oligopeptide, etc.) had been reported for HCC therapy. Li et al. designed 5dual-ligand glycyrrhetinic acid and galactose-modified chitosan NPs by using the ionic gelation method as novel hepatoma-targeted drug delivery systems to further improve the targeting capability to HCC (Figure 3A). The dual-targeted NPs conquered the unsatisfactory targeting capacity and uptake efficiency of the single-ligand modified drug delivery system and represented an effective and safe drug delivery system for targeted therapy of HCC (171). Further, Xiang et al. developed a facile yet efficient strategy toward dual-targeting ligand-functionalized NPs for precise HCC therapy and potential clinical translation to solve the problems of sophisticated chemical design, multi-step synthesis and purification procedures of most reported NPs with dual-targeted properties

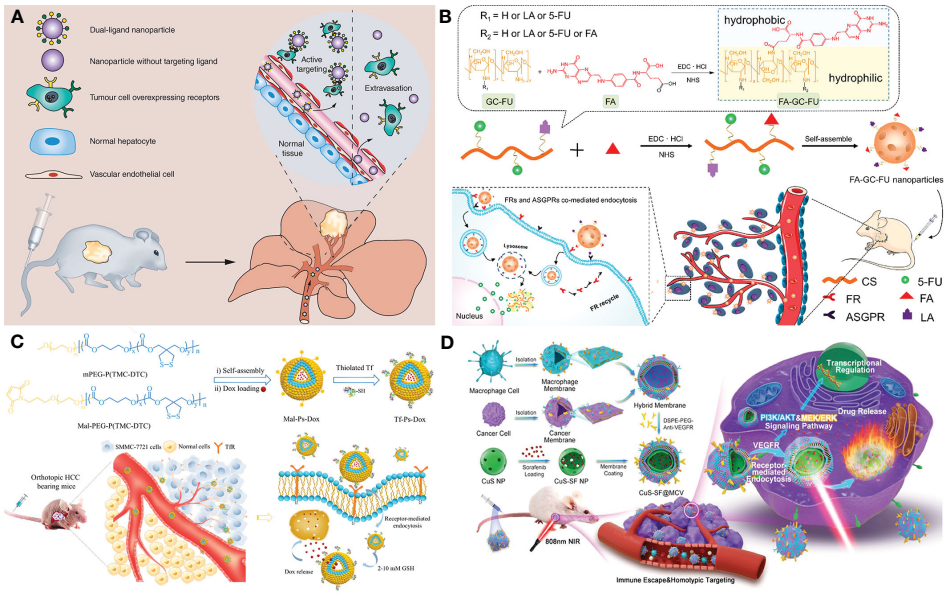

FIGURE 3
Applications of nano-based drug delivery systems in HCC. **(A)** Schematic representation of the dual-ligand glycyrrhetinic acid and galactose-modified chitosan nanoparticles with dual-ligand targeting hepatoma cells after intravenous administration in tumor-bearing mice model, through enhanced permeability and retention effect and active targeting between lactobionic acid and glycyrrhetinic acid on the nanoparticles and their receptors on hepatoma cells. Adapted with permission from ref (171). Copyright 2020, Future Medicine Ltd. **(B)** Schematic illustration of the facile synthesis of FA-GC-FU and its self-assembled micelle NPs with dual-targeting ligands of FA and LA for hepatoma-targeted delivery of 5-FU. Adapted with permission from ref (173). Copyright 2020, American Chemical Society. **(C)** Schematic illustration of the preparation of transferrin-guided, reduction-responsive and reversibly cross-linked polymersomal doxorubicin (Tf-Ps-Dox), and the targeted therapy of orthotopic hepatocellular carcinoma of Tf-Ps-Dox *in vivo*. Adapted with permission from ref (174). Copyright 2019, Elsevier. **(D)** Schematic illustration of the generation of macrophage–cancer hybrid membrane-coated, sorafenib-loaded and anti-VEGFR-modified CuS NPs for PTT against hepatocellular carcinoma. Adapted with permission from ref (175). Copyright 2020, Elsevier.

(Figure 3B). Folate (FA) was introduced as a hydrophobic and targeting component to a hydrophilic macromolecular prodrug (galactosylated chitosan-5-fluorouracil acetic acid (GC-FU)) to afford FA-GC-FU formulation that can self-assemble into NPs without the necessity of physical cross-linking. The FA-GC-FU NPs can target the over-expressed folate receptors (FRs) and asialoglycoprotein receptors (ASGPRs) on the surface of HCC cells, leading to greater targeting efficiency for enhanced therapeutic efficiency of HCC *in vitro* and *in vivo* (173). To provide a potent and low-toxic treatment modality for HCC, transferrin-guided polymersomal doxorubicin (Tf-Ps-Dox) was fabricated with controlled transferrin density, small size, and high drug loading through ligand postmodification strategy by Wei et al. (Figure 3C). The Tf-Ps-Dox NPs resulted in up to three-fold more accumulation and longer survival time than non-targeted Ps-Dox and clinically viable liposomal Dox (Lipo-Dox) (174). Biomimetic NPs coated with cell membranes have been widely concerned in targeted anti-tumor therapy due to the enhanced biocompatibility and specificity for homotypic cells. Ji et al. constructed cancer cell-macrophage hybrid membrane-coated hollow CuS NPs encapsulating sorafenib and surface modified with anti-VEGFR antibodies (CuS-SF@CMV) (Figure 3D). The CuS-SF@CMV NPs enhanced synergistic photothermal therapy (PTT) and chemotherapy against HCC owing to their immune evasion, tumor cell targeting and drug loading capacities, along with an inherent photo-thermal conversion ability (175). Compared with antibodies, aptamers with the advantages of low molecular weights and lack of immunogenicity show more stability, low cost and equal binding affinities, making them be used as promising targeting moiety candidates. Chakraborty et al. compared the therapeutic potential of phosphorothioate-modified TLS 9a aptamer (L5)-functionalized drug nano-carrier (PTX-NPL5) with other nano-carrier formulas, including previously reported HCC cell-targeting aptamers and non-aptamer ligands functionalized NPs. The results indicated that PTX-NPL5 had the highest potency in inducing selective apoptosis in neoplastic hepatocytes *via* a mitochondrial-dependent apoptotic pathway and did not produce any notable toxic effects in healthy hepatocytes, thus unveiling a new and safer option in targeted therapy for HCC (176).

Although ICIs have shown significant promise for cancer treatment, there are still challenges with efficacy, patient variability and off-target effects when immunomodulators are used (177). Immunomodulators like proteins have limited delivery potential when administered freely. Study has indicated that NPs have the potential to significantly improve delivery by protecting immunomodulators and enhancing their interaction with immune cells (178). Thus, nanomedicines-based immunotherapy has recently received widespread attention as a newly introduced strategy for tumor treatment (179–181). As an anticancer immune-boosting strategy, checkpoint inhibitors are typically monoclonal antibodies that target PD-1, PD-L1 or CTLA4. However, the usage of free antibodies is limited by

stability concerns. To improve these therapies by enhancing efficacy and reducing side effects, NPs have been utilized for both monoclonal antibody (anti-PD-1) and small interfering RNAs (siRNAs) delivery, which disrupt immune checkpoints (182, 183). Immunogenic cell death (ICD) is one type of cell death that causes an activation of the immune response (184). Many studies have revealed that drugs that are able to induce ICD are of great significance for cancer therapy (184). Metallic material-derived NPs usually have photothermal therapy (PTT) and photodynamic therapy (PDT) effects, which not only can be used as photosensitizer, but also have great potential for cancer immunotherapy due to ICD. For example, Dong et al. designed a multifunctional FA-CuS/DTX@PEI-CpG NPs (FA-CD@PP-CpG) for synergistic PDT, PTT and docetaxel (DTX)-enhanced immunotherapy (185). FA-CD@PP-CpG can improve immunotherapy effects, such as promoting infiltration of CTLs, suppressing myeloidderived suppressor cells (MDSCs) and enhancing antitumor efficacy on 4T1-tumor-bearing mice. Chemotherapeutic agents such as platinum-based drugs and Dox were identified that not only induce cell apoptosis, but also trigger ICD in tumor cells, leading to activated cytotoxic T cells mediating the anti-cancer immune responses (186). Zhu et al. (180) encapsulated Dox and PD-L1 siRNA (siPD-L1) into block copolymer PEG-PLA (NPDox/siPD L1) to evaluate the effects of Dox on the ICD in the PD-L1 knockdown tumor cells and tumor-bearing animal models. The results demonstrated that the treatment of NPDox/siPD-L1 significantly increased the ICD induction in the HCC cells, supporting the adjunctive role of blocking PD-L1 in the augment of ICD. Additionally, *in vivo* study supported that treatment of NPDox/siPD-L1 significantly inhibited tumor growth.

Epigenetic changes alter the TME by changing gene expressions and silencing tumor-suppressor genes. Hence, DNA methylation and histone modifications are the potential therapeutic targets in cancer therapy (187). However, current epigenetic drugs in cancer therapy are restricted by poor bioavailability, undesired side effects and cytotoxicity to normal tissues (188). Drug delivery system provides the opportunity to overcome the above limitations and improve therapeutic efficacy, owing to delivering high concentration of drugs to the tumor tissue with minimal side effects to healthy tissue. Meanwhile, the integration of two or more anti-tumor therapeutic methods has been proven to improve the therapeutic efficacy compared to the mono-therapy approaches (189, 190). Ruttala et al. developed a transferrin-anchored albumin nanoplatform with PEGylated lipid bilayers (Tf-L-APVN) for the targeted co-delivery of paclitaxel and vorinostat in solid tumors (191). Paclitaxel is an important chemotherapeutic drug with a broad spectrum of activity against multiple solid tumors. However, high toxicity, poor aqueous solubility and poor biodistribution restricted its therapeutic efficacy (192). As an HDACi, vorinostat plays a crucial role in epigenetic transcriptional regulation. The co-loading of paclitaxel and vorinostat could effectively modify the pharmacokinetics and toxicity profiles, control the release of drugs and maintain synergistic drug ratios for maximum therapeutic benefits. The Tf-L-APVN significantly enhanced the synergistic effects of paclitaxel and vorinostat on the proliferation of HepG2 cancer cells and displayed excellent anti-tumor efficacy in HepG2 tumor-bearing mice, making it great potential for HCC therapy.

The above-mentioned researches proved that nanomedicine is one of the novel strategies to help the generation of new therapeutic procedures for HCC. However, challenges and drawbacks in different nanostructures have restricted their applications in the clinic, resulting only a few nano-carriers have successfully entered clinical trials for HCC therapy. Physicochemical characteristics of nanomaterials including size, composition, structure, surface modifications, charge, porosity and aggregation behavior are one of the main challenges, and so, reproducible standards are necessary for improving the quality assessment of nanomaterials. Safety and biocompatibility concerns are also challenges in the translation of nanomedicine products to the clinic due to triggering adverse responses. Although the biomimetic multifunctional nanostructures using different biological compartments such as cell membranes or whole cells have been utilized to overcome the limitation, refining and standardizing requirements for the approval of nanomaterials are also necessary. Additionally, the complexity of the TME brings challenges for drug delivery. To introduce nanomedicine as an extraordinary tool for HCC therapy, more efforts should be made to investigate the easy routes to synthesize therapeutic nanomaterials and ensure their biosafety, cytotoxicity and drug efficiency, besides, multidisciplinary collaboration of different scientific areas is still needed to fully address all challenges.

6 Conclusion and perspectives

HCC is a malignant tumor with high morbidity and mortality, which seriously threatens the health of people all over the world. Immunotherapy has opened a new direction for HCC treatment and is gradually transforming the management of HCC patients. However, due to the suppressed tumor immune microenvironment of HCC, some patients are not sensitive to immunotherapy, which hinders the application and development of HCC immunotherapy. Here, we summarize the roles of HDACis, a class of epigenetic regulatory drugs, in enhancing HCC immunotherapy. HDACis have been shown to exhibit superior immunomodulatory capacity in a variety of tumors, including HCC, and have strong tumor suppressor function in conjunction with immunotherapies such as ICIs. The specific mechanisms include enhancing tumor immunogenicity and regulating TME. These results indicate that HDACis are an excellent adjunct drug for immunotherapy, and the two drugs have a stronger synergistic effect while playing their respective anti-tumor functions. However, the choice of drugs for HDACis is a challenge that combination therapy has to face, which is related to the multipotency of HDACi. On the one hand, HDACs can regulate a variety of non-histone targets, and inhibition of one HDAC may lead to multiple outcomes. On the other hand, some HDACis lack selectivity (pan-HDACis) and can inhibit multiple HDACs, which may lead to toxicity to healthy cells. Furthermore, the dosage of HDACis and the interaction between drugs in combination therapy must be carefully considered. Further studies should focus on synthesizing more selective HDACis and trying better combination therapies to reduce possible adverse

effects. In addition to drug combination therapy strategies, nanomaterial-based drug delivery systems also open up new directions for improving the therapeutic efficacy of HCC. Based on its advantages of good stability, good targeting, special physicochemical properties and biological effects, NDDS can effectively overcome the drug resistance mechanisms of some tumors, and has achieved impressive results. How to ensure the biosafety of the drug delivery systems, effectively control the cost, and develop uniform nanomedicine application standards will be the main challenges faced by NDDS in HCC treatment.

Author contributions

YL and YZ designed this study. CS, ML and YD drafted the manuscript. CS performed drawing and organization of figures. YL, YZ, CS, ML, YD, XJ, XH and FX revised the manuscript. All authors read and approved the final manuscript. All authors contributed to the article and approved the submitted version.

Funding

This work was funded by the National Natural Science Foundation of China, No. 82003262; China Postdoctoral Science Foundation, No. 2019TQ0221 and No. 2019M663517; Post-Doctor Research Project, West China Hospital, Sichuan University, No. 2019HXBH059; Key R&D Program of Sichuan Provincial Department of Science and Technology (Major Science and Technology Project) 2022YFS0095; Sichuan University postdoctoral interdisciplinary Innovation Fund.

Acknowledgments

The authors would like to gratefully acknowledge Prof. Chunhai Fan (Shanghai Jiao Tong University), Prof. Nan Chen and Assistant Prof. Min Yin (Shanghai Normal University) for their instructive suggestions to refine the manuscript. Figures 1, 2 were created with Biorender.com (https://biorender.com/).

Conflict of interest

The authors declare that the research was conducted in the absence of any commercial or financial relationships that could be construed as a potential conflict of interest.

Publisher's note

References

1. Sung H, Ferlay J, Siegel RL, Laversanne M, Soerjomataram I, Jemal A, et al. Global cancer statistics 2020: globocan estimates of incidence and mortality worldwide for 36 cancers in 185 countries. *CA Cancer J Clin* (2021) 71(3):209–49. doi: 10.3322/caac.21660

2. Llovet JM, Kelley RK, Villanueva A, Singal AG, Pikarsky E, Roayaie S, et al. Hepatocellular carcinoma. *Nat Rev Dis Primers* (2021) 7(1):6. doi: 10.1038/s41572-020-00240-3

3. Forner A, Reig M, Bruix J. Hepatocellular carcinoma. *Lancet* (2018) 391 (10127):1301–14. doi: 10.1016/s0140-6736(18)30010-2

4. Wang ZJ, Liu WH, Shi JY, Chen N, Fan CH. Nanoscale delivery systems for cancer immunotherapy. *Mater Horiz* (2018) 5(3):344–62. doi: 10.1039/c7mh00991g

5. Kennedy LB, Salama AKS. A review of cancer immunotherapy toxicity. *CA Cancer J Clin* (2020) 70(2):86–104. doi: 10.3322/caac.21596

6. Leone V, Ali A, Weber A, Tschaharganeh DF, Heikenwalder M. Liver inflammation and hepatobiliary cancers. *Trends Cancer* (2021) 7(7):606–23. doi: 10.1016/j.trecan.2021.01.012

7. Sangro B, Sarobe P, Hervás-Stubbs S, Melero I. Advances in immunotherapy for hepatocellular carcinoma. *Nat Rev Gastroenterol Hepatol* (2021) 18(8):525–43. doi: 10.1038/s41575-021-00438-0

8. Dermani FK, Samadi P, Rahmani G, Kohlan AK, Najafi R. Pd-1/Pd-L1 immune checkpoint: potential target for cancer therapy. *J Cell Physiol* (2019) 234(2):1313–25. doi: 10.1002/jcp.27172

9. Vanella V, Festino L, Vitale MG, Alfano B, Ascierto PA. Emerging pd-1/Pd-L1 antagonists for the treatment of malignant melanoma. *Expert Opin Emerg Drugs* (2021) 26(2):79–92. doi: 10.1080/14728214.2021.1901884

10. Wang J, Ye Y, Yu J, Kahkoska AR, Zhang X, Wang C, et al. Core-shell microneedle gel for self-regulated insulin delivery. *ACS Nano* (2018) 12(3):2466–73. doi: 10.1021/acsnano.7b08152

11. Bellmunt J, Powles T, Vogelzang NJ. A review on the evolution of pd-1/Pd-L1 immunotherapy for bladder cancer: the future is now. *Cancer Treat Rev* (2017) 54:58–67. doi: 10.1016/j.ctrv.2017.01.007

12. Ansell SM, Lesokhin AM, Borrello I, Halwani A, Scott EC, Gutierrez M, et al. Pd-1 blockade with nivolumab in relapsed or refractory hodgkin's lymphoma. *N Engl J Med* (2015) 372(4):311–9. doi: 10.1056/NEJMoa1411087

13. Baker H. Pd-1 inhibition in advanced merkel-cell carcinoma. *Lancet Oncol* (2016) 17(6):e225. doi: 10.1016/s1470-2045(16)30112-7

14. Havel JJ, Chowell D, Chan TA. The evolving landscape of biomarkers for checkpoint inhibitor immunotherapy. *Nat Rev Cancer* (2019) 19(3):133–50. doi: 10.1038/s41568-019-0116-x

15. Hato T, Goyal L, Greten TF, Duda DG, Zhu AX. Immune checkpoint blockade in hepatocellular carcinoma: current progress and future directions. *Hepatology* (2014) 60(5):1776–82. doi: 10.1002/hep.27246

16. Trujillo JA, Sweis RF, Bao R, Luke JJ. T Cell-inflamed versus non-T cell-inflamed tumors: a conceptual framework for cancer immunotherapy drug development and combination therapy selection. *Cancer Immunol Res* (2018) 6(9):990–1000. doi: 10.1158/2326-6066.Cir-18-0277

17. El-Khoueiry AB, Sangro B, Yau T, Crocenzi TS, Kudo M, Hsu C, et al. Nivolumab in patients with advanced hepatocellular carcinoma (Checkmate 040): an open-label, non-comparative, phase 1/2 dose escalation and expansion trial. *Lancet* (2017) 389(10088):2492–502. doi: 10.1016/s0140-6736(17)31046-2

18. Zhu AX, Finn RS, Edeline J, Cattan S, Ogasawara S, Palmer D, et al. Pembrolizumab in patients with advanced hepatocellular carcinoma previously treated with sorafenib (Keynote-224): a non-randomised, open-label phase 2 trial. *Lancet Oncol* (2018) 19(7):940–52. doi: 10.1016/s1470-2045(18)30351-6

19. Wang J, Li J, Tang G, Tian Y, Su S, Li Y. Clinical outcomes and influencing factors of pd-1/Pd-L1 in hepatocellular carcinoma. *Oncol Lett* (2021) 21(4):279. doi: 10.3892/ol.2021.12540

20. Zongyi Y, Xiaowu L. Immunotherapy for hepatocellular carcinoma. *Cancer Lett* (2020) 470:8–17. doi: 10.1016/j.canlet.2019.12.002

21. Tolsma TO, Hansen JC. Post-translational modifications and chromatin dynamics. *Essays Biochem* (2019) 63(1):89–96. doi: 10.1042/ebc20180067

22. Neganova ME, Klochkov SG, Aleksandrova YR, Aliev G. Histone modifications in epigenetic regulation of cancer: perspectives and achieved progress. *Semin Cancer Biol* (2020) 83:452–71. doi: 10.1016/j.semcancer.2020.07.015

23. Bates SE. Epigenetic therapies for cancer. *N Engl J Med* (2020) 383(7):650–63. doi: 10.1056/NEJMra1805035

24. Hauser AT, Robaa D, Jung M. Epigenetic small molecule modulators of histone and DNA methylation. *Curr Opin Chem Biol* (2018) 45:73–85. doi: 10.1016/j.cbpa.2018.03.003

25. Yang G-J, Wang W, Mok SWF, Wu C, Law BYK, Miao X-M, et al. Selective inhibition of lysine-specific demethylase 5a (Kdm5a) using a Rhodium(Iii) complex for triple-negative breast cancer therapy. *Angew Chem Int Ed Engl* (2018) 57(40):13091–5. doi: 10.1002/anie.201807305

26. Yang G-J, Zhong H-J, Ko C-N, Wong S-Y, Vellaisamy K, Ye M, et al. Identification of a Rhodium(Iii) complex as a Wee1 inhibitor against Tp53-mutated triple-negative breast cancer cells. *Chem Commun (Camb)* (2018) 54(20):2463–6. doi: 10.1039/c7cc09384e

27. Zhao C, Dong H, Xu Q, Zhang Y. Histone deacetylase (Hdac) inhibitors in cancer: a patent review (2017-present). *Expert Opin Ther Pat* (2020) 30(4):263–74. doi: 10.1080/13543776.2020.1725470

28. Poole RM. Belinostat: first global approval. *Drugs* (2014) 74(13):1543–54. doi: 10.1007/s40265-014-0275-8

29. Eleutherakis-Papaiakovou E, Kanellias N, Kastritis E, Gavriatopoulou M, Terpos E, Dimopoulos MA. Efficacy of panobinostat for the treatment of multiple myeloma. *J Oncol* (2020) 2020:7131802. doi: 10.1155/2020/7131802

30. Eckschlager T, Plch J, Stiborova M, Hrabeta J. Histone deacetylase inhibitors as anticancer drugs. *Int J Mol Sci* (2017) 18(7):1414. doi: 10.3390/ijms18071414

31. Zhou M, Yuan M, Zhang M, Lei C, Aras O, Zhang X, et al. Combining histone deacetylase inhibitors (Hdacis) with other therapies for cancer therapy. *Eur J Med Chem* (2021) 226:113825. doi: 10.1016/j.ejmech.2021.113825

32. Wang X, Waschke BC, Woolaver RA, Chen SMY, Chen Z, Wang JH. Hdac inhibitors overcome immunotherapy resistance in b-cell lymphoma. *Protein Cell* (2020) 11(7):472–82. doi: 10.1007/s13238-020-00694-x

33. Deng S, Hu Q, Zhang H, Yang F, Peng C, Huang C. Hdac3 inhibition upregulates pd-L1 expression in b-cell lymphomas and augments the efficacy of anti-Pd-L1 therapy. *Mol Cancer Ther* (2019) 18(5):900–8. doi: 10.1158/1535-7163.MCT-18-1068

34. Grunewald CM, Schulz WA, Skowron MA, Hoffmann MJ, Niegisch G. Tumor immunotherapy-the potential of epigenetic drugs to overcome resistance. *Trans Cancer Res* (2018) 7(4):1151–60. doi: 10.21037/tcr.2018.06.24

35. Grumetti L, Lombardi R, Iannelli F, Pucci B, Avallone A, Di Gennaro E, et al. Epigenetic approaches to overcome fluoropyrimidines resistance in solid tumors. *Cancers (Basel)* (2022) 14(3):695. doi: 10.3390/cancers14030695

36. Luo Y, Yin M, Mu C, Hu X, Xie H, Li J, et al. Engineering female germline stem cells with exocytotic polymer dots. *Adv Mater* (2023):e2210458. doi: 10.1002/adma.202210458

37. Mitchell MJ, Billingsley MM, Haley RM, Wechsler ME, Peppas NA, Langer R. Engineering precision nanoparticles for drug delivery. *Nat Rev Drug Discov* (2021) 20 (2):101–24. doi: 10.1038/s41573-020-0090-8

38. Ma P, Sun Y, Chen J, Li H, Zhu H, Gao X, et al. Enhanced anti-hepatocarcinoma efficacy by Glut1 targeting and cellular microenvironment-responsive pamam-camptothecin conjugate. *Drug Deliv* (2018) 25(1):153–65. doi: 10.1080/10717544.2017.1419511

39. Wang M, Zhao J, Zhang L, Wei F, Lian Y, Wu Y, et al. Role of tumor microenvironment in tumorigenesis. *J Cancer* (2017) 8(5):761–73. doi: 10.7150/jca.17648

40. Jenne CN, Kubes P. Immune surveillance by the liver. *Nat Immunol* (2013) 14 (10):996–1006. doi: 10.1038/ni.2691

41. Ringelhan M, Pfister D, O'Connor T, Pikarsky E, Heikenwalder M. The immunology of hepatocellular carcinoma. *Nat Immunol* (2018) 19(3):222–32. doi: 10.1038/s41590-018-0044-z

42. Heymann F, Peusquens J, Ludwig-Portugall I, Kohlhepp M, Ergen C, Niemietz P, et al. Liver inflammation abrogates immunological tolerance induced by kupffer cells. *Hepatology* (2015) 62(1):279–91. doi: 10.1002/hep.27793

43. Hou J, Zhang H, Sun B, Karin M. The immunobiology of hepatocellular carcinoma in humans and mice: basic concepts and therapeutic implications. *J Hepatol* (2020) 72(1):167–82. doi: 10.1016/j.jhep.2019.08.014

44. Pfister D, Núñez NG, Pinyol R, Govaere O, Pinter M, Szydlowska M, et al. Nash Limits anti-tumour surveillance in immunotherapy-treated hcc. *Nature* (2021) 592 (7854):450–6. doi: 10.1038/s41586-021-03362-0

45. Zheng C, Zheng L, Yoo JK, Guo H, Zhang Y, Guo X, et al. Landscape of infiltrating T cells in liver cancer revealed by single-cell sequencing. *Cell* (2017) 169 (7):1342–56.e16. doi: 10.1016/j.cell.2017.05.035

46. Hoechst B, Ormandy LA, Ballmaier M, Lehner F, Krüger C, Manns MP, et al. A new population of myeloid-derived suppressor cells in hepatocellular carcinoma patients induces Cd4(+)Cd25(+)Foxp3(+) T cells. *Gastroenterology* (2008) 135 (1):234–43. doi: 10.1053/j.gastro.2008.03.020

47. Kalathil S, Lugade AA, Miller A, Iyer R, Thanavala Y. Higher frequencies of Garp(+)Ctla-4(+)Foxp3(+) T regulatory cells and myeloid-derived suppressor cells in hepatocellular carcinoma patients are associated with impaired T-cell functionality. *Cancer Res* (2013) 73(8):2435–44. doi: 10.1158/0008-5472.Can-12-3381

48. Giraud J, Chalopin D, Blanc J-F, Saleh M. Hepatocellular carcinoma immune landscape and the potential of immunotherapies. *Front Immunol* (2021) 12:655697. doi: 10.3389/fimmu.2021.655697

49. Llovet JM, Castet F, Heikenwalder M, Maini MK, Mazzaferro V, Pinato DJ, et al. Immunotherapies for hepatocellular carcinoma. *Nat Rev Clin Oncol* (2022) 19(3):151–72. doi: 10.1038/s41571-021-00573-2

50. Kole C, Charalampakis N, Tsakatikas S, Vailas M, Moris D, Gkotsis E, et al. Immunotherapy for hepatocellular carcinoma: a 2021 update. *Cancers (Basel)* (2020) 12 (10):2859. doi: 10.3390/cancers12102859

51. Pinter M, Jain RK, Duda DG. The current landscape of immune checkpoint blockade in hepatocellular carcinoma: a review. *JAMA Oncol* (2021) 7(1):113–23. doi: 10.1001/jamaoncol.2020.3381

52. Khemlina G, Ikeda S, Kurzrock R. The biology of hepatocellular carcinoma: implications for genomic and immune therapies. *Mol Cancer* (2017) 16(1):149. doi: 10.1186/s12943-017-0712-x

53. Mody K, Feldman R, Reddy SK, Reynolds GA, McMillan JM, Johnson E. Pd-1/Pd-L1 expression and molecular associations in hpb malignancies. *J Clin Oncol* (2016) 34(4):289. doi: 10.1200/jco.2016.34.4_suppl.289

54. Yau T, Park J-W, Finn RS, Cheng A-L, Mathurin P, Edeline J, et al. Nivolumab versus sorafenib in advanced hepatocellular carcinoma (Checkmate 459): a randomised, multicentre, open-label, phase 3 trial. *Lancet Oncol* (2022) 23(1):77–90. doi: 10.1016/S1470-2045(21)00604-5

55. Yau T, Hsu C, Kim T-Y, Choo S-P, Kang Y-K, Hou M-M, et al. Nivolumab in advanced hepatocellular carcinoma: sorafenib-experienced Asian cohort analysis. *J Hepatol* (2019) 71(3):543–52. doi: 10.1016/j.jhep.2019.05.014

56. Yau T, Kang Y-K, Kim T-Y, El-Khoueiry AB, Santoro A, Sangro B, et al. Efficacy and safety of nivolumab plus ipilimumab in patients with advanced hepatocellular carcinoma previously treated with sorafenib: the checkmate 040 randomized clinical trial. *JAMA Oncol* (2020) 6(11):e204564. doi: 10.1001/jamaoncol.2020.4564

57. D'Alessio A, Fulgenzi CAM, Nishida N, Schönlein M, von Felden J, Schulze K, et al. Preliminary evidence of safety and tolerability of atezolizumab plus bevacizumab in patients with hepatocellular carcinoma and child-pugh a and b cirrhosis: a real-world study. *Hepatology* (2022) 76(4):1000–12. doi: 10.1002/hep.32468

58. Lee MS, Ryoo B-Y, Hsu C-H, Numata K, Stein S, Verret W, et al. Atezolizumab with or without bevacizumab in unresectable hepatocellular carcinoma (Go30140): an open-label, multicentre, phase 1b study. *Lancet Oncol* (2020) 21(6):808–20. doi: 10.1016/S1470-2045(20)30156-X

59. Finn RS, Qin S, Ikeda M, Galle PR, Ducreux M, Kim T-Y, et al. Atezolizumab plus bevacizumab in unresectable hepatocellular carcinoma. *N Engl J Med* (2020) 382 (20):1894–905. doi: 10.1056/NEJMoa1915745

60. Zhu AX, Abbas AR, de Galarreta MR, Guan Y, Lu S, Koeppen H, et al. Molecular correlates of clinical response and resistance to atezolizumab in combination with bevacizumab in advanced hepatocellular carcinoma. *Nat Med* (2022) 28(8):1599–611. doi: 10.1038/s41591-022-01868-2

61. Finn RS, Ryoo B-Y, Merle P, Kudo M, Bouattour M, Lim HY, et al. Pembrolizumab as second-line therapy in patients with advanced hepatocellular carcinoma in keynote-240: a randomized, double-blind, phase iii trial. *J Clin Oncol* (2020) 38(3):193–202. doi: 10.1200/JCO.19.01307

62. Duan J, Cui L, Zhao X, Bai H, Cai S, Wang G, et al. Use of immunotherapy with programmed cell death 1 vs programmed cell death ligand 1 inhibitors in patients with cancer: a systematic review and meta-analysis. *JAMA Oncol* (2020) 6(3):375–84. doi: 10.1001/jamaoncol.2019.5367

63. Agdashian D, ElGindi M, Xie C, Sandhu M, Pratt D, Kleiner DE, et al. The effect of anti-Ctla4 treatment on peripheral and intra-tumoral T cells in patients with hepatocellular carcinoma. *Cancer Immunol Immunother* (2019) 68(4):599–608. doi: 10.1007/s00262-019-02299-8

64. Zhou G, Sprengers D, Boor PPC, Doukas M, Schutz H, Mancham S, et al. Antibodies against immune checkpoint molecules restore functions of tumor-infiltrating T cells in hepatocellular carcinomas. *Gastroenterology* (2017) 153 (4):1107–19. doi: 10.1053/j.gastro.2017.06.017

65. Iñarrairaegui M, Melero I, Sangro B. Immunotherapy of hepatocellular carcinoma: facts and hopes. *Clin Cancer Res* (2018) 24(7):1518–24. doi: 10.1158/1078-0432.CCR-17-0289

66. Duffy AG, Ulahannan SV, Makorova-Rusher O, Rahma O, Wedemeyer H, Pratt D, et al. Tremelimumab in combination with ablation in patients with advanced hepatocellular carcinoma. *J Hepatol* (2017) 66(3):545–51. doi: 10.1016/j.jhep.2016.10.029

67. Chew V, Lai L, Pan L, Lim CJ, Li J, Ong R, et al. Delineation of an immunosuppressive gradient in hepatocellular carcinoma using high-dimensional

proteomic and transcriptomic analyses. *Proc Natl Acad Sci USA* (2017) 114(29):E5900–E9. doi: 10.1073/pnas.1706559114

68. Yarchoan M, Xing D, Luan L, Xu H, Sharma RB, Popovic A, et al. Characterization of the immune microenvironment in hepatocellular carcinoma. *Clin Cancer Res* (2017) 23(23):7333–9. doi: 10.1158/1078-0432.CCR-17-0950

69. Guo M, Yuan F, Qi F, Sun J, Rao Q, Zhao Z, et al. Expression and clinical significance of lag-3, Fgl1, pd-L1 and Cd8t cells in hepatocellular carcinoma using multiplex quantitative analysis. *J Transl Med* (2020) 18(1):306. doi: 10.1186/s12967-020-02469-8

70. Guo M, Qi F, Rao Q, Sun J, Du X, Qi Z, et al. Serum lag-3 predicts outcome and treatment response in hepatocellular carcinoma patients with transarterial chemoembolization. *Front Immunol* (2021) 12:754961. doi: 10.3389/fimmu.2021.754961

71. Lee WJ, Lee YJ, Choi ME, Yun KA, Won CH, Lee MW, et al. Expression of lymphocyte-activating gene 3 and T-cell immunoreceptor with immunoglobulin and itim domains in cutaneous melanoma and their correlation with programmed cell death 1 expression in tumor-infiltrating lymphocytes. *J Am Acad Dermatol* (2019) 81(1):219–27. doi: 10.1016/j.jaad.2019.03.012

72. Sanchez-Correa B, Lopez-Sejas N, Duran E, Labella F, Alonso C, Solana R, et al. Modulation of nk cells with checkpoint inhibitors in the context of cancer immunotherapy. *Cancer Immunol Immunother* (2019) 68(5):861–70. doi: 10.1007/s00262-019-02336-6

73. Zhang P-F, Gao C, Huang X-Y, Lu J-C, Guo X-J, Shi G-M, et al. Cancer cell-derived exosomal Circuhrf1 induces natural killer cell exhaustion and may cause resistance to anti-Pd1 therapy in hepatocellular carcinoma. *Mol Cancer* (2020) 19(1):110. doi: 10.1186/s12943-020-01222-5

74. Tan S, Xu Y, Wang Z, Wang T, Du X, Song X, et al. Tim-3 hampers tumor surveillance of liver-resident and conventional nk cells by disrupting Pi3k signaling. *Cancer Res* (2020) 80(5):1130–42. doi: 10.1158/0008-5472.CAN-19-2332

75. Butterfield LH. Immunotherapeutic strategies for hepatocellular carcinoma. *Gastroenterology* (2004) 127(5 Suppl 1):S232–S41. doi: 10.1053/j.gastro.2004.09.038

76. Palmer DH, Midgley RS, Mirza N, Torr EE, Ahmed F, Steele JC, et al. A phase ii study of adoptive immunotherapy using dendritic cells pulsed with tumor lysate in patients with hepatocellular carcinoma. *Hepatology* (2009) 49(1):124–32. doi: 10.1002/hep.22626

77. Aranda F, Vacchelli E, Eggermont A, Galon J, Sautès-Fridman C, Tartour E, et al. Trial watch: peptide vaccines in cancer therapy. *Oncoimmunology* (2013) 2(12):e26621. doi: 10.4161/onci.26621

78. Coulie PG, Van den Eynde BJ, van der Bruggen P, Boon T. Tumour antigens recognized by T lymphocytes: At the core of cancer immunotherapy. *Nat Rev Cancer* (2014) 14(2):135–46. doi: 10.1038/nrc3670

79. Tagliamonte M, Petrizzo A, Mauriello A, Tornesello ML, Buonaguro FM, Buonaguro L. Potentiating cancer vaccine efficacy in liver cancer. *Oncoimmunology* (2018) 7(10):e1488564. doi: 10.1080/2162402X.2018.1488564

80. Wang Y, Zhao Q, Zhao B, Zheng Y, Zhuang Q, Liao N, et al. Remodeling tumor-associated neutrophils to enhance dendritic cell-based hcc neoantigen nano-vaccine efficiency. *Adv Sci (Weinh)* (2022) 9(11):e2105631. doi: 10.1002/advs.202105631

81. Zuo B, Zhang Y, Zhao K, Wu L, Qi H, Yang R, et al. Universal immunotherapeutic strategy for hepatocellular carcinoma with exosome vaccines that engage adaptive and innate immune responses. *J Hematol Oncol* (2022) 15(1):46. doi: 10.1186/s13045-022-01266-8

82. Rosenberg SA, Restifo NP. Adoptive cell transfer as personalized immunotherapy for human cancer. *Science* (2015) 348(6230):62–8. doi: 10.1126/science.aaa4967

83. Rosenberg SA, Yang JC, Sherry RM, Kammula US, Hughes MS, Phan GQ, et al. Durable complete responses in heavily pretreated patients with metastatic melanoma using T-cell transfer immunotherapy. *Clin Cancer Res* (2011) 17(13):4550–7. doi: 10.1158/1078-0432.CCR-11-0116

84. Lee JH, Lee J-H, Lim Y-S, Yeon JE, Song T-J, Yu SJ, et al. Adjuvant immunotherapy with autologous cytokine-induced killer cells for hepatocellular carcinoma. *Gastroenterology* (2015) 148(7):1383–91. doi: 10.1053/j.gastro.2015.02.055

85. Yu SJ, Ma C, Heinrich B, Brown ZJ, Sandhu M, Zhang Q, et al. Targeting the crosstalk between cytokine-induced killer cells and myeloid-derived suppressor cells in hepatocellular carcinoma. *J Hepatol* (2019) 70(3):449–57. doi: 10.1016/j.jhep.2018.10.040

86. Dal Bo M, De Mattia E, Baboci L, Mezzalira S, Cecchin E, Assaraf YG, et al. New insights into the pharmacological, immunological, and car-T-Cell approaches in the treatment of hepatocellular carcinoma. *Drug Resist Update* (2020) 51:100702. doi: 10.1016/j.drup.2020.100702

87. Akce M, Zaidi MY, Waller EK, El-Rayes BF, Lesinski GB. The potential of car T cell therapy in pancreatic cancer. *Front Immunol* (2018) 9:2166. doi: 10.3389/fimmu.2018.02166

88. Li D, Li N, Zhang Y-F, Fu H, Feng M, Schneider D, et al. Persistent polyfunctional chimeric antigen receptor T cells that target glypican 3 eliminate orthotopic hepatocellular carcinomas in mice. *Gastroenterology* (2020) 158(8):2250–65. doi: 10.1053/j.gastro.2020.02.011

89. Wang C-J, Xiao C-W, You T-G, Zheng Y-X, Gao W, Zhou Z-Q, et al. Interferon-A enhances antitumor activities of oncolytic adenovirus-mediated il-24 expression in hepatocellular carcinoma. *Mol Cancer* (2012) 11:31. doi: 10.1186/1476-4598-11-31

90. Llovet JM, Sala M, Castells L, Suarez Y, Vilana R, Bianchi L, et al. Randomized controlled trial of interferon treatment for advanced hepatocellular carcinoma. *Hepatology* (2000) 31(1):54–8. doi: 10.1002/hep.510310111

91. Zhou J, Wang W, Li Q. Potential therapeutic targets in the tumor microenvironment of hepatocellular carcinoma: reversing the protumor effect of tumor-associated macrophages. *J Exp Clin Cancer Res* (2021) 40(1):73. doi: 10.1186/s13046-021-01873-2

92. Sharma P, Hu-Lieskovan S, Wargo JA, Ribas A. Primary, adaptive, and acquired resistance to cancer immunotherapy. *Cell* (2017) 168(4):707–23. doi: 10.1016/j.cell.2017.01.017

93. Morad G, Helmink BA, Sharma P, Wargo JA. Hallmarks of response, resistance, and toxicity to immune checkpoint blockade. *Cell* (2021) 184(21):5309–37. doi: 10.1016/j.cell.2021.09.020

94. Brown ZJ, Yu SJ, Heinrich B, Ma C, Fu Q, Sandhu M, et al. Indoleamine 2,3-dioxygenase provides adaptive resistance to immune checkpoint inhibitors in hepatocellular carcinoma. *Cancer Immunol Immunother* (2018) 67(8):1305–15. doi: 10.1007/s00262-018-2190-4

95. Snahnicanova Z, Kasubova I, Kalman M, Grendar M, Mikolajcik P, Gabonova E, et al. Genetic and epigenetic analysis of the beta-2-Microglobulin gene in microsatellite instable colorectal cancer. *Clin Exp Med* (2020) 20(1):87–95. doi: 10.1007/s10238-019-00601-7

96. Castagnoli L, Cancila V, Cordoba-Romero SL, Faraci S, Talarico G, Belmonte B, et al. Wnt signaling modulates pd-L1 expression in the stem cell compartment of triple-negative breast cancer. *Oncogene* (2019) 38(21):4047–60. doi: 10.1038/s41388-019-0700-2

97. Kornberg RD. Chromatin structure: a repeating unit of histones and DNA. *Science* (1974) 184(4139):868–71. doi: 10.1126/science.184.4139.868

98. Yang G-J, Ko C-N, Zhong H-J, Leung C-H, Ma D-L. Structure-based discovery of a selective Kdm5a inhibitor that exhibits anti-cancer activity *Via* inducing cell cycle arrest and senescence in breast cancer cell lines. *Cancers (Basel)* (2019) 11(1):92. doi: 10.3390/cancers11010092

99. Dawson MA, Kouzarides T. Cancer epigenetics: from mechanism to therapy. *Cell* (2012) 150(1):12–27. doi: 10.1016/j.cell.2012.06.013

100. McIntyre RL, Daniels EG, Molenaars M, Houtkooper RH, Janssens GE. From molecular promise to preclinical results: hdac inhibitors in the race for healthy aging drugs. *EMBO Mol Med* (2019) 11(9):e9854. doi: 10.15252/emmm.201809854

101. Hesham HM, Lasheen DS, Abouzid KAM. Chimeric hdac inhibitors: comprehensive review on the hdac-based strategies developed to combat cancer. *Med Res Rev* (2018) 38(6):2058–109. doi: 10.1002/med.21505

102. Biersack B, Polat S, Höpfner M. Anticancer properties of chimeric hdac and kinase inhibitors. *Semin Cancer Biol* (2022) 83:472–86. doi: 10.1016/j.semcancer.2020.11.005

103. Gregoretti IV, Lee Y-M, Goodson HV. Molecular evolution of the histone deacetylase family: functional implications of phylogenetic analysis. *J Mol Biol* (2004) 338(1):17–31. doi: 10.1016/j.jmb.2004.02.006

104. Li G, Jiang H, Chang M, Xie H, Hu L. Hdac6 A-tubulin deacetylase: a potential therapeutic target in neurodegenerative diseases. *J Neurol Sci* (2011) 304(1-2):1–8. doi: 10.1016/j.jns.2011.02.017

105. Wang P, Wang Z, Liu J. Role of hdacs in normal and malignant hematopoiesis. *Mol Cancer* (2020) 19(1):5. doi: 10.1186/s12943-019-1127-7

106. Dong L, Dong Q, Chen Y, Li Y, Zhang B, Zhou F, et al. Novel Hdac5-interacting motifs of Tbx3 are essential for the suppression of e-cadherin expression and for the promotion of metastasis in hepatocellular carcinoma. *Signal Transduct Target Ther* (2018) 3:22. doi: 10.1038/s41392-018-0025-6

107. Kim TW, Lee HG. Apigenin induces autophagy and cell death by targeting Ezh2 under hypoxia conditions in gastric cancer cells. *Int J Mol Sci* (2021) 22(24):13455. doi: 10.3390/ijms222413455

108. Reßing N, Schliehe-Diecks J, Watson PR, Sönnichsen M, Cragin AD, Schöler A, et al. Development of fluorinated peptoid-based histone deacetylase (Hdac) inhibitors for therapy-resistant acute leukemia. *J Med Chem* (2022) 65(22):15457–72. doi: 10.1021/acs.jmedchem.2c01418

109. Ho TCS, Chan AHY, Ganesan A. Thirty years of hdac inhibitors: 2020 insight and hindsight. *J Med Chem* (2020) 63(21):12460–84. doi: 10.1021/acs.jmedchem.0c00830

110. Shi Y, Dong M, Hong X, Zhang W, Feng J, Zhu J, et al. Results from a multicenter, open-label, pivotal phase ii study of chidamide in relapsed or refractory peripheral T-cell lymphoma. *Ann Oncol* (2015) 26(8):1766–71. doi: 10.1093/annonc/mdv237

111. Li W, Sun Z. Mechanism of action for hdac inhibitors-insights from omics approaches. *Int J Mol Sci* (2019) 20(7):1616. doi: 10.3390/ijms20071616

112. Qiu Q, Yang L, Feng Y, Zhu Z, Li N, Zheng L, et al. Hdac I/Iib selective inhibitor purinostat mesylate combined with Gls1 inhibition effectively eliminates cml stem cells. *Bioact Mater* (2023) 21:483–98. doi: 10.1016/j.bioactmat.2022.08.006

113. Xiao K, Li Y-P, Wang C, Ahmad S, Vu M, Kuma K, et al. Disulfide cross-linked micelles of novel hdac inhibitor thailandepsin a for the treatment of breast cancer. *Biomaterials* (2015) 67:183–93. doi: 10.1016/j.biomaterials.2015.07.033

114. Zhang S, Zhan L, Li X, Yang Z, Luo Y, Zhao H. Preclinical and clinical progress for hdac as a putative target for epigenetic remodeling and functionality of immune cells. *Int J Biol Sci* (2021) 17(13):3381–400. doi: 10.7150/ijbs.62001

115. He S, Dong G, Li Y, Wu S, Wang W, Sheng C. Potent dual Bet/Hdac inhibitors for efficient treatment of pancreatic cancer. *Angew Chem Int Ed Engl* (2020) 59 (8):3028–32. doi: 10.1002/anie.201915896

116. Buurman R, Gürlevik E, Schäffer V, Eilers M, Sandbothe M, Kreipe H, et al. Histone deacetylases activate hepatocyte growth factor signaling by repressing microrna-449 in hepatocellular carcinoma cells. *Gastroenterology* (2012) 143(3):811–20. doi: 10.1053/j.gastro.2012.05.033

117. Marquardt JU, Gomez-Quiroz L, Arreguin Camacho LO, Pinna F, Lee Y-H, Kitade M, et al. Curcumin effectively inhibits oncogenic nf-Kb signaling and restrains stemness features in liver cancer. *J Hepatol* (2015) 63(3):661–9. doi: 10.1016/j.jhep.2015.04.018

118. Yeo W, Chung HC, Chan SL, Wang LZ, Lim R, Picus J, et al. Epigenetic therapy using belinostat for patients with unresectable hepatocellular carcinoma: a multicenter phase I/Ii study with biomarker and pharmacokinetic analysis of tumors from patients in the Mayo phase ii consortium and the cancer therapeutics research group. *J Clin Oncol Off J Am Soc Clin Oncol* (2012) 30(27):3361–7. doi: 10.1200/JCO.2011.41.2395

119. Bitzer M, Horger M, Giannini EG, Ganten TM, Wörns MA, Siveke JT, et al. Resminostat plus sorafenib as second-line therapy of advanced hepatocellular carcinoma - the shelter study. *J Hepatol* (2016) 65(2):280–8. doi: 10.1016/j.jhep.2016.02.043

120. Ito R, Miyanishi K, Kubo T, Hamaguchi K, Osuga T, Tanaka S, et al. Synergistic antitumor effect of histone deacetylase class iia inhibitor with lenvatinib in hepatocellular carcinoma. *Hepatol Int* (2023). doi: 10.1007/s12072-023-10484-2

121. Tsai C-L, Liu W-L, Hsu F-M, Yang P-S, Yen R-F, Tzen K-Y, et al. Targeting histone deacetylase 4/Ubiquitin-conjugating enzyme 9 impairs DNA repair for radiosensitization of hepatocellular carcinoma cells in mice. *Hepatol (Baltimore Md)* (2018) 67(2):586–99. doi: 10.1002/hep.29328

122. Lin Z-Z, Hu MCT, Hsu C, Wu Y-M, Lu Y-S, Ho J-AA, et al. Synergistic efficacy of telomerase-specific oncolytic adenoviral therapy and histone deacetylase inhibition in human hepatocellular carcinoma. *Cancer Lett* (2023) 556:216063. doi: 10.1016/j.canlet.2023.216063

123. Xiao Q, Liu H, Wang H-S, Cao M-T, Meng X-J, Xiang Y-L, et al. Histone deacetylase inhibitors promote epithelial-mesenchymal transition in hepatocellular carcinoma *Via* ampk-Foxo1-Ulk1 signaling axis-mediated autophagy. *Theranostics* (2020) 10(22):10245–61. doi: 10.7150/thno.47045

124. Fernández-Barrena MG, Arechederra M, Colyn L, Berasain C, Avila MA. Epigenetics in hepatocellular carcinoma development and therapy: the tip of the iceberg. *JHEP Rep* (2020) 2(6):100167. doi: 10.1016/j.jhepr.2020.100167

125. Cai J, Li B, Zhu Y, Fang X, Zhu M, Wang M, et al. Prognostic biomarker identification through integrating the gene signatures of hepatocellular carcinoma properties. *EBioMedicine* (2017) 19:18–30. doi: 10.1016/j.ebiom.2017.04.014

126. Zhao J, Gray SG, Greene CM, Lawless MW. Unmasking the pathological and therapeutic potential of histone deacetylases for liver cancer. *Expert Rev Gastroenterol Hepatol* (2019) 13(3):247–56. doi: 10.1080/17474124.2019.1568870

127. Bae HJ, Jung KH, Eun JW, Shen Q, Kim HS, Park SJ, et al. Microrna-221 governs tumor suppressor Hdac6 to potentiate malignant progression of liver cancer. *J Hepatol* (2015) 63(2):408–19. doi: 10.1016/j.jhep.2015.03.019

128. Lee Y-H, Seo D, Choi K-J, Andersen JB, Won M-A, Kitade M, et al. Antitumor effects in hepatocarcinoma of isoform-selective inhibition of Hdac2. *Cancer Res* (2014) 74(17):4752–61. doi: 10.1158/0008-5472.CAN-13-3531

129. Wu H, Yang T-Y, Li Y, Ye W-L, Liu F, He X-S, et al. Tumor necrosis factor receptor-associated factor 6 promotes hepatocarcinogenesis by interacting with histone deacetylase 3 to enhance c-myc gene expression and protein stability. *Hepatology* (2020) 71(1):148–63. doi: 10.1002/hep.30801

130. Zhang L-Z, Yang J-E, Luo Y-W, Liu F-T, Yuan Y-F, Zhuang S-M. A P53/Lnc-Ip53 negative feedback loop regulates tumor growth and chemoresistance. *Adv Sci (Weinh)* (2020) 7(21):2001364. doi: 10.1002/advs.202001364

131. Lytle NK, Barber AG, Reya T. Stem cell fate in cancer growth, progression and therapy resistance. *Nat Rev Cancer* (2018) 18(11):669–80. doi: 10.1038/s41568-018-0056-x

132. Demircioglu F, Wang J, Candido J, Costa ASH, Casado P, de Luxan Delgado B, et al. Cancer associated fibroblast fak regulates malignant cell metabolism. *Nat Commun* (2020) 11(1):1290. doi: 10.1038/s41467-020-15104-3

133. Bi L, Ren Y, Feng M, Meng P, Wang Q, Chen W, et al. Hdac11 regulates glycolysis through the Lkb1/Ampk signaling pathway to maintain hepatocellular carcinoma stemness. *Cancer Res* (2021) 81(8):2015–28. doi: 10.1158/0008-5472.CAN-20-3044

134. Wu J, Zhu P, Lu T, Du Y, Wang Y, He L, et al. The long non-coding rna Lnchdac2 drives the self-renewal of liver cancer stem cells *Via* activation of hedgehog signaling. *J Hepatol* (2019) 70(5):918–29. doi: 10.1016/j.jhep.2018.12.015

135. Wang L-Z, Ramírez J, Yeo W, Chan M-YM, Thuya W-L, Lau J-YA, et al. Glucuronidation by Ugt1a1 is the dominant pathway of the metabolic disposition of belinostat in liver cancer patients. *PLoS One* (2013) 8(1):e54522. doi: 10.1371/journal.pone.0054522

136. Roca MS, Moccia T, Iannelli F, Testa C, Vitagliano C, Minopoli M, et al. Hdac class I inhibitor domatinostat sensitizes pancreatic cancer to chemotherapy by targeting cancer stem cell compartment *Via* Foxm1 modulation. *J Exp Clin Cancer Res* (2022) 41 (1):83. doi: 10.1186/s13046-022-02295-4

137. Xu W, Liu H, Liu Z-G, Wang H-S, Zhang F, Wang H, et al. Histone deacetylase inhibitors upregulate snail *Via* Smad2/3 phosphorylation and stabilization of snail to promote metastasis of hepatoma cells. *Cancer Lett* (2018) 420:1–13. doi: 10.1016/j.canlet.2018.01.068

138. Wang X, Waschke BC, Woolaver RA, Chen Z, Zhang G, Piscopio AD, et al. Histone deacetylase inhibition sensitizes Pd1 blockade-resistant b-cell lymphomas. *Cancer Immunol Res* (2019) 7(8):1318–31. doi: 10.1158/2326-6066.CIR-18-0875

139. Que Y, Zhang X-L, Liu Z-X, Zhao J-J, Pan Q-Z, Wen X-Z, et al. Frequent amplification of hdac genes and efficacy of hdac inhibitor chidamide and pd-1 blockade combination in soft tissue sarcoma. *J Immunother Cancer* (2021) 9(2):e001696. doi: 10.1136/jitc-2020-001696

140. Blaszczak W, Liu G, Zhu H, Barczak W, Shrestha A, Albayrak G, et al. Immune modulation underpins the anti-cancer activity of hdac inhibitors. *Mol Oncol* (2021) 15 (12):3280–98. doi: 10.1002/1878-0261.12953

141. Zheng H, Zhao W, Yan C, Watson CC, Massengill M, Xie M, et al. Hdac inhibitors enhance T-cell chemokine expression and augment response to pd-1 immunotherapy in lung adenocarcinoma. *Clin Cancer Res an Off J Am Assoc For Cancer Res* (2016) 22(16):4119–32. doi: 10.1158/1078-0432.CCR-15-2584

142. Chu Y, Yahr A, Huang B, Ayello J, Barth M, S Cairo M. Romidepsin alone or in combination with anti-Cd20 chimeric antigen receptor expanded natural killer cells targeting burkitt lymphoma *in vitro* and in immunodeficient mice. *Oncoimmunology* (2017) 6(9):e1341031. doi: 10.1080/2162402X.2017.1341031

143. Yang W, Feng Y, Zhou J, Cheung OK-W, Cao J, Wang J, et al. A selective Hdac8 inhibitor potentiates antitumor immunity and efficacy of immune checkpoint blockade in hepatocellular carcinoma. *Sci Transl Med* (2021) 13(588):eaaz6804. doi: 10.1126/scitranslmed.aaz6804

144. Bugide S, Gupta R, Green MR, Wajapeyee N. Ezh2 inhibits nk cell-mediated antitumor immunity by suppressing Cxcl10 expression in an Hdac10-dependent manner. *Proc Natl Acad Sci USA* (2021) 118(30):e2102718118. doi: 10.1073/pnas.2102718118

145. Qiu W, Wang B, Gao Y, Tian Y, Tian M, Chen Y, et al. Targeting histone deacetylase 6 reprograms interleukin-17-Producing helper T cell pathogenicity and facilitates immunotherapies for hepatocellular carcinoma. *Hepatol (Baltimore Md)* (2020) 71(6):1967–87. doi: 10.1002/hep.30960

146. Xie H, Zhang Q, Zhou H, Zhou J, Zhang J, Jiang Y, et al. Microrna-889 is downregulated by histone deacetylase inhibitors and confers resistance to natural killer cytotoxicity in hepatocellular carcinoma cells. *Cytotechnology* (2018) 70(2):513–21. doi: 10.1007/s10616-017-0108-1

147. Baumeister SH, Freeman GJ, Dranoff G, Sharpe AH. Coinhibitory pathways in immunotherapy for cancer. *Annu Rev Immunol* (2016) 34:539–73. doi: 10.1146/annurev-immunol-032414-112049

148. Galluzzi L, Chan TA, Kroemer G, Wolchok JD, López-Soto A. The hallmarks of successful anticancer immunotherapy. *Sci Transl Med* (2018) 10(459):eaat7807. doi: 10.1126/scitranslmed.aat7807

149. Li T, Zhang C, Hassan S, Liu X, Song F, Chen K, et al. Histone deacetylase 6 in cancer. *J Hematol Oncol* (2018) 11(1):111. doi: 10.1186/s13045-018-0654-9

150. Woods DM, Sodré AL, Villagra A, Sarnaik A, Sotomayor EM, Weber J. Hdac inhibition upregulates pd-1 ligands in melanoma and augments immunotherapy with pd-1 blockade. *Cancer Immunol Res* (2015) 3(12):1375–85. doi: 10.1158/2326-6066.CIR-15-0077-T

151. Gao Y, Nihira NT, Bu X, Chu C, Zhang J, Kolodziejczyk A, et al. Acetylation-dependent regulation of pd-L1 nuclear translocation dictates the efficacy of anti-Pd-1 immunotherapy. *Nat Cell Biol* (2020) 22(9):1064–75. doi: 10.1038/s41556-020-0562-4

152. Perez-Ruiz E, Minute L, Otano I, Alvarez M, Ochoa MC, Belsue V, et al. Prophylactic tnf blockade uncouples efficacy and toxicity in dual ctla-4 and pd-1 immunotherapy. *Nature* (2019) 569(7756):428–32. doi: 10.1038/s41586-019-1162-y

153. Neuwelt AJ, Kimball AK, Johnson AM, Arnold BW, Bullock BL, Kaspar RE, et al. Cancer cell-intrinsic expression of mhc ii in lung cancer cell lines is actively restricted by Mek/Erk signaling and epigenetic mechanisms. *J Immunother Cancer* (2020) 8(1):e000441. doi: 10.1136/jitc-2019-000441

154. Hopewell EL, Zhao W, Fulp WJ, Bronk CC, Lopez AS, Massengill M, et al. Lung tumor nf-Kb signaling promotes T cell-mediated immune surveillance. *J Clin Invest* (2013) 123(6):2509–22. doi: 10.1172/JCI67250

155. Ji R-R, Chasalow SD, Wang L, Hamid O, Schmidt H, Cogswell J, et al. An immune-active tumor microenvironment favors clinical response to ipilimumab. *Cancer Immunol Immunother* (2012) 61(7):1019–31. doi: 10.1007/s00262-011-1172-6

156. Hirano M, Imai Y, Kaito Y, Murayama T, Sato K, Ishida T, et al. Small-molecule hdac and akt inhibitors suppress tumor growth and enhance immunotherapy in multiple myeloma. *J Exp Clin Cancer Res* (2021) 40(1):110. doi: 10.1186/s13046-021-01909-7

157. Raulet DH. Roles of the Nkg2d immunoreceptor and its ligands. *Nat Rev Immunol* (2003) 3(10):781–90. doi: 10.1038/nri1199

158. Lanier LL. Nkg2d receptor and its ligands in host defense. *Cancer Immunol Res* (2015) 3(6):575–82. doi: 10.1158/2326-6066.CIR-15-0098

159. Liu E, Marin D, Banerjee P, Macapinlac HA, Thompson P, Basar R, et al. Use of car-transduced natural killer cells in Cd19-positive lymphoid tumors. *N Engl J Med* (2020) 382(6):545–53. doi: 10.1056/NEJMoa1910607

160. Fiegler N, Textor S, Arnold A, Rölle A, Oehme I, Breuhahn K, et al. Downregulation of the activating Nkp30 ligand B7-H6 by hdac inhibitors impairs tumor cell recognition by nk cells. *Blood* (2013) 122(5):684–93. doi: 10.1182/blood-2013-02-482513

161. Llopiz D, Ruiz M, Villanueva L, Iglesias T, Silva L, Egea J, et al. Enhanced anti-tumor efficacy of checkpoint inhibitors in combination with the histone deacetylase inhibitor belinostat in a murine hepatocellular carcinoma model. *Cancer Immunol Immunother* (2019) 68(3):379–93. doi: 10.1007/s00262-018-2283-0

162. Korfhage J, Lombard DB. Malignant peripheral nerve sheath tumors: from epigenome to bedside. *Mol Cancer Res* (2019) 17(7):1417–28. doi: 10.1158/1541-7786.MCR-19-0147

163. Goswami S, Apostolou I, Zhang J, Skepner J, Anandhan S, Zhang X, et al. Modulation of Ezh2 expression in T cells improves efficacy of anti-Ctla-4 therapy. *J Clin Invest* (2018) 128(9):3813–8. doi: 10.1172/JCI99760

164. Xiao G, Jin L-L, Liu C-Q, Wang Y-C, Meng Y-M, Zhou Z-G, et al. Ezh2 negatively regulates pd-L1 expression in hepatocellular carcinoma. *J Immunother Cancer* (2019) 7(1):300. doi: 10.1186/s40425-019-0784-9

165. He MX, Yu L, Yang YY, Zou BH, Ma W, Yu M, et al. Delivery of triptolide with reduction-sensitive polymer nanoparticles for liver cancer therapy on patient-derived xenografts models. *Chin Chem Lett* (2020) 31(12):3178–82. doi: 10.1016/j.cclet.2020.05.034

166. Yang Y, Yu Y, Chen H, Meng X, Ma W, Yu M, et al. Illuminating platinum transportation while maximizing therapeutic efficacy by gold nanoclusters *Via* simultaneous near-Infrared-I/Ii imaging and glutathione scavenging. *ACS Nano* (2020) 14(10):13536–47. doi: 10.1021/acsnano.0c05541

167. Liu Y, Bhattarai P, Dai Z, Chen X. Photothermal therapy and photoacoustic imaging *Via* nanotheranostics in fighting cancer. *Chem Soc Rev* (2019) 48(7):2053–108. doi: 10.1039/c8cs00618k

168. Sedighi M, Mahmoudi Z, Abbaszadeh S, Eskandari MR, Saeinasab M, Sefat F. Nanomedicines for hepatocellular carcinoma therapy: challenges and clinical applications. *Mater Today Commun* (2023) 34:105242. doi: 10.1016/j.mtcomm.2022.105242

169. Sedighi M, Sieber S, Rahimi F, Shahbazi MA, Rezayan AH, Huwyler J, et al. Rapid optimization of liposome characteristics using a combined microfluidics and design-of-Experiment approach. *Drug Deliv Trans Res* (2019) 9(1):404–13. doi: 10.1007/s13346-018-0587-4

170. Herranz-Blanco B, Shahbazi MA, Correia AR, Balasubramanian V, Kohout T, Hirvonen J, et al. Ph-switch nanoprecipitation of polymeric nanoparticles for multimodal cancer targeting and intracellular triggered delivery of doxorubicin. *Adv Healthc Mater* (2016) 5(15):1904–16. doi: 10.1002/adhm.201600160

171. Li M, Wang Y, Jiang S, Gao Y, Zhang W, Hu S, et al. Biodistribution and biocompatibility of glycyrrhetinic acid and galactose-modified chitosan nanoparticles as a novel targeting vehicle for hepatocellular carcinoma. *Nanomedicine* (2020) 15 (2):145–61. doi: 10.2217/nnm-2018-0455

172. Fu Y, Urban DJ, Nani RR, Zhang Y-F, Li N, Fu H, et al. Glypican-3-Specific antibody drug conjugates targeting hepatocellular carcinoma. *Hepatology* (2019) 70 (2):563–76. doi: 10.1002/hep.30326

173. Xiang Y, Huang W, Huang C, Long J, Zhou Y, Liu Y, et al. Facile fabrication of nanoparticles with dual-targeting ligands for precise hepatocellular carcinoma therapy *in vitro* and *in vivo*. *Mol Pharm* (2020) 17(9):3223–35. doi: 10.1021/acs.molpharmaceut.0c00327

174. Wei Y, Gu X, Cheng L, Meng F, Storm G, Zhong Z. Low-toxicity transferrin-guided polymersomal doxorubicin for potent chemotherapy of orthotopic hepatocellular carcinoma *in vivo*. *Acta Biomater* (2019) 92:196–204. doi: 10.1016/j.actbio.2019.05.034

175. Ji B, Cai H, Yang Y, Peng F, Song M, Sun K, et al. Hybrid membrane camouflaged copper sulfide nanoparticles for photothermal-chemotherapy of hepatocellular carcinoma. *Acta biomaterialia* (2020) 111:363–72. doi: 10.1016/j.actbio.2020.04.046

176. Chakraborty S, Dlie ZY, Chakraborty S, Roy S, Mukherjee B, Besra SE, et al. Aptamer-functionalized drug nanocarrier improves hepatocellular carcinoma toward normal by targeting neoplastic hepatocytes. *Mol Ther Nucleic Acids* (2020) 20:34–49. doi: 10.1016/j.omtn.2020.01.034

177. Marshall HT, Djamgoz MBA. Immuno-oncology: emerging targets and combination therapies. *Front Oncol* (2018) 8:315. doi: 10.3389/fonc.2018.00315

178. Urbanavicius D, Alvarez T, Such GK, Johnston APR, Mintern JD. The potential of nanoparticle vaccines as a treatment for cancer. *Mol Immunol* (2018) 98:2–7. doi: 10.1016/j.molimm.2017.12.022

179. Huang J, Yang B, Peng Y, Huang JS, Wong SHD, Bian LM, et al. Nanomedicine-boosting tumor immunogenicity for enhanced immunotherapy. *Adv Funct Mater* (2021) 31(21):2011171. doi: 10.1002/adfm.202011171

180. Zhu HZ, Zhou WJ, Wan YF, Ge K, Lu J, Jia CK. Nanomedicine-mediated induction of immunogenic cell death and prevention of pd-L1 overexpression for enhanced hepatocellular carcinoma therapy. *Cancer Nanotechnol* (2020) 11(1):15. doi: 10.1186/s12645-020-00072-6

181. van der Meel R, Sulheim E, Shi Y, Kiessling F, Mulder WJM, Lammers T. Smart cancer nanomedicine. *Nat Nanotechnol* (2019) 14(11):1007–17. doi: 10.1038/s41565-019-0567-y

182. Deng H, Zhang Z. The application of nanotechnology in immune checkpoint blockade for cancer treatment. *J Control Release* (2018) 290:28–45. doi: 10.1016/j.jconrel.2018.09.026

183. Wang C, Sun W, Wright G, Wang AZ, Gu Z. Inflammation-triggered cancer immunotherapy by programmed delivery of cpg and anti-Pd1 antibody. *Adv Mater* (2017) 29(15):1770101. doi: 10.1002/adma.201700761

184. Galluzzi L, Buque A, Kepp O, Zitvogel L, Kroemer G. Immunogenic cell death in cancer and infectious disease. *Nat Rev Immunol* (2017) 17(2):97–111. doi: 10.1038/nri.2016.107

185. Chen L, Zhou LL, Wang CH, Han Y, Lu YL, Liu J, et al. Tumor-targeted drug and cpg delivery system for phototherapy and docetaxel-enhanced immunotherapy with polarization toward M1-type macrophages on triple negative breast cancers. *Adv Mater* (2019) 31(52):1904997. doi: 10.1002/adma.201904997

186. Jessup JM, Kabbout M, Korokhov N, Joun A, Tollefson AE, Wold WSM, et al. Adenovirus and oxaliplatin cooperate as agnostic sensitizers for immunogenic cell death in colorectal carcinoma. *Hum Vaccines Immunother* (2020) 16(3):636–44. doi: 10.1080/21645515.2019.1665960

187. Singh M, Kumar V, Sehrawat N, Yadav M, Chaudhary M, Upadhyay SK, et al. Current paradigms in epigenetic anticancer therapeutics and future challenges. *Semin Cancer Biol* (2022) 83:422–40. doi: 10.1016/j.semcancer.2021.03.013

188. Roberti A, Valdes AF, Torrecillas R, Fraga MF, Fernandez AF. Epigenetics in cancer therapy and nanomedicine. *Clin Epigenet* (2019) 11:81. doi: 10.1186/s13148-019-0675-4

189. Guo JF, Yu Z, Sun DD, Zou YF, Liu Y, Huang L. Two nanoformulations induce reactive oxygen species and immunogenetic cell death for synergistic chemo-immunotherapy eradicating colorectal cancer and hepatocellular carcinoma. *Mol Cancer* (2021) 20(1):10. doi: 10.1186/s12943-020-01297-0

190. Guo JF, Yu Z, Das M, Huang L. Nano codelivery of oxaliplatin and folinic acid achieves synergistic chemo-immunotherapy with 5-fluorouracil for colorectal cancer and liver metastasis. *ACS Nano* (2020) 14(4):5075–89. doi: 10.1021/acsnano.0c01676

191. Ruttala HB, Ramasamy T, Poudal BK, Choi Y, Choi JY, Kim J, et al. Molecularly targeted Co-delivery of a histone deacetylase inhibitor and paclitaxel by lipid-protein hybrid nanoparticles for synergistic combinational chemotherapy. *Oncotarget* (2017) 8(9):14925–40. doi: 10.18632/oncotarget.14742

192. Hou L, Zhong T, Cheng P, Long B, Shi L, Meng X, et al. Self-assembled peptide-paclitaxel nanoparticles for enhancing therapeutic efficacy in colorectal cancer. *Front Bioeng Biotechnol* (2022) 10:938662. doi: 10.3389/fbioe.2022.938662

frontiers | Frontiers in Oncology

TYPE Original Research
PUBLISHED 19 June 2023
DOI 10.3389/fonc.2023.1169537

OPEN ACCESS

EDITED BY
Maria Lina Tornesello,
G. Pascale National Cancer Institute Foundation (IRCCS), Italy

REVIEWED BY
Susan Costantini,
G. Pascale National Cancer Institute Foundation (IRCCS), Italy
Jinghan Wang,
Tongji University, China

*CORRESPONDENCE
Hannes Jansson
hannes.jansson@ki.se

†These authors have contributed equally to this work and share senior authorship

RECEIVED 22 February 2023
ACCEPTED 05 June 2023
PUBLISHED 19 June 2023

CITATION
Jansson H, Cornillet M, Sun D, Filipovic I, Sturesson C, O'Rourke CJ, Andersen JB, Björkström NK and Sparrelid E (2023) Preoperative immunological plasma markers TRAIL, CSF1 and TIE2 predict survival after resection for biliary tract cancer. *Front. Oncol.* 13:1169537. doi: 10.3389/fonc.2023.1169537

Preoperative immunological plasma markers TRAIL, CSF1 and TIE2 predict survival after resection for biliary tract cancer

Hannes Jansson[1]*, Martin Cornillet[2], Dan Sun[2], Iva Filipovic[2], Christian Sturesson[1], Colm J. O'Rourke[3], Jesper B. Andersen[3], Niklas K. Björkström[2†] and Ernesto Sparrelid[1†]

[1]Division of Surgery and Oncology, Department of Clinical Science, Intervention and Technology, Karolinska Institutet, Karolinska University Hospital, Stockholm, Sweden, [2]Center for Infectious Medicine, Department of Medicine Huddinge, Karolinska Institutet, Karolinska University Hospital, Stockholm, Sweden, [3]Biotech Research and Innovation Centre (BRIC), Department of Health and Medical Sciences, University of Copenhagen, Copenhagen, Denmark

Introduction: Systemic inflammatory markers have been validated as prognostic factors for patients with biliary tract cancer (BTC). The aim of this study was to evaluate specific immunologic prognostic markers and immune responses by analyzing preoperative plasma samples from a large prospectively collected biobank.

Methods: Expression of 92 proteins representing adaptive and innate immune responses was investigated in plasma from 102 patients undergoing resection for BTC 2009-2017 (perihilar cholangiocarcinoma n=46, intrahepatic cholangiocarcinoma n=27, gallbladder cancer n=29), by means of a high-throughput multiplexed immunoassay. Association with overall survival was analyzed by Cox regression, with internal validation and calibration. Tumor tissue bulk and single-cell gene expression of identified markers and receptors/ligands was analyzed in external cohorts.

Results: Three preoperative plasma markers were independently associated with survival: TRAIL, TIE2 and CSF1, with hazard ratios (95% confidence intervals) 0.30 (0.16-0.56), 2.78 (1.20-6.48) and 4.02 (1.40-11.59) respectively. The discrimination of a preoperative prognostic model with the three plasma markers was assessed with concordance-index 0.70, while the concordance-index of a postoperative model with histopathological staging was 0.66. Accounting for subgroup differences, prognostic factors were assessed for each type of BTC. TRAIL and CSF1 were prognostic factors in intrahepatic cholangiocarcinoma. In independent cohorts, TRAIL-receptor expression was higher in tumor tissue and seen in malignant cells, with TRAIL and CSF1 expressed by intra- and peritumoral immune cells. Intratumoral TRAIL-activity was decreased compared to peritumoral immune cells, while CSF1-activity was increased. The highest CSF1 activity was seen in intratumoral macrophages, while the highest TRAIL-activity was seen in peritumoral T-cells.

Discussion: In conclusion, three preoperative immunological plasma markers were prognostic for survival after surgery for BTC, providing good discrimination, even compared to postoperative pathology. TRAIL and CSF1, prognostic factors in intrahepatic cholangiocarcinoma, showed marked differences in expression and activity between intra- and peritumoral immune cells.

KEYWORDS

cholangiocarcinoma (CCA), gallbladder cancer (GBC), prognostic biomarkers, tumor associated macrophage (TAM), biliary tract cancer (BTC)

1 Introduction

Patients with biliary tract cancer (cholangiocarcinoma and gallbladder cancer) have a high risk of tumor recurrence after curative intent surgery, with poor long-term survival outcomes. A majority of patients are diagnosed with cancer recurrence within five years after surgery for cholangiocarcinoma or oncological resection for gallbladder cancer (1–4), and a median overall survival of approximately two to four years has been reported in reviews, meta-analyses and multicenter cohorts (2, 5–7). Established prognostic factors such as histopathological tumor extension, tumor grade and lymph node metastasis (2, 8, 9) are only available after tumor resection, impeding a preoperative risk stratification. Prognostic value of a systemic inflammatory response (as assessed by markers such as C-reactive protein [CRP], albumin or white cell counts) for overall survival has been indicated in several types of malignancies (e.g. colorectal cancer, pancreatic cancer, breast cancer and prostate cancer) (10), including biliary tract cancer (11). Previously, general inflammatory markers in plasma (CRP, albumin) were validated as independent negative prognostic factors for overall survival for patients with resectable biliary tract cancer (BTC) (12). The aim of this study was to identify new candidate preoperative prognostic markers and to further characterize the immune response in BTC.

2 Materials and methods

2.1 Study design

Patients undergoing primary resection for perihilar cholangiocarcinoma (pCCA), intrahepatic cholangiocarcinoma (iCCA) or gallbladder cancer (GBC) at Karolinska University Hospital, a tertiary referral center (Stockholm, Sweden), in the period January 2009 to January 2017 were assessed for inclusion in the development and internal validation cohort of this study. Patients undergoing resection for suspected BTC with benign tumors on postoperative histopathology, as well as patients with confirmed BTC found unresectable at surgical exploration, were also included as controls. The study was approved by the Regional Ethical Review Board of Stockholm and conducted in accordance with Good Clinical Practice and the Declaration of Helsinki. All patients included in the biobank provided written informed consent. The study was reported in accordance with the REMARK guidelines for prognostic studies (13), with the REMARK checklist presented in Supplementary Table 1. Analysis of tumor tissue expression of candidate prognostic markers and corresponding receptors/ligands was performed with gene expression data from independent and public cohorts of BTC patients, including patients from different geographic regions.

2.2 Sample size calculation

With two-sided $p<0.05$ and a power of 80%, a minimal sample size of n=88 was estimated as necessary to identify a prognostic marker with a hazard ratio of 2.0, assuming a median follow-up of 4 years, a yearly censoring ratio of 10 percent and a median overall survival of 24 months for unexposed patients (12, 14).

2.3 Patient inclusion

One-hundred and seven patients operated with primary resection for BTC were selected for inclusion in the development and internal validation cohort: all resected pCCA patients with plasma samples available in biobank (resected confirmed pCCA n=47), and random samples from all patients operated for iCCA (resected confirmed iCCA n=28) and GBC (resected confirmed GBC n=32). Furthermore, 29 patients with confirmed BTC found unresectable on exploration and 32 patients resected on suspicion of BTC with a benign lesion on final postoperative histopathology were included. Two patients not operated with primary resection (one case of re-resection and one patient undergoing transplantation) were excluded from analysis, as well as seven patients where samples did not pass internal quality control for the proximity extension assay (resectable BTC n=5, unresectable BTC n=2). Finally, 102 resected patients with confirmed BTC, 27 patients with confirmed BTC found unresectable and 32 patients resected with a benign lesion on final postoperative histopathology were included for analysis. The study flow chart for BTC patients is presented in Figure 1.

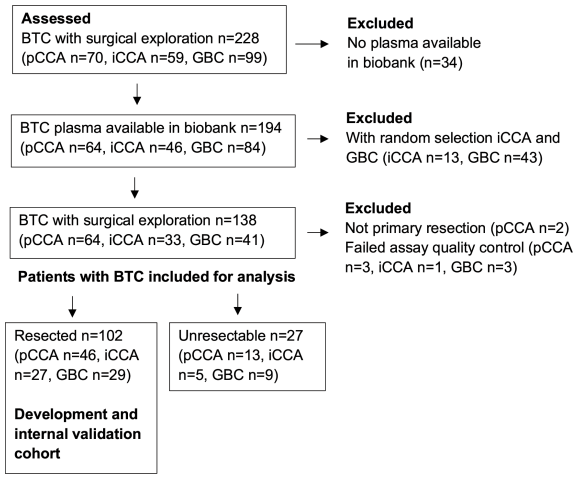

FIGURE 1
Study flow chart for the inclusion of patients with BTC. BTC, biliary tract cancer; GBC, galibladder cancer; iCCA, intrahepatic cholangiocarcinoma; pCCA, perihilar cholangiocarcinoma.

2.4 Sample preparation and multiplex immunoassay analysis

EDTA plasma samples were collected preoperatively at the day of surgery, centrifuged, aliquoted, frozen and stored at -80° Celsius. For Proximity Extension Assay-analysis (PEA), plasma samples were thawed on ice, and 20 microliters transferred to 96 well plates. PEA employs paired oligonucleotide coupled antibodies for detection of each analyte, with relative quantification of protein expression by polymerase chain reaction (PCR) (15). The full panel of analytes for the PEA (Immuno-Oncology I) is presented in Supplementary Table 2. Internal quality control of the immunoassay, extension and detection steps in each sample was performed with assay-specific protein-, antibody- and double stranded oligonucleotide controls respectively, while interplate control was performed with a set of 92 oligonucleotide duplexes. Relative quantification for each analyte by PEA was expressed as Normalized Protein Expression units (NPX) in Log2 scale, after normalization of PCR quantification cycle values for intra- and interassay variation using the detection and interplate controls. PEA analysis was performed at an institutional core facility (SciLifeLab, Clinical Biomarker Facility, Uppsala University, Uppsala, Sweden) blinded to all outcome data. The PEA has been validated for preserved analytical precision with hyperlipidemia and hyperbilirubinemia corresponding to 8-10 times upper reference values (16). No patient in the development and internal validation cohort underwent surgery with a bilirubin >190 micromoles/litre. The Immuno-Oncology I-panel has also been validated for interference of hemolysate in plasma, allowing up to 5-10% hemolysis of a sample for reliable detection of 84 of 92 proteins, while eight proteins in the panel were identified as more sensitive for interference by hemolysate (Adenosine deaminase, Arginase-1, Caspase-8, C-X-C-motif chemokine 11, Galectin-9, Granzyme-B, Granzyme-H and Interleukin-18) (16).

2.5 Outcome variables and clinicopathological data

The primary outcome was overall survival calculated from the date of surgery. Clinical data were retrospectively collected from quality registries and the electronic health record. Last follow-up was 11 Aug 2019. Demographic and clinicopathological variables collected were: age, sex, preoperative physical status classification according to the American Society of Anesthesiologists, diagnosis of primary sclerosing cholangitis, cirrhosis or diabetes, tumor extension stage, lymph node metastasis (N1), lymphovascular- and perineural invasion, microscopically tumor-positive resection margin (R1) and tumor differentiation (grade). Histopathological staging was reported according to the 7th edition of the AJCC/TNM guidelines and tumor grade according to the College of American Pathologists (17, 18).

2.6 Gene expression analyses

The following gene expression datasets were analyzed: GSE107943 (19), GSE138709 (20), GSE89749 (21), GSE26566 (22) (Gene Expression Omnibus), EGAD00001001693 (23) (European Genome-Phenome Archive, study ID: EGAS00001000950), E-MTAB-6389 (24) (ArrayExpress), OEP001105 (25) (Biosino), phs001404.v1.p1 (26) (dbGaP) and HRA000863 (27) (Genome Sequence Archive). Differential expression was analyzed using limma 3.50.0 (28) for microarray data and DESeq2 1.34.0 (29) for sequencing data. For single-cell RNA-sequencing data from HRA000863, raw BAM files were converted back to FASTQ format using the CellRanger 6.1.2 (30) *bamtofastq* command and read counts per gene per cell were obtained by CellRanger *count* (30). For processed expression data from GSE138709 and HRA000863, analysis was performed in R 4.1.1 with the Seurat 4.0.4 package (31). Data were normalized and scaled after filtering out cells with gene counts below 500 or greater than 3 000, as well as cells with a percentage of mitochondrial genes above 5. Data from different samples were then integrated by Harmony (32). For HRA000863 (27) and GES138709 (20) datasets, a total of 239 760 and 28 261 cells were clustered by principal component analysis and visualized with uniform manifold approximation and projection (UMAP), respectively. Clusters were annotated by mapping to references for immune cells according to CITE-seq data (31), annotation of malignant cells according to copy number variation (CNV) scores (with a cut off score of 3 for malignancy) calculated using InferCNV 1.8.1 (33), and by using cell markers for hepatocytes (not present in HRA000863), cholangiocytes, fibroblasts and endothelial cells (20). Differential expression of biomarkers between different cell types or between cells from tumor and periphery were tested using FindMarkers() with logfc.threshold and min.pct set to 0. Modelling of cytokine activities from single-cell transcriptome profiles were performed using the Cytokine Signaling Analyzer (CytoSig) v0.1 (34). Specifically, counts per gene were first converted to transcripts per million (TPM) and $\log_2$-transformed, and expression values

across all cells were mean centralized. Permutation tests were used to compare activity Z-scores obtained from Cytosig between tumor and periphery samples. That is, after obtaining the mean of Z-scores of a particular cell type for either tumor or periphery samples; that mean was compared to the mean of same number of cells randomly chosen (with replacement) from that cell type regardless of sample location. This process was repeated 10 000 times, and an empirical p-value was calculated as [10 000 - $N_{Mean\_real\ >Mean\_permutation}$]/ 10 000.

2.7 Statistical analysis

Statistical analyses were performed in R (R 3.5.3 and 4.1.1, R Foundation for Statistical Computing; RStudio 1.1.463, 1.4.1717 and 2021.09.0, RStudio Inc, Boston, USA), SPSS Statistics v25 and v28 (IBM, New York, USA) and Olink Insights Stat Analysis (Olink Proteomics, Uppsala, Sweden). Inclusion of iCCA and GBC patients was performed with random sampling from all consecutively operated iCCA and GBC patients respectively in SPSS. Imputation of missing data was used for independent variables included in regression analysis. For proteomics data, values below the limit of detection were imputed as left-censored data missing not at random by a quantile regression method (35). For other variables, multivariate imputation was performed (36). Demographic and clinicopathological characteristics at baseline were reported with unimputed data. Correlations among variables were assessed with Spearman's rank correlation, and visualized with heatmaps after hierarchical clustering according to the degree of correlation (37). For Cox regression analysis, the proportionality of hazards assumption was tested with scaled Schoenfeld residuals (38). To account for multiple comparisons in evaluation of univariable prognostic value, the Bonferroni-Holm corrected p-values were calculated and variables with an adjusted univariable p-value <0.20 were included in multivariable models. For variable selection in Cox regression modelling, backward elimination was applied with stopping criterion unadjusted p=0.157, equivalent to the Akaike information criterion (39). Differential protein expression between patient subgroups was analyzed by independent t-test, with corrected p-values according to the Benjamini-Hochberg method and illustrated with volcano plots. Additionally, non-parametric analysis was performed by Mann-Whitney U test.

The discriminatory ability of multivariable prognostic models was assessed with concordance indices (c-index) where a c-index of 0.50 would indicate no predictive ability and a c-index of 1.00 would indicate perfect predictive ability (40). The calibration of predictions for specified time points was assessed with calibration curves (40). To account for overfitting, internal validation of multivariable models by bootstrap resampling was performed (resamples n=600) (40). For survival analysis with Kaplan-Meier curves and Cox regression, SPSS and in R the survival and rms packages were used (38, 40). Survival curves were compared using the log-rank test. For survival analyses with gene expression data, patients were stratified into groups according to marker expression above/below the median. Significance tests were all two-sided and p-values <0.05 were considered statistically significant.

3 Results

Baseline characteristics and clinicopathological variables for the 102 included patients resected for BTC and 27 patients with unresectable BTC are presented in Table 1. There were 75 deaths during a median follow-up of 67 months (95% CI 55-79 months) among the 102 resected BTC patients, while all 27 patients found unresectable at exploration were followed to death. No patients were censored before 24 months after surgery. Median overall

TABLE 1 Demographic and clinicopathological characteristics of BTC patients.

Variable	BTC resected n=102	Missing data BTC resected	BTC unresectable n=27	Missing data BTC unresectable	p-value
Age Y, md (IQR)	66 (54-71)	–	65 (60-70)	–	0.81$
Sex F, n (%)	52 (51)	–	14 (52)	–	0.94
BMI, md (IQR)	25 (23-29)	–	24 (23-30)	–	0.94$
Diabetes, n (%)	13 (13)	–	5 (19)	–	0.53&
Cirrhosis, n (%)	5 (5)	–	2 (7)	–	0.64&
ASA≥3, n (%)	30 (29)	–	8 (30)	–	0.98
GPS≥1, n (%)	55 (54)	17	20 (74)	6	0.007*
PSC, n (%)	12 (12)	–	1 (4)	–	0.30&
PVE, n (%)	18 (18)	–	3 (11)	–	0.56&
BTC subgroup:					0.68
pCCA, n (%)	46 (45)	–	13 (48)	–	

(Continued)

TABLE 1 Continued

Variable	BTC resected n=102	Missing data BTC resected	BTC unresectable n=27	Missing data BTC unresectable	p-value
iCCA, n (%)	27 (27)	–	5 (19)	–	
GBC, n (%)	29 (28)	–	9 (33)	–	
Major resection, n (%)#	73 (72)	–			
CD≥3, n (%)#	47 (46)	–			
Postoperative mortality, n (%)#	10 (10)	–			
T≥3, n (%)#	45 (44)	1			
N1, n (%)#	49 (48)	12			
Pn1, n (%)#	73 (72)	7			
LV1, n (%)#	77 (75)	7			
R1, n (%)#	65 (64)	2			
Grade≥2, n (%)#	79 (77)	9			

ASA, American Society of Anesthesiologists; BMI, body mass index; BTC, biliary tract cancer; CD, Clavien-Dindo complication grade; F, female; GBC, gallbladder cancer; GPS, Glasgow prognostic score; iCCA, intrahepatic cholangiocarcinoma; IQR, interquartile range; LV1, lymphovascular invasion; md, median; N1, lymph node metastasis; pCCA, perihilar cholangiocarcinoma; Pn1, perineural invasion; Postoperative mortality, in-hospital postoperative mortality (not limited to 90 days). PSC, primary sclerosing cholangitis; PVE, portal vein embolization; R1, microscopically tumor positive resection margin; T, tumor extension; Y, years.
#: Reported for resected patients; $: Mann-Whitney U; &: Fisher Exact test; * p<0.05.

survival was 20 months (95% CI 16-24 months) for all BTC patients, 23 months for resected patients (95% CI 17-29 months) and 7 months for unresectable patients (95% CI 0-14 months).

3.1 Analysis of plasma protein expression

Of the 92 proteins analyzed by PEA, 14 proteins were not detected in >75% of samples. A list of the 78 proteins included for further analysis is presented in Supplementary Table 3. No proteins were differentially expressed between resected and unresectable BTC patients (Supplementary Table 4).

To illustrate correlation of expression and identify non-redundant candidate markers, all proteins analyzed in BTC patients were grouped by hierarchical clustering, according to the degree of correlation. Two main clusters were formed (Figure 2; Supplementary Table 5), with the larger cluster subdivided into three subgroups. The smaller main cluster (cluster 1) contained three proteins related to the external induction of apoptosis, together with VEGFR2. The larger main cluster (cluster 2) contained proteins including effector molecules, chemokines, mitogens and other regulators of immune cell proliferation and differentiation.

The correlation of the plasma proteins with other clinicopathological variables and established prognostic factors was also evaluated and is illustrated in Supplementary Figure 1. Demographic and clinicopathological variables (age, sex, tumor stage, lymph node metastasis, perineural invasion, lympho-vascular invasion, tumor grade) were not internally strongly correlated, with the strongest correlation found between tumor stage and tumor grade (r = 0.37) and between lympho-vascular and perineural invasion (r = 0.27). The strongest correlation between demographic/clinicopathological variables and plasma proteins analyzed by PEA was seen between age and Pleiotrophin (PTN, r = 0.59).

3.2 Uni- and multivariable survival analysis

Association of the 78 proteins with overall survival after resection surgery was investigated by univariable Cox regression analysis (Supplementary Table 6). Six proteins were found to be associated to overall survival with univariable adjusted p-value <0.20 (unadjusted p-value <0.005) and are presented in Table 2 and with Kaplan-Meier curves in Supplementary Figure 2.

The protein with a positive association to survival was located in cluster 1 (TRAIL/TNFSF10, death receptor ligand, one of the effector mechanisms of macrophages and NK-cells), and five proteins with a negative association were located in two subgroups of cluster 2 (TNFSF14, an effector and regulator of T-cell activity; CSF1/M-CSF, a regulator of monocyte proliferation, differentiation and function; IL6, inducer of acute phase response and regulator of lymphocyte and monocyte differentiation; IL8, chemotactic for neutrophils, basophils and T-cells; and TIE2/TEK, angiopoietin receptor and a regulator of angiogenesis). The six proteins associated with overall survival were included in multivariable analysis (events per variable 75/6 = 12.5) with three proteins selected by backward elimination (Table 2), representing separate clusters/subgroups in the hierarchical clustering analysis (TRAIL: cluster 1, CSF and TIE2: separate subgroups cluster 2).

10.3389/fonc.2023.1169537

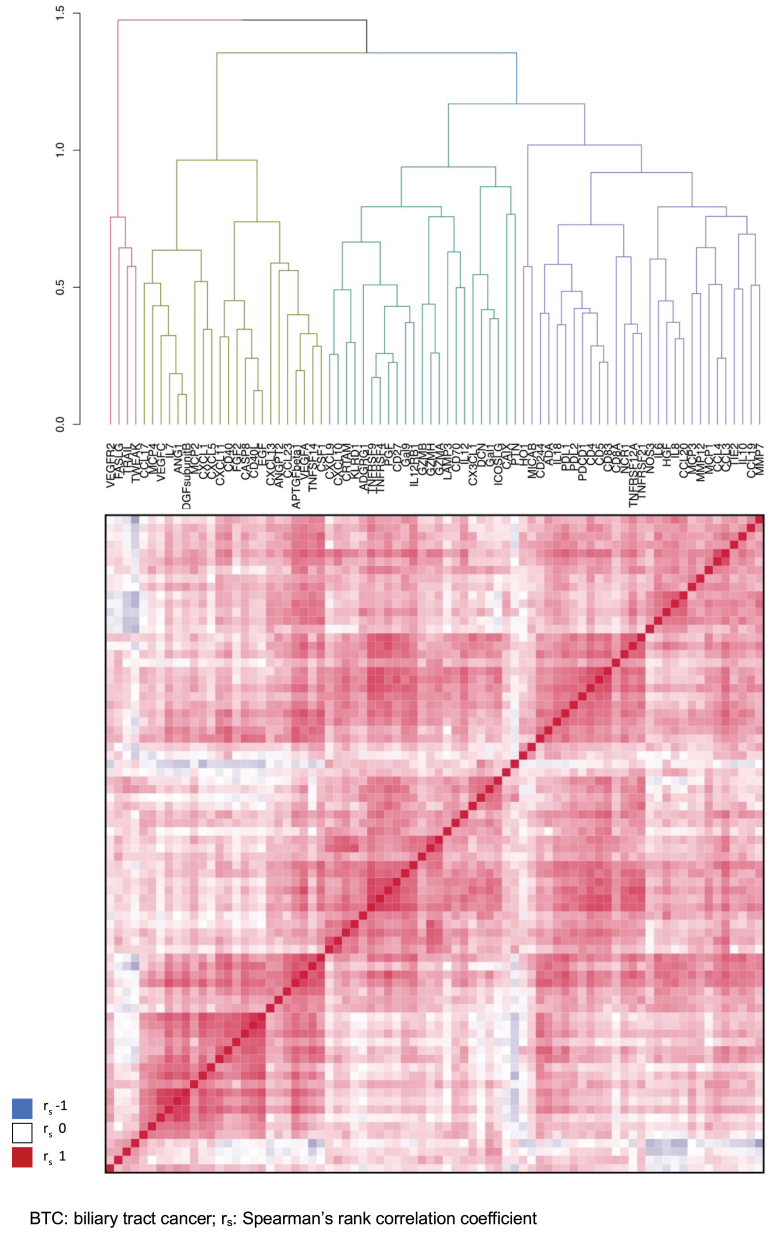

FIGURE 2
Correlation matrix for the expression of 78 proteins in plasma of patients with BTC, hierarchically clustered. BTC, biliary tract cancer; rs: Spearman's rank correlation coefficient.

3.3 Discrimination of pre- and postoperative prognostic models

The discriminatory ability of the three preoperative candidate markers TRAIL, CSF1 and TIE2 for overall survival after resection was assessed with a c-index of 0.71 for the three markers combined. C-indices for the separate markers were 0.61, 0.65 and 0.63 for TRAIL, CSF1 and TIE2 respectively. The prognostic ability of postoperative pathology (T-stage, N-status, perineural invasion, lympho-vascular invasion, tumor grade, resection margin) was assessed with a c-index of 0.70. Adding the three preoperative candidate markers to a combined model with postoperative pathology increased the c-index to 0.74. Internal validation of the prognostic value was performed with bootstrap correction, where the corrected c-index for the three preoperative candidate markers was 0.70, while the corrected c-index for postoperative pathology was 0.66. The corrected c-index for a model with the three preoperative candidate markers added to postoperative pathology was 0.72.

A validated preoperative prognostic factor, Glasgow prognostic score (GPS, calculated from albumin and CRP concentrations: CRP>10 mg/L or albumin<35 g/L = 1 point each), was analyzed with a corrected c-index of 0.65. In the analysis of correlation of plasma protein expression and other clinicopathological/prognostic variables, there was a moderate correlation between GPS and CSF1 (r=0.49) and between GPS and TIE2 (r=0.42), where GPS and TIE2 grouped together in hierarchical clustering (Supplementary Figure 1).

TABLE 2 Uni- and multivariable Cox regression analyses (resected BTC n=102).

Variable	Univariable HR (95% CI)	p-value unadjusted (adjusted)	Multivariable HR (95% CI)	p-value all	Multivariable HR (95% CI) selected	p-value selected
TRAIL	0.35 (0.18-0.67)	<0.001* (0.096)$	0.29 (0.14-0.59)	<0.001*	0.30 (0.16-0.56)	<0.001*
TNFSF14	1.84 (1.33-2.54)	<0.001* (0.015)*	1.13 (0.71-1.78)	0.61		
CSF1	6.52 (2.42-17.54)	<0.001* (0.013)*	4.04 (1.03-15.81)	0.045*	4.02 (1.40-11.59)	0.010*
IL6	1.31 (1.10-1.56)	0.003* (0.15)$	0.92 (0.72-1.20)	0.55		
IL8	1.34 (1.13-1.59)	<0.001* (0.056)$	1.00 (0.77-1.30)	0.98		
TIE2	4.33 (1.97-9.51)	<0.001* (0.016)*	2.82 (1.09-7.32)	0.033*	2.78 (1.20-6.48)	0.018*

BTC, biliary tract cancer; CSF1, colony-stimulating factor 1; IL6, interleukin 6; IL8, interleukin 8; CI, confidence interval; HR, hazard ratio; TIE2, tyrosine kinase with immunoglobulin-like and EGF-like domains 2; TRAIL, TNF-related apoptosis-inducing ligand.
* p<0.05; $ p<0.20.

A preoperative prognostic model including the three candidate markers together with the GPS was assessed with a c-index of 0.71, and a bootstrap corrected c-index of 0.69. A postoperative prognostic model including pathological variables together with GPS was assessed with c-index 0.75, and corrected c-index of 0.71. Multivariable models including both pre- and postoperative factors are presented in Supplementary Table 7.

3.4 Calibration of preoperative prognostic markers

The calibration of a preoperative prognostic model with the three candidate markers TRAIL, CSF1 and TIE2 was assessed for one-, three- and five-year overall survival, as illustrated with calibration plots in Supplementary Figure 3 (bootstrap corrected preoperative models indicated by the blue lines, uncorrected models indicated by the black lines). Actual survival at one year was lower than predicted by the preoperative model (Supplementary Figure 3A), while at three years and five years the model underestimated survival predicted below 60% and 40% respectively (Supplementary Figures 3B, C).

3.5 Subgroup analyses and internal validation of disease specific prognostic models

The prognostic value of the three identified plasma markers within each BTC subgroup (iCCA, pCCA and GBC) was further analyzed (Supplementary Table 8). For the iCCA group, TRAIL and CSF1 retained prognostic value while TIE2 (p=0.52) did not. For the pCCA group, TRAIL was a significant prognostic factor while TIE2 (p=0.05) and CSF1 (p=0.17) were not. For gallbladder cancer, CSF1 and TIE2 but not TRAIL (p=0.15), remained prognostic.

The prognostic performance of three disease-specific preoperative prognostic models including GPS was evaluated with bootstrap correction to account for overfitting. The corrected c-indices for models specific for iCCA (TRAIL, CSF1, GPS), pCCA (TRAIL, TIE2, GPS) and GBC (CSF1, TIE2) were 0.78 (uncorrected 0.80), 0.65 (uncorrected 0.68) and 0.74 (uncorrected 0.75) respectively. A cholangiocarcinoma-specific (iCCA + pCCA) prognostic model with only TRAIL and GPS had a c-index of 0.69 (uncorrected 0.69).

3.6 Comparison of plasma protein expression in BTC and benign controls

The differential expression of plasma proteins between BTC patients and patients with benign histopathology after resection for suspected BTC was analyzed, with expression levels of 25 proteins significantly higher and with no proteins showing lower expression in patients with BTC (Supplementary Table 9; Supplementary Figure 4). CSF1 and TIE2, but not TRAIL, was higher in patients with malignancy. Excluding TRAIL from the preoperative prognostic model for patients with BTC did not improve discrimination (c-index 0.65, bootstrap corrected c-index 0.64).

The five proteins found with higher levels of expression in malignancy and with the most statistically significant difference compared to patients with benign lesions were IL6, PGF, CSF1, MMP12 and HGF, with a significant difference also on non-parametric testing (PGF, CSF1, MMP12: p<0.001; IL6, HGF: p=0.004). There was a considerable overlap in expression levels for these proteins between the benign group and the BTC group (Supplementary Figure 5A). CSF1, PGF and MMP12 had the highest area under the receiver operating curve values for predicting malignancy (all: AUROC=0.69), with CSF1 and PGF showing slightly better performance according to precision-recall curve analysis (Supplementary Figure 5B).

3.7 Analysis of tumor tissue-specific expression of plasma markers and receptors/ligands

The tumor tissue-specific expression of the three identified plasma markers and their respective receptors (*CSF1*: *CSF1-R*; *TRAIL*: *TRAIL-R1/TNFRSF10A*, *TRAIL-R2/TNFRSF10B*, *TRAIL-R3/TNFRSF10C* and *TRAIL-R4/TNFRSF10D*) or ligands (*TIE2/TEK*: *ANGPT1*, *ANGPT2* and *ANGPT4*) was then analyzed with gene expression data from two external surgical CCA cohorts with samples included from both tumor and normal surrounding liver: GSE107943 published by Ahn et al. (19) (Korea, sequencing, n=30, iCCA, hepatitis B/C 13%, recurrence and survival data with median follow-up 30.5 months) and GSE26566 published by Andersen et al. (22) (USA, Belgium and Australia, microarray, matched samples n=58, iCCA and pCCA) (Figure 3).

Seven out of the 11 genes analyzed were differentially expressed in tumor compared to surrounding liver in the GSE107943 dataset, and expression levels of three of the same seven proteins were likewise higher (*TRAIL-R1/TNFRSF10A*, *ANGPT2*) or lower (*TIE2/TEK*) in tumors in the GSE26566 dataset (Figure 3).

3.8 Cell type-specific expression of markers and receptors/ligands in tumor tissue

By interrogation of single-cell gene expression data for iCCA in two datasets, published by Song et al. (27) (China, tumor samples n=14 [from patients n=14]/surrounding non-tumor liver samples n=14, hepatitis B 29%) and Zhang et al. (20) (China, tumor samples n=5 [from patients n=4]/surrounding non-tumor liver samples n=3, hepatitis B 50%), the cell type-specific expression of markers and their receptors or ligands was examined (Figure 4; Supplementary Tables 10–14).

In both datasets, expression of *TRAIL* and *TRAIL-R1/TNFRSF10A* was higher in malignant cells, compared to the average of other cell types in tumor and surrounding liver tissue (Supplementary Tables 11, 12). *TRAIL* was similarly highly expressed by monocytes, T-cells, cholangiocytes and endothelial cells (Figure 4A; Supplementary Table 10). Expression of *TRAIL-R2/TNFRSF10B* and *TRAIL-R4/TNFRSF10D* was significantly higher in endothelial cells compared to the average of other cell types (Figure 4A; Supplementary Tables 10–12). *TRAIL-R2/TNFRSF10B* was expressed by a large fraction of the malignant cells (Song et al: 26.3%, Zhang et al: 26.1%), and at higher average levels than the other *TRAIL* receptors (Supplementary Tables 10–12).

TIE2/TEK was mainly expressed by endothelial cells and *TIE2/TEK* ligands *ANGPT1* and *ANGPT2* were mainly expressed by fibroblasts (Supplementary Tables 10–12). *CSF1* was most highly expressed by T-cells, NK-cells, fibroblasts and endothelial cells. When comparing intratumoral immune cells to the same immune cell type in surrounding liver, *TRAIL* expression was higher in intratumoral CD8+ T-cells, but significantly lower in intratumoral macrophages compared to macrophages outside of the tumor (Figure 5; Supplementary Tables 13, 14). Expression of *CSF1* was significantly higher in intratumoral CD8+/CD4+ T-cells and NK-cells compared with T-cells and NK-cells in surrounding liver.

Comparing the cytokine activities of intra- and peritumoral immune cells in the larger Song et al. dataset, CSF1 activity was generally increased intratumorally, while TRAIL activity was generally decreased (Figure 4B). The highest immune cell CSF1 activity was seen in intratumoral macrophages, while the highest TRAIL activity was seen in peritumoral T-cells. The TRAIL activity in tumor cells and intratumoral cholangiocytes was higher compared to peritumoral cholangiocytes.

Similarly, in the Zhang et al. dataset, the highest immune cell CSF1 activity was seen in intratumoral macrophages, while the highest TRAIL activity in immune cells was seen in peritumoral T-cells (Supplementary Figure 6). In both single-cell datasets, the

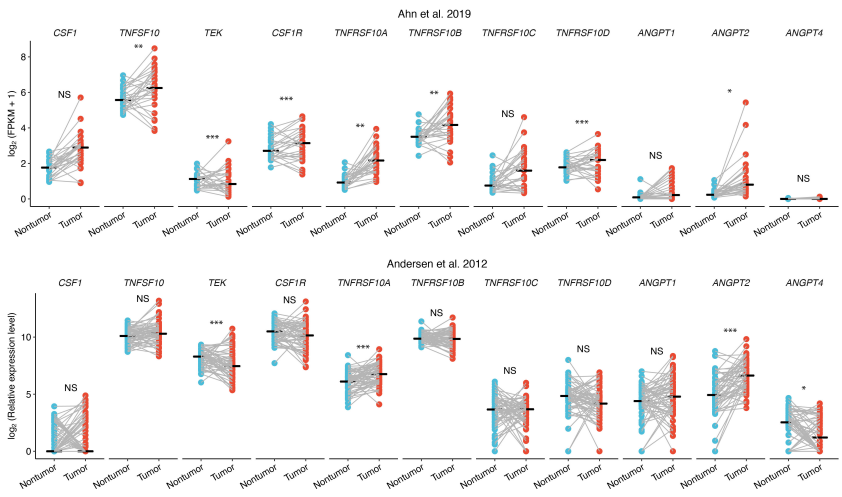

FIGURE 3
Differential gene expression of markers and ligands/receptors in CCA tissue, tumor tissue (red) and surrounding liver (blue). NS, not significant; * adjusted p<0.05; ** adjusted p<0.01; *** adjusted p<0.001.

10.3389/fonc.2023.1169537

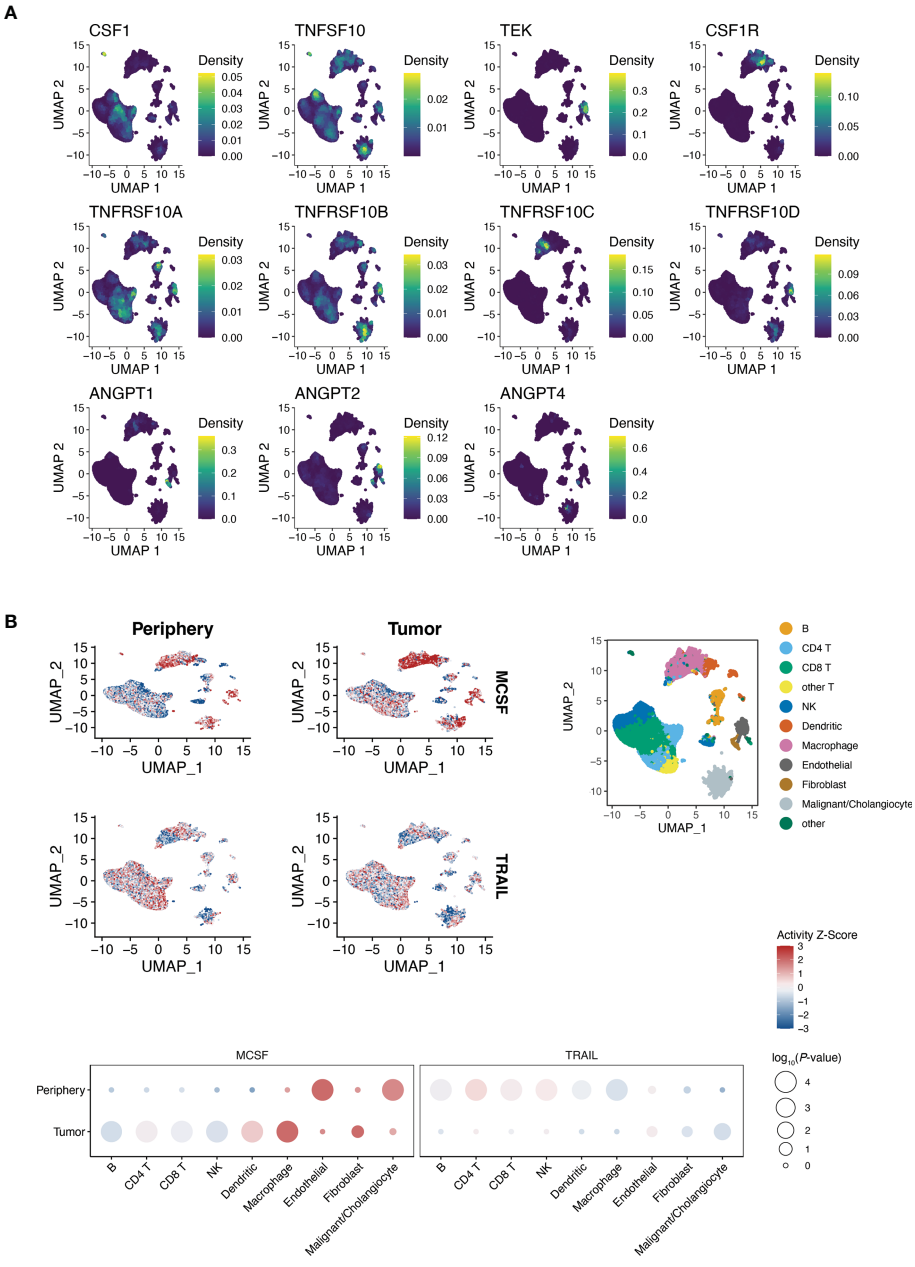

FIGURE 4
(A, B) Single-cell gene expression of markers and receptors/ligands in iCCA (Song et al. (27)), clusters by cell type (right top panel **B**). **(B)** Cytokine activity intratumorally vs. peritumorally. Activity Z-scores trimmed to [-3, 3] to facilitate visualization. P-values in balloon plots calculated by permutation tests (see Patients and methods).

highest non-immune cell tumor stroma TRAIL activity was seen in endothelial cells.

3.9 Prognostic influence of tumor tissue expression of markers and receptors/ligands

The prognostic influence of tumor tissue expression of the identified markers and their receptors or ligands was analyzed using recurrence and survival data available for the GSE107943 dataset (19) (Figure 6, disease-free survival 6A, overall survival 6B; Supplementary Figure 7). Expression levels of three receptors (*CSF1-R* p=0.02, *TRAIL-R2/TNFRSF10B* p=0.02, *TRAIL-R4/TNFRSF10D* p=0.02) were associated to disease-free survival, while no significant association was seen to overall survival for these genes (*CSF1-R* p=0.19, *TRAIL-R2/TNFRSF10B* p=0.52, *TRAIL-R4/TNFRSF10D* p=0.08). Survival analyses according to expression of the remaining receptors and ligands are presented in Supplementary Figure 7 (disease-free survival 7A, overall survival

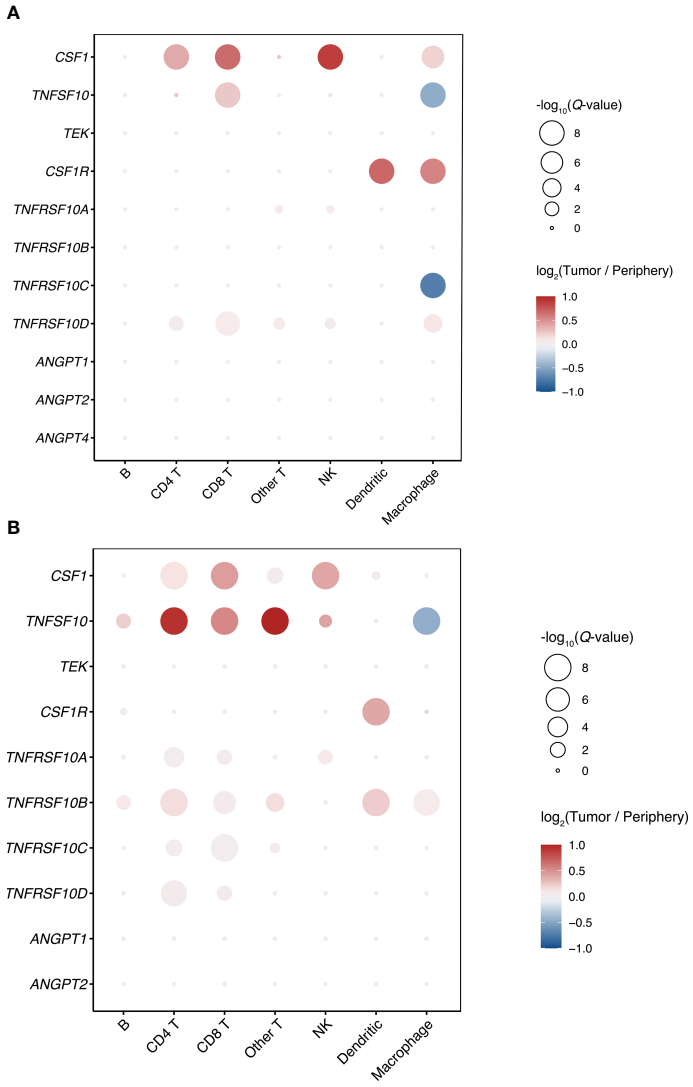

FIGURE 5
Differences in gene expression of markers and receptors/ligands between intratumoral and peritumoral immune cells in iCCA. **(A)** Song et al. (27) **(B)** Zhang et al. (20).

7B). The disease-free and overall survival curves stratified according to expression of *TRAIL-R1*/*TNFRSF10A* did not reach statistical significance (disease-free survival p=0.08, overall survival 0.07). While *CSF1-R* was negatively associated to disease-free survival, expression of *TRAIL-R2*/*TNFRSF10B* and *TRAIL-R4*/*TNFRSF10D* was positively associated to disease-free survival.

For further investigation of BTC tumor tissue expression and the possible prognostic influence in a wider setting, gene expression data from six additional cohorts was interrogated. Three datasets represented diverse iCCA cohorts, from Japan (23) (Nakamura et al, RNA sequencing, n=112, hepatitis B 5%, hepatitis C 3%), France (24) (Job et al, n=72, microarray, hepatitis B 5%, hepatitis C 3%) and China (25) (Dong et al, RNA sequencing, n=224, alpha-fetoprotein [AFP] ≥21ng/ml 10%, hepatitis B 27%). Two datasets represented multinational mixed cholangiocarcinoma cohorts: Jusakul et al. (21) (Singapore, Thailand, South Korea, Romania, France, Brazil; microarray, iCCA/pCCA/distal CCA/extrahepatic CCA, n=115, fluke positive 43%, hepatitis B 8%, hepatitis C 3%) and Andersen et al. (22) (Australia, Belgium, France, Germany, Italy, USA, microarray, iCCA/pCCA, expanded cohort n=178, hepatitis C 4%). One dataset, from Nepal et al. (26), represented a multinational GBC cohort (China, Chile; RNA sequencing, n=44, hepatitis B 4%). While the indicated positive prognostic value for disease-free survival of *TRAIL-R* expression in iCCA tumor tissue in the Ahn et al. cohort was supported by overall survival data from the Job et al. cohort (*TRAIL-R1*/*TNFSFR10A* p=0.03, *TRAIL-R2*/*TNFSFR10B* p=0.16, *TRAIL-R4*/*TNFSFR10D* p=0.006), such an association was not seen in the cohorts from Nakamura et al. or Dong et al. (Supplementary Figure 8). In the later cohort instead, a negative association to overall survival was seen for *TRAIL-R1*/

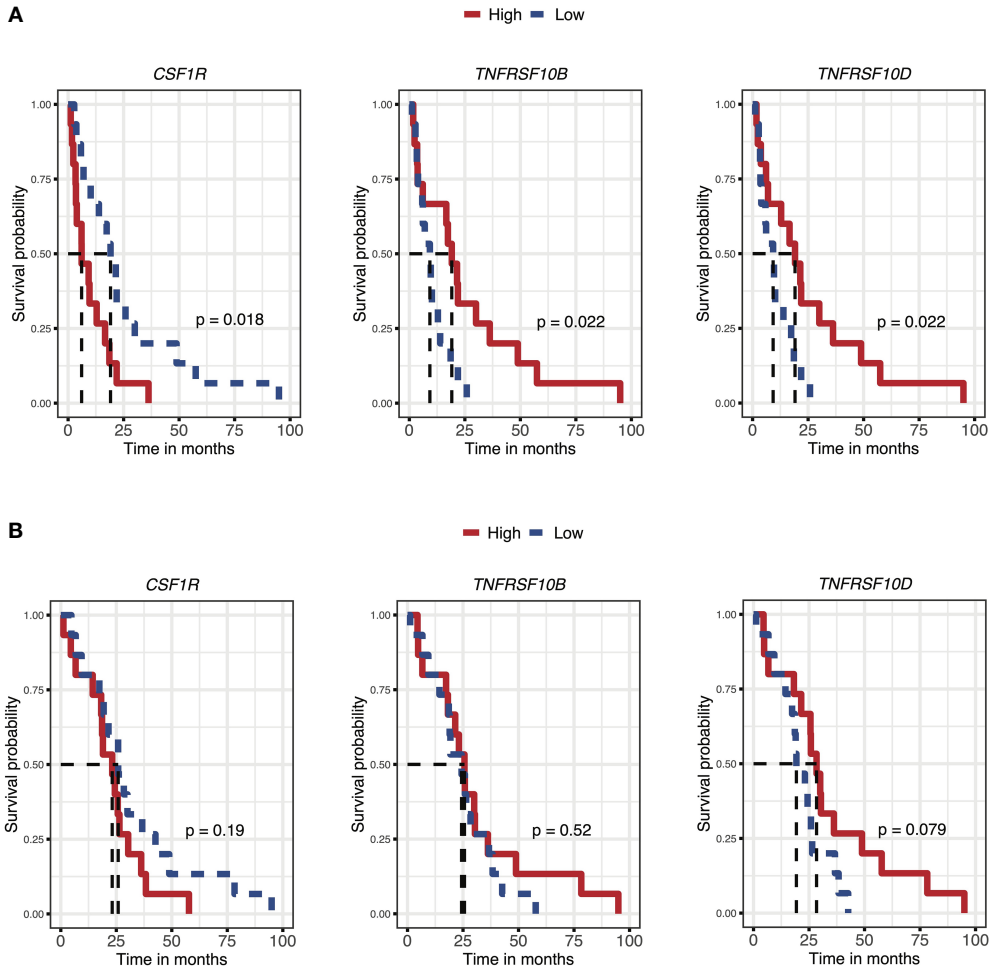

FIGURE 6
Prognostic influence of iCCA tumor tissue gene expression of markers and receptors/ligands, for disease-free survival **(A)** and overall survival **(B)** (Ahn et al. (19)).

TNFSFR10A (p=0.005) and *TRAIL-R4/TNFSFR10D* (p=0.04). A negative prognostic value was seen for tumor tissue *CSF1* expression only in the cohort from Nakamura et al. (p=0.047). No other associations to survival were seen.

4 Discussion

Long term survival outcomes for patients undergoing resection for BTC remain poor, with a median overall survival of approximately two to four years. While multimodal therapy is under current development, prognostic factors to allow preoperative risk stratification and development of better tailored treatments remain ill-defined.

In a previous study, general inflammatory markers were validated as preoperative prognostic factors (12). The present analysis, of samples from a unique prospectively collected biobank, was therefore aimed at identifying more specific immunologic prognostic markers and to better characterize immune responses in BTC.

By means of a high-throughput multiplexed immunoassay three candidate preoperative plasma markers were identified, with a combined prognostic value for survival similar to that of established postoperative pathology. TRAIL/TNFSF10 was identified as a positive prognostic factor in both iCCA and pCCA. CSF1/M-CSF was identified as a negative prognostic factor in iCCA and GBC. TIE2/TEK was identified as a significant negative prognostic factor in GBC.

To clarify the tumor-specific expression of the identified prognostic markers and receptors or ligands, analyses were performed across four separate datasets investigating BTC tissues and surrounding liver by means of microarray, next-generation sequencing and single-cell sequencing. Over all three platforms and in demographically diverse cohorts, higher *TRAIL-R1/TNFSFR10A* was seen in tumor tissue/cholangiocarcinoma cells. With single-cell analysis of iCCA tissues from two separate cohorts, higher *TRAIL-R1/TNFRSF10A* expression was seen specifically in malignant cells. The ligand *TRAIL/TNFSF10* was expressed by intratumoral T-cells, B-cells, NK-cells, monocytes, malignant cells, normal cholangiocytes and endothelial cells. The expression of *TRAIL/TNFSF10* was higher in intratumoral CD8+ T-cells as compared to

CD8+ T-cells in surrounding tissue, but decreased in intratumoral macrophages. *CSF1/M-CSF* was expressed by T-cells, NK-cells, fibroblasts and endothelial cells. This altogether suggests a possible important role of a T-cell-/NK-cell/monocyte-mediated TRAIL-R1/TNFRSF10A-dependent anti-tumor activity in cholangiocarcinoma. While tumor infiltrating monocytes exhibited higher CSF1/M-CSF activity compared to peritumoral monocytes, they had lower *TRAIL/TNFSF10* expression. The strong negative prognostic value of the macrophage colony-stimulating factor CSF1/M-CSF in iCCA, with higher expression shown specifically in iCCA tumor-infiltrating T-cells, furthermore, implicates tumor associated macrophages as important actors in the promotion of tumor progression (24, 41). Additionally, an interplay between inflammatory factors and a local tumor promoting environment has been described in BTC (42, 43), with a role of myeloid-derived suppressor cells (41, 43). Finally, an anti-tumor activity of TRAIL/TNFSF10 in cholangiocarcinoma can also rely on additional mechanisms, namely activation of other TRAIL receptors than TRAIL-R1/TNFRSF10A, and targeting of other tumor promoting cells than just the tumor cells (44). In single cell analysis of iCCA, *TRAIL-R2/TNFRSF10B* was most highly expressed by endothelial cells but also expressed by tumor cells, immune cells, fibroblasts and cholangiocytes. A recent investigation of the iCCA T-cell and myeloid compartments exhibited agonistic TRAIL/TNFSF10 signaling as one significant interaction between regulatory T-cells and myeloid cells, where the TRAIL/TNFSF10-TRAIL-R2/TNFRSF10B interaction was most pronounced for dendritic cells (45). TRAIL-stimulation via TRAIL-R2/TNFRSF10B has been proposed to induce dendritic cell maturation rather than apoptosis (46). In both of the single-cell cohorts reported here, dendritic cells were the immune cells with the highest expression of *TRAIL-R2/TNFRSF10B*.

Further investigating the role of TRAIL in cholangiocarcinoma tumor tissue, there was an indication of a positive prognostic value in tissue expression of both *TRAIL-R2/TNFRSF10B* and *TRAIL-R4/TNFRSF10D* with a significant association to disease-free survival in the cohort from Ahn et al. (19) (GSE107943). This was furthermore supported by analysis of the cohort from Job et al. (24) (E-MTAB-6389) where *TRAIL-R1/TNFRSF10A* and *TRAIL-R4/TNFRSF10D* were significantly associated to overall survival. No association of *TRAIL-R* expression with survival was seen in the third iCCA cohort from Nakamura et al. (23), or in the mixed CCA cohorts from Andersen et al. (22) (GSE26566) and Jusakul et al. (21) (GSE89749). While disease-free survival was better for patients with high *TRAIL-R2/TNFRSF10B* and *TRAIL-R4/TNFRSF10D*, no significant association was seen between *TRAIL-R* expression and overall survival in the GSE107943 cohort from Ahn et al, possibly reflecting the low number of events and limited follow-up for the overall survival outcome (deaths = 17, median follow-up 30.5 months) (19).

In one iCCA cohort, the OEP001105 dataset reported by Dong et al. (25), *TRAIL-R* expression was instead negatively associated with survival. It has been established that cancer cells including CCA cell lines can develop resistance to TRAIL-induced apoptosis (47), with TRAIL-signaling instead contrarily inducing a tumor promoting inflammatory secretome, suggested to affect the tumor microenvironment (48). Underlying differences in tumor etiology and biology between the different investigated iCCA cohorts could also be one explanation to discrepancies in prognostic implications. Notably, in the Dong et al. cohort, the prevalence of underlying viral hepatitis was above 25% and approximately 10 percent of patients had a preoperative plasma AFP above 20 ng/mL (25). This AFP level has been used by a previous study as a cut off to exclude patients with possible mixed hepatocellular carcinoma-cholangiocarcinoma (HCC-CCA) (49). In the cohorts reported by Ahn et al. (19) (GSE107943) and Job et al. (24) (E-MTAB-6389) patients with HCC-CCA were excluded. It has been suggested that HCC cells can show considerable resistance to TRAIL-induced apoptosis (50), whereas no reports on this matter specific for HCC-CCA were found.

TRAIL-R4/TNFSRF10D, with a truncated intracellular death domain, can act as a decoy and antagonistic TRAIL receptor. However, in data from three cohorts, tumor tissue expression of *TRAIL-R4/TNFRSF10D* showed a similar prognostic influence as expression of the agonistic TRAIL receptors *TRAIL-R1/TNFRSF10A* and *TRAIL-R2/TNFRSF10B*: a congruent positive association to disease-free survival or overall survival in two cohorts, and to negative survival in one cohort. Distinctive TRAIL-signal responses in different cell types could be one possible explanation to such associations. As was the case with *TRAIL-R2/TNFRSF10B*, the highest *TRAIL-R4/TNFRSF10D* expression in iCCA was noted in endothelial cells.

Plasma TIE2/TEK, the angiopoietin receptor, was a strong negative prognostic factor for survival specifically in the GBC subgroup. Plasma TIE2 has been investigated as a biomarker during treatment with VEGFR inhibitor in advanced BTC (51). In the tumor micro-environment of several cancers, a subset of TIE2-expressing tumor associated macrophages has been described, with proangiogenic activity and negative prognostic value (52), implicating the interplay between tumor associated macrophages and angiogenesis as a possible therapeutic target (53). In an analysis of TIE2-expressing tumor associated macrophages in pCCA, a positive association to survival was instead found (54). As opposed to some other types of highly vascularized malignancies, CCA tissues can be characterized by a dense fibrous stroma (4, 54). Whereas VEGFR inhibition alone has failed to show improved outcomes in BTC, a targeted combined inhibition of VEGFR and TIE2 recently showed a significant effect on progression-free survival of BTC in a phase two randomized control trial (55). Importantly, the vascular endothelium can have several roles, not only with regards to tumor angiogenesis but also in the regulation of immune cell infiltration and itself acting as a regulator of immune cell function (56).

While prognostic associations of soluble factors in plasma may reflect mechanistic processes in tumor and peritumoral tissue, it is also possible that the plasma protein profile reflects a systemic host response to malignancy or concurrent inflammatory conditions. Two of the identified prognostic markers, CSF1/M-CSF and TIE2/TEK, were differentially expressed in malignancy compared to benign controls. This was also the case with IL6, which in this study showed a univariable association to survival in resected patients and previously has been validated as a prognostic factor

in advanced BTC (11), with mixed previous reports on possible diagnostic value (57, 58). Levels of differentially expressed proteins overlapped between the malignant and benign groups, with predictive value for the highest expression levels, but low sensitivity. While beyond the scope of this study, the possible diagnostic value of CSF1/M-CSF and PGF in combination with other factors should be investigated in specialized diagnostic studies. To clarify the role of infiltrating immune cells and the tumor microenvironment on one hand, and the systemic inflammatory response in BTC on the other, further analyses of CCA and GBC tissue, including single-cell and spatial transcriptomics and histopathology, are motivated. That no proteins were significantly differentially expressed between patients undergoing resection and patients with unresectable tumors could reflect that patients with resectable (localized) and unresectable (advanced/metastasized) tumors represent a spectrum of disease rather than clear-cut separated categories. Indeed, in pancreatic cancer, a malignancy with similarly poor long-term prognosis, patients with localized tumors undergoing resection have been found to harbor distant micrometastases (59, 60). Secondly, the small sample-size with only 27 patients with unresectable tumors limited the statistical power of this study to detect a significant difference in expression between patients with resectable and unresectable BTC.

An important strength of the current study was a dedicated prospective research biobank allowing the inclusion of a comparatively large cohort of patients resected for BTC, a group of rare cancers most often diagnosed at an unresectable stage. Furthermore, patients were followed for a median time of more than five years after surgery, allowing an accurate analysis of long-term survival. Other strengths include the method for relative quantification of protein expression by multiplexed immunoassay with strong internal quality controls minimizing variability. Finally, the findings from the plasma biomarker screening were put in a comprehensive context with analysis of tissue gene expression for markers and receptors/ligands in both tumor and surrounding liver tissue from patients with BTC in demographically varied cohorts.

The study also had several important limitations. Firstly, the sample size was limited and calculated to allow the identification of a prognostic marker for patients with BTC of any subtype. With differences in prognostic value seen between BTC subgroups, most importantly for TIE2, a larger sample size would have permitted further analyses and reduced the risk of error and overfitting. While inclusion and sample collection in the biobank were prospective, collection of clinical follow-up data was retrospective, and no further postoperative biobank samples were included in the protocol precluding analysis of temporal dynamics in biomarker expression. Furthermore, while prognostic associations for the bulk tissue expression of markers and receptors/ligands in external cohorts was studied in all subgroups of BTC, single cell analysis was limited to the iCCA subgroup.

In conclusion, with this analysis of a unique prospectively collected biobank three preoperative prognostic factors could be identified in plasma from patients with BTC, with plasma TRAIL/TNFSF10 determined as a novel positive prognostic factor in both iCCA and pCCA. With subgroup analyses and interrogation of external cohorts, the heterogeneity both between and within BTC subgroups was underscored, a factor of vital importance when developing future targeted treatments. A negative prognostic value of plasma CSF1/M-CSF was seen in iCCA and GBC, further implicating tumor-associated macrophages and the interplay between inflammatory activity and tumor progression as a possible therapeutic target in BTC. TRAIL and CSF1, both prognostic factors in iCCA, exhibited marked differences in expression and activity between intratumoral and peritumoral immune cells on single-cell analysis. The negative prognostic value of plasma TIE2/TEK in GBC mandates further investigation of proangiogenic and inflammatory activity in GBC tumor tissue. Validation of predictive value in external and prospective cohorts will be the next step in the development of disease-specific preoperative prognostic models for patients with BTC.

Data availability statement

The raw data supporting the conclusions of this article will be made available by the authors, without undue reservation.

Ethics statement

This study involving human participants was reviewed and approved by the Regional Ethical Review Board of Stockholm. All patients included in the biobank provided their written informed consent.

Author contributions

Conceptualization: HJ, MC, CS, NB, ES. Methodology: all authors. Investigation: HJ, MC, DS, IF, CO'R, JA, NB, ES. Writing – original draft: HJ, DS, MC, NB, ES. Writing – review and editing: all authors. Funding acquisition: HJ, MC, NB, ES. Resources: JA, NB, ES. Supervision: MC, NB, ES. All authors contributed to the article and approved the submitted version.

Funding

This study was supported by grants from the Center for Innovative Medicine at Karolinska Institutet, the Swedish Society for Medical Research (SSMF) and Region Stockholm. HJ was supported by grants from the Royal Swedish Academy of Sciences and Region Stockholm. ES was supported by grants from the Bengt Ihre Foundation, the Center for Innovative Medicine at Karolinska Institutet, the Swedish Society for Medical Research (SSMF) and Region Stockholm. The funding sources were not involved in the design or conduct of the research, the analysis or interpretation of the data, the writing of the report or the decision to submit the article for publication.

Conflict of interest

The authors declare that the research was conducted in the absence of any commercial or financial relationships that could be construed as a potential conflict of interest.

Publisher's note

All claims expressed in this article are solely those of the authors and do not necessarily represent those of their affiliated organizations, or those of the publisher, the editors and the reviewers. Any product that may be evaluated in this article, or claim that may be made by its manufacturer, is not guaranteed or endorsed by the publisher.

Supplementary material

The Supplementary Material for this article can be found online at: https://www.frontiersin.org/articles/10.3389/fonc.2023.1169537/full#supplementary-material

References

1. Groot Koerkamp B, Wiggers JK, Allen PJ, Besselink MG, Blumgart LH, Busch OR, et al. Recurrence rate and pattern of perihilar cholangiocarcinoma after curative intent resection. *J Am Coll Surg* (2015) 221:1041–9. doi: 10.1016/j.jamcollsurg.2015.09.005

2. Mavros MN, Economopoulos KP, Alexiou VG, Pawlik TM. Treatment and prognosis for patients with intrahepatic cholangiocarcinoma: systematic review and meta-analysis. *JAMA Surg* (2014) 149:565–74. doi: 10.1001/jamasurg.2013.5137

3. Vega EA, Newhook TE, Kawaguchi Y, Qiao W, De Bellis M, Okuno M, et al. Conditional recurrence-free survival after oncologic extended resection for gallbladder cancer: an international multicenter analysis. *Ann Surg Oncol* (2021) 28:2675–82. doi: 10.1245/s10434-021-09626-3

4. Banales JM, Marin JJG, Lamarca A, Rodrigues PM, Khan SA, Roberts LR, et al. Cholangiocarcinoma 2020: the next horizon in mechanisms and management. *Nat Rev Gastroenterol Hepatol* (2020) 17:557–88. doi: 10.1038/s41575-020-0310-z

5. Rangarajan K, Simmons G, Manas D, Malik H, Hamady ZZ. Systemic adjuvant chemotherapy for cholangiocarcinoma surgery: a systematic review and meta-analysis. *Eur J Surg Oncol* (2020) 46:684–93. doi: 10.1016/j.ejso.2019.11.499

6. Hartog H, Ijzermans JN, van Gulik TM, Groot Koerkamp B. Resection of perihilar cholangiocarcinoma. *Surg Clin North Am* (2016) 96:247–67. doi: 10.1016/j.suc.2015.12.008

7. Altman AM, Kizy S, Marmor S, Huang JL, Denbo JW, Jensen EH. Current survival and treatment trends for surgically resected intrahepatic cholangiocarcinoma in the united states. *J Gastrointest Oncol* (2018) 9:942–52. doi: 10.21037/jgo.2017.11.06

8. Bird NTE, McKenna A, Dodd J, Poston G, Jones R, Malik H. Meta-analysis of prognostic factors for overall survival in patients with resected hilar cholangiocarcinoma. *Br J Surg* (2018) 105:1408–16. doi: 10.1002/bjs.10921

9. Margonis GA, Gani F, Buettner S, Amini N, Sasaki K, Andreatos N, et al. Rates and patterns of recurrence after curative intent resection for gallbladder cancer: a multi-institution analysis from the US extra-hepatic biliary malignancy consortium. *HPB (Oxford)* (2016) 18:872–8. doi: 10.1016/j.hpb.2016.05.016

10. Dolan RD, Laird BJA, Horgan PG, McMillan DC. The prognostic value of the systemic inflammatory response in randomised clinical trials in cancer: a systematic review. *Crit Rev Oncol Hematol* (2018) 132:130–7. doi: 10.1016/j.critrevonc.2018.09.016

11. Hogdall D, O'Rourke CJ, Dehlendorff C, Larsen OF, Jensen LH, Johansen AZ, et al. Serum IL6 as a prognostic biomarker and IL6R as a therapeutic target in biliary tract cancers. *Clin Cancer Res* (2020) 26:5655–67. doi: 10.1158/1078-0432.CCR-19-2700

12. Jansson H, Cornillet M, Bjorkstrom NK, Sturesson C, Sparrelid E. Prognostic value of preoperative inflammatory markers in resectable biliary tract cancer - validation and comparison of the Glasgow prognostic score and modified Glasgow prognostic score in a Western cohort. *Eur J Surg Oncol* (2020) 46:804–10. doi: 10.1016/j.ejso.2019.12.008

13. McShane LM, Altman DG, Sauerbrei W, Taube SE, Gion M, Clark GM, et al. Reporting recommendations for tumor marker prognostic studies (REMARK). *J Natl Cancer Inst* (2005) 97:1180–4. doi: 10.1093/jnci/dji237

14. Sample size calculators. UCSF clinical & translational science institute . Available at: https://sample-size.net/sample-size-survival-analysis/ (Accessed 14 March 2022).

15. Assarsson E, Lundberg M, Holmquist G, Bjorkesten J, Thorsen SB, Ekman D, et al. Homogenous 96-plex PEA immunoassay exhibiting high sensitivity, specificity, and excellent scalability. *PloS One* (2014) 9:e95192. doi: 10.1371/journal.pone.0095192

16. *Olink immuno-oncology I - validation data v 2.0*. Uppsala, Sweden: Olink Proteomics (2018).

17. Edge SB. *American Joint committee on cancer. AJCC cancer staging manual. 7th*. New York: Springer (2010).

18. *Protocol for the examination of specimens from patients with carcinoma of the intrahepatic bile ducts. college of American pathologists* (2021). Available at: https://www.cap.org/protocols-and-guidelines/cancer-reporting-tools/cancer-protocols (Accessed 14 March 2022).

19. Ahn KS, O'Brien D, Kang YN, Mounajjed T, Kim YH, Kim TS, et al. Prognostic subclass of intrahepatic cholangiocarcinoma by integrative molecular-clinical analysis and potential targeted approach. *Hepatol Int* (2019) 13:490–500. doi: 10.1007/s12072-019-09954-3

20. Zhang M, Yang H, Wan L, Wang Z, Wang H, Ge C, et al. Single-cell transcriptomic architecture and intercellular crosstalk of human intrahepatic cholangiocarcinoma. *J Hepatol* (2020) 73:1118–30. doi: 10.1016/j.jhep.2020.05.039

21. Jusakul A, Cutcutache I, Yong CH, Lim JQ, Huang MN, Padmanabhan N, et al. Whole-genome and epigenomic landscapes of etiologically distinct subtypes of cholangiocarcinoma. *Cancer Discov* (2017) 7:1116–35. doi: 10.1158/2159-8290.CD-17-0368

22. Andersen JB, Spee B, Blechacz BR, Avital I, Komuta M, Barbour A, et al. Genomic and genetic characterization of cholangiocarcinoma identifies therapeutic targets for tyrosine kinase inhibitors. *Gastroenterology* (2012) 142:1021–31.e15. doi: 10.1053/j.gastro.2011.12.005

23. Nakamura H, Arai Y, Totoki Y, Shirota T, Elzawahry A, Kato M, et al. Genomic spectra of biliary tract cancer. *Nat Genet* (2015) 47:1003–10. doi: 10.1038/ng.3375

24. Job S, Rapoud D, Dos Santos A, Gonzalez P, Desterke C, Pascal G, et al. Identification of four immune subtypes characterized by distinct composition and functions of tumor microenvironment in intrahepatic cholangiocarcinoma. *Hepatology* (2020) 72:965–81. doi: 10.1002/hep.31092

25. Dong L, Lu D, Chen R, Lin Y, Zhu H, Zhang Z, et al. Proteogenomic characterization identifies clinically relevant subgroups of intrahepatic cholangiocarcinoma. *Cancer Cell* (2022) 40:70–87.e15. doi: 10.1016/j.ccell.2021.12.006

26. Nepal C, Zhu B, O'Rourke CJ, Bhatt DK, Lee D, Song L, et al. Integrative molecular characterisation of gallbladder cancer reveals micro-environment-associated subtypes. *J Hepatol* (2021) 74:1132–44. doi: 10.1016/j.jhep.2020.11.033

27. Song G, Shi Y, Meng L, Ma J, Huang S, Zhang J, et al. Single-cell transcriptomic analysis suggests two molecularly subtypes of intrahepatic cholangiocarcinoma. *Nat Commun* (2022) 13:1642. doi: 10.1038/s41467-022-29164-0

28. Ritchie ME, Phipson B, Wu D, Hu Y, Law CW, Shi W, et al. Limma powers differential expression analyses for RNA-sequencing and microarray studies. *Nucleic Acids Res* (2015) 43:e47. doi: 10.1093/nar/gkv007

29. Love MI, Huber W, Anders S. Moderated estimation of fold change and dispersion for RNA-seq data with DESeq2. *Genome Biol* (2014) 15:550. doi: 10.1186/s13059-014-0550-8

30. Zheng GX, Terry JM, Belgrader P, Ryvkin P, Bent ZW, Wilson R, et al. Massively parallel digital transcriptional profiling of single cells. *Nat Commun* (2017) 8:14049. doi: 10.1038/ncomms14049

31. Hao Y, Hao S, Andersen-Nissen E, Mauck WM 3rd, Zheng S, Butler A, et al. Integrated analysis of multimodal single-cell data. *Cell* (2021) 184:3573–87.e29. doi: 10.1016/j.cell.2021.04.048

32. Korsunsky I, Millard N, Fan J, Slowikowski K, Zhang F, Wei K, et al. Fast, sensitive and accurate integration of single-cell data with harmony. *Nat Methods* (2019) 16:1289–96. doi: 10.1038/s41592-019-0619-0

33. *inferCNV of the trinity CTAT project. klarman cell observatory, broad institute of MIT and Harvard* (2019). Available at: https://github.com/broadinstitute/inferCNV (Accessed 14 April 2022).

34. Jiang P, Zhang Y, Ru B, Yang Y, Vu T, Paul R, et al. Systematic investigation of cytokine signaling activity at the tissue and single-cell levels. *Nat Methods* (2021) 18:1181–91. doi: 10.1038/s41592-021-01274-5

35. Lazar C. *imputeLCMD: a collection of methods for left-censored missing data imputation*. R package version 2.0. Available at: https://cran.r-project.org/web/packages/imputeLCMD.

36. van Buuren S, Groothuis-Oudshoorn K. Mice: multivariate imputation by chained equations in r. *J Stat Software* (2011) 45:1–67. doi: 10.18637/jss.v045.i03

37. Broman KW. R/qtlcharts: interactive graphics for quantitative trait locus mapping. *Genetics* (2015) 199:359–61. doi: 10.1534/genetics.114.172742

38. Therneau TM, Grambsch PM. *Modeling survival data: extending the cox model*. New York: Springer (2000).

39. Heinze G, Wallisch C, Dunkler D. Variable selection - a review and recommendations for the practicing statistician. *Biom J* (2018) 60:431–49. doi: 10.1002/bimj.201700067

40. Harrell FE. *Regression modeling strategies : with applications to linear models, logistic regression, and survival analysis*. New York: Springer (2001).

41. Loeuillard E, Yang J, Buckarma E, Wang J, Liu Y, Conboy CB, et al. Targeting tumor-associated macrophages and granulocytic-myeloid-derived suppressor cells augments pd-1 blockade in cholangiocarcinoma. *J Clin Invest* (2020) 130(10):5380–96. doi: 10.1172/JCI137110

42. Kobayashi S, Werneburg NW, Bronk SF, Kaufmann SH, Gores GJ. Interleukin-6 contributes to mcl-1 up-regulation and TRAIL resistance via an akt-signaling pathway in cholangiocarcinoma cells. *Gastroenterology* (2005) 128:2054–65. doi: 10.1053/j.gastro.2005.03.010

43. Ware MBZ, Zaidi M, Yang J, Turgeon MK, Krasinskas A, Mace TA, et al. Suppressive myeloid cells are expanded by biliary tract cancer-derived cytokines in vitro and associate with aggressive disease. *Br J Cancer* (2020) 123(9):1377–86. doi: 10.1038/s41416-020-1018-0

44. Dominguez GA, Condamine T, Mony S, Hashimoto A, Wang F, Liu Q, et al. Selective targeting of myeloid-derived suppressor cells in cancer patients using DS-8273a, an agonistic TRAIL-R2 antibody. *Clin Cancer Res* (2017) 23:2942–50. doi: 10.1158/1078-0432.CCR-16-1784

45. Alvisi G, Termanini A, Soldani C, Portale F, Carriero R, Pilipow K, et al. Multimodal single-cell profiling of intrahepatic cholangiocarcinoma defines hyperactivated tregs as a potential therapeutic target. *J Hepatol* (2022) 77:1359–72. doi: 10.1101/2022.03.06.483155

46. Cho YS, Challa S, Clancy L, Chan FK. Lipopolysaccharide-induced expression of TRAIL promotes dendritic cell differentiation. *Immunology* (2010) 130:504–15. doi:? 10.1111/j.1365-2567.2010.03266.x

47. Fingas CD, Blechacz BR, Smoot RL, Guicciardi ME, Mott J, Bronk SF, et al. A smac mimetic reduces TNF related apoptosis inducing ligand (TRAIL)-induced invasion and metastasis of cholangiocarcinoma cells. *Hepatology* (2010) 52:550–61. doi: 10.1002/hep.23729

48. Hartwig T, Montinaro A, von Karstedt S, Sevko A, Surinova S, Chakravarthy A, et al. The TRAIL-induced cancer secretome promotes a tumor-supportive immune microenvironment via CCR2. *Mol Cell* (2017) 65:730–42.e5. doi: 10.1016/j.molcel.2017.01.021

49. Jiang W, Zeng ZC, Tang ZY, Fan J, Sun HC, Zhou J, et al. A prognostic scoring system based on clinical features of intrahepatic cholangiocarcinoma: the fudan score. *Ann Oncol* (2011) 22:1644–52. doi: 10.1093/annonc/mdq650

50. Pei Z, Chu L, Zou W, Zhang Z, Qiu S, Qi R, et al. An oncolytic adenoviral vector of smac increases antitumor activity of TRAIL against HCC in human cells and in mice. *Hepatology* (2004) 39:1371–81. doi: 10.1002/hep.20203

51. Backen AC, Lopes A, Wasan H, Palmer DH, Duggan M, Cunningham D, et al. Circulating biomarkers during treatment in patients with advanced biliary tract cancer receiving cediranib in the UK ABC-03 trial. *Br J Cancer* (2018) 119:27–35. doi: 10.1038/s41416-018-0132-8

52. Turrini R, Pabois A, Xenarios I, Coukos G, Delaloye JF, Doucey MA. TIE-2 expressing monocytes in human cancers. *Oncoimmunology* (2017) 6:e1303585. doi: 10.1080/2162402X.2017.1303585

53. Huang H, Lai JY, Do J, Liu D, Li L, Del Rosario J, et al. Specifically targeting angiopoietin-2 inhibits angiogenesis, Tie2-expressing monocyte infiltration, and tumor growth. *Clin Cancer Res* (2011) 17:1001–11. doi: 10.1158/1078-0432.CCR-10-2317

54. Atanasov G, Hau HM, Dietel C, Benzing C, Krenzien F, Brandl A, et al. Prognostic significance of TIE2-expressing monocytes in hilar cholangiocarcinoma. *J Surg Oncol* (2016) 114:91–8. doi: 10.1002/jso.24249

55. Demols A, Borbath I, Van den Eynde M, Houbiers G, Peeters M, Marechal R, et al. Regorafenib after failure of gemcitabine and platinum-based chemotherapy for locally advanced/metastatic biliary tumors: REACHIN, a randomized, double-blind, phase II trial. *Ann Oncol* (2020) 31:1169–77. doi: 10.1016/j.annonc.2020.05.018

56. Motz GT, Santoro SP, Wang LP, Garrabrant T, Lastra RR, Hagemann IS, et al. Tumor endothelium FasL establishes a selective immune barrier promoting tolerance in tumors. *Nat Med* (2014) 20:607–15. doi: 10.1038/nm.3541

57. Cuenco J, Wehnert N, Blyuss O, Kazarian A, Whitwell HJ, Menon U, et al. Identification of a serum biomarker panel for the differential diagnosis of cholangiocarcinoma and primary sclerosing cholangitis. *Oncotarget* (2018) 9:17430–42. doi: 10.18632/oncotarget.24732

58. Sandanayake NS, Sinclair J, Andreola F, Chapman MH, Xue A, Webster GJ, et al. A combination of serum leucine-rich alpha-2-glycoprotein 1, CA19-9 and interleukin-6 differentiate biliary tract cancer from benign biliary strictures. *Br J Cancer* (2011) 105:1370–8. doi: 10.1038/bjc.2011.376

59. Thorban S, Roder JD, Siewert JR. Detection of micrometastasis in bone marrow of pancreatic cancer patients. *Ann Oncol* (1999) 10 Suppl 4:111–3. doi: 10.1093/annonc/10.suppl_4.S111

60. Evans DB. What makes a pancreatic cancer resectable? *Am Soc Clin Oncol Educ Book* (2018) 38:300–5. doi: 10.1200/EDBK_200861

frontiers | Frontiers in Oncology

TYPE Original Research
PUBLISHED 17 August 2023
DOI 10.3389/fonc.2023.1216097

OPEN ACCESS

EDITED BY
Francesco Vasuri,
Azienda Ospedaliero-Universitaria di Bologna, Italy

REVIEWED BY
Andrea Benedetti Cacciaguerra,
Polytechnic University of Marche, Italy
Christian Cotsoglou,
Ospedale di Vimercate - ASST Brianza, Italy

*CORRESPONDENCE
Nobuyoshi Hiraoka
nhiraoka@ncc.go.jp

RECEIVED 03 May 2023
ACCEPTED 27 July 2023
PUBLISHED 17 August 2023

CITATION
Nagashima D, Esaki M, Nara S, Ban D, Takamoto T, Mizui T, Shimada K and Hiraoka N (2023) Novel insights into the intraepithelial spread of extrahepatic cholangiocarcinoma: clinicopathological study of 382 cases on extrahepatic cholangiocarcinoma.
Front. Oncol. 13:1216097.
doi: 10.3389/fonc.2023.1216097

Novel insights into the intraepithelial spread of extrahepatic cholangiocarcinoma: clinicopathological study of 382 cases on extrahepatic cholangiocarcinoma

Daisuke Nagashima[1,2,3,4], Minoru Esaki[2], Satoshi Nara[2], Daisuke Ban[2], Takeshi Takamoto[2], Takahiro Mizui[2], Kazuaki Shimada[2] and Nobuyoshi Hiraoka[1,3,4]*

[1]Division of Molecular Pathology, National Cancer Center Research Institute, Tokyo, Japan, [2]Department of Hepatobiliary and Pancreatic Surgery, National Cancer Center Hospital, Tokyo, Japan, [3]Department of Molecular Oncology, Jikei University Graduate School of Medicine, Tokyo, Japan, [4]Division of Innovative Pathology and Laboratory Medicine, National Cancer Center Exploratory Oncology Research & Clinical Trial Center (EPOC), Tokyo, Japan

Background: Extrahepatic cholangiocarcinoma (eCCA) is a rare and aggressive disease and consisted of conventional eCCA and intraductal papillary neoplasm of the bile duct (IPNB). Intraepithelial spread (IES) of cancer cells beyond the invasive area is often observed in IPNBs; however, the prevalence of IES remains to be examined in conventional eCCAs. Here, we evaluated the clinicopathological features of eCCAs according to tumor location, with a focus on the presence of IES. The IES extension was also compared among biliary tract cancers (BTCs).

Methods: We examined the prevalence and clinicopathological significance of IES in eCCAs (n=382) and the IES extension of BTCs, including gallbladder (n=172), cystic duct (n=20), and ampullary cancers (n=102).

Results: Among the invasive eCCAs, IPNB had a higher rate of IES (89.2%) than conventional eCCAs (57.0%). Among conventional eCCAs, distal eCCAs (75.4%) had a significantly higher prevalence of IES than perihilar eCCAs (41.3%). The presence of IES was associated with a significantly higher survival rate in patients with distal eCCAs (P=0.030). Extension of the IES into the cystic duct (CyD) in distal eCCAs that cancer cells reached the junction of the CyD was a favorable prognostic factor (P<0.001). The association of survival with IES, either on the extrahepatic bile duct or on the CyD, differed depending on the tumor location and type of eCCA. The extension properties of IES were also dependent on different types of tumors among BTCs; usually, the IES incidence became higher

than 50% in the tissues that the tumor developed, whereas IES extension to other tissues decreased the incidence.

Conclusion: Thus, eCCAs have different clinicopathological characteristics depending on the tumor location and type.

KEYWORDS

intraepithelial spread, extrahepatic cholangiocarcinoma, biliary tract cancer, tumor location, patient outcome

Introduction

The biliary tract comprises the intrahepatic bile duct (IHBD), extrahepatic bile duct (EHBD), cystic duct (CyD), gallbladder, and ampulla of Vater. Biliary tract cancers (BTCs) are rare and aggressive, and because of limited treatment options, they are associated with poor outcomes (1, 2). Extrahepatic cholangiocarcinoma (eCCA) accounts for approximately one-third of BTCs (3). The incidence of eCCA varies geographically, with a high incidence in east Asia, although it has increased worldwide (4, 5). Owing to the differences of clinicopathological characteristics of eCCAs dependent on anatomical location, eCCAs are currently categorized as perihilar and distal eCCAs to be evaluated in different tumor-node-metastasis (TNM) classifications (6). The accumulated findings suggest that the differences of eCCAs characteristics may be based on not only simply location differences but also biological properties of cancer cells raised in different anatomical locations (7–10). Thus, further clinicopathological characterization and exploration of molecular alterations in eCCA are needed.

Intraepithelial spread (IES) of cancer cells beyond the invasive area is found in several cancers, including BTCs (11–16). Extensive IES may represent a less aggressive behavior of the tumor and is associated with better patient outcome in eCCA (11, 13, 15) and pancreatic ductal adenocarcinoma (PDAC) (12, 16). Recent reports also indicated that the presence of IES without invasive cancer cells in the bile duct margin is not an unfavorable factor (14, 17–19). The previous studies have characterized eCCAs with extensive IES as unique eCCAs that show macroscopic papillary type and histological papillary adenocarcinoma with a high incidence and long-term prognosis. These features of tumors with extensive IES are very similar to those of intraductal papillary neoplasms of the bile duct (IPNBs) and its derived invasive cancers, entities that first appeared in the 2010 World Health Organization (WHO) classification after published reports. IPNBs are grossly visible premalignant neoplasms with intraductal papillary or villous growth of epithelial neoplastic cells, and intrahepatic IPNBs show better outcome compared to extrahepatic IPNBs (20). Since previous IES studies analyzed eCCAs without dividing IPNBs from the conventional eCCAs (11, 13, 15), it remains to be investigated if reported characteristics of IES are also relevant to conventional eCCAs. In addition, the extensive properties of the IES have not been characterized, especially the extension of the IES beyond the borders among different tissues. The EHBD connects continuously to different tissues, such as the CyD and ampullary ducts, and through them to the gallbladder and duodenum.

In this study, we investigated the clinicopathological features of eCCAs (n=382) in terms of tumor location, with a focus on the presence of IES. We also compared the incidence and extension properties of IES among BTCs, including eCCAs, gallbladder cancers (GBCs, n=172), cystic duct cancers (CyDCs, n=20), and ampullary cancers (AVCs, n=102).

Materials and methods

Patients of eCCAs

We retrospectively evaluated 382 eCCA patients who underwent surgical resection at the National Cancer Center Hospital between January 2002 and March 2022. All the patients included in this study underwent macroscopic curative resection of conventional eCCAs or IPNBs that developed during EHBD. We excluded patients who had received any therapy before surgery and those with inadequate IES data. In addition, cases of hospital death after surgical resection, cases with unknown causes of death, or early death not due to eCCAs within 12 months after surgical resection were excluded. Finally, 305 patients were included in this study. For survival analyses, cases of carcinoma *in situ* of conventional eCCA were excluded. Supplementary Figure 1 describes the details of patient selection.

Surgical procedures were performed based on the location of the primary tumor. Among 305 patients, 140 (45.9%) underwent hepatectomy with extrahepatic bile duct resection, 124 (40.7%) underwent pancreaticoduodenectomy, 17 (5.6%) underwent combined hepatectomy and pancreaticoduodenectomy, and 24 (7.9%) underwent extrahepatic bile duct resection. Para-aortic lymph node sampling was performed when lymph node metastasis was suspected. In our hospital, adjuvant therapy is not routinely performed after surgery, although adjuvant S-1 therapy has become a standard of care according to the results of the JCOG1202 study since October 2021 (21). Only four patients underwent adjuvant chemotherapy with S-1 during the study period. Clinical and radiological follow-ups were scheduled on a

3-month basis for a few years after resection. The median follow-up period was 41.0 months for all 305 patients. Recurrence was confirmed by radiological examination and elevation of tumor markers. The date of recurrence was defined as the date on which clinicians confirmed recurrence in medical records. The census date was December 31, 2022. According to previous studies, early recurrence is defined as any recurrence within 12 months after surgery (22, 23).

Patients with GBCs, CyDCs, or AVCs

To assess the incidence and extent of IES in BTCs, 102 cases of AVC, 174 cases of GBC, and 20 cases of CyDC were included, all of which were surgically resected at the National Cancer Center Hospital between January 2002 and March 2022. Supplementary Table 1 shows the demographics of the patients with GBC, AVC, and CyDC. AVCs raised in the common, bile, or pancreatic ducts of the ampulla of Vater were selected for this assessment.

Pathological examination

All of the BTCs were examined pathologically and classified according to the WHO classification (2, 24, 25) and the International Union against Cancer (UICC) TNM classification 8th edition (6). We had some modification about tumor location as mentioned later. Macroscopic types of eCCA and the following histopathological variables were evaluated following the Japanese Society of Biliary Surgery (JSBS) classification (26): lymphatic, venous, and perineural invasions that were classified into negative (−), slightly positive (1+), moderately positive (2+), and markedly positive (3+) based on their event frequencies. For the survival and correlation analyses, "high" and "low" grades were determined based on these values; high grade to be combined with 2+ and 3+ and low grade to be - and 1+. According to the JSBS classification (27), the right and left hepatic ducts and their confluence were defined as the (peri)hilar duct (Bph), common hepatic duct, and common bile duct, and were divided into three portions as follows: superior (Bs), middle (Bm), and inferior (Bi) portions of the EHBD. Bs and Bm were defined as the respective portions in the upper and lower halves of the bile duct length from the confluence of the right and left hepatic ducts to the upper margin of the pancreas, and Bi was defined as the portion from the upper margin of the pancreas to the ampulla of Vater. In some analyses, we combined Bph and Bs eCCAs as perihilar eCCAs, and Bm and Bi eCCAs as distal eCCAs. IHBD was defined as the hepatic side of the bile duct from the third branch (e.g., segmental ducts 5 and 8) of the hepatic duct in this study. All patients with stage IV disease were diagnosed on the basis of para-aortic lymph node involvement. Surgically resected specimens were fixed in 10% formalin and cut into serial slices 5 mm thick. All sections were stained with hematoxylin and eosin for pathological examination. IES was defined as the intraepithelial spread of cancer cells beyond the invasive area. IES contained lesions corresponded to biliary intraepithelial neoplasia, high grade (BilIN-3), intraductal papillary neoplasm of the bile duct (IPNB), intracholecystic papillary neoplasm (ICPN), intraampullary papillary tubular neoplasm (IAPN), and cancerous duct. IES was diagnosed only when the cancer cells extended along the biliary tract. IES was not applied when cancer cells had stromal invasion beyond the biliary tract structure without extension along the biliary tract and the cancer cells re-entered the biliary tract mucosal epithelial layer. We defined that "intraepithelial extension of cancer cells on duodenum" was present when intraepithelial extension of cancer cells on ampullary common duct continued to extend to the duodenum epithelial layer. The length of the IES was described using a 5 mm scale in general.

Statistical analysis

Statistical analyses were performed using JMP version 12.2 (SAS Institute, Cary, NC, USA) and the StatView-J software version 5.0 (Abacus Concepts, Berkeley, CA, USA). Continuous data were expressed as median (range) and compared using the Mann–Whitney U test. Categorical variables were compared between groups using Pearson's chi-square test or Fisher's exact test, as appropriate. Relapse-free survival (RFS) was defined as the interval between the date of surgery and time of recurrence. Overall survival (OS) was calculated based on the time from surgery to death from any cause or last follow-up. Survival data were estimated using the Kaplan–Meier method and examined using the log-rank test. Factors found to be significant in the univariate analysis were subjected to multivariate analysis using the Cox proportional hazards model. Differences at $P < 0.05$ were considered statistically significant.

Results

Clinicopathological characteristics of eCCAs

Details of the surgical and clinicopathological features are presented in Table 1. Among 284 patients with invasive eCCAs, those with Bph eCCAs were significantly younger than those with other conventional eCCAs. The female ratio in Bph eCCAs was significantly higher than that in Bs and Bi eCCAs, and similar tendencies were found in Bm eCCAs and invasive IPNBs. The total tumor sizes of Bph eCCAs were significantly smaller than those of Bs and Bm eCCAs, whereas the sizes of the tumor area with stromal invasion of cancer cells (invasive tumor sizes) of Bi eCCAs and invasive IPNBs were significantly smaller than those of the other conventional eCCAs.

Approximately 80% of conventional invasive eCCAs belong to the nodular-infiltrating macroscopic type. In contrast, more than 85% of invasive IPNB cases were papillary types. The incidence of poorly differentiated adenocarcinomas in Bph eCCAs was significantly lower than that in other conventional eCCAs. Invasive IPNBs predominantly include papillary adenocarcinomas. The invasion depth tended to be lower in invasive IPNBs than in conventional eCCAs. The frequencies of portal vein or artery invasion of cancer cells were much higher in Bph and Bs eCCAs, as the portal vein or artery exists nearer to the EHBD in these

10.3389/fonc.2023.1216097

TABLE 1A Clinicopathological variables of invasive extrahepatic cholangiocarcinomas (n = 284).

	Bph eCCA n= 96	Bs eCCA n= 42	Bm eCCA n= 59	Bi eCCA n= 59	IPNB n= 28
Age, year [range]	65 [19-83]	70 [39-87]	68 [44-82]	71 [41-83]	74.5 [33-82]
Female/Male	29/67	5/37	12/47	10/49	4/24
Macroscopic type					
nodular-infiltrating	78 (81.3)	33 (78.6)	47 (79.7)	40 (67.8)	2 (7.1)
nodular-expanding	1 (1.0)	0 (0)	1 (1.7)	3 (5.1)	1 (3.6)
papillary-infiltrating	3 (3.1)	4 (9.5)	4 (6.8)	8 (13.6)	17 (60.7)
papillary-expanding	0 (0)	1 (2.4)	1 (1.7)	0 (0)	8 (28.6)
flat-infiltrating	13 (13.5)	4 (9.5)	6 (10.2)	8 (13.6)	0 (0)
flat-expanding	1 (1.0)	0 (0)	0 (0)	0 (0)	0 (0)
Total tumor size, mm [range]	40 [15-150]	50 [20-90]	55 [15-120]	50 [20-100]	57.5 [15-120]
Invasive tumor size, mm [range]	35 [15-120]	35 [20-90]	40 [15-70]	30 [15-70]	22.5 [5-50]
Histology (histological grade)					
Tub1 (G1)	19 (19.8)	9 (21.4)	10 (17.0)	10 (17.0)	3 (10.7)
Tub2 (G2)	71 (74.0)	23 (54.8)	37 (62.7)	30 (50.8)	6 (21.4)
Por (G3)	4 (4.2)	8 (19.1)	10 (17.0)	15 (25.4)	1 (3.6)
Pap (G1)	0 (0)	1 (2.4)	2 (3.4)	2 (3.4)	18 (64.3)
AS (G3)	2 (2.1)	1 (2.4)	0 (0)	2 (3.4)	0 (0)
Depth of invasion					
fm	0 (0)	1 (2.4)	1 (1.7)	0 (0)	7 (25.0)
ss	88 (91.7)	38 (90.5)	58 (98.3)	59 (100)	20 (71.4)
se	7 (7.3)	2 (4.8)	0 (0)	0 (0)	1 (3.6)
si	1 (1.0)	1 (2.4)	0 (0)	0 (0)	0 (0)
Portal vein invasion					
presence	39 (40.6)	2 (4.8)	5 (8.5)	1 (1.7)	1 (3.6)
absence	57 (59.4)	40 (95.2)	54 (91.5)	58 (98.3)	27 (96.4)
Artery invasion					
presence	12 (12.5)	7 (16.7)	0 (0)	0 (0)	0 (0)
absence	84 (87.5)	35 (83.3)	59 (100)	59 (100)	28 (100)
Lymphatic invasion					
high	46 (47.9)	15 (35.7)	31 (52.5)	29 (49.2)	8 (28.6)
low	50 (52.1)	27 (64.3)	28 (47.5)	30 (50.8)	20 (71.4)
Venous invasion					
high	64 (66.7)	20 (47.6)	25 (42.4)	27 (45.8)	6 (21.4)
low	32 (33.3)	22 (52.4)	34 (57.6)	32 (54.2)	22 (78.6)
Perineural invasion					
high	72 (75.0)	38 (90.5)	52 (88.1)	44 (74.6)	8 (28.6)
low	24 (25.0)	4 (9.5)	7 (11.9)	15 (25.4)	20 (71.4)
Surgical procedure					

(Continued)

TABLE 1A Continued

	Bph eCCA n= 96	Bs eCCA n= 42	Bm eCCA n= 59	Bi eCCA n= 59	IPNB n= 28
EBDR	2 (2.1)	7 (16.7)	7 (11.9)	1 (1.7)	6 (21.4)
PD	0 (0)	6 (14.3)	41 (69.5)	57 (96.6)	17 (60.7)
Hepatectomy	87 (90.6)	28 (66.7)	5 (8.5)	0 (0)	4 (14.3)
HPD	7 (7.3)	1 (2.4)	6 (10.2)	1 (1.7)	1 (3.6)
Major vessel resection					
PVR	15 (15.6)	2 (4.8)	10 (17.0)	2 (3.4)	0 (0)
HAR	5 (5.4)	3 (7.1)	1 (1.7)	1 (1.7)	0 (0)
PVR+HAR	7 (7.5)	0 (0)	1 (1.7)	0 (0)	0 (0)
Bile duct margin status					
presence with invasive cancer	24 (25.0)	12 (28.6)	8 (13.6)	2 (3.4)	0 (0)
presence with non-invasive cancer	14 (14.6)	11 (26.2)	18 (30.5)	11 (18.6)	8 (28.6)
absence	58 (60.4)	19 (45.2)	33 (55.9)	46 (78.0)	20 (71.4)
Residual tumor status					
microscopic residual tumor	40 (41.7)	24 (57.1)	32 (54.2)	16 (27.1)	10 (35.7)
no residual tumor	56 (58.3)	18 (42.9)	27 (45.8)	43 (72.9)	18 (64.3)
Recurrence					
presence	71 (74.0)	27 (64.3)	41 (69.5)	30 (50.8)	15 (53.6)
absence	25 (26.0)	15 (35.7)	18 (30.5)	29 (49.2)	13 (46.4)
Early recurrence					
presence	29 (30.2)	10 (23.8)	22 (37.3)	15 (25.4)	5 (17.9)
absence	67 (69.8)	32 (76.2)	37 (62.7)	44 (74.6)	23 (82.1)

Values given are the number of patients (percentage) unless otherwise indicated.
AS, adenosquamous carcinoma; Bi, inferior portion of EHBD; Bm, middle portion of EHBD; Bph, (peri)hilar bile duct; Bs, superior portion of EHBD; eCCA, extrahepatic cholangiocarcinoma; EHBD, extrahepatic bile duct; EBDR, extrahepatic bile duct resection; fm, fibromusclar layer; HAR, hepatic artery resection; HPD, hepatopancreatoduodenectomy; IPNB, intraductal papillary neoplasm of the bile duct; Pap, papillary adenocarcinoma; Por, poorly differentiated adenocarcinoma; PD, pancreaticoduodenectomy; PVR, Portal vein resection; se, exposed on serosal surface; si, infiltration beyond the serosa to other tissues; ss, subserosal tissue; Tub1, well differentiated tubular adenocarcinoma; Tub2, moderately differentiated tubular adenocarcinoma.

regions compared to other sites. The lymphatic, vascular, and perineural invasion of tumor cells tended to be lower in invasive IPNBs than in conventional eCCAs. Venous invasion was significantly higher in Bph eCCAs than in other conventional eCCAs and invasive IPNBs. Perineural invasion was significantly lower in Bi eCCAs than in Bs and Bm eCCAs. The rates of residual tumor-free tumors (R0) were significantly higher in Bi eCCAs than in other conventional eCCAs. The rates of positive bile duct margins with invasive cancers and positive residual tumor status with invasive cancers were significantly higher in Bph and Bs eCCAs than in Bi eCCA and invasive IPNBs.

Patients with noninvasive IPNBs had significantly better survival than those with invasive eCCAs, including invasive IPNBs (Supplementary Figure 2). The survival outcomes of invasive IPNBs were significantly better than those of Bm or Bph eCCAs, but not significantly different from those of Bs or Bi eCCAs. The survival curve of Bi eCCAs was similar to that of invasive IPNBs for both RFS and OS, and the 5-year and 10-year survival rates were similar. The survival outcomes of patients with Bi eCCAs were significantly better than those of patients with Bph and Bm eCCAs in terms of both RFS and OS.

Clinicopathological characteristics of invasive eCCAs with IES along EHBD

IES was observed in 60.2% of invasive eCCAs (Figure 1). The incidence of IES in Bph or Bs eCCAs was significantly lower than in Bm or Bi eCCAs or invasive IPNBs (Figure 1D). Table 2A summarizes the extent and distribution of IES in invasive eCCAs. Invasive IPNBs had the highest incidence (P <0.001) and longer duration of IES than invasive conventional eCCAs. The incidence peak of IES was at lengths of ≥10 and <20 mm in conventional eCCAs and at lengths of ≥20 and <30 mm in invasive IPNBs. The IES extended further to the liver-side in invasive eCCAs.

Patients with invasive eCCAs and IES showed significantly longer survival times than those without IES (P = 0.039) (Figure 2A). Similar survival associations were found in patients

10.3389/fonc.2023.1216097

TABLE 1B Clinicopathological variables of invasive extrahepatic cholangiocarcinomas (n = 284).

	Bph eCCA n= 96	Bs eCCA n= 42	IPNB-perihilar n= 8		Bm eCCA n= 59	Bi eCCA n= 59	IPNB-distal n= 20
TMN classification							
T category							
T1	0 (0)	11 (26.2)	5 (62.5)	T1	19 (32.2)	7 (11.9)	11 (55.0)
T2a	19 (19.8)	25 (59.5)	2 (25.0)	T2	30 (50.8)	42 (71.2)	6 (30.0)
T2b	36 (37.5)	2 (4.8)	1 (12.5)	T3	10 (17.0)	10 (17.0)	3 (15.0)
T3	31 (32.3)	4 (9.5)	0 (0)	T4	0 (0)	0 (0)	0 (0)
T4	10 (10.4)	0 (0)	0 (0)				
N category							
N0	49 (51.0)	17 (40.5)	7 (87.5)	N0	26 (44.1)	35 (59.3)	13 (65.0)
N1	33 (34.4)	19 (45.2)	1 (12.5)	N1	24 (40.7)	15 (25.4)	2 (10.0)
N2	14 (14.6)	6 (14.3)	0 (0)	N2	9 (15.3)	9 (15.3)	5 (25.0)
M category							
M0	91 (94.8)	38 (90.5)	8 (100)	M0	57 (96.6)	55 (93.2)	18 (90.0)
M1	5 (5.2)	4 (9.5)	0 (0)	M1	2 (3.4)	4 (6.8)	2 (10.0)
Stage							
I	0 (0)	6 (14.3)	5 (62.5)	I	9 (15.3)	7 (11.9)	9 (45.0)
II	35 (36.5)	9 (21.4)	2 (25.0)	IIA	22 (37.3)	24 (40.7)	5 (25.0)
IIIA	10 (10.4)	2 (4.8)	0 (0)	IIB	17 (28.8)	18 (30.5)	1 (5.0)
IIIB	3 (3.1)	0 (0)	0 (0)	IIIA	9 (15.3)	6 (10.2)	3 (15.0)
IIIC	31 (32.3)	17 (40.5)	1 (12.5)	IIIB	0 (0)	0 (0)	0 (0)
IVA	12 (12.5)	4 (9.5)	0 (0)	IV	2 (3.4)	4 (6.8)	2 (10.0)
IVB	5 (5.2)	4 (9.5)	0 (0)				

Values given are the number of patients (percentage) unless otherwise indicated.
IPNB was not classified by tumor location due to small number of cases.

with invasive conventional eCCAs, but without statistical significance (Figure 2B). IES was not associated with outcomes in perihilar eCCAs (Figure 2C), although patients with IES showed significantly longer OS in distal eCCAs (P = 0.030) (Figure 2D). When survival was evaluated at each location in invasive conventional eCCAs and invasive IPNBs, significant differences in RFS (P = 0.039) and OS (P = 0.025) were observed in Bm eCCAs (Supplementary Figure 3). Multivariate analyses of patients with distal eCCAs (Table 3) revealed that the IES was not a significant predictor of RFS or OS. In distal eCCAs, the presence of IES significantly correlated with a lower female-to-male ratio, larger total tumor size, higher positive bile duct margins, and a higher positive residual tumor status (Supplementary Table 2).

Clinicopathological characteristics of invasive eCCAs with IES along CyD

The IES on the EHBD reached the junction of the CyD and often extended beyond the junction and continuously into both the CyD and the other side of the EHBD. When invasive eCCAs in which cancer cells reached the junction of the CyD were selected and assessed, the incidence of IES along with CyD (CyD-IES) was lower than that of IES on EHBD in all locations of the conventional and invasive eCCAs (Figure 1D and Table 2B). 60.0% of Bi eCCAs had CyD-IES and 30% of the other conventional eCCAs had CyD-IES, and their CyD-IES extended rarely to the gallbladder (Table 2B). In contrast, 75.0% of IPNBs had CyD-IES, and 57.1% had IES on the gallbladder when IPNBs reached the border between the CyD and the gallbladder.

In patients with invasive eCCAs, as well as those with invasive conventional eCCAs, patients with CyD-IES showed significantly longer survival times for both RFS (P = 0.037 and P = 0.016) and OS (P = 0.006 and P = 0.004, respectively) than patients without CyD-IES (Figures 3A, B). Perihilar eCCAs had a low incidence of CyD-IES, and there were no associations between CyD-IES and patient outcomes (Figure 3C). Patients with CyD-IES in distal eCCAs had significantly longer survival than those without CyD-IES for both RFS (P = 0.043) and OS (P = 0.018) (Figure 3). Multivariate survival analysis of patients with invasive conventional eCCAs revealed that

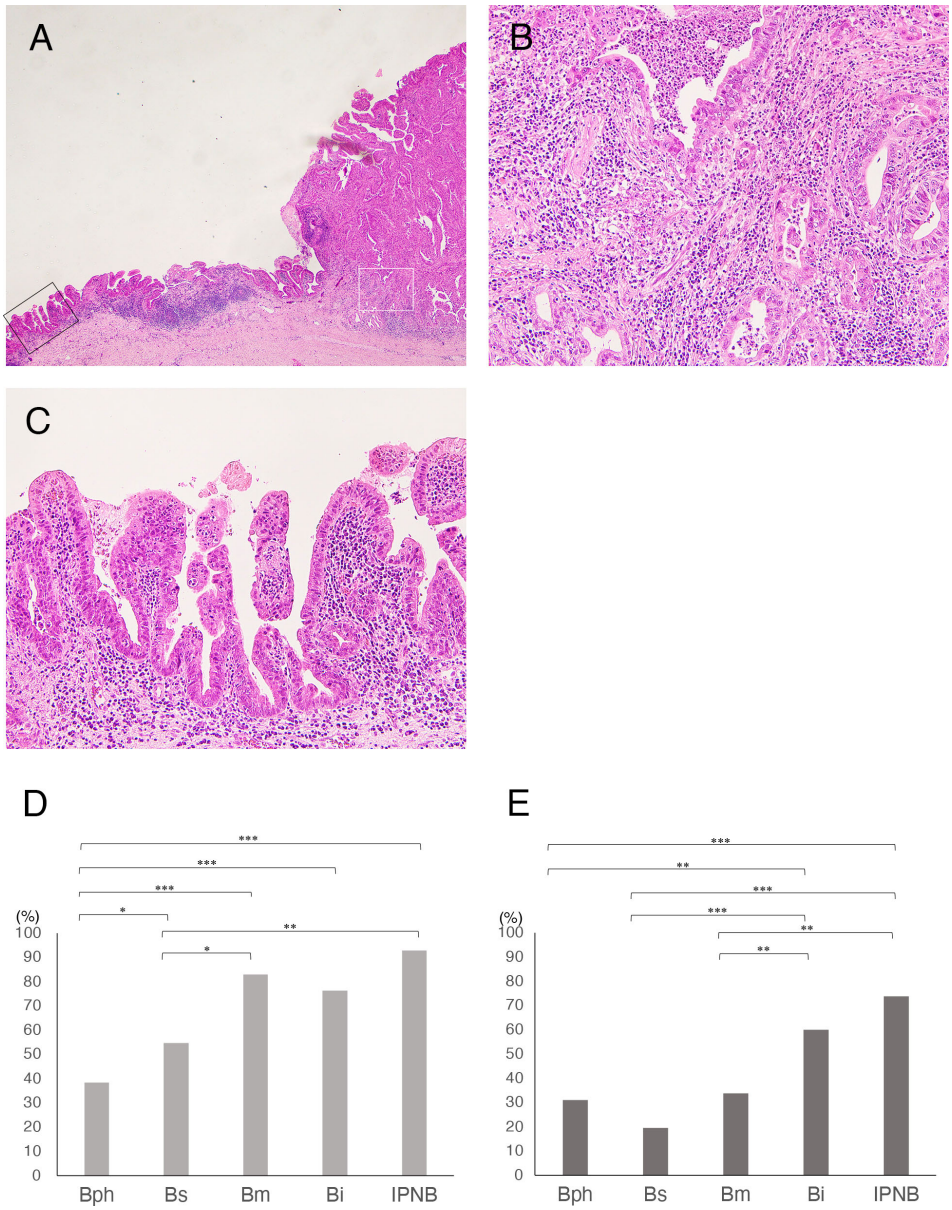

FIGURE 1
(A-C) Histology of intraepithelial spread (IES) of cancer cells in extrahepatic cholangiocarcinomas (eCCAs). **(A)** Main tumor mass with stromal invasion of cancer cells at right and IES extended along epithelial layers of the bile duct in very low-power view. **(B)** Histology of cancer area with stromal invasion in middle power view, corresponding to white square in A. **(C)** Histology of IES showing proliferation of cancer cells in epithelial layer with a low papillary structure in middle power view, corresponding to black square in A. **(D, E)** Comparison of incidence of intraepithelial spread in invasive eCCAs. **(D)** Bar graph shows incidence of IES along extrahepatic bile duct in invasive eCCAs. **(E)** Bar graph shows incidence of IES along with cystic duct (CyD) in invasive eCCAs that cancer cells reached the junction of CyD. Differences are examined by chi-square test. IPNB is not classified by tumor location because of small number of cases. *P< 0.05; **P< 0.01; ***P< 0.001.

the CyD-IES was not a significant predictor of RFS or OS (Table 3). Multivariate survival analysis of patients with distal eCCAs also revealed that the CyD-IES was not a significant predictor of RFS or OS (Supplementary Table 3). CyD-IES closely correlated with tumor location, perineural invasion, and early recurrence of distal eCCAs (Supplementary Table 4).

Distal eCCA cases reaching the junction of the CyD were divided into three groups according to IES patterns: eCCAs with CyD-IES as group A, eCCAs with only IES as group B, and eCCAs without any IES or CyD-IES as group C (Supplementary Figure 4). Group A contained 5 eCCAs with only CyD-IES and 42 cases with both CyD-IES and IES. Survival analyses revealed that group A had longer survival and group C had shorter survival, with significant differences in both RFS (P = 0.002) and OS (P < 0.001) (Supplementary Figure 5). Group B also showed longer survival compared with that of group C for both RFS (P = 0.024) and OS (P = 0.034) (Supplementary Figure 5). All survival rates were higher in group A than in group B.

TABLE 2A Intraepithelial spread of extrahepatic cholangiocarcinomas along with extrahepatic bile duct.

	Bph eCCA n= 96	Bs eCCA n= 42	Bm eCCA n= 59	Bi eCCA n= 59	invasive IPNB n= 28
IES, mm					
0	62 (64.6)	19 (45.2)	13 (22.0)	16 (27.1)	3 (10.7)
0 <, < 10	12 (12.5)	6 (14.3)	10 (16.9)	6 (10.2)	3 (10.7)
10 ≤, < 20	12 (12.5)	9 (21.4)	19 (32.2)	22 (37.3)	7 (25.0)
20 ≤, < 30	5 (5.2)	5 (11.9)	8 (13.6)	7 (11.9)	9 (32.1)
30 ≤, < 40	3 (3.1)	2 (4.8)	5 (8.5)	6 (10.2)	3 (10.7)
40 ≤, < 50	1 (1.0)	0 (0)	3 (5.1)	1 (1.7)	0 (0)
50 ≤, < 60	1 (1.0)	1 (2.4)	0 (0)	0 (0)	3 (10.7)
60 ≤	0 (0)	0 (0)	1 (1.7)	1 (1.7)	0 (0)
Distribution of IES					
liver-side dominant	17 (50.0)	12 (52.2)	18 (39.1)	30 (69.8)	13 (52.0)
duodenal-side dominant	14 (41.2)	10 (43.5)	24 (52.2)	10 (23.3)	8 (32.0)
equivalent	3 (8.8)	1 (4.3)	4 (8.7)	3 (7.0)	4 (16.0)

Incidence and profiles of IES in BTCs; IES in eCCAs extended into IHBD and ampullary area

Some properties of the IES on the EHBD of the eCCAs are described above and depicted in Figure 4. Liver-side IES was ended on the IHBD in 60.4%, on the bile ducts of the borderline area between the IHBD and EHBD (i.e., hepatic ducts and the second branches) in 37.5%, and on the confluence of the right and left hepatic ducts in 2.1% of conventional eCCA cases who underwent hepatectomy with liver-side IES (Table 4A). In perihilar eCCAs, IES on EHBD was mostly ended on the EHBD in front of the IHBD, and extension of IES into the IHBD from the EHBD was very rare, whereas 95.5% of cases with IES on IHBD had stromal invasion in the IHBD area. In distal eCCAs, cases of IES on IHBD were rare, with longer IES. Liver-side IES ended on the IHBD in 12.5% of patients, on the confluence of the right and left hepatic ducts in 25.0%, and on EHBD distal to the confluence of the hepatic ducts in 37.5% of patients with IPNB who underwent hepatectomy with liver-side IES. When cancer cells reached the EHBD in front of the IHBD, IES on the IHBD was found in 61.7% of patients. Thus, the liver-side IES from the EHBD often ended in front of the IHBD and extended to the IHBD in a limited conventional eCCAs with a long length of IES or in a part of perihilar eCCAs with stromal invasion of the IHBD.

Duodenal-side IES ended in the ampullary common duct in 20.3%, in the ampullary bile duct in 42.2%, and in 37.5% of patients with conventional eCCA who underwent pancreatoduodenectomy with duodenal-side IES (Table 4B). Duodenal-side IES ended in the ampullary common duct in 30.8%, in the ampullary bile duct in 46.2%, and in 23.1% of patients with IPNB who underwent pancreatoduodenectomy with duodenal-side IES. Thus, the duodenal-side IES on EHBD and the ampullary duct were similar to one tissue without barriers, although it did not reach the duodenum.

IES in CyDCs

The incidence of IES in CyDCs was 80.0%; IES on CyD was found in 25.0% of cases; IES on the gallbladder in 65.0%; IES on EHBD in 40.0% (liver-side in 30.0% and duodenal-side in 15.0%); and no IES on the IHBD, ampullary common duct, or duodenum. The IES from CyDCs extended in both directions of the gallbladder and EHBD in 40.0% of the cases. The incidence of IES in conventional CyDCs and ICPNs is shown in Figure 4 and Supplementary Table 5. CyDCs had a high frequency of IES on both the gallbladder and EHBD, especially in ICPN showing a very high frequency of IES; their incidences were 53% and 27% in conventional CyDCs and 100% and 80% in ICPNs, respectively.

IES of GBCs

IES on the gallbladder was often observed in GBCs, although IES extending into the CyD and EHBD was not observed, which was found in 8.1% and 1.2% of GBCs, respectively. This series contained 30.2% ICPN cases, and ICPNs showed a similar incidence of IES on CyD as conventional GBCs, as shown in Figure 4A and Supplementary Table 5. However, in conventional GBCs and ICPNs that reached the borders between the CyD and the gallbladder, IES on the CyD was found in 62.5% and 100% of cases, respectively (Figure 4B). Thus, GBCs often have an IES, although the IES extension is usually limited to the gallbladder. The low incidence of IES on the CyD in both conventional GBCs and ICPNs

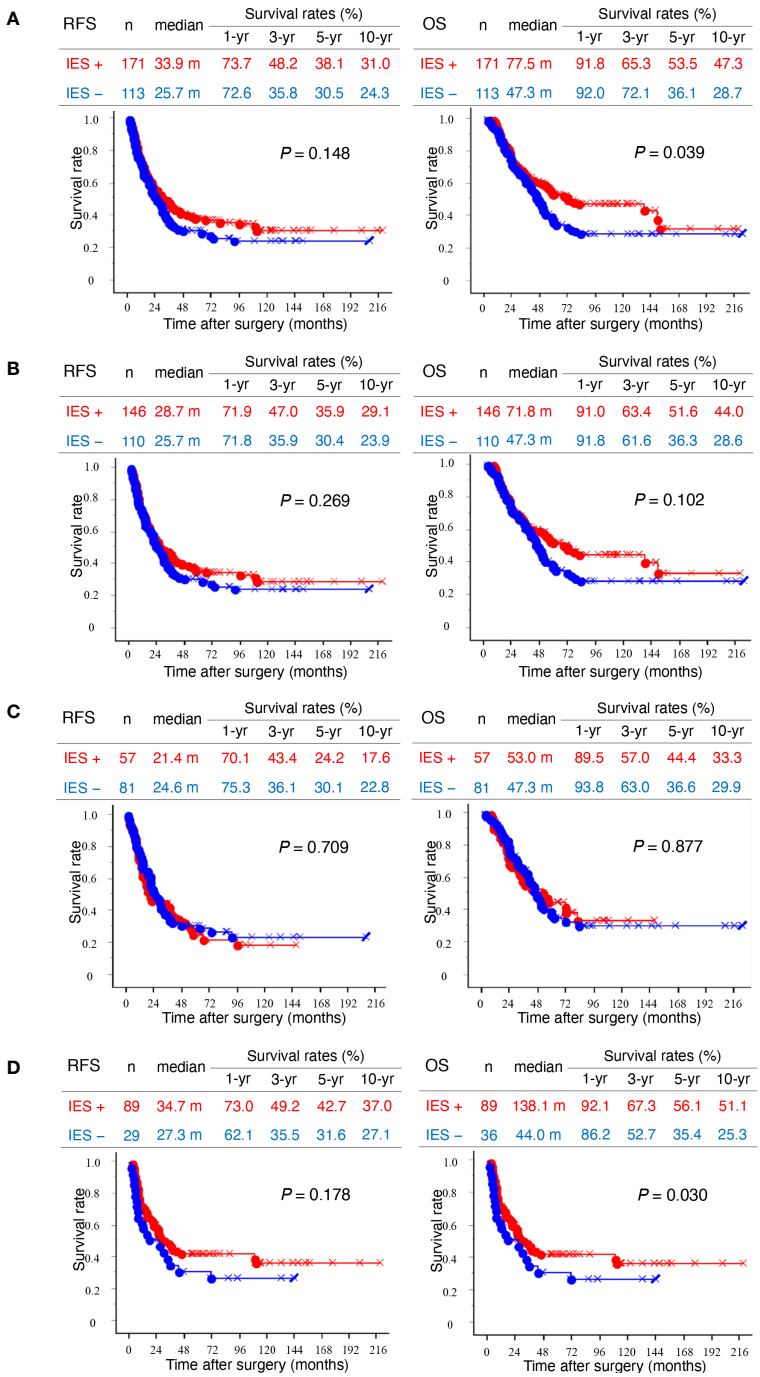

FIGURE 2
Kaplan–Meier survival curves. **(A)** Left and right panels show recurrence-free survival (RFS) and overall survival (OS), respectively. Kaplan–Meier curves of total invasive extrahepatic cholangiocarcinomas (eCCAs) with intraepithelial spread (IES) (red) and without IES (blue) are compared. **(B)** Kaplan–Meier curves of invasive conventional eCCAs with IES (red) and without IES (blue) are compared. **(C)** Kaplan–Meier curves of perihilar eCCAs with IES (red) and without IES (blue) are compared. **(D)** Kaplan–Meier curves of distal eCCAs with IES (red) and without IES (blue) are compared. Differences are examined by a log-rank test.

was presumed to be because the tumor cells did not reach the border between the gallbladder and the CyD.

IES of AVCs

The incidence of IES was investigated in AVCs raised in the ampulla of Vater, except for the ampullary duodenum, which was 60.8%, 54.0%, and 76.9% in total AVCs, conventional AVCs, and IAPNs, respectively. Three directions of the IES beyond the ampulla of Vater were found: the EHBD, main pancreatic duct (MPD), and duodenum. The incidences of these IES are shown in Figure 4B and Supplementary Table 5. These IESs beyond the ampulla of Vater were usually of short length (Supplementary Table 6); IES on EHBD with ≤5 mm in length was in 54.5% of conventional AVCs and in

TABLE 2B Intraepithelial spread of extrahepatic cholangiocarcinomas along with cystic duct.

	Bph eCCA n= 45	Bs eCCA n= 41	Bm eCCA n= 59	Bi eCCA n= 45	invasive IPNB n= 24
CyD-IES, mm					
0	31 (68.9)	33 (80.5)	39 (66.1)	18 (40.0)	6 (25.0)
0 <, < 10	7 (15.6)	1 (2.4)	5 (8.5)	4 (8.9)	5 (20.8)
10 ≤, < 20	6 (13.3)	3 (7.3)	8 (13.6)	10 (22.2)	6 (25.0)
20 ≤, < 30	1 (2.2)	3 (7.3)	2 (3.4)	7 (15.6)	4 (16.7)
30 ≤	0 (0)	1 (2.4)	5 (8.5)	6 (13.3)	3 (12.5)
Status of IES-CyD					
a part of CyD	11 (78.6)	3 (37.5)	12 (60.0)	19 (70.4)	11 (61.1)
entire CyD	2 (14.3)	4 (50.0)	5 (25.0)	7 (25.9)	3 (16.7)
GB and entire CyD	1 (7.1)	1 (12.5)	3 (15.0)	1 (3.7)	4 (22.2)

Values given are the number of patients (percentage) unless otherwise indicated.
Bi, inferior portion of EHBD; Bm, middle portion of EHBD; Bph, (peri)hilar bile duct; Bs, superior portion of EHBD; CyD, cystic duct; CyD-IES, IES along with CyD; eCCA, extrahepatic cholangiocarcinoma; EHBD, extrahepatic bile duct; GB, gallbladder; IES, intraepithelial spread; IPNB, intraductal papillary neoplasm of the bile duct

58.3% of IAPNs; IES on MPD with ≤5 mm in length was in 57.1% of conventional AVCs and in 70.0% of IAPNs. In 98.0% of conventional AVCs, the extension of the IES ended at the border between the ampullary common duct and the duodenum (Figure 5), whereas 30.8% of IAPN cases had the IES extending beyond the border into the duodenum (Figure 4B). There was no IES reaching the IHBD, CyD, or gallbladder, except in one case of IAPN that spread to the CyD. Thus, IES extensions into the EHBD and MPD were found in approximately 20% and 15% of cases, respectively, and short length in both conventional AVCs and IAPNs, although intraepithelial spread on the duodenum was found in approximately 1/3 of IAPNs but not in conventional AVCs.

Discussion

eCCAs are rare and show aggressive behaviors (2), and their clinicopathological characteristics vary depending on their anatomical location (7–10). IES may be a hallmark of one type of extension in cancer biology, in which intraepithelial extension of cancer cells may be predominant over stromal invasion. Hence, stromal invasion is relatively weak in case of IES. This study revealed that the presence of IES was associated with favorable outcomes in eCCAs, although this was dependent on tumor location and type. The incidence and extension properties of IES are also characterized by the tumor location and type. Compared to conventional eCCAs, invasive IPNBs showed a high incidence and a longer extension of IES, often spreading beyond the tissue borders. Invasive IPNBs with IES were also associated with good prognosis. In conventional eCCAs, the incidence of IES was significantly higher in distal eCCAs than in perihilar eCCAs, although the length of the IES extension was comparable (Figure 1). The presence of IES was associated with better outcomes in conventional eCCAs and a significantly longer survival time for OS in distal eCCAs (Figure 2). The presence of CyD-IESs was significantly associated with better outcomes in total invasive eCCAs, invasive conventional eCCAs, and distal eCCAs. The incidence of CyD-IES was higher in distal eCCAs than in perihilar eCCAs, which was reduced to 35–80% of that of IES in each conventional eCCAs. CyD-IES and IES often overlap in the same eCCA cases, and the CyD-IES could more effectively stratify eCCAs to predict patient outcomes. When invasive eCCAs reach the junction of the CyD, CyD-IES is a more useful prognostic factor than IES. It is implied that clinicopathological characteristics are apparently different between perihilar eCCAs and distal eCCAs, and further among Bph, Bs, Bm, and Bi eCCAs, the differences may be due to not only simple location differences but also the biological properties of cancer cells.

The incidence and extension properties of IES also differ depending on the different types of BTCs. All BTCs showed common characteristics in that the incidence of IES was more than a half in tissues that the tumor raised, although IES extension to other tissues beyond the borders decreased the incidence. In addition to these common rules, the incidence and properties of IES differed depending on the tumor location and type (Figure 4). These properties may be useful for determining the primary sites of BTCs.

The presence of IES was a favorable prognostic factor in patients with conventional eCCA in this series. The extensive IES defined as more than 20 mm in length beyond the invasive area, is associated with better patient outcome in eCCAs in the previous reports (11, 13, 15). The extensive IES (≥ 20 mm) was not prognostic in our series, even if the cohort was combined with conventional eCCAs and invasive IPNBs, or was divided by anatomical locations. This discrepancy may be due to the cohort used in the present study. In previous studies (11, 13), researchers have analyzed invasive eCCAs combined with conventional eCCAs and invasive IPNBs, and such cohorts had much higher rates of patients with perihilar eCCAs (74.5% and 82.6%, respectively) than those in this study (51.4%). Since the incidence of IES-positive cases in perihilar eCCAs was low, most of the IES-positive cases in

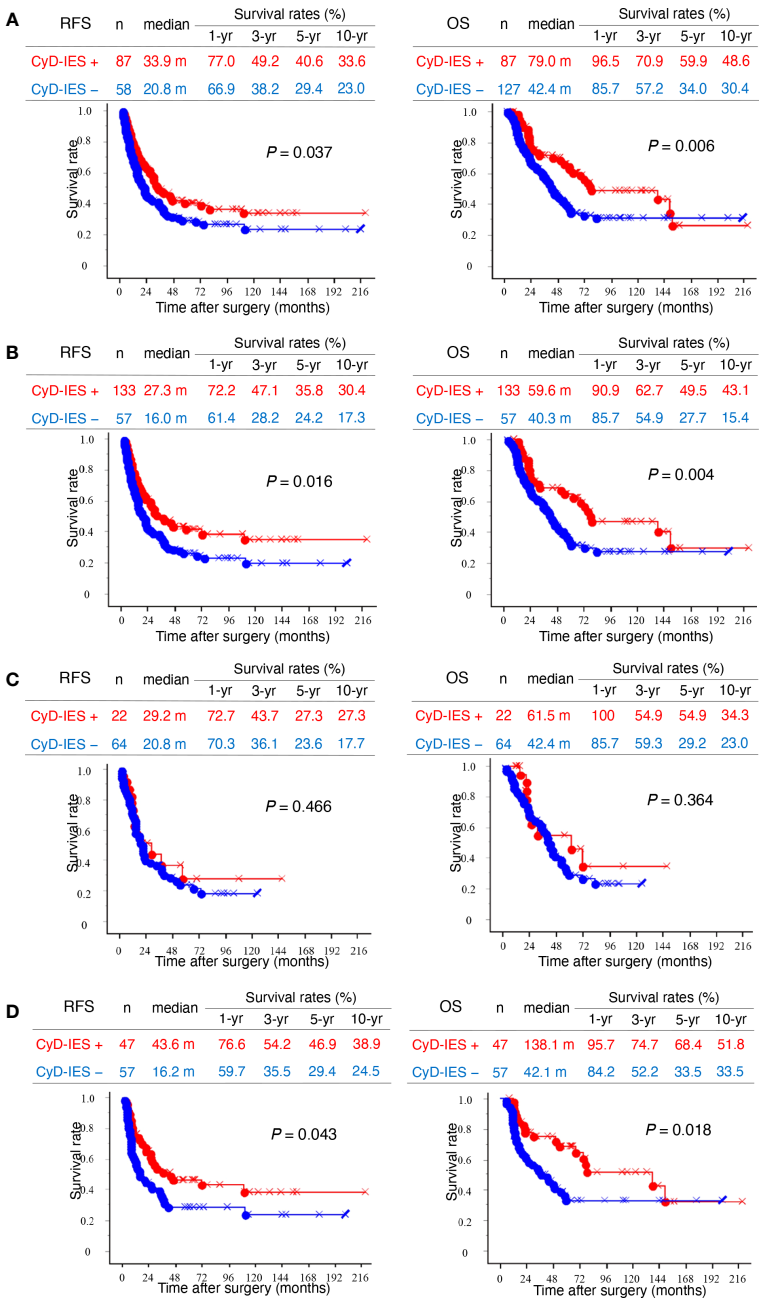

FIGURE 3
Kaplan–Meier survival curves. **(A)** Left and right panels show recurrence-free survival (RFS) and overall survival (OS), respectively. Kaplan–Meier curves of total invasive extrahepatic cholangiocarcinomas (eCCAs) with intraepithelial spread along with cystic duct (CyD-IES) (red) and without CyD-IES (blue) are compared. **(B)** Kaplan–Meier curves of invasive conventional eCCAs with CyD-IES (red) and without CyD-IES (blue) are compared. **(C)** Kaplan–Meier curves of perihilar eCCAs with CyD-IES (red) and without CyD-IES (blue) are compared. **(D)** Kaplan–Meier curves of distal eCCAs with CyD-IES (red) and without CyD-IES (blue) are compared. Differences are examined by a log-rank test.

previous studies were invasive IPNBs, and IES-negative cases were conventional perihilar eCCAs; therefore, the differences in patient outcomes might be significant.

In this study, Bph eCCAs showed unique clinicopathological characteristics compared to other eCCAs. Patients with Bph eCCAs tended to be younger females. Compared to eCCAs, intrahepatic cholangiocarcinoma (iCCA) develops predominantly in males but is more common in females, and the peak incidence age in iCCA is approximately ten years younger than that in eCCAs (28). It is suggested that Bph eCCAs might be similar to iCCAs. Bph eCCAs had much more venous invasion, together with a low incidence of IES in perihilar eCCAs, which is consistent with the aggressive behavior and poor outcomes of perihilar eCCAs. In addition, Bph eCCAs showed unique features in the incidence and properties of IES, especially IES on IHBD, compared to other conventional eCCAs. In contrast, Bi eCCAs showed lower perineural invasion and a higher incidence of IES and CyD-IES, with a better prognosis, similar to that of invasive IPNBs (Supplementary Figure 1).

TABLE 3 Univariate and multivariate analysis of conventional extrahepatic cholangiocarcinomas reached to junction of cystic duct (n = 190).

	Recurrence-free survival				Overall survival			
Variables	Univariate		Multivariate		Univariate		Multivariate	
	HR (95% CI)	P value	HR (95% CI)	P value	HR (95% CI)	P value	HR (95% CI)	P value
Age (>69/≤69 years)	0.979 (0.689-1.388)	0.903			0.922 (0.619-1.365)	0.687		
Gender (female/male)	1.293 (0.829-1.948)	0.249			1.498 (0.929-2.329)	0.095		
Tumor location (perihilar/distal)	1.253 (0.881-1.780)	0.208			1.315 (0.889-1.945)	0.170		
Total tumor size (>55/≤55 mm)	1.325 (0.932-1.878)	0.117			1.143 (0.771-1.685)	0.503		
Invasive tumor size (>40/≤40 mm)	1.673 (1.175-2.375)	0.004	1.139 (0.778-1.666)	0.501	1.523 (1.026-2.250)	0.037	1.028 (0.665-1.582)	0.902
CyD-IES (absence/presence)	1.571 (1.085-2.317)	0.016	1.275 (0.869-1.905)	0.217	1.824 (1.198-2.853)	0.005	1.500 (0.970-2.380)	0.068
Histological grade (G2+G3/G1)	2.153 (1.328-3.722)	0.001	1.893 (1.157-3.295)	0.010	1.982 (1.167-3.639)	0.010	1.767 (1.023-3.285)	0.041
Lymphatic invasion (high/low)	2.288 (1.608-3.272)	<0.001	1.799 (1.180-2.752)	0.006	2.824 (1.900-4.237)	<0.001	1.987 (1.235-3.220)	0.005
Venous invasion (high/low)	2.031 (1.430-2.898)	<0.001	1.243 (0.819-1.894)	0.307	2.558 (1.724-3.835)	<0.001	1.477 (0.930-2.367)	0.997
Perineural invasion (high/low)	2.237 (1.342-4.012)	0.001	1.422 (0.816-2.643)	0.222	2.027 (1.180-3.760)	0.009	1.193 (0.663-2.302)	0.570
Residual tumor status (microscopic residual tumor/no residual tumor)	1.941 (1.357-2.804)	<0.001	1.764 (1.194-2.629)	0.004	1.612 (1.090-2.405)	0.017	1.487 (0.960-2.318)	0.076
Lymph node metastasis (presence/absence)	2.272 (1.591-3.272)	<0.001	1.321 (0.878-2.000)	0.182	2.527 (1.698-3.809)	<0.001	1.117 (0.913-2.308)	0.117

CyD, cystic duct; CyD-IES, IES along with CyD; IES, intraepithelial spread.

The biliary tree differentiates from a few different anlagen raised in the hepatic diverticulum during embryonic development; the proximal part of the hepatic ducts and intrahepatic bile ducts are developed from the ductal plate that appears in the hepatic hilus in the developing liver; the distal part of hepatic ducts, common hepatic duct, and common bile duct are formed from the caudal part of the liver bud, and the gallbladder with the cystic duct is formed from the gallbladder anlage (29–31). These tissue borders based on embryonic development almost correspond to the extension of IES in BTCs, with some tissue-dependent modifications.

The border between the IHBD and EHBD is sometimes difficult to determine because there are many variations in bile duct branching, including in this area. Certain IHBD are the liver side of the third branch of the bile duct (e.g., segmental ducts 5 and 8), and certain EHBD are the duodenal side of the common hepatic duct, while it is possible that the border between the IHBD and EHBD might vary by individual within the perihilar bile ducts between them. Most endpoints of the liver-side IES were found in this area (Table 4A). It was assumed that the endpoints of the liver-side IES represented the border. The incidence of IES in perihilar eCCAs was lower, and IES in IHBD was rare when IES extended from the EHBD to the IHBD in conventional eCCAs. In contrast, most perihilar eCCA with IES on IHBD had stromal invasion of the IHBD area without IES on EHBD. It is possible that some of these perihilar eCCAs developed from the IHBD and extended from the IES to the IHBD.

The duodenal-side IES extended on the EHBD and ampullary ducts, as they are one tissue without potential extension barriers. This might be reasonable because both ducts develop into one tube in the embryonic developmental stage. The actual duodenal-side tissue border should be at the border between the ampullary common duct and the duodenum. The IES of conventional AVCs that develop in the common duct or ampullary bile duct usually ends at the common duct-duodenal border, and in 30% of IAPNs, the intraepithelial spread extends beyond the border into the duodenum.

CyD develops from the gallbladder anlage during the embryonic stage, and the histological structure of CyD is the same as that of EHBD, but different from that of the gallbladder, suggesting that CyD is similar to a zone of brackish water. CyD may overlap biologically (i.e., molecular expression) with EHBD and the gallbladder. The incidence of IES in the gallbladder from conventional CyDCs that reached the border between the gallbladder and CyD and the incidence of IES in the CyD from

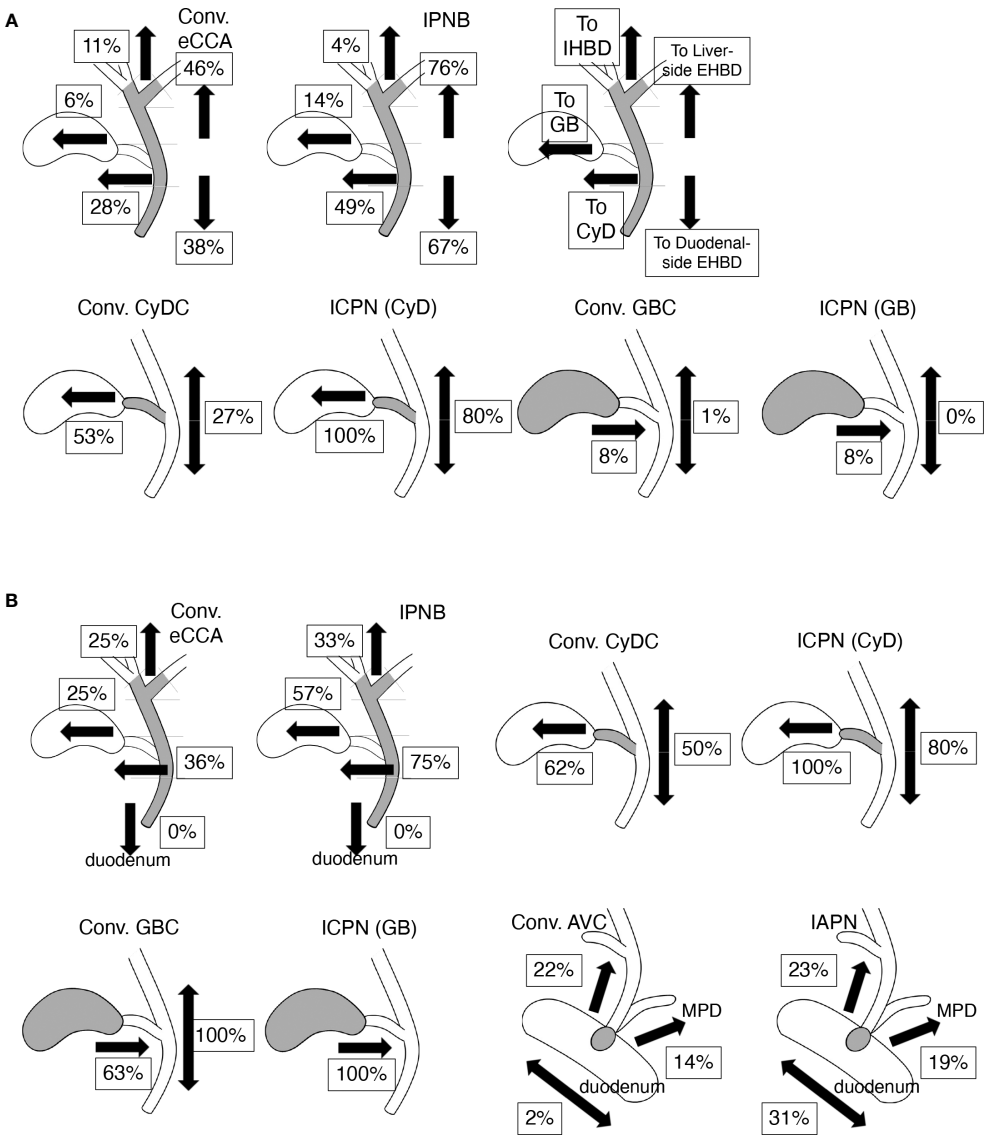

FIGURE 4
Incidence and profiles of intraepithelial spread (IES) of bile tract cancers (BTCs). Values indicate percentages of IES in each tissue and each direction on biliary tract. Values represent incidence that ratio of positive case among total cases in **(A)** and values represent incidence ratio of positive case to cases in which cancer cells reach tissue border closest to the assessed IES (e.g., the junction of CyD for assessing IES on EHBD in CyDCs) in **(B)**. **(A)** The incidence and profiles of IES in conventional (conv.) extrahepatic cholangiocarcinomas (eCCAs) and intraductal papillary neoplasms of the bile duct (IPNBs) are shown in upper line. Incidence of IES in liver- or duodenal-side on extrahepatic bile duct (EHBD) is shown on right side in each panel. Incidences of IES on intrahepatic bile duct (IHBD), IES on gallbladder (GB), and IES on cystic duct (CyD) are shown on the left side in each panel. Incidence of IES in the gallbladder and EHBD in conventional (conv.) cystic duct cancers (CyDCs) or intracholecystic papillary neoplasms (ICPNs) arising from CyD are depicted in the lower line. Incidence of IES in CyD and EHBD in the conventional (conv.) gallbladder cancers (GBCs) or ICPNs arising in gallbladder are also found on the lower line. **(B)** The incidence of IES extended to various tissues other than the tissue in which the tumors developed in BTCs. The incidence values of IES beyond the ampullary area, including IES on the EHBD, IES on main pancreatic duct (MPD), intraepithelial spread into the duodenum in conventional ampullary cancers (conv. AVCs), and intraampullary papillary tubular neoplasms (IAPNs) are shown in the lower right panels.

conventional GBCs that reached the border were almost the same (62% and 63%, respectively) (Figure 4B). Similarly, the incidence of IES in the gallbladder from the ICPNs of the CyD and that of IES in CyD from the ICPNs of the gallbladder were both 100%. It is suggested that the CyD and the gallbladder might be recognized as similar tissues by GBCs and CyDCs with respect to IES extension, as represented by the developmental event in which these tissues develop from the gallbladder anlage. Fifty percent of conventional CyDCs that reached the junction of the CyD had an IES on the EHBD, and 36% of conventional eCCAs reached the junction of the CyD with the CyD-IES. This difference in incidence might be attributed to the difference in distances from the invasive cancers to the junction of the CyD.

IPNB, ICPN, and IAPN are thought to be counterpart entities of pancreatic intraductal papillary mucinous neoplasms. The extension property of IES from ICPNs is similar to that of IPNBs, in which IES often extends beyond tissue borders compared to conventional types of cancers and has a relatively longer length. However, ICPNs spread

TABLE 4A Intraepithelial spread of extrahepatic cholangiocarcinomas directed to intrahepatic bile ducts.

		perihilar eCCA cases undertaken hepatectomy with liver-side IES (n=39)	distal eCCA cases undertaken hepatectomy with liver-side IES (n=9)	invasive IPNB cases undertaken hepatectomy with liver-side IES (n=8)
liver-side end position of IES				
at IHBD		22*	7	1
at EHBD in front of IHBD	around the confluence of and on the second branches **	8	2	0
	hepatic ducts	8	0	2
at confluence of right and left hepatic ducts		1	0	1
at EHBD distal to the confluence of hepatic ducts	Bs	0	0	4

*containing 21 cases with stromal invasion reached to IHBD area and one case with IES extended from Bs. **right posterior or anterior sectoral ducts or segmental ducts of 2, 3, or 4. Bs, superior portion of EHBD; eCCA, extrahepatic cholangiocarcinoma; EHBD, extrahepatic bile duct; IES, intraepithelial spread; IHBD, intrahepatic bile duct; IPNB, intraductal papillary neoplasm of the bile duct.

TABLE 4B Intraepithelial spread of extrahepatic cholangiocarcinomas directed to ampullary area.

		perihilar eCCA cases undertaken pancreatoduodenectomy with duodenal-side IES (n=8)	distal eCCA cases undertaken pancreatoduodenectomy with duodenal-side IES (n=56)	IPNB cases undertaken pancreatoduodenectomy with duodenal-side IES (n=13)
duodenal-side end position of IES				
at duodenum		0	0	0
at ampullary area	ampullary common duct	0	13	4
	ampullary bile duct	2	25	6
at EHBD	Bi	6	18	3

Bi, inferior portion of EHBD; eCCA, extrahepatic cholangiocarcinoma; EHBD, extrahepatic bile duct; IES, intraepithelial spread; IHBD, intrahepatic bile duct; IPNB, intraductal papillary neoplasm of the bile duct.

more frequently beyond the border between the gallbladder and CyD compared to IPNBs. This difference may be explained by the distance from the main tumor. Similarly, both IPNBs and ICPNs of the CyD extended the IES frequently *via* the junction of the CyD, although the ICPNs of the gallbladder did not reach the junction. In contrast, IAPNs revealed different characteristics from IPNBs and ICPNs in the incidence and extension properties of IES, which did not have a longer IES. IAPNs had similar properties to conventional AVCs in IES for EHBD and MPD. However, IAPNs showed an apparently higher frequency of intraepithelial spread into the duodenum compared to conventional AVCs. It is necessary to characterize these similar entities to establish their positions.

From a clinical standpoint, perioperative chemotherapy is a standard strategy, even for resectable eCCAs and PDACs. The presence of IES revealed by pathological investigation may be an indicator of the postoperative treatment strategy. More importantly, the different incidences of IES and related outcomes suggest biological differences between perihilar and distal eCCAs. Along with integrative molecular profiling analyses, targeted therapies have been developed for advanced eCCAs and iCCAs (32–34). Genetic or molecular alterations in CCAs related to tumor localization and the presence of IES are still limited. Investigating molecular or genetic differences is imperative for identifying clinical features and establishing targeted therapeutic options.

This study has several limitations. First, this was a retrospective study conducted in a single-center cohort. Second, differences in the adapted surgical procedures, including lymph node dissection, could affect survival outcomes. However, this study included a relatively large number of eCCAs, and the therapeutic strategy did not change significantly during the study period. Additionally, a

10.3389/fonc.2023.1216097

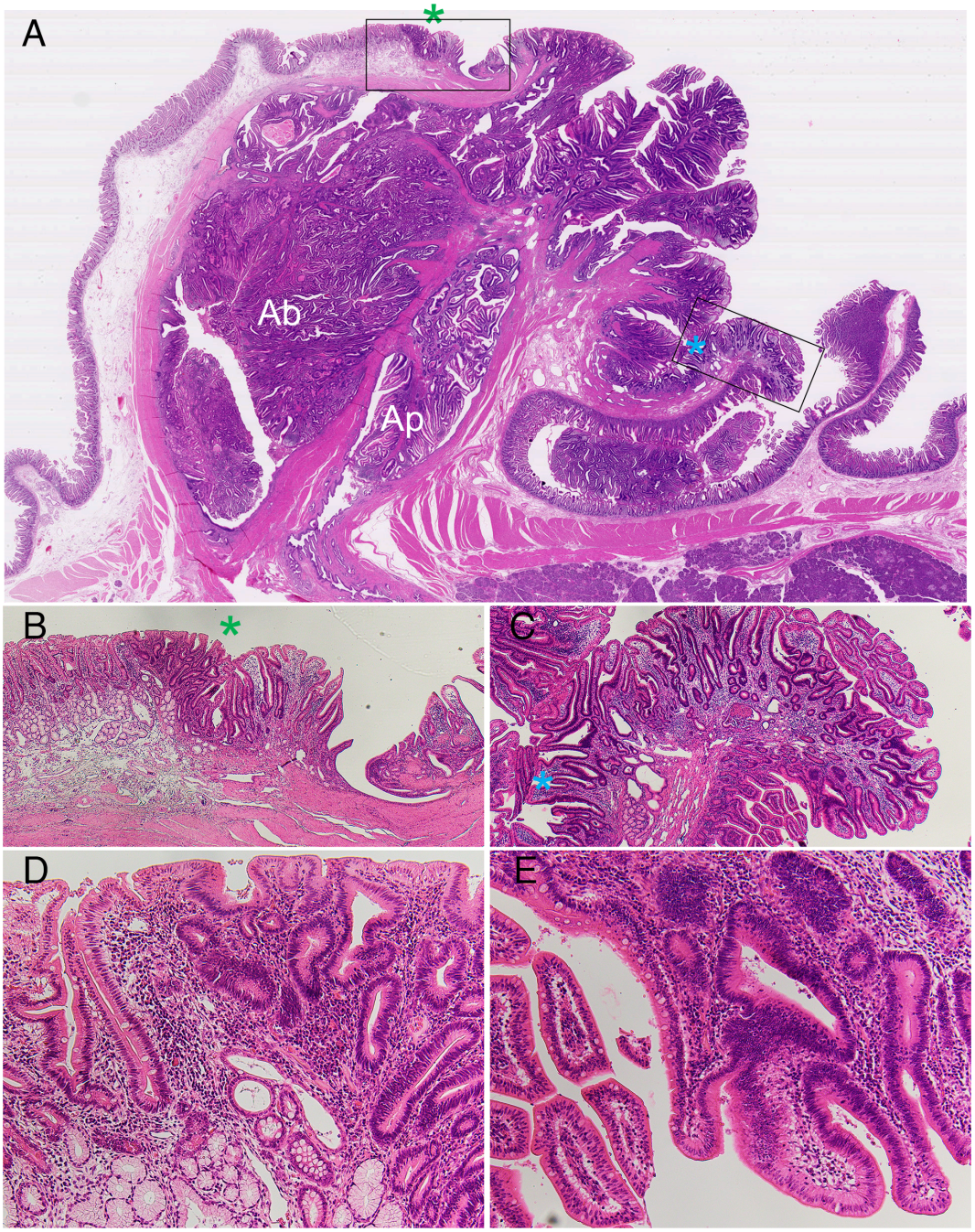

FIGURE 5
Histology of intraepithelial spread of cancer cells from ampullary common duct to duodenum in ampullary cancer. At an opening of ampullary common duct surrounded by Oddi sphincter, Oddi sphincter anastomoses to muscularis mucosa in duodenal mucosal layer (*). An opening of common duct is covered by epithelial cells of common duct that continue to the duodenal covering epithelium on the border of *. The Brunner's glands are found in the duodenum. Right and left side borders are indicated by blue-colored * and green-colored *. Cancer cells with papillary growth extend along common duct and replace the existing covering epithelium beyond the borders (*). **(A)** is loupe figure; **(B, C)** are in low power view corresponded to left and right squares in **(A)** respectively; **(D, E)** are in middle power view.

pathological diagnosis was made based on a detailed pathological examination in each case. This consistency in the treatment and diagnosis is an advantage of this study. As there are still few studies investigating IES in eCCAs, further investigation is required to identify IES and their characteristics.

In conclusion, the IES was a favorable factor in patients with eCCA, although it was not as strongly favorable as previously reported. CyD-IES is also a favorable factor and may be more useful for IES when eCCAs reach the CyD junction. The clinicopathological characteristics of eCCAs vary depending on their anatomical location and type, especially between perihilar and distal eCCAs. The incidence and extension properties of IES also differ depending on the different types of BTCs. We hypothesize that the extension profiles of the IES may represent

the tumor cell origin as well as the biological characteristics of cancer.

Data availability statement

The datasets used and analyzed during the current study are available from the corresponding author upon reasonable request.

Ethics statement

This study was approved by the Institutional Review Board of National Cancer Center Hospital, Japan (#2016-006). Informed consent was obtained from all patients, and all clinical assessments were conducted in accordance with the principles of the Declaration of Helsinki.

Author contributions

Study concept and design: DN and NH. Acquisition of data, analysis, and interpretation of data: DN and NH. Drafting of the manuscript: DN. Critical revision of the manuscript for important intellectual content: ME, SN, DB, TT, TM, KS, and NH. Obtained funding: NH. Technical or material support: ME, SN, DB, TT, TM, KS, and NH. Study supervision, NH. All authors contributed to the article and approved the submitted version.

Funding

This work was supported by a Grant-in-Aid for Scientific Research from the Ministry of Education, Culture, Sports, Science and Technology of Japan, #21K07139 (NH), and the Japan Agency for Medical Research and Development, #21ck0106540 (NH).

Acknowledgments

The authors thank Ms. Sachiko Miura, Toshiko Sakaguchi, and Chizu Kina for excellent techniques. We are grateful to the National Cancer Center Biobank for the tissue samples used in this study.

Conflict of interest

The authors declare that the research was conducted in the absence of any commercial or financial relationships that could be construed as a potential conflict of interest.

Publisher's note

Supplementary material

The Supplementary Material for this article can be found online at: https://www.frontiersin.org/articles/10.3389/fonc.2023.1216097/full#supplementary-material

References

1. Nakanuma Y, Klimstra DS, Komuta M, Zen Y. Intrahepatic cholangiocarcinoma. In: Carneiro F, editor. *World Health Organization Classification of Tumours 5th Edition Digestive System Tumours*. Lyon: IARC Press (2019). p. 254–9.

2. Roa JC, Adsay NV, Arola J, Tsui WM, Zen Y. Carcinoma of the extrahepatic bile ducts. In: Carneiro F, editor. *World Health Organization Classification of Tumours 5th Edition Digestive System Tumours*. Lyon: IARC Press (2019). p. 289–91.

3. Van Dyke AL, Shiels MS, Jones GS, Pfeiffer RM, Petrick JL, Beebe-Dimmer JL, et al. Biliary tract cancer incidence and trends in the United States by demographic group, 1999-2013. *Cancer* (2019) 125:1489–98. doi: 10.1002/cncr.31942

4. Florio AA, Ferlay J, Znaor A, Ruggieri D, Alvarez CS, Laversanne M, et al. Global trends in intrahepatic and extrahepatic cholangiocarcinoma incidence from 1993 to 2012. *Cancer* (2020) 126:2666–78. doi: 10.1002/cncr.32803

5. Valle JW, Kelley RK, Nervi B, Oh DY, Zhu AX. Biliary tract cancer. *Lancet* (2021) 397:428–44. doi: 10.1016/S0140-6736(21)00153-7

6. Brierley JD, Gospodarowicz MK, Wittekind C. *TNM classification of Malignant tumours*. Hoboken, NJ: Wiley-Blackwell (2017).

7. Akita M, Fujikura K, Ajiki T, Fukumoto T, Otani K, Azuma T, et al. Dichotomy in intrahepatic cholangiocarcinomas based on histologic similarities to hilar cholangiocarcinomas. *Mod Pathol* (2017) 30:986–97. doi: 10.1038/modpathol.2017.22

8. Boottanun P, Ino Y, Shimada K, Hiraoka N, Angata K, Narimatsu H. Association between the expression of core 3 synthase and survival outcomes of patients with cholangiocarcinoma. *Oncol Lett* (2021) 22:760. doi: 10.3892/ol.2021.13021

9. Hiraoka N, Nitta H, Ohba A, Yoshida H, Morizane C, Okusaka T, et al. Details of human epidermal growth factor receptor 2 status in 454 cases of biliary tract cancer. *Hum Pathol* (2020) 105:9–19. doi: 10.1016/j.humpath.2020.08.006

10. Ishida K, Osakabe M, Eizuka M, Tai S, Sugimoto R, Fujita Y, et al. The expression of gastrointestinal differentiation markers in extrahepatic cholangiocarcinoma: clinicopathological significance based on tumor location. *Hum Pathol* (2019) 92:91–100. doi: 10.1016/j.humpath.2019.08.002

11. Igami T, Nagino M, Oda K, Nishio H, Ebata T, Yokoyama Y, et al. Clinicopathologic study of cholangiocarcinoma with superficial spread. *Ann Surg* (2009) 249:296–302. doi: 10.1097/SLA.0b013e318190a647

12. Kawahira H, Hasebe T, Kinoshita T, Sasaki S, Konishi M, Nakagori T, et al. The intraductal carcinoma component is a significant prognostic parameter in patients with invasive ductal carcinoma of the pancreas. *Jpn J Cancer Res* (2002) 93:1138–44. doi: 10.1111/j.1349-7006.2002.tb01216.x

13. Nakanishi Y, Zen Y, Kawakami H, Kubota K, Itoh T, HIrano S, et al. Extrahepatic bile duct carcinoma with extensive intraepithelial spread: a clinicopathological study of 21 cases. *Mod Pathol* (2008) 21:807–16. doi: 10.1038/modpathol.2008.65

14. Ojima H, Kanai Y, Iwasaki M, Hiraoka N, Shimada K, Sano T, et al. Intraductal carcinoma component as a favorable prognostic factor in biliary tract carcinoma. *Cancer Sci* (2009) 100:62–70. doi: 10.1111/j.1349-7006.2008.01009.x

15. Sakamoto E, Nimura Y, Hayakawa N, Kamiya J, Kondo S, Nagino M, et al. The pattern of infiltration at the proximal border of hilar bile duct carcinoma: a histologic

analysis of 62 resected cases. *Ann Surg* (1998) 227:405–11. doi: 10.1097/00000658-199803000-00013

16. Takahashi H, Oda T, Hasebe T, Aoyagi Y, Kinoshita T, Konishi M, et al. Biologically different subgroups of invasive ductal carcinoma of the pancreas: Dpc4 status according to the ratio of intraductal carcinoma components. *Clin Cancer Res* (2004) 10:3772–9. doi: 10.1158/1078-0432.CCR-03-0120

17. Sasaki R, Takeda Y, Funato O, Nitta H, Kawamura H, Uesugi N, et al. Significance of ductal margin status in patients undergoing surgical resection for extrahepatic cholangiocarcinoma. *World J Surg* (2007) 31:1788–96. doi: 10.1007/s00268-007-9102-7

18. Tsukahara T, Ebata T, Shimoyama Y, Yokoyama Y, Igami T, Sugawara G, et al. Residual Carcinoma *In Situ* at the Ductal Stump has a Negative Survival Effect: An Analysis of Early-stage Cholangiocarcinomas. *Ann Surg* (2017) 266:126–32. doi: 10.1097/SLA.0000000000001944

19. Wakai T, Shirai Y, Moroda T, Yokoyama N, Hatakeyama K. Impact of ductal resection margin status on long-term survival in patients undergoing resection for extrahepatic cholangiocarcinoma. *Cancer* (2005) 103:1210–6. doi: 10.1002/cncr.20906

20. You Y, Choi SH, Choi DW, Heo JS, Han IW, Jang KT, et al. Recurrence after resection for intraductal papillary neoplasm of bile duct (IPNB) according to tumor location. *J Gastrointest Surg* (2020) 24:804–12. doi: 10.1007/s11605-019-04235-8

21. Nakachi K, Ikeda M, Konishi M, Nomura S, Katayama H, Kataoka T, et al. Adjuvant S-1 compared with observation in resected biliary tract cancer (JCOG1202, ASCOT): a multicentre, open-label, randomised, controlled, phase 3 trial. *Lancet* (2023) 401:195–203. doi: 10.1016/S0140-6736(22)02038-4

22. Ito Y, Abe Y, Egawa T, Kitago M, Itano O, Kitagawa Y. Predictive factors of early recurrence in patients with distal cholangiocarcinoma after pancreaticoduodenectomy. *Gastroenterol Res Pract* (2018) 2018:6431254. doi: 10.1155/2018/6431254

23. Sahara K, Tsilimigras DI, Toyoda J, Miyake K, Ethun CG, Maithel SK, et al. Defining the risk of early recurrence following curative-intent resection for distal cholangiocarcinoma. *Ann Surg Oncol* (2021) 28:4205–13. doi: 10.1245/s10434-021-09811-4

24. Adsay NV, Reid MD. Ampullary adenocarcinoma. In: Carneiro F, editor. *World Health Organization Classification of Tumours 5th Edition Digestive System Tumours*. Lyon: IARC Press (2019). p. 127–30.

25. Roa JC, Adsay NV, Arola J, Tsui WM, Zen Y. Carcinoma of the gallbladder. In: Carneiro F, editor. *World Health Organization Classification of Tumours 5th Edition Digestive System Tumours*. Lyon: IARC Press (2019). p. 283–8.

26. Miyazaki M, Ohtsuka M, Miyakawa S, Nagino M, Yamamoto M, Kokudo N, et al. Classification of biliary tract cancers established by the Japanese Society of Hepato-Biliary-Pancreatic Surgery: 3(rd) English edition. *J Hepatobiliary Pancreat Sci* (2015) 22:181–96. doi: 10.1002/jhbp.211

27. Japanese Society of Biliary Surgery. *Classification of Biliary Tract Carcinoma. 2nd English Edition*. Tokyo: Kanehara & Co., Ltd. (2004).

28. Siegel RL, Miller KD, Fuchs HE, Jemal A. Cancer statistics, 2022. *CA Cancer J Clin* (2022) 72:7–33. doi: 10.3322/caac.21708

29. Ando H. Embryology of the biliary tract. *Dig Surg* (2010) 27:87–9. doi: 10.1159/000286463

30. Lemaigre FP. Development of the intrahepatic and extrahepatic biliary tract: A framework for understanding congenital diseases. *Annu Rev Pathol* (2020) 15:1–22. doi: 10.1146/annurev-pathmechdis-012418-013013

31. Tan CE, Moscoso GJ. The developing human biliary system at the porta hepatis level between 29 days and 8 weeks of gestation: a way to understanding biliary atresia. *Part 1. Pathol Int* (1994) 44:587–99. doi: 10.1111/j.1440-1827.1994.tb01719.x

32. Lee MS, Menter DG, Kopetz S. Right versus left colon cancer biology: integrating the consensus molecular subtypes. *J Natl Compr Canc Netw* (2017) 15:411–9. doi: 10.6004/jnccn.2017.0038

33. Mazzaferro V, El-Rayes BF, Droz Dit Busset M, Cotsoglou C, Harris WP, Damjanov N, et al. Derazantinib (ARQ 087) in advanced or inoperable FGFR2 gene fusion-positive intrahepatic cholangiocarcinoma. *Br J Cancer* (2019) 120:165–71. doi: 10.1038/s41416-018-0334-0

34. Sia D, Hoshida Y, Villanueva A, Roayaie S, Ferrer J, Tabak B, et al. Integrative molecular analysis of intrahepatic cholangiocarcinoma reveals 2 classes that have different outcomes. *Gastroenterology* (2013) 144:829–40. doi: 10.1053/j.gastro.2013.01.001

frontiers | Frontiers in Pharmacology

TYPE Original Research
PUBLISHED 05 September 2023
DOI 10.3389/fphar.2023.1234342

OPEN ACCESS

EDITED BY
Maria Lina Tornesello,
G. Pascale National Cancer Institute Foundation (IRCCS), Italy

REVIEWED BY
Rui Dai,
Massachusetts General Hospital and Harvard Medical School, United States
Kang Wang,
Eastern Hepatobiliary Surgery Hospital, China

*CORRESPONDENCE
Minshan Chen,
chenmsh@sysucc.org.cn
Yaojun Zhang,
zhangyuj@sysucc.org.cn

†These authors have contributed equally to this work

RECEIVED 04 June 2023
ACCEPTED 21 August 2023
PUBLISHED 05 September 2023

CITATION
Yang Z, Fu Y, Wu W, Hu Z, Pan Y, Wang J, Chen J, Hu D, Zhou Z, Chen M and Zhang Y (2023), Comparison of hepatic arterial infusion chemotherapy with mFOLFOX vs. first-line systemic chemotherapy in patients with unresectable intrahepatic cholangiocarcinoma. *Front. Pharmacol.* 14:1234342. doi: 10.3389/fphar.2023.1234342

Comparison of hepatic arterial infusion chemotherapy with mFOLFOX vs. first-line systemic chemotherapy in patients with unresectable intrahepatic cholangiocarcinoma

Zhenyun Yang[1,2†], Yizhen Fu[1,2†], Weijie Wu[1,2†], Zili Hu[1,2], Yangxun Pan[1,2], Juncheng Wang[1,2], Jinbin Chen[1,2], Dandan Hu[1,2], Zhongguo Zhou[1,2], Minshan Chen[1,2*] and Yaojun Zhang[1,2*]

[1]State Key Laboratory of Oncology in South China, Collaborative Innovation Center for Cancer Medicine, Sun Yat-Sen University Cancer Center, Guangzhou, Guangdong, China, [2]Department of Liver Surgery, Sun Yat-Sen University Cancer Center, Guangzhou, Guangdong, China

Background: Systemic chemotherapy (SC) remains the only first-line treatment for unresectable intrahepatic cholangiocarcinoma (iCCA). Hepatic arterial infusion chemotherapy (HAIC) has been recently proven to be effective in managing hepatocellular carcinoma (HCC). Hence, our study aims to investigate the safety and efficacy of HAIC in treating unresectable iCCA patients.

Methods: We reviewed 146 patients with unresectable iCCA who had received HAIC or SC between March 2016 and March 2022 in a retrospective manner. Outcomes of patients and safety were compared between the HAIC and SC groups.

Results: There were 75 and 71 patients in the HAIC and SC groups, respectively. The median OS in the HAIC and SC groups was 18.0 and 17.8 months (p = 0.84), respectively. The median PFS in the HAIC and SC groups was 10.8 and 11.4 months (p = 0.59), respectively. However, the HAIC group had significantly longer intrahepatic progression-free survival (IPFS) than the SC group (p = 0.035). The median IPFS in the HAIC and SC groups was 13.7 and 11.4 months, respectively. According to the OS (p = 0.047) and PFS (p = 0.009), single-tumor patients in the HAIC group appeared to benefit more. In addition, the overall incidence of adverse events (AEs) was lower in the HAIC group than that in the SC group.

Conclusion: Our study revealed that HAIC was a safe and effective therapeutic regimen for unresectable iCCA with better intrahepatic tumor control when compared to SC. Meanwhile, patients with single tumor were more likely to benefit from HAIC than SC.

KEYWORDS

intrahepatic cholangiocarcinoma, hepatic arterial infusion chemotherapy, systemic chemotherapy, overall survival, progression-free survival, adverse events

Introduction

Intrahepatic cholangiocarcinoma (iCCA) is the second most frequent primary liver cancer with a poor prognosis and high level of malignancy (Bridgewater et al., 2014; Sirica et al., 2019; Valle et al., 2021). The incidence of iCCA is higher in Thailand and China (6 per 100,000 people) than that in Western Europe and North America (0·35 to 2 per 100,000 people) (Banales et al., 2016; Oh et al., 2022). Over the next 20–30 years, the incidence of iCCA will increase ten-fold worldwide (Rodriguez and Pennington, 2018; Dong et al., 2022). Surgical resection is currently the first-line and curative therapy for iCCA management. However, most iCCA patients are diagnosed at a late stage as a result of the absence of specific clinical symptoms and limited treatment modalities for iCCA (Rizvi and Gores, 2013; Bupathi et al., 2017; Rizvi et al., 2018).

Currently, the first-line systemic chemotherapy (SC) for biliary tract cancer is gemcitabine plus cisplatin (GEMCIS), with a median overall survival (OS) of 11.7 months (Valle et al., 2010). Oxaliplatin plus gemcitabine (GEMOX) is also a common treatment regimen for biliary tract cancer patients in Asia, with a similar median OS compared to GEMCIS (Fiteni et al., 2014; Kim et al., 2019). The FOLFOX regimen may be an option for the palliative treatment of advanced cholangiocarcinoma (Nehls et al., 2002; Caparica et al., 2019; Lamarca et al., 2021).

Hepatic arterial infusion chemotherapy (HAIC) enables the delivery of chemotherapy drugs directly into the liver. Tumors derive most of their nutrients from the arteries, whereas the liver derives nutrients from the portal vein, which may reduce systemic adverse events (AEs) from systemic chemotherapy (Kemeny et al., 1984; Cercek et al., 2020). Meanwhile, previous studies have clarified that HAIC is useful for advanced iCCA and has shown higher tumor control rates compared to systemic chemotherapy (Kasai et al., 2014; Cercek et al., 2020). However, there was no study comparing HAIC with FOLFOX and first-line systemic chemotherapy in relation to patients' outcomes and AEs.

Herein, the current study compares the clinical outcomes and tumor response of patients with unresectable iCCA treated with HAIC and SC. In addition, the assessment of safety and AEs were also vital in this retrospective study.

Materials and methods

Patients' recruitment and selection criteria

This is a retrospective study, and the study subjects consisted of 146 patients diagnosed with iCCA who were initially treated with HAIC or first-line SC between March 2016 and March 2022 at Sun Yat-sen University Cancer Center, China. Participants were included if they conformed to the following criteria: (Bridgewater et al., 2014) age 18 years old or elder; (Sirica et al., 2019) histopathological evidence confirmation of iCCA; (Valle et al., 2021) confirmed records of primary HAIC or first-line SC; (Oh et al., 2022) an Eastern Cooperative Oncology Group (ECOG) score of 2 or below; and (Banales et al., 2016) complete medical follow-up data. Patients were excluded based on the following exclusion criteria: (Bridgewater et al., 2014) patients with any other malignant tumor and (Sirica et al., 2019) patients who had contraindications to HAIC and SC.

Treatment procedures

HAIC was performed according to our previously reported protocol (Li et al., 2022). Femoral artery puncture and catheterization were performed on day 1 of the HAIC cycle, and the patient was transferred to the inpatient ward for drug infusion through the hepatic artery. Oxaliplatin was administered at 130 mg/m^2 from 0 to 2 h on day 1; leucovorin was administered at 400 mg/m^2 from 2 to 3 h on day 1; fluorouracil was administered at 400 mg/m^2 from hour 3 on day 1. Infusional fluorouracil was given at 2400 mg/m^2 over 23 h or 46 h. HAIC cycles were performed every 3 weeks. In the GEMCIS group, each cycle comprised cisplatin (25 mg per square meter of body-surface area), followed by gemcitabine (1,000 mg per square meter), which was administered on days 1 and 8 every 3 weeks. In the GEMOX group, each cycle comprised oxaliplatin (85 mg/m2) on day 1 and gemcitabine (1,000 mg per square meter) between days 1 and 8 every 3 weeks. HAIC or SC was suspended at 24 weeks or because of disease progression, unacceptable toxic effects, or patient's own choice. As a part of treatment, HAIC or SC may be combined with the PD-1 inhibitor or tyrosine kinase inhibitor according to the needs of the condition and patient's own choice.

Data collection

All clinical data were obtained from the medical records of the Sun Yat-sen University Cancer Center. Demographic and clinical characteristics included age, sex, hepatitis infection status, ECOG, aspartate aminotransferase (AST), alanine transaminase (ALT), albumin (ALB), total bilirubin (TBIL), carcinoembryonic antigen (CEA), carbohydrate antigen 19–9 (CA19–9), white blood cell count (WBC), platelet count (PLT), creatinine (CRE), largest tumor size, tumor number, macroscopic vascular invasion, lymph node metastasis, extra-hepatic metastasis, and tumor–node–metastasis (TNM) stages. A summary of demographic and clinical characteristics is presented in Table 1. The blood tests and tumor burdens were measured within 5 days before the treatment. After treatment had been initiated, the radiological response was evaluated by magnetic resonance imaging (MRI) or computed tomography (CT) performed at baseline and every 6 weeks. Response Evaluation Criteria in Solid Tumors (RECIST)1.1 and modified RECIST (mRECIST) were used for evaluating the tumor response (Eisenhauer et al., 2009; Llovet and Lencioni, 2020).

Overall survival (OS) was defined as the time interval from first-line treatment to cancer-related death. Progression-free survival (PFS) was defined as the interval from first-line treatment to disease progression, iCCA relapse, or the date of death from iCCA or the date of the last follow-up. Intrahepatic progression-free survival (IPFS) was defined as the interval from the first-line treatment to intrahepatic tumor progression, iCCA relapse, or the date of death from iCCA or the date of the last follow-up, regardless of extrahepatic metastasis.

TABLE 1 Baseline characteristics of two group patients.

Variable	HAIC group (n = 75)	SC group (n = 71)	*p*-value
Age (years)	54 (28–78)	57 (32–80)	0.152
Gender (men/women)	52/23 (69.3/30.7)	40/31 (56.3/43.7)	0.104
Hepatitis (yes/no)	34/41 (45.3/54.7)	25/46 (35.2/64.8)	0.213
ECOG (1–2/0)	45/30 (60/40)	40/31 (56.3/43.7)	0.654
Preoperative blood tests			
AST (IU/L)	35.8 (14.8–169.1)	30.5 (11.8–174)	0.311
ALT (IU/L)	27.6 (7.4–179.4)	23.7 (8.5–209.2)	0.999
ALB (g/L)	41.5 (25.9–53.5)	41.4 (30.6–48)	0.316
TBIL (umol/L)	12.5 (5.4–69.5)	11.6 (3.8–256)	0.492
CEA (ng/mL)	4.2 (0.3–6,395)	4.6 (0.5–8,952)	0.945
CA19–9(U/mL)	90.1 (1.0–200000)	152 (0.6–200000)	0.531
WBC(10^9/L)	8.0 (4.4–26.6)	8.4 (4.7–14.8)	0.177
PLT (10^9/L)	272 (66–490)	232 (81–578)	0.302
CRE(umol/L)	66.4 (30.6–133)	62.5 (30.6–133)	0.683
Tumor burden			
Largest tumor size, cm (>10/≤10)	25/50 (33.3/66.7)	14/57 (19.7/80.3)	0.063
Tumor numbers (single/multiple)	25/50 (33.3/66.7)	22/49 (31/69)	0.762
Macrovascular invasion (yes/no)	23/52 (30.7/69.3)	18/53 (25.4/74.6)	0.475
Lymph node metastasis (yes/no)	51/24 (68/32)	47/24 (66.2/33.8)	0.817
Extrahepatic metastasis (yes/no)	17/58 (22.7/77.3)	24/47 (33.8/66.2)	0.135
TNM stage (III-IV/II)	56/19 (74.7/25.3)	56/15 (78.9/21.1)	0.548
Cycle times	4 (2–8)	3 (2–7)	0.628
Combination therapy (yes/no)	32/43 (42.6/57.3)	26/45 (36.6/63.4)	0.455

Values are presented as the median (range) or n (%).
Abbreviations: HAIC, hepatic arterial infusion chemotherapy; SC, systemic chemotherapy; ECOG, Eastern Cooperative Oncology Group; AST, aspartate transaminase; ALT, alanine transaminase; ALB, albumin; TBIL, total bilirubin; CEA, carcinoembryonic antigen; CA19–9, carbohydrate antigen 19–9; WBC, white blood cell; PLT, platelet count; CRE, creatinine; TNM, tumor–node–metastasis.

Statistical analysis

Non-normally distributed data were expressed as medians and ranges. Continuous parametric variables were analyzed by the unpaired Student's *t*-test, and continuous non-parametric variables were analyzed by the Mann–Whitney *U* test. Categorical data were analyzed by Pearson's correlation coefficient, chi-squared test with continuity corrections, or Fisher's exact probability method. Forward LR-based univariate and multivariate Cox regression analyses were conducted to identify independent predictive variables. The OS and PFS were shown by Kaplan–Meier curves, and differences between the groups were compared using the results of the log-rank test. The *p*-value <0.05 was considered statistically significant. All the analyses were performed using SPSS 25.0 software (SPSS Inc., Chicago, IL) and R version 4.0.1.

Results

Patient characteristics

Between March 2016 and March 2022, 146 patients diagnosed with iCCA who initially received HAIC or first-line SC were selected at Sun Yat-sen University Cancer Center, China. There were 75 patients in the HAIC group and 71 patients in the SC group (Figure 1). Detailed characteristics of each group are shown in Table 1. No significant baseline differences existed between the HAIC and SC groups.

In the HAIC group, the median age was 54 years old, 52 patients were male subjects, the largest tumor size of 25 (33.3%) patients was longer than 10 cm, a majority of patients had multiple tumors (66.7%), a total of 23 (30.7%) patients had macrovascular invasion, 51 (68%) patients had lymph node metastasis, and 17 (22.7%) patients had extra-hepatic metastasis. In the SC group, the

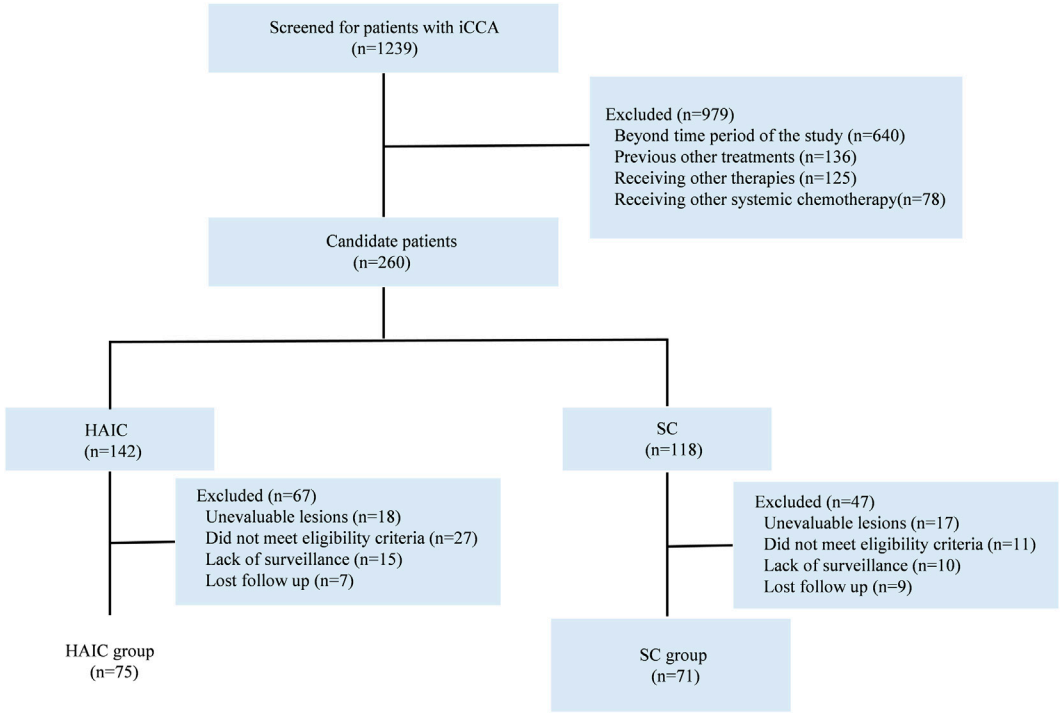

FIGURE 1
Flowchart for patient inclusion. Abbreviations: iCCA, intrahepatic cholangiocarcinoma; HAIC, hepatic arterial infusion chemotherapy; SC, systemic chemotherapy.

median age was 57 years old, and 40 patients were male subjects, the largest tumor size of 14 (19.7%) patients was longer than 10 cm, a majority of patients had multiple tumors (69%), a total of 18 (25.4%) patients had macrovascular invasion, 47 (66.2%) patients had lymph node metastasis, and 24 (33.8%) patients had extra-hepatic metastasis. According to characteristics of a tumor, most patients in this study had large tumor burden and advanced iCCA.

Univariate and multivariate Cox regression analyses in the cohorts

Prognostic factors of all clinical variables were analyzed in univariate analysis. Univariate analyses showed that ECOG, tumor number, extra-hepatic metastasis, and TNM stages were significant risk factors for patients' OS. Univariate analysis for PFS showed that ECOG, CA19–9, and extra-hepatic metastasis were significant risk factors. More details are described in Table 2. The multivariate Cox proportional analysis revealed that ECOG ($p < 0.001$) and extra-hepatic metastasis ($p = 0.026$) were significant and independent prognostic factors of OS (Table 2). The multivariate Cox proportional analysis revealed that ECOG ($p < 0.001$), CA19–9 ($p = 0.02$), macrovascular invasion ($p = 0.02$), and extra-hepatic metastasis ($p = 0.001$) were significant and independent prognostic factors of PFS (Table 2).

Tumor response and patient survival

The median OS in the HAIC and SC groups was 18.0 and 17.8 months, respectively. Meanwhile, the median PFS times in the HAIC and SC groups were 10.8 and 11.4 months, respectively. There was no significant difference between the two groups in OS ($p = 0.84$; Figure 2A) and PFS ($p = 0.59$; Figure 2B). However, patients in the HAIC group had significantly longer IPFS than patients in the SC group ($p = 0.035$; Figure 2C). The median IPFS in the HAIC and SC groups was 13.7 and 11.4 months, respectively. The median follow-up in the HAIC and SC group was 16.8 and 17.7 months, respectively (Supplementary Figure S1). Patients in the SC group were divided into two subgroups (GEMCIS and GEMOX). GEMCIS and GEMOX were compared with HAIC in OS and PFS (Supplementary Figure S2).

The subgroup analyses of OS and PFS are shown in Figure 3. HAIC provided a clinical benefit for OS and PFS in tumor number subgroups. Single-tumor patients appeared to benefit more from it in terms of OS ($p = 0.047$; Supplementary Figure S3A) and PFS ($p = 0.009$; Supplementary Figure S3B). The intrahepatic tumor responses of the patients are shown in Table 3. On the basis of RECIST1.1 and mRECIST criteria, HAIC showed an ORR two times higher than SC (40% vs. 16.9%, $p = 0.002$, RECIST1.1; 45.3% vs. 21.2%, $p = 0.002$, mRECIST). The optimal response for intrahepatic target lesions by patients according to RECIST1.1 criteria is shown in the waterfall plot in Figure 4.

TABLE 2 Univariate and multivariate Cox regression analyses of risk factors for overall survival and progression-free survival.

Variable	OS				PFS			
	Univariate		Multivariate		Univariate		Multivariate	
	HR (95% CI)	*p*-value	HR (95% CI)	*p*-value	HR (95% CI)	*p*-value	HR (95% CI)	*p*-value
Age, y (>/≤50)	0.99 (0.59–1.67)	0.96			0.78 (0.51–1.22)	0.28		
Gender (men/women)	1.05 (0.65–1.67)	0.85			1.17 (0.74–1.86)	0.5		
Hepatitis (yes/no)	1.29 (0.82–2.03)	0.27			1.29 (0.82–2.00)	0.27		
ECOG (≥1/0)	13.48 (5.83–31.17)	<0.001	13.18 (5.7–30.5)	<0.001	4.22 (2.39–7.44)	<0.001	4.52 (2.53–8.06)	<0.001
ALB, g/L, (>/≤35)	0.60 (0.29–1.21)	0.16			0.68 (0.35–1.33)	0.26		
TBIL, umol/L, (>/≤17.1)	1.21 (0.70–2.11)	0.49			1.62 (0.94–2.78)	0.08		
CA19–9,U/mL, (>/≤100)	0.98 (0.62–1.54)	0.92			1.68 (1.08–2.59)	0.02	1.69 (1.09–2.62)	0.02
CEA, ng/mL (>5/≤5)	1.54 (0.76–3.10)	0.23			1.21 (0.58–2.51)	0.61		
Largest tumor size (>/≤10 cm)	1.49 (0.93–2.39)	0.09			0.81 (0.51–1.3)	0.39		
Tumor numbers (>1/1)	1.65 (1.05–2.61)	0.03			1.28 (0.81–2.02)	0.29		
Macrovascular invasion (yes/no)	0.77 (0.46–1.29)	0.33			1.55 (0.94–2.56)	0.08	1.79 (1.08–2.99)	0.02
Lymph node metastasis (yes/no)	0.83 (0.51–1.33)	0.43			1.19 (0.75–1.89)	0.47		
Extrahepatic metastasis (yes/no)	1.86 (1.17–2.95)	0.008	1.69 (1.01–2.67)	0.026	2.12 (1.37–3.29)	0.001	2.12 (1.35–3.32)	0.001
TNM stage (III-IV/II)	1.76 (1.0–3.1)	0.05			1.70 (0.97–2.97)	0.06		
Therapy (SC/HAIC)	0.95 (0.61–1.51)	0.84			1.13 (0.72–1.77)	0.59		

p-value <0.05 is statistically significant in both univariate and multivariate analyses.
Abbreviations: ECOG, Eastern Cooperative Oncology Group; ALB, albumin; TBIL, total bilirubin; CA19–9 carbohydrate antigen 19–9; CEA, carcinoembryonic antigen; TNM, tumor–node–metastasis; SC, systemic chemotherapy; HAIC, hepatic artery infusion chemotherapy.

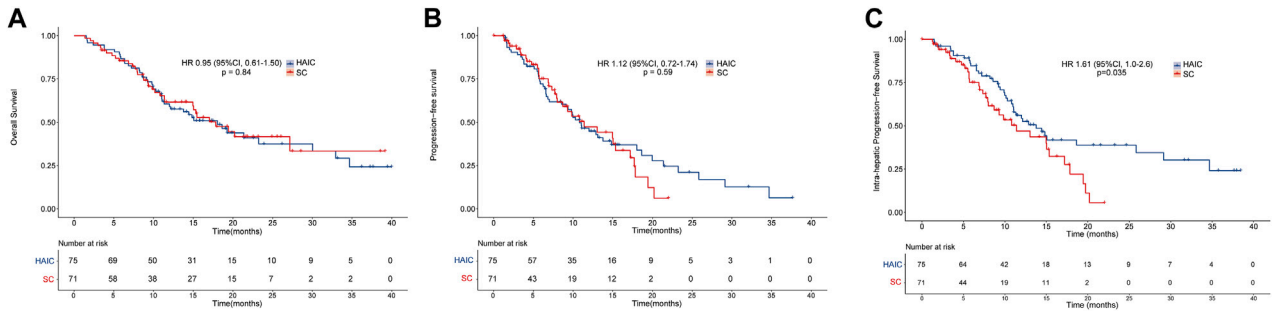

FIGURE 2
Overall survival and progression-free survival of the two groups of patients. Kaplan–Meier curves of **(A)** overall survival, **(B)** progression-free survival, and **(C)** intrahepatic progression-free survival for patients in the HAIC and SC groups.

Adverse events and safety

In general, the SC resulted in more AEs than those in HAIC (Table 4). The frequencies of rash (3 [4%] vs. 20 [28.2%]; $p < 0.001$), vomiting (27 [36%] vs. 51 [71.8%]; $p < 0.001$), fatigue (19 [25.3%] vs. 35 [49.3%]; $p < 0.001$), leukopenia (9 [12%] vs. 20 [28.2%]; $p = 0.014$), anemia (13 [17.3%] vs. 33 [46.5%]; $p < 0.001$), and sensory neuropathy (9 [12%] vs. 18 [25.4%]; $p = 0.038$) were lower in the HAIC group. Meanwhile, the overall incidence of serious AEs was higher in the SC group than that in the HAIC group. The frequencies of grades 3–4 vomiting (1 [1.3%] vs. 8 [11.2%]; $p = 0.032$), leukopenia (0 [0] vs. 5 [7%]; $p = 0.025$), and anemia (0 [0] vs. 6 [8.5%]; $p = 0.012$) were significantly higher in the SC group than those in the HAIC group. There were no significant differences in the frequencies of fever (15 [20%] vs. 10 [14.1%]; $p = 0.343$), abdominal pain (19 [25.3%] vs. 13 [18.3%]; $p = 0.305$), diarrhea (2 [2.7%] vs. 2 [2.8%]; $p = 1.000$), neutropenia (6 [8%] vs. 9 [12.7%]; $p = 0.352$),

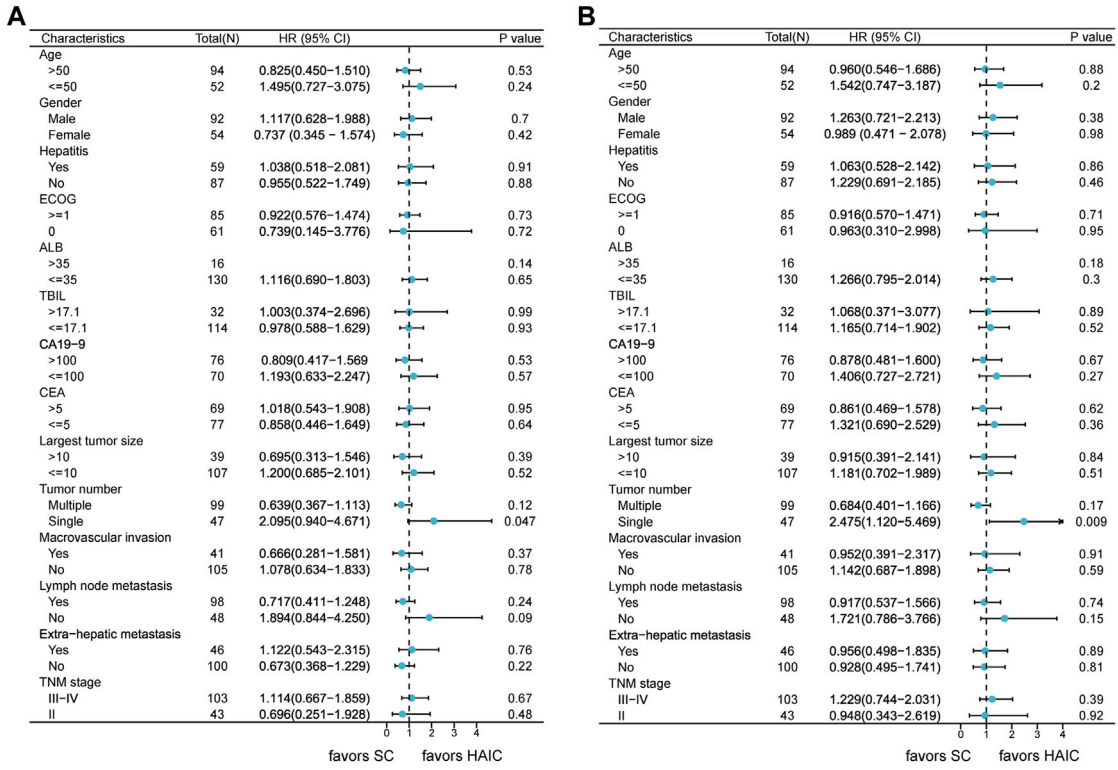

FIGURE 3
Forest plots of **(A)** overall survival and **(B)** progression-free survival in different patient subgroups. Abbreviations: HR, hazard ratio; CI, confidence interval; ECOG, Eastern Cooperative Oncology Group; ALB, albumin; TBIL, total bilirubin; CA19−9, carbohydrate antigen 19−9; CEA, carcinoembryonic antigen; TNM, tumor−node−metastasis.

TABLE 3 Intra-hepatic tumor responses evaluated by RECIST1.1 and mRECIST criteria.

Response	RECIST1.1			mRECIST		
	HAIC group (*n* = 75)	SC group (*n* = 71)	*p*-value	HAIC group (*n* = 75)	SC group (n = 71)	*p*-value
CR	0	0	–	2 (2.7%)	0	-
PR	30 (40%)	12 (16.9%)	–	32 (42.6%)	15 (21.1%)	-
SD	36 (48%)	51 (71.8%)	–	32 (42.6%)	48 (67.6%)	-
PD	9 (12%)	8 (11.2%)	–	9 (26.7%)	8 (31%)	-
ORR	30 (40%)	12 (16.9%)	0.002	34 (45.3%)	15 (21.1%)	0.002
DCR	66 (88%)	63 (88.7%)	0.89	66 (88%)	63 (88.7%)	0.89

Abbreviations: HAIC, hepatic arterial infusion chemotherapy; SC, systemic chemotherapy; CR, complete response; PR, partial response; SD, stable disease; PD, progressive disease; ORR, objective response rate; DCR, disease control rate.

thrombocytopenia (8 [10.7%] vs. 16 [22.5%]; $p = 0.053$), elevated ALT (20 [26.7%] vs. 16 [22.5%]; $p = 0.563$), elevated AST (30 [40%] vs. 24 [33.8%]; $p = 0.438$), hyperbilirubinemia (12 [16%] vs. 10 [14.1%]; $p = 0.746$), hypoalbuminemia (37 [49.3%] vs. 34 [47.9%]; $p = 0.861$), and elevated creatinine (8 [10.7%] vs. 6 [8.5%]; $p = 0.649$). In the HAIC group, three (4%) patients delayed and discontinued treatment because of AEs. In the SC group, seven (9.86%) patients delayed and discontinued the treatment because of AEs.

Discussion

It is widely acknowledged that iCCA is a gastrointestinal adenocarcinoma with a high level of malignancy and poor prognosis. In addition, most of the patients with iCCA cannot receive surgery because of advanced disease in iCCA, and these patients with unresectable iCCA undergo chemotherapy to control tumor development. Over the past years, GEMCIS and GEMOX have become the standard first-line chemotherapy regimen

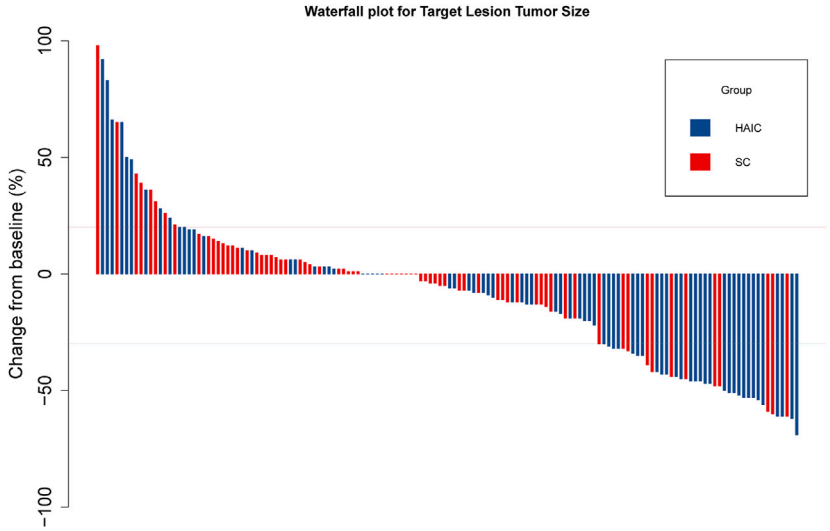

FIGURE 4
Waterfall plot for tumor size changes in intrahepatic target lesions. Abbreviations: PD, progressive disease; PR, partial response.

TABLE 4 Objective treatment-related adverse events.

Adverse event	Any grade			Grades 3–4		
	HAIC group (*n* = 75)	SC group (*n* = 71)	*p*-value	HAIC group (*n* = 75)	SC group (*n* = 71)	*p*-value
Rash	3 (4%)	20 (28.2%)	<0.001	0	0	–
Fever	15 (20%)	10 (14.1%)	0.343	0	0	–
Abdominal pain	19 (25.3%)	13 (18.3%)	0.305	3 (4%)	0	0.245
Vomiting	27 (36%)	51 (71.8%)	<0.001	1 (1.3%)	8 (11.2%)	0.032
Fatigue	19 (25.3%)	35 (49.3%)	0.003	0	0	–
Diarrhea	2 (2.7%)	2 (2.8%)	1.000	0	0	–
Leukopenia	9 (12%))	20 (28.2%)	0.014	0	5 (7.0%)	0.025
Neutropenia	6 (8%)	9 (12.7%)	0.352	1 (1.3%)	4 (5.6%)	0.331
Anemia	13 (17.3%)	33 (46.5%)	<0.001	0	6 (8.5%)	0.012
Thrombocytopenia	8 (10.7%)	16 (22.5%)	0.053	0	3 (4.2%)	0.112
Elevated ALT	20 (26.7%)	16 (22.5%)	0.563	1 (1.3%)	1 (1.4%)	1.000
Elevated AST	30 (40%)	24 (33.8%)	0.438	2 (2.7%)	2 (2.8%)	1.000
Hyperbilirubinemia	12 (16%)	10 (14.1%)	0.746	2 (2.7%)	1 (1.4%)	1.000
Hypoalbuminemia	37 (49.3%)	34 (47.9%)	0.861	0	1 (1.4%)	0.486
Elevated creatinine	8 (10.7%)	6 (8.5%)	0.649	0	0	–
Sensory neuropathy	9 (12%)	18 (25.4%)	0.038	0	0	–

Some patients may have multiple immune-related adverse events.
Abbreviations: HAIC, hepatic arterial infusion chemotherapy; SC, systemic chemotherapy; ALT, alanine aminotransferase; AST, aspartate aminotransferase.

(Okusaka et al., 2010; Valle et al., 2010; Fiteni et al., 2014; Grenader et al., 2015). However, the occurrence of AEs is an urgent problem to be solved for SC. There is also an urgent need to find a regimen to reduce the occurrence of AEs while achieving similar survival benefits. Localized arterial treatment such as HAIC, TACE, and transarterial radioembolization (TARE) might be important treatment options for advanced cholangiocarcinoma (Mosconi et al., 2021; Ishii et al., 2022; Schaarschmidt et al., 2023). A previous study clarified that patients receiving TARE as first-line therapy had a 68.6% disease control rate and a median OS of 12 months (Schaarschmidt et al., 2023). In addition, a systemic review and meta-analysis demonstrated that the median OS after

TACE was 14.2 months, while after TARE, it was 13.5 months for advanced iCCA (Mosconi et al., 2021). Meanwhile, few previous studies indicated that HAIC combined with systemic gemcitabine (GEM) and oxaliplatin may be an effective therapy for patients with advanced iCCA (Marumoto et al., 2014; Cercek et al., 2020). A retrospective study indicated the mFOLFOX regimen used in HAIC could be a new option for patients with iCCA (Cai et al., 2021). Some prospective studies demonstrated that HAIC with mFOLFOX had relatively low toxicity for hepatocellular carcinoma (HCC) (He et al., 2019; Li et al., 2022; Lyu et al., 2022; Li et al., 2023). Although these studies focused on HCC patients, the safety of HAIC with mFOLFOX was still of clinical significance for patients with iCCA, and HAIC with FOLFOX might be a feasible and promising regimen for treating iCCA patients.

In the current study of 146 patients, we compared HAIC with the first-line SC (GEMCIS and GEMOX) and found that patients in the HAIC group had significantly longer IPFS than patients in the SC group and that HAIC showed an ORR higher than SC. In subgroup analyses, single-tumor patients appeared to benefit from considering HAIC in terms of OS and PFS, indicating that HAIC might have a better efficacy than SC in relatively early-stage unresectable iCCA patients and that HAIC could control liver lesions better than SC. One potential explanation for this is that HAIC can provide higher concentrations of the chemotherapeutic agents in the liver than SC, therefore contributing to control tumor in the liver. As is known to all, the liver possesses a dual blood supply. In detail, the hepatic artery provides nearly all of the tumor's blood flow, and the portal vein supplies blood to the non-neoplastic liver parenchyma. HAIC could preferentially deliver more chemotherapeutic agents to the hepatic artery, which contributes to controlling tumors in the liver.

We also found that patients with unresectable iCCA had similar OS and PFS after HAIC or SC treatment, suggesting that HAIC had a similar clinical efficiency to SC in the outcomes of patients. Although HAIC could better control intrahepatic tumors compared to SC, there were no significant differences in the outcome of patients. It could be explained by the fact that in this study, most patients were at the advanced stage and had extrahepatic metastases. The progression of extrahepatic lesions resulted in the death of patients, and HAIC had a poor control effect on extrahepatic lesions. Therefore, it would be an excellent clinical treatment strategy to add immune therapy and targeted therapy or SC on the basis of HAIC for those patients with extrahepatic metastasis.

Safety and the incidence of AEs are also important indicators for evaluating the chemotherapy regimen apart from the therapeutic effect. The common objective treatment-related AEs observed in this study were rash, fever, abdominal pain, vomiting, fatigue, diarrhea, leukopenia, neutropenia, anemia, thrombocytopenia, elevated ALT, elevated AST, hyperbilirubinemia, hypoalbuminemia, elevated creatinine, and sensory neuropathy. In general, the ratio of AEs in the HAIC group was lower than that in the SC group. The frequencies of rash, vomiting, fatigue, leukopenia, anemia, and sensory neuropathy were also lower in the HAIC group. Hematologic toxicity and liver function damage were the main grade 3-4 AEs in this study. In addition, the frequencies of grade 3–4 AEs were lower in the HAIC group. One possible reason for this is that HAIC enables the delivery of chemotherapy drugs directly into the liver, causing a relatively low systemic blood concentration of drugs. However, SC is the intravenous administration of chemotherapy drugs. In order to achieve the effect of killing liver tumors, the systemic blood concentration of the drug must be at a high level to cause damage to various systems in the body. It is also possible that the liver could clear the drugs via first-pass metabolism to approach diminish systemic toxic effects (Ensminger and Gyves, 1983; Cohen and Kemeny, 2003; Cercek et al., 2020). Meanwhile, most of these AEs were controlled after symptomatic treatment for the HAIC group and would not affect the next session. Therefore, HAIC may be a safe and effective therapeutic regimen for treating patients with unresectable iCCA.

This study also had few limitations. First, it was a retrospective study, and all of the patients came from a single center; thus, further prospective, large-sample, and randomized studies are needed to confirm our findings. Second, the relatively small sample size was limited by the generalizability of our results, and there was a risk of type II error. Finally, more bench-scale research studies are needed to determine the intrinsic mechanism guiding HAIC for patients with iCCA.

In conclusion, this study demonstrated that HAIC was a safe and effective therapeutic regimen in the cohort of 146 patients with unresectable iCCA. Meanwhile, our study indicated that patients with single tumor are most likely to benefit from HAIC than SC.

Data availability statement

The raw data supporting the conclusion of this article will be made available by the authors, without undue reservation.

Ethics statement

The studies involving humans were approved by the Institutional Review Board of the Sun Yat-sen University Cancer Center. The studies were conducted in accordance with the local legislation and institutional requirements. The participants provided their written informed consent to participate in this study.

Author contributions

ZY: conceptualization, methodology, software, formal analysis, and writing—original draft; YF: methodology, software, and formal analysis; WW: conceptualization, software, resources, and data curation; ZH: resources and investigation; YP: resources and investigation; DH: resources and investigation; ZZ: supervision and data curation; MC: conceptualization, funding acquisition, project administration, and supervision; YZ: conceptualization, methodology, project administration, supervision, and writing—review and editing. All authors contributed to the article and approved the submitted version.

Funding

This work is funded by the National Natural Science Foundation of China (No: 82103566).

Acknowledgments

The authors would like to thank Bullet Edits Limited for the linguistic editing and proofreading of the manuscript.

Conflict of interest

The authors declare that the research was conducted in the absence of any commercial or financial relationships that could be construed as a potential conflict of interest.

Publisher's note

All claims expressed in this article are solely those of the authors and do not necessarily represent those of their affiliated organizations, or those of the publisher, the editors, and the reviewers. Any product that may be evaluated in this article, or claim that may be made by its manufacturer, is not guaranteed or endorsed by the publisher.

Supplementary material

The Supplementary Material for this article can be found online at: https://www.frontiersin.org/articles/10.3389/fphar.2023.1234342/full#supplementary-material

SUPPLEMENTARY FIGURE S1
Median follow-up times of the **(A)** HAIC and **(B)** SC groups calculated by the reversed Kaplan–Meier method.

SUPPLEMENTARY FIGURE S2
Overall survival and progression-free survival of the two groups of patients. Kaplan–Meier curves of **(A)** overall survival and **(B)** progression-free survival for patients in the HAIC, GEMCIS, and GEMOX groups.

SUPPLEMENTARY FIGURE S3
Subgroup analysis for the overall survival and progression-free survival of the two groups of patients. Kaplan–Meier curves of **(A)** overall survival and **(B)** progression-free survival for patients with single tumor.

References

Banales, J. M., Cardinale, V., Carpino, G., Marzioni, M., Andersen, J. B., Invernizzi, P., et al. (2016). Expert consensus document: cholangiocarcinoma: current knowledge and future perspectives consensus statement from the European network for the study of cholangiocarcinoma (ENS-CCA). *Nat. Rev. Gastroenterol. Hepatol.* 13 (5), 261–280. doi:10.1038/nrgastro.2016.51

Bridgewater, J., Galle, P. R., Khan, S. A., Llovet, J. M., Park, J. W., Patel, T., et al. (2014). Guidelines for the diagnosis and management of intrahepatic cholangiocarcinoma. *J. Hepatol.* 60 (6), 1268–1289. doi:10.1016/j.jhep.2014.01.021

Bupathi, M., Ahn, D. H., and Bekaii-Saab, T. (2017). Therapeutic options for intrahepatic cholangiocarcinoma. *Hepatobiliary Surg. Nutr.* 6 (2), 91–100. doi:10.21037/hbsn.2016.12.12

Cai, Z., He, C., Zhao, C., and Lin, X. (2021). Survival comparisons of hepatic arterial infusion chemotherapy with mFOLFOX and transarterial chemoembolization in patients with unresectable intrahepatic cholangiocarcinoma. *Front. Oncol.* 11, 611118. doi:10.3389/fonc.2021.611118

Caparica, R., Lengelé, A., Bekolo, W., and Hendlisz, A. (2019). FOLFIRI as second-line treatment of metastatic biliary tract cancer patients. *Autops. Case Rep.* 9 (2), e2019087. doi:10.4322/acr.2019.087

Cercek, A., Boerner, T., Tan, B. R., Chou, J. F., Gönen, M., Boucher, T. M., et al. (2020). Assessment of hepatic arterial infusion of floxuridine in combination with systemic gemcitabine and oxaliplatin in patients with unresectable intrahepatic cholangiocarcinoma: a phase 2 clinical trial. *JAMA Oncol.* 6 (1), 60–67. doi:10.1001/jamaoncol.2019.3718

Cohen, A. D., and Kemeny, N. E. (2003). An update on hepatic arterial infusion chemotherapy for colorectal cancer. *Oncologist* 8 (6), 553–566. doi:10.1634/theoncologist.8-6-553

Dong, L., Lu, D., Chen, R., Lin, Y., Zhu, H., Zhang, Z., et al. (2022). Proteogenomic characterization identifies clinically relevant subgroups of intrahepatic cholangiocarcinoma. *Cancer Cell* 40 (1), 70–87.e15. doi:10.1016/j.ccell.2021.12.006

Eisenhauer, E. A., Therasse, P., Bogaerts, J., Schwartz, L. H., Sargent, D., Ford, R., et al. (2009). New response evaluation criteria in solid tumours: revised RECIST guideline (version 1.1). *Eur. J. Cancer* 45 (2), 228–247. doi:10.1016/j.ejca.2008.10.026

Ensminger, W. D., and Gyves, J. W. (1983). Clinical pharmacology of hepatic arterial chemotherapy. *Semin. Oncol.* 10 (2), 176–182.

Fiteni, F., Nguyen, T., Vernerey, D., Paillard, M. J., Kim, S., Demarchi, M., et al. (2014). Cisplatin/gemcitabine or oxaliplatin/gemcitabine in the treatment of advanced biliary tract cancer: a systematic review. *Cancer Med.* 3 (6), 1502–1511. doi:10.1002/cam4.299

Grenader, T., Nash, S., Plotkin, Y., Furuse, J., Mizuno, N., Okusaka, T., et al. (2015). Derived neutrophil lymphocyte ratio may predict benefit from cisplatin in the advanced biliary cancer: the ABC-02 and BT-22 studies. *Ann. Oncol.* 26 (9), 1910–1916. doi:10.1093/annonc/mdv253

He, M., Li, Q., Zou, R., Shen, J., Fang, W., Tan, G., et al. (2019). Sorafenib plus hepatic arterial infusion of oxaliplatin, fluorouracil, and leucovorin vs sorafenib alone for hepatocellular carcinoma with portal vein invasion: A randomized clinical trial. *JAMA Oncol.* 5 (7), 953–960. doi:10.1001/jamaoncol.2019.0250

Ishii, M., Itano, O., Morinaga, J., Shirakawa, H., and Itano, S. (2022). Potential efficacy of hepatic arterial infusion chemotherapy using gemcitabine, cisplatin, and 5-fluorouracil for intrahepatic cholangiocarcinoma. *PLoS One* 17 (4), e0266707. doi:10.1371/journal.pone.0266707

Kasai, K., Kooka, Y., Suzuki, Y., Suzuki, A., Oikawa, T., Ushio, A., et al. (2014). Efficacy of hepatic arterial infusion chemotherapy using 5-fluorouracil and systemic pegylated interferon α-2b for advanced intrahepatic cholangiocarcinoma. *Ann. Surg. Oncol.* 21 (11), 3638–3645. doi:10.1245/s10434-014-3766-7

Kemeny, N., Daly, J., Oderman, P., Shike, M., Chun, H., Petroni, G., et al. (1984). Hepatic artery pump infusion: toxicity and results in patients with metastatic colorectal carcinoma. *J. Clin. Oncol.* 2 (6), 595–600. doi:10.1200/JCO.1984.2.6.595

Kim, S. T., Kang, J. H., Lee, J., Lee, H. W., Oh, S. Y., Jang, J. S., et al. (2019). Capecitabine plus oxaliplatin versus gemcitabine plus oxaliplatin as first-line therapy for advanced biliary tract cancers: a multicenter, open-label, randomized, phase III, noninferiority trial. *Ann. Oncol.* 30 (5), 788–795. doi:10.1093/annonc/mdz058

Lamarca, A., Palmer, D. H., Wasan, H. S., Ross, P. J., Ma, Y. T., Arora, A., et al. (2021). Second-line FOLFOX chemotherapy versus active symptom control for advanced biliary tract cancer (ABC-06): a phase 3, open-label, randomised, controlled trial. *Lancet Oncol.* 22 (5), 690–701. doi:10.1016/S1470-2045(21)00027-9

Li, Q. J., He, M. K., Chen, H. W., Fang, W. Q., Zhou, Y. M., Xu, L., et al. (2022). Hepatic arterial infusion of oxaliplatin, fluorouracil, and leucovorin versus transarterial chemoembolization for large hepatocellular carcinoma: a randomized phase III trial. *J. Clin. Oncol.* 40 (2), 150–160. doi:10.1200/JCO.21.00608

Li, S. H., Mei, J., Cheng, Y., Li, Q., Wang, Q. X., Fang, C. K., et al. (2023). Postoperative adjuvant hepatic arterial infusion chemotherapy with FOLFOX in hepatocellular carcinoma with microvascular invasion: a multicenter, phase III, randomized study. *J. Clin. Oncol.* 41 (10), 1898–1908. doi:10.1200/JCO.22.01142

Llovet, J. M., and Lencioni, R. (2020). mRECIST for HCC: performance and novel refinements. *J. Hepatol.* 72 (2), 288–306. doi:10.1016/j.jhep.2019.09.026

Lyu, N., Wang, X., Li, J. B., Lai, J. F., Chen, Q. F., Li, S. L., et al. (2022). Arterial chemotherapy of oxaliplatin plus fluorouracil versus sorafenib in advanced hepatocellular carcinoma: a biomolecular exploratory, randomized, phase III trial (FOHAIC-1). *J. Clin. Oncol.* 40 (5), 468–480. doi:10.1200/JCO.21.01963

Marumoto, M., Yamasaki, T., Marumoto, Y., Saeki, I., Harima, Y., Urata, Y., et al. (2014). Systemic gemcitabine combined with hepatic arterial infusion chemotherapy with cisplatin, 5-fluorouracil, and isovorin for the treatment of advanced intrahepatic cholangiocarcinoma: a pilot study. *Hepatogastroenterology* 61 (129), 162–167.

Mosconi, C., Solaini, L., Vara, G., Brandi, N., Cappelli, A., Modestino, F., et al. (2021). Transarterial chemoembolization and radioembolization for unresectable intrahepatic cholangiocarcinoma-a systemic review and meta-analysis. *Cardiovasc Interv. Radiol.* 44 (5), 728–738. doi:10.1007/s00270-021-02800-w

Nehls, O., Klump, B., Arkenau, H. T., Hass, H. G., Greschniok, A., Gregor, M., et al. (2002). Oxaliplatin, fluorouracil and leucovorin for advanced biliary system

adenocarcinomas: a prospective phase II trial. *Br. J. Cancer* 87 (7), 702–704. doi:10.1038/sj.bjc.6600543

Oh, D. Y., Lee, K. H., Lee, D. W., Yoon, J., Kim, T. Y., Bang, J. H., et al. (2022). Gemcitabine and cisplatin plus durvalumab with or without tremelimumab in chemotherapy-naive patients with advanced biliary tract cancer: an open-label, single-centre, phase 2 study. *Lancet Gastroenterol. Hepatol.* 7 (6), 522–532. doi:10.1016/S2468-1253(22)00043-7

Okusaka, T., Nakachi, K., Fukutomi, A., Mizuno, N., Ohkawa, S., Funakoshi, A., et al. (2010). Gemcitabine alone or in combination with cisplatin in patients with biliary tract cancer: a comparative multicentre study in Japan. *Br. J. Cancer* 103 (4), 469–474. doi:10.1038/sj.bjc.6605779

Rizvi, S., and Gores, G. J. (2013). Pathogenesis, diagnosis, and management of cholangiocarcinoma. *Gastroenterology* 145 (6), 1215–1229. doi:10.1053/j.gastro.2013.10.013

Rizvi, S., Khan, S. A., Hallemeier, C. L., Kelley, R. K., and Gores, G. J. (2018). Cholangiocarcinoma - evolving concepts and therapeutic strategies. *Nat. Rev. Clin. Oncol.* 15 (2), 95–111. doi:10.1038/nrclinonc.2017.157

Rodriguez, H., and Pennington, S. R. (2018). Revolutionizing precision oncology through collaborative proteogenomics and data sharing. *Cell* 173 (3), 535–539. doi:10.1016/j.cell.2018.04.008

Schaarschmidt, B. M., Kloeckner, R., Dertnig, T., Demircioglu, A., Müller, L., Auer, T. A., et al. (2023). Real-life experience in the treatment of intrahepatic cholangiocarcinoma by (90)Y radioembolization: a multicenter retrospective study. *J. Nucl. Med.* 64 (4), 529–535. doi:10.2967/jnumed.122.264598

Sirica, A. E., Gores, G. J., Groopman, J. D., Selaru, F. M., Strazzabosco, M., Wei Wang, X., et al. (2019). Intrahepatic cholangiocarcinoma: continuing challenges and translational advances. *Hepatology* 69 (4), 1803–1815. doi:10.1002/hep.30289

Valle, J., Wasan, H., Palmer, D. H., Cunningham, D., Anthoney, A., Maraveyas, A., et al. (2010). Cisplatin plus gemcitabine versus gemcitabine for biliary tract cancer. *N. Engl. J. Med.* 362 (14), 1273–1281. doi:10.1056/NEJMoa0908721

Valle, J. W., Kelley, R. K., Nervi, B., Oh, D. Y., and Zhu, A. X. (2021). Biliary tract cancer. *Lancet* 397 (10272), 428–444. doi:10.1016/S0140-6736(21)00153-7

frontiers | Frontiers in Immunology

TYPE Original Research
PUBLISHED 19 October 2023
DOI 10.3389/fimmu.2023.1254158

OPEN ACCESS

EDITED BY
Daniel Neureiter,
Salzburger Landeskliniken, Austria

REVIEWED BY
Chi Ma,
National Institutes of Health (NIH), United States
Matthias Ocker,
Charité University Medicine Berlin, Germany

*CORRESPONDENCE
Jian Gao
982213482@qq.com

RECEIVED 06 July 2023
ACCEPTED 06 October 2023
PUBLISHED 19 October 2023

CITATION
Tang C, He Q, Feng J, Liao Z, Peng Y and Gao J (2023) Portal vein tumour thrombosis radiotherapy improves the treatment outcomes of immunotherapy plus bevacizumab in hepatocellular carcinoma: a multicentre real-world analysis with propensity score matching. *Front. Immunol.* 14:1254158. doi: 10.3389/fimmu.2023.1254158

Portal vein tumour thrombosis radiotherapy improves the treatment outcomes of immunotherapy plus bevacizumab in hepatocellular carcinoma: a multicentre real-world analysis with propensity score matching

Cuiping Tang[1,2], Qin He[3], Jian Feng[4], Ziyue Liao[1], Yunli Peng[5] and Jian Gao[1*]

[1]Department of Gastroenterology and Hepatology, Second Affiliated Hospital of Chongqing Medical University, Chongqing, China, [2]Department of Graduate, The Second Clinical College of Chongqing Medical University, Chongqing, China, [3]Department of Gastroenterology and Hepatology, The First People's Hospital of Mianyang (SiChuan Mianyang 404 Hospital), Sichuan, China, [4]Department of Oncology, Bishan Hospital of Chongqing Medical University, Chongqing, China, [5]Department of Gastroenterology and Hepatology, Bishan Hospital of Chongqing Medical University, Chongqing, China

Background: This study aimed to evaluate the efficacy and safety of sequential immune checkpoint inhibitors (ICIs) plus bevacizumab therapy after radiotherapy for portal vein tumour thrombosis (PVTT) in patients with hepatocellular carcinoma (HCC).

Methods: Retrospective data were collected from 113 patients with HCC with PVTT. Patients in the PVTT radiotherapy (radiotherapy + ICIs + bevacizumab) and control groups (ICIs + bevacizumab) were enrolled according to propensity score matching (PSM) analysis (1:1). The differences in progression-free survival (PFS), objective response rate (ORR), disease control rate (DCR), and potential factors affecting PFS between the groups were analysed. The adverse events (AEs) were compared between the two groups.

Results: There were 47 patients in the two groups after PSM (1:1). The differences in neutrophil and lymphocyte counts, neutrophil-to-lymphocyte ratio (NLR), CRP, and CD4, CD8, and CD4-to-CD8 ratio before and after radiotherapy for PVTT ($P < 0.05$) in the PVTT radiotherapy group were significant. The patients in the PVTT radiotherapy group had a longer PFS (median, 9.6 *vs.* 5.4 months, $P < 0.001$), and the PFS rates of 3, 6, 9, and 12 months were 97.87% *vs.* 94.19%,

10.3389/fimmu.2023.1254158

80.85% *vs.* 44.68%, 53.19% *vs.* 6.38%, and 23.40% *vs.* 0.00%, respectively ($P < 0.001$). There were also significant differences in the ORR (48.94% *vs.* 27.66%, $P = 0.0339$) and DCR (97.87% *vs.* 82.98%, $P = 0.0141$) between the two groups, and no serious AEs were observed. Multivariate Cox analysis showed that AFP expression, gross classification of HCC, PVTT type, extrahepatic metastasis, PVTT radiotherapy, and reduction in PVTT were independent factors influencing PFS ($P < 0.05$).

Conclusions: Sequential ICIs plus bevacizumab therapy after radiotherapy for PVTT in patients with HCC is safe and feasible and may further prolong the PFS of patients.

KEYWORDS

hepatocellular carcinoma, portal vein tumour thrombosis, radiotherapy, immune checkpoint inhibitors, bevacizumab

1 Introduction

Hepatocellular carcinoma (HCC) has the clinical characteristics of insidious onset, rapid progression, early recurrence, poor prognosis, and high morbidity and mortality (1). Approximately three in four liver blood samples come from the portal vein system, and HCC is prone to invade the portal vein system to form portal vein tumour thrombosis (PVTT), with an incidence of ~44–66.2% (2). Patients with HCC and PVTT often had liver reserve damage, tumour invasion, and portal hypertension manifestations. PVTT is one of the most severe prognostic factors of HCC, and the median survival time of the patients without treatment was 2.7–4.0 months (2). Percutaneous portal vein stenting can open the portal vein to protect liver function and reduce portal hypertension; however, it cannot prevent the progression of PVTT. However, there is no international consensus on the diagnostic and treatment criteria for PVTT complicated by HCC, which causes great difficulties in the selection of treatment and prediction of efficacy. Transhepatic arterial chemotherapy and embolisation (TACE) is the standard treatment for patients with unresectable HCC. However, TACE has lower efficacy and safety than hepatectomy for patients with HCC and PVTT (3). The current Barcelona clinic liver cancer (BCLC) classification of HCC with PVTT is at an advanced stage; therefore, sorafenib or lenvatinib is generally recommended as first-line therapy for these patients (2). Although evidence for the efficacy of systemic therapy for advanced HCC is expanding, data on treatment guidance for a subgroup of patients with HCC with PVTT remain limited.

The liver is the "immune preferential organ", the immune system in the liver is not sensitive to foreign bodies for its functional needs, resulting in the escape of primary liver tumour cells from the immune system's surveillance and attack, also known as "immune escape". Immunocheckpoint inhibitors (ICIs) such as programmed death-1/programmed death ligand 1 (PD-1/PD-L1) enable autoimmune cells to play an anti-tumour role by relieving the inhibition of immune cells. The FDA approved nivolumab as a second-line treatment for patients with HCC after sorafenib treatment in 2017, marking the official entry into the immunological era of HCC treatment. With the release of clinical results, CheckMate040 (4), KEYNOTE-240 (5), KEYNOTE-224 (6), SHR-1210 (7), pembrolizumab (PD-1), and atezolizumab (PD-L1) have been recommended as treatment options for HCC in multiple clinical guidelines, both domestically and overseas. Clinical research IMbrave 150 (8) and ORIENT-32 (9) showed better progression-free survival (PFS) and overall survival (OS) when ICIs plus bevacizumab were used as the first-line treatment for patients with advanced-stage HCC. However, the results of current clinical trials showed that the objective response rate (ORR) of ICIs plus bevacizumab treatment was still low. Therefore, there is an urgent need to explore combination treatments to improve treatment response rates.

The release of tumour antigens is an initial factor in the seven key links of immunotherapy. Tumour cells become necrotic after radiotherapy, and the immune system is fully activated, releasing tumour antigens (10). Therefore, PVTT radiotherapy combined with ICIs is theoretically feasible for the treatment of HCC. However, no relevant clinical studies have been conducted thus

Abbreviations: PVTT, portal vein tumour thrombosis; HCC, hepatocellular carcinoma; ICIs, immune checkpoint inhibitors; PFS, progression-free survival; ORR, objective response rate; DCR, disease control rate; AEs, adverse events; TACE, Transhepatic Arterial Chemotherapy and Embolization; BCLC, Barcelona Clinical staging system; PD-1, programmed death-1; PD-L1, programmed death-Ligand 1; CT, computerized tomography; MRI, magnetic resonance imaging; DSA, digital subtraction angiography; ECOG-PS score, Eastern Cooperative Oncology Group performance status score; INR, international normalized ratio; CNCL, China liver cancer staging; HBV-DNA, hepatitis B virus deoxyribonucleic acid; AFP, serum alpha fetoprotein; IMRT, Intensity-modulated radiation therapy; PTV, planning target volume; TBIL, total bilirubin; ALT, Alamine aminotransferase; AST, Aspartate aminotransferase; PT, prothrombin time; CRP, C-reactive protein; NLR, Neutrophils to Lymphocytes Ratio (NLR); CR, complete response; PR, partial response; SD, stable disease; PD, progressive disease; OS, overall survival; ECG, Electrocardiograph.

far. Our study aimed to investigate the changes in immune-related indicators after radiotherapy for PVTT in patients with HCC, to evaluate the efficacy and safety of sequential ICIs plus bevacizumab therapy after radiotherapy for PVTT, and to preliminarily explore the factors affecting the efficacy in these patients.

2 Methods

2.1 Inclusion and exclusion criteria

Inclusion criteria: HCC was diagnosed clinically or pathologically according to the diagnostic criteria of the American Liver Association. All patients were found with PVTT by ultrasound B, computerized tomography (CT), magnetic resonance imaging (MRI) or digital subtraction angiography (DSA). Patients had no history of anti-tumour therapy and met the indications of medical and local treatments. None of them had received chemotherapy, targeted molecular drugs, PD-1/PD-L1 immunotherpay, et al. The control group was treated with ICIs plus bevacizumab as the first-line treatment, and the PVTT radiotherapy group was treated with radiotherapy of PVTT followed by ICIs plus bevacizumab. The interval between radiotherapy of PVTT and systemic treatment must less than 1 month; Eastern Cooperative Oncology Group performance status score (ECOG-PS score) 0-1; Child-Pugh class A or B; Complete follow-up data were available.

Exclusion criteria: Suspected non-PVTT formation, PVTT intervention and other treatment history, combined with severe heart, liver and renal insufficiency, unable to complete treatment, bleeding tendency, significantly prolonged coagulation time, international normalized ratio (INR) >1.5, ECOG-PS score ≥2, Child-Pugh class C or D, systemic treatment after more than 1 month of PVTT radiotherapy, accompanied by other primary tumour or serious disease. Patients with red-color sign, severe esophagogastric fundus varices, history of hematemesis, aggressive tumour which had struck a major blood vessel were excluded. Rigor criteria including blinding, randomization of groups, and power analysis are not relevant to the study.

2.2 Clinical data

According to the inclusion and exclusion criteria, patients with PVTT diagnosed in the Second Affiliated Hospital of Chongqing Medical University, Sichuan Mianyang 404 Hospital and Bishan Hospital Affiliated to Chongqing Medical University from January 1, 2020 to June 31, 2022 were collected and selected. The sex, age, smoking history, alcohol consumption, diabetes, hypertension, cardiovascular disease, China liver cancer staging (CNCL), Child-Pugh class, ECOG-PS score Cause of hepatitis, liver cirrhosis, Quantity of hepatitis B virus deoxyribonucleic acid (HBV-DNA), serum alpha fetoprotein (AFP) expression, tumour gross classification of primary liver cancer (giant, massive, nodular, diffuse), Classification of PVTT, tumour metastasis and ICIs treatment of every patients were recorded.

2.3 Treatment

2.3.1 Radiotherapy

Intensity-modulated radiation therapy (IMRT) was used as external radiotherapy for PVTT. The radiotherapy target volume was delineated by a radiologist under CT guidance with a total dose of 45 Gy (3 Gy ×15 fractions) for planning target volume (PTV), and radiotherapy was performed weekly from Monday to Friday.

2.3.2 ICIs + bevacizumab therapy

PD-1 inhibitors Sintilimab (injection, 100 mg/bottle, Xinda Biopharmaceutical (Suzhou) Co. Ltd) 200 mg every 3 weeks, Camrelizumab (injection, 200 mg/bottle, Suzhou Shengdia Biomedicine Co. Ltd) 200 mg every 3 weeks, or PD-L1 inhibitor Atezolizumab (injection, 1200 mg/bottle, Roche Diagnostics GmbH) 1200 mg every 3 weeks, plus bevacizumab (injection, 100 mg/bottle, Roche Pharma (Switzerland) Ltd. or Qilu Pharmaceutical Co. Ltd) 15 mg/kg every 3 weeks therapy was continued within 1–2 weeks after the end of PVTT radiotherapy. The control group received PD-1/PD-L1 inhibitors plus bevacizumab as first-line treatment. PD-1/PD-L1 inhibitors and bevacizumab were administered every 21 d until discontinuation, delay in intolerable side effects, or serious treatment-related adverse events (AEs).

2.4 Observe indicators

PVTT radiotherapy group: Hematological indicators including Albumin, total bilirubin (TBIL), Alamine aminotransferase (ALT), Aspartate aminotransferase (AST), prothrombin time (PT), hemoglobin, neutrophils, lymphocytes, C-reactive protein (CRP) within 3 days before radiotherapy and before systemic treatment (or within 2 weeks after the end of radiotherapy), and neutrophils-to-lymphocytes ratio (NLR) and CD4-to-CD8 lymphocytes ratio were calculated.

Follow-up: All patients underwent liver-enhanced CT or MRI every 6-8 weeks during the treatment. All patients were evaluated according to RECIST1.1 criteria and divided into complete response (CR), partial response (PR), stable disease (SD), and progressive disease (PD). Survival analysis: Progression-free survival (PFS) was defined as the time from initial treatment to first tumour progression, death, or the end of follow-up. The concept of PFS in our study refers to disease progression regardless of local (liver), distant (metastasis), or NVPT progression. The ORR was defined as the proportion of patients whose tumour volume reduced to a prespecified value and maintained a minimum duration and was calculated as the sum of CR and PR (CR+PR), whereas the disease control rate (DCR) was defined as the proportion of patients whose tumours had shrunk or remained stable for a certain period of time, including CR, PR, and SD cases (CR+PR+SD). PFS and AEs were analysed in both groups.

2.5 Statistical analysis

Propensity score matching (PSM) analysis was used to minimise potential confounders and selection bias and to balance the patient baseline characteristics between groups. The propensity score was estimated for each patient using a multivariate logistic regression model, and 1:1 group matching was performed using the nearest-neighbour matching method without replacement. Variables including sex, age, smoking history, alcohol consumption, diabetes, hypertension, cardiovascular disease, CNCL staging, Child-Pugh class, ECOG performance status score, cause of hepatitis, liver cirrhosis, quantity of HBV DNA, AFP expression, gross classification of primary liver cancer, classification of PVTT, tumour metastasis, and ICIs were matched. A calliper width of 0.2 standard deviations was set to prevent poor matching.

The primary endpoints of this study were PFS, ORR, and DCR, and the secondary endpoints were adverse events. Descriptive statistical methods were used to summarise the baseline characteristics of the patients. SPSS version 26.0 (RRID: SCR_002865, IBM, Armonk, New York, USA) (https://www.ibm.com/spss), and GraphPad Prism (version 9.0; RRID: SCR_002798, GraphPad Software, CA) (https://www.graphpad.com) were used to analyse the data. Statistical Tests and measurement data were analysed using t-tests. Enumeration data were analysed by χ^2 test, Cox regression model was used for survival analysis, and $P < 0.05$ was considered statistically significant.

3 Results

3.1 General information

A total of 113 patients with complete data were screened according to the inclusion and exclusion criteria, of whom 55 were treated with ICIs plus bevacizumab after PVTT radiotherapy (PVTT radiotherapy group) and 58 were treated with ICIs plus bevacizumab therapy (control group). Overall, 47 patients in the PVTT radiotherapy group and 47 in the control group were enrolled in the PSM analysis (1:1), whereas eight patients in the PVTT radiotherapy group and 9 in the control group (17 patients) were excluded by PSM.

Characteristics including sex, age, smoking history, smoking history, drinking, diabetes, hypertension, cardiovascular disease, CNCL staging, Child–Pugh class, ECOG performance status score, cause of hepatitis, liver cirrhosis, quantity of HBV DNA, AFP expression, gross classification of primary liver cancer, classification of PVTT, tumour metastasis, and ICIs were matched and are shown in Table 1. There were no significant differences in the baseline characteristics between the two groups ($P > 0.05$).

3.2 Analysis of indicators before and after radiotherapy of PVTT in patients with HCC

A total of 55 patients with PVTT radiotherapy and ICIs plus bevacizumab therapy group, the hemoglobin, neutrophils, lymphocytes, CRP, albumin, total bilirubin, ALT, AST,

TABLE 1 Characteristics of all patients in the two groups.

	Total group (n=113)		*P* value	PSM group (1:1) (n=96)		*P value*
	PVTT radiotherapy group(n=55)	Control group (n=58)		PVTT radiotherapy group (n=47)	Control group (n=47)	
Sex			0.91			0.77
Male	47 (85.45)	50 (86.21)		41 (87.23)	40 (85.11)	
Female	8 (14.55)	8 (13.79)		6 (12.77)	7 (14.89)	
Age(years)			–			–
Median	52	54		50	56	
Range	32-72	16-79		32-70	16-79	
Smoking history			0.92			0.53
Former	26 (47.27)	28 (48.28)		23 (48.94)	20 (42.55)	
Never	29 (52.73)	30 (51.72)		24 (51.06)	27 (57.45)	
Alcohol consumption			0.85			0.51
Yes	17 (30.91)	17 (29.31)		17 (36.17)	14 (29.79)	

(Continued)

10.3389/fimmu.2023.1254158

TABLE 1 Continued

	Total group (n=113)		*P* value	PSM group (1:1) (n=96)		*P value*
	PVTT radiotherapy group(n=55)	Control group (n=58)		PVTT radiotherapy group (n=47)	Control group (n=47)	
No	38 (69.09)	41 (70.69)		30 (63.83)	33 (70.21)	
Diabetes			0.50			> 0.99
Yes	8 (14.55)	6 (10.34)		6 (12.77)	6 (12.77)	
No	47 (85.45)	52 (89.66)		41 (87.23)	41 (87.23)	
Hypertension			0.92			0.46
Yes	7 (12.73)	7 (12.07)		3 (6.38)	5 (10.64)	
No	48 (87.27)	51 (87.93)		44 (93.62)	42 (89.36)	
Cardiovascular disease			0.28			> 0.99
Yes	3 (5.45)	1 (1.72)		1 (2.13)	1 (2.13)	
No	52 (94.55)	57 (98.28)		46 (97.87)	46 (97.87)	
CNCLstaging			0.32			0.67
IIIa stage	34 (61.82)	41 (70.69)		28 (59.57)	30 (63.83)	
IIIb stage	21 (38.18)	17 (29.31)		19 (40.43)	17 (36.17)	
Child-Pugh class			0.30			0.37
A(5-6 score)	50 (90.91)	49 (84.48)		42 (89.36)	39 (82.98)	
B(7-9 score)	5 (9.09)	9 (15.52)		5 (10.63)	8 (17.02)	
ECOG performance status score			0.55			0.65
0	18 (32.73)	16 (27.59)		15 (31.91)	13 (27.66)	
1	37 (67.27)	42 (72.41)		32 (68.09)	34 (72.34)	
Cause of hepatitis			0.74			0.22
Hepatitis B(HBeAg/Carrier)	4 9(23/26) (89.09)	49 (15/34) (84.48)		43 (22/21) (91.49)	39 (12/27) (82.98)	
Hepatitis C	1 (1.82)	1 (1.83)		0 (0.00)	0 (0.00)	
NAFLD	5 (9.09)	8 (13.79)		4 (8.51)	8 (17.02)	
Liver cirrhosis			0.63			> 0.99
Yes	30 (54.55)	29 (50.00)		26 (55.32)	26 (55.32)	
No	25 (45.45)	29 (50.00)		21 (44.68)	21 (44.68)	
Quantity of HBV-DNA			0.42			0.81
$0\sim1\times10^3$	24 (48.98)	28 (57.14)		22 (51.46)	21 (53.85)	
$>1\times10^3$	25 (51.02)	21 (42.86)		21 (48.84)	18 (46.15)	
AFP expression (ng/ml)			0.92			0.97
≥400	22 (40.00)	25 (43.10)		18 (38.30)	19 (40.43)	
20~399	16 (29.09)	15 (25.86)		13 (27.66)	13 (27.66)	
<20	17 (30.91)	18 (31.04)		16 (34.04)	15 (31.91)	
Gross classification of primary liver cancer			0.45			0.52
Giant	17 (39.91)	16 (27.59)		16 (34.04)	13 (27.66)	

(Continued)

10.3389/fimmu.2023.1254158

TABLE 1 Continued

	Total group (n=113)		*P* value	PSM group (1:1) (n=96)		*P* value
	PVTT radiotherapy group(n=55)	Control group (n=58)		PVTT radiotherapy group (n=47)	Control group (n=47)	
Massive	19 (34.55)	15 (25.86)		14 (29.79)	11 (23.40)	
Nodular	15 (27.27)	24 (41.38)		14 (29.79)	21 (44.68)	
Diffuse	4 (7.27)	3 (5.17)		3 (6.38)	2 (4.26)	
Classification of PVTT			0.57			0.65
Type I	6 (10.91)	7 (12.07)		4 (8.51)	5 (10.64)	
Type II	26 (47.27)	20 (34.48)		21 (44.68)	15 (31.91)	
Type III	19 (34.55)	25 (43.10)		18 (38.30)	22 (46.81)	
Type IV	4 (7.27)	6 (10.35)		4 (8.51)	5 (10.64)	
Tumour metastasis			0.72			0.90
Intrahepatic	36 (65.45)	42 (72.41)		29 (61.70)	33 (70.21)	
Lung	12 (21.82)	8 (13.79)		11 (23.40)	8 (17.02)	
Lymphonodi coeliaci	18 (32.73)	12 (20.69)		13 (27.66)	11 (23.40)	
Bone	2 (3.64)	1 (1.72)		2 (4.26)	1 (2.13)	
Kidney	1 (1.82)	1 (1.72)		1 (2.13)	1 (2.13)	
Spleen	1 (1.82)	1 (1.72)		1 (2.13)	1 (2.13)	
Omentum	0 (0.00)	1 (1.72)		0 (0.00)	1 (2.13)	
ICIs			0.95			> 0.99
PD-L1 inhibitor	3 (5.45)	3 (5.17)		2 (4.26)	2 (4.26)	
PD-1 inhibitor	52 (94.55)	55 (94.83)		45 (95.74)	45 (95.74)	

PVTT radiotherapy group, Radiotherapy+ICIs+Bevacizumab; Control group, ICIs+Bevacizumab; ICIs, immuno-checkpoint inhibitors; CNCL, China Liver Cancer Staging; ECOG, Eastern Cooperative Oncology Group; NAFLD, non-alcoholic fatty liver disease; APF, alpha-fetoprotein; PVTT, portal vein tumour thrombosis; PD-L1, programmed cell death-ligand1; PD-1, programmed cell death-1.

prothrombin time, CD4, CD8 in routine analysis of blood, liver function and coagulation were collected within 1 week before and 2 weeks after PVTT radiotherapy, NLR and CD4/CD8 lymphocyte ratio were calculated (Table 2). All the indexes mentioned above were tested by paired t-test, and the immune-related indexes including neutrophil (3.09 ± 1.39 *vs.* 4.97 ± 1.65, t = 12.68, $P < 0.05$), lymphocyte (0.96 ± 0.43 *vs.* 0.45 ± 0.27, t = 8.27, $P < 0.05$), CRP (25.30 ± 38.35 *vs.* 41.87 ± 41.88, t = 3.18, $P < 0.05$), CD4 (490.33 ± 54.57 *vs.* 295.96 ± 35.26, t = 45.34, $P < 0.05$) and CD8 (270.93 ± 31.24 *vs.* 186.47 ± 24.30, t = 8.27, $P < 0.05$) before and after PVTT radiotherapy were statistically significant ($P < 0.05$). NLR increased from 3.57 ± 1.73 to 14.98 ± 10.74 (t = 8.24, $P < 0.05$), CD4/CD8 ratio decreased from 1.81 ± 0.10 to 1.59 ± 0.11 (t = 17.23, $P < 0.05$). Shown in Table 2.

3.3 Survival analysis (PFS, ORR, and DCR)

The median PFS of patients in PVTT radiotherapy group was 9.6 months, and the PFS rates at 3, 6, 9, and 12 months were 46 (97.87%), 38 (80.85%), 25 (53.19%), and 11 (23.40%), respectively. The median survival PFS was 5.4 months in the control group, and the PFS rates at 3, 6, 9, and 12 months were 43 (91.49%), 21 (44.68%), 3 (6.38%), and 0 (0.00%), respectively (Table 3). PFS rates (Figure 1A) and stage IIIa (Figure 1B) and IIIb (Figure 1C) PFS rates of the PVTT radiotherapy group were better than those of the control group ($P < 0.001$), as shown in Figure 1.

Compared with the control group, the patients in PVTT radiotherapy group with CR were five cases *vs.* two cases (10.64% *vs.* 4.26%), PR were 18 cases *vs.* 11 cases (38.30% *vs.* 23.40%), SD patients were 23 cases *vs.* 26 cases (48.94% *vs.* 55.32%), PD patients were one case *vs.* eight cases (2.13% *vs.* 27.66%), including one patient with hyper-progression in the control group, ORR were 23 cases *vs.* 13 cases (48.94% *vs.* 27.66%), and DCR were 46 cases *vs.* 39 cases (97.87% *vs.* 82.98%). There were significant differences in the best response between the two groups (P = 0.0351), ORR (P = 0.0339) and DCR (P = 0.0141) (Table 3). Based on RECISIT1.1, the waterfall plot showed optimal tumour regression in the PVTT radiotherapy combined with systemic therapy group (Figure 2A) and systemic therapy-only groups (Figure 2a), and there were no significant

10.3389/fimmu.2023.1254158

TABLE 2 Comparison of the index before and after radiotherapy for PVTT in the PVTT radiotherapy group (Radiotherapy + ICIs + Antiangiogenic) (n=55).

	Before radiotherapy (x±s)	After radiotherapy (x±s)	*t*	*P*
Hemoglobin(g/L)	129.69 ± 20.78	127.78 ± 20.90	0.96	0.34
Neutrophil(10^9/L)	3.09 ± 1.39	4.97 ± 1.65	12.68	< 0.05
Lymphocyte(10^9/L)	0.96 ± 0.43	0.45 ± 0.27	8.27	< 0.05
NLR	3.57 ± 1.73	14.98 ± 10.74	8.24	< 0.05
CRP (mg/L)	25.30 ± 38.35	41.87 ± 41.88	3.18	< 0.05
Albumin (g/dL)	38.85 ± 4.54	44.28 ± 45.78	0.89	0.38
TBIL (μmol/L)	18.35 ± 12.77	25.83 ± 59.43	1.10	0.28
ALT (U/L)	52.55 ± 46.98	40.27 ± 24.27	1.80	0.07
AST (U/L)	65.27 ± 48.75	56.13 ± 38.65	1.30	0.20
PT (s)	14.00 ± 1.23	13.88 ± 1.29	0.98	0.33
CD4(a/uL)	490.33 ± 54.57	295.96 ± 35.26	45.34	< 0.05
CD8(a/uL)	270.93 ± 31.24	186.47 ± 24.30	31.43	< 0.05
CD4/CD8 ratio	1.81 ± 0.10	1.59 ± 0.11	17.23	< 0.05

PVTT, portal vein tumour thrombosis; ICIs, immuno-checkpoint inhibitors; NLR, Neutrophil-to-Lymphocyte Ratio; CRP, C-reactive protein; TBIL, Total bilirubin; ALT, Alamine aminotransferase; AST, Aspartate aminotransferase; PT, Prothrombin time.

differences in optimal tumour regression between the two groups at stage IIIa (Figure 2B, b) and IIIb (Figure 2C, c). The spider plot shows regression or growth in the PVTT radiotherapy combined with systemic therapy group (Figure 3A), and systemic therapy-only groups (Figure 3a) at each follow-up, and there were no significant differences between the two groups in terms of stage IIIa (Figure 3B, b) and IIIb (Figure 3C, c). A total of 42 patients experienced OS events by the end of data collection in June 2022 of this research, and the maturity of the current OS data reached 37.17%. Continued follow-up of OS data will be presented in further research.

TABLE 3 Survival analysis and response evaluation of patients in the two groups after PSM (1:1) (RECIST 1.1 version).

	PVTT radiotherapy group (Radiotherapy+ICIs+ Bevacizumab)			Control group (ICIs+Bevacizumab)			*P*
	Total (n=47)	IIIa stage (n=28)	IIIb stage (n=19)	Total (n=47)	IIIa stage (n=30)	IIIb stage (n=17)	
mPFS [months (95% CI)]	9.6 (1.187-2.664)	10.5 (1.004-2.812)	6.8 (0.8416-3.115)	5.4 (0.3754-0.8428)	6.25 (0.3556-0.9962)	4.2 (0.3210-1.188)	*< 0.001*
PFS Rate [n (%)]							*< 0.001*
3 Months	46 (97.87)	28 (100.00)	18 (94.74)	43 (91.49)	29 (96.67)	14 (82.35)	
6 Months	38 (80.85)	25 (89.29)	13 (68.42)	21 (44.68)	19 (63.33)	2 (11.76)	
9 Months	25 (53.19)	19 (67.86)	6 (31.58)	3 (6.38)	3 (10.00)	0 (0.00)	
12 Months	11 (23.40)	9 (32.14)	2 (10.53)	0 (0.00)	0 (0.00)	0 (0.00)	
Best response [n (%)]							*0.0351*
CR	5 (10.64)	3 (10.71)	2 (10.53)	2 (4.26)	1 (3.33)	1 (5.88)	
PR	18 (38.30)	12 (42.86)	6 (31.58)	11 (23.40)	9 (30.00)	2 (11.76)	
SD	23 (48.94)	13 (46.43)	10 (52.63)	26 (55.32)	18 (60.00)	8 (47.06)	
PD	1 (2.13)	0 (0.00)	1 (5.26)	8 (17.02)	2 (6.67)	6 (35.29)	
ORR [n (%)]	23 (48.94)	15 (53.57)	8 (42.11)	13 (27.66)	10 (33.33)	3 (17.65)	*0.0339*
DCR [n (%)]	46 (97.87)	28 (100.00)	18 (94.74)	39 (82.98)	28 (93.33)	11 (64.71)	*0.0141*

PSM, propensity score matching; RECIST, Response Evaluation Criteria in Solid Tumors; ICIs, immuno-checkpoint inhibitors; mPFS, Median progression-free survival; CR, complete response; PR, partial response; SD, stable disease; PD, progression disease; ORR (objective response rate)= CR+PR; DCR (disease control rate)= CR+PR+SD.
The italic values means that the data were statistically significant.

10.3389/fimmu.2023.1254158

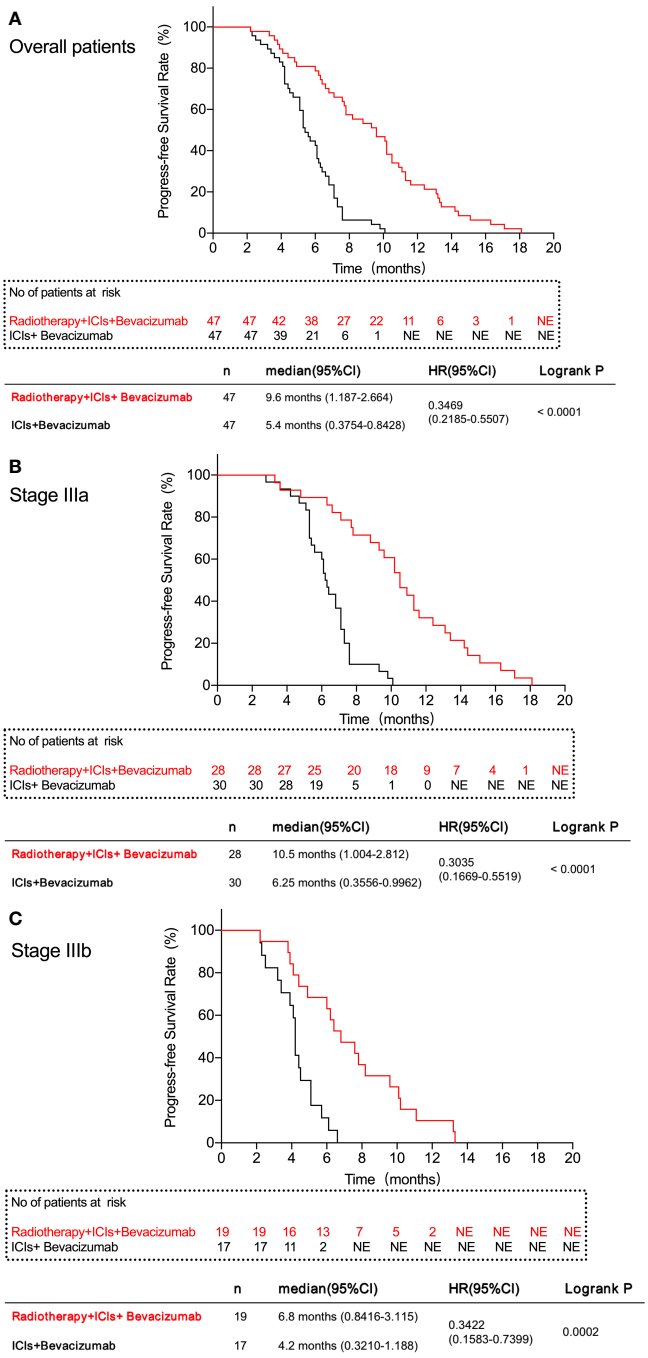

FIGURE 1
Progress-free survival rate of patients in this study. **(A)** All patients in the two groups. **(B)** patients with IIIa stage in the two groups. **(C)** patients with IIIb stage in the two groups. The results show that the PVTT radiotherapy group had a better FPS rate than the control group.

3.4 Analysis of risk factors of PFS

Sex, age, smoking, alcohol consumption, diabetes, hypertension, cardiovascular disease, child-pugh grade, ECOG-PS score, whether B viral hepatitis, whether cirrhosis, AFP lever before treatment (< 400ng/ml or ≥400 ng/ml), HBV-DNA lever (0-1×10^3 or >1×10^3), whether giant HCC, PVTT type (I-II or III-IV), whether extrahepatic metastasis, whether PVTT was treated with radiotherapy, and whether there was reduction of PVTT were analyzed by univariate Cox analysis. The results suggested that the expression of AFP before treatment (HR 1.950, 95%*CI* 1.271-2.992, $P = 0.002$), giant HCC (HR 2.211, 95%*CI* 1.397-3.499, $P = 0.001$), PVTT type (HR 2.211, 95%*CI* 1.859-4.788, $P < 0.001$), extrahepatic metastasis (HR 1.921, 95%*CI* 1.177-3.133, $P = 0.009$), radiotherapy for PVTT (HR 0.227, 95%*CI*

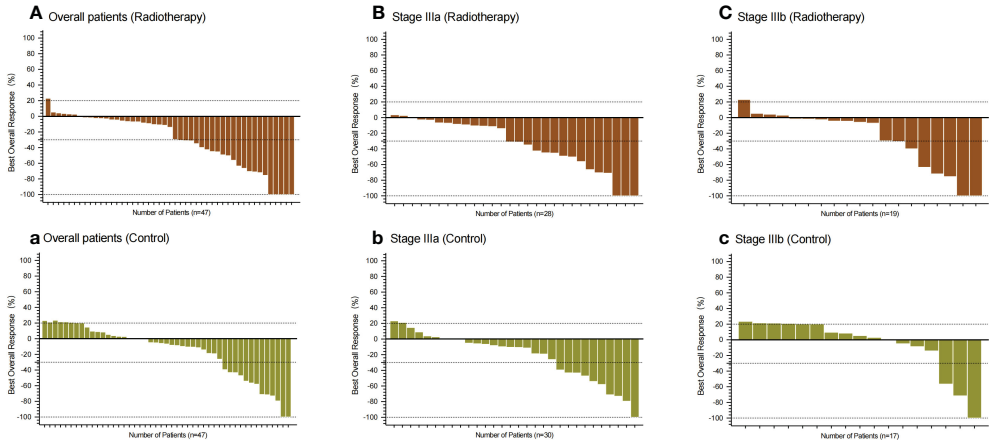

FIGURE 2
Waterfall plot showing the best percentage change from baseline in the sum of the target lesions in patients. **(A–C)** All patients, patients with IIIa stage, and patients with IIIb stage in the PVTT radiotherapy group, respectively. **(a, b, c)** All patients, patients with IIIa stage, and patients with IIIb stage in the control group, respectively. Assessed using RECIST1.1 with image measurements before and after treatment. There were no statistically significant differences between the two groups in both subgroups.

0.135-0.328, $P < 0.001$), and reduction of PVTT (HR 0.107, 95%CI 0.049-0.233, $P < 0.001$) were the influencing factors of PFS (Table 4). The P value equal to 0.2 was used as the boundary to screen out the factors with significant differences in $P < 0.2$ of factors mentioned above, multivariate Cox regression analysis was conducted to further analyze the influencing factors of PFS. The results has showed that: the level of AFP before treatment (HR 1.702, 95%*CI* 1.081-2.681, $P = 0.022$), giant HCC (HR 1.753, 95%*CI* 1.064-2.889, $P = 0.028$), PVTT type (HR 1.796, 95%*CI* 1.061-3.041, $P = 0.029$), extrahepatic metastasis (HR 2.105, 95%*CI* 1.240-3.572, $P = 0.006$), radiotherapy for PVTT (HR 0.231, 95%*CI* 0.133-0.401, $P < 0.001$), and the reduction of PVTT (HR 0.175, 95%*CI* 0.073-0.416, $P < 0.001$) were the independent influencing factors for PFS (Table 4).

3.5 Toxicity

There were no significant differences in AEs between the PVTT radiotherapy and control groups ($P > 0.05$). The main AEs of any grade in the two groups included weight loss (70.21% and 65.96%), hypertension (48.94% and 51.06%), decreased appetite (46.81% and 53.19%), proteinuria (46.81% and 48.94%), hand-foot syndrome (42.55% and 38.20%), fatigue (40.43% and 42.55%), hypothyroidism (29.79% and 31.91%), pruritus (29.79% and 34.04%), *et al.* (Table 5). No significant increase in cTn, electrocardiographic (ECG) changes, or clinical symptoms of cardiac dysfunction were found in either group. Patients of AEs Grade ≥ 3 in PVTT radiotherapy group compared with the control group, there were 6 cases *vs.* 7 cases

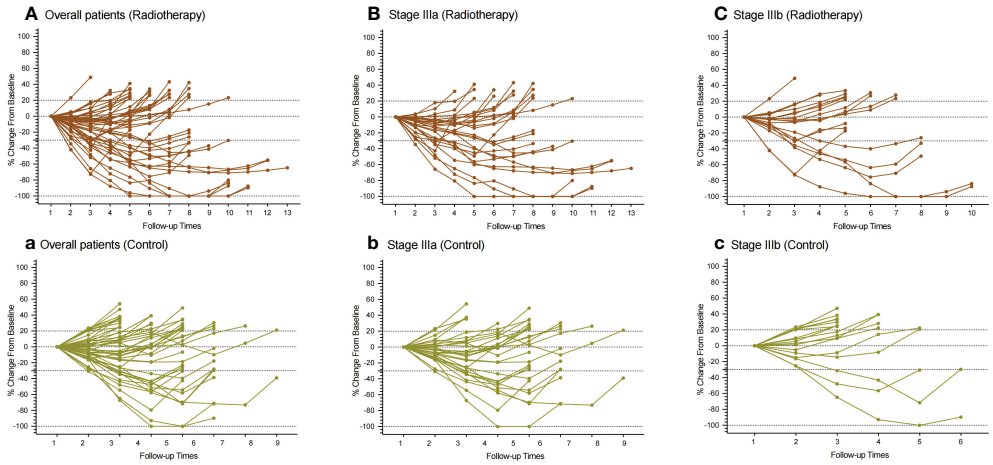

FIGURE 3
Spider plot showing the regression or growth changing from baseline in the sum of the target lesions of patients. **(A–C)**: All patients, patients with IIIa stage, and patients with IIIb stage in the PVTT radiotherapy group, respectively. **(a, b, c)** All patients, patients with IIIa stage, and patients with IIIb stage in the control group, respectively. Assessed using RECIST1.1 with image measurements before and after treatment. There were no statistically significant differences between the two groups in both subgroups.

10.3389/fimmu.2023.1254158

TABLE 4 Univariate and multivariate Cox regression analyses of risk factors for progression-free survival following PSM (1:1).

Variable	Univariate Cox Analysis			Multivariate Cox analysis		
	HR	95% *CI*	*P* value	HR	95% *CI*	*P* value
Sex (male *vs.* female)	1.103	0.612-1.989	0.745			
Age (years) (≤ 60 *vs.* > 60)	1.105	0.672-1.643	0.827			
Smoking (yes *vs.* no)	0.911	0.599-1.385	0.662			
Alcohol consumption (yes *vs.* no)	0.902	0.581-1.400	0.645			
Diabetes (yes *vs.* no)	0.757	0.445-1.286	0.303			
Hypertension (yes *vs.* no)	1.177	0.563-2.462	0.666			
Cardiovascular disease (yes *vs.* no)	1.641	0.401-6.720	0.491			
Child-Pugh grading (A *vs.* B)	1.460	0.804-2.649	0.214			
ECOG-PS (0 *vs.*1)	0.721	0.589-1.442	0.922			
Hepatitis B (yes vs. no)	0.979	0.530-1.808	0.945			
Liver cirrhosis (yes *vs.* no)	1.330	0.879-2.012	0.177			
HBV-DNA (0~1×10^3 *vs.*>1×10^3)	1.153	0.758-1.754	0.506			
AFP (<400 ng/ml *vs.* ≥ 400ng/ml)	*1.950*	*1.271-2.992*	*0.002*	*1.702*	*1.081-2.681*	*0.022*
Gross (giant *vs.* others)	*2.211*	*1.397-3.499*	*0.001*	*1.753*	*1.064-2.889*	*0.028*
Extrahepatic metastasis (yes *vs.* no)	*1.921*	*1.177-3.133*	*0.009*	*2.105*	*1.240-3.572*	*0.006*
PVTT (Type I-II *vs.*Type III-IV)	*2.984*	*1.859-4.788*	*<0.001*	*1.796*	*1.061-3.041*	*0.029*
PVTT Radiotherapy (yes vs. no)	*0.227*	*0.135-0.382*	*<0.001*	*0.231*	*0.133-0.401*	*<0.001*
Reduction of PVTT (yes vs. no)	*0.107*	*0.049-0.233*	*<0.001*	*0.175*	*0.073-0.416*	*<0.001*

ECOG-PS, Eastern Cooperative Oncology Group performance status score; APF, alpha-fetoprotein; PVTT, portal vein tumour thrombosis.
The italic values means that the data were statistically significant.

TABLE 5 Treatment-related adverse events in the two groups following PSM (1:1).

Adverse Event	Any Grade			Grade ≥ 3		
	PVTT radiotherapy group (n=47)	Control group (n=47)	*P* value	PVTT radiotherapy group (n=47)	Control group (n=47)	*P* value
Weight loss	33 (70.21)	31 (65.96)	0.658	6 (12.77)	7 (14.89)	0.765
Hypertension	23 (48.94)	24 (51.06)	0.837	11 (23.40)	9 (19.15)	0.614
Decreased appetite	22 (46.81)	25 (53.19)	0.536	3 (6.38)	6 (12.77)	0.293
Proteinuria	22 (46.81)	23 (48.94)	0.836	5(10.64)	6 (12.77)	0.748
Hand-foot syndrome	20 (42.55)	18 (38.20)	0.674	5 (10.64)	6 (12.77)	0.748
Fatigue	19 (40.43)	20 (42.55)	0.834	0 (0.00)	1 (2.13)	0.315
Hypothyroidism	14 (29.79)	16 (34.04)	0.658	0 (0.00)	0 (0.00)	–
Pruritus	14 (29.79)	15 (31.91)	0.823	4 (8.51)	4 (8.51)	1.000
Hypoalbuminemia	13 (27.66)	12 (25.53)	0.815	0 (0.00)	1 (2.13)	0.315
Headache	12 (25.53)	10 (21.28)	0.626	0 (0.00)	0 (0.00)	–
Rash	10 (21.28)	13 (27.66)	0.472	2 (4.26)	1 (2.13)	0.557
Increased AST	10 (21.28)	9 (19.15)	0.797	1 (2.13)	0 (0.00)	0.315
Increased ALT	9 (19.15)	11 (23.40)	0.614	1 (2.13)	0 (0.00)	0.315

(Continued)

10.3389/fimmu.2023.1254158

TABLE 5 Continued

Adverse Event	Any Grade			Grade ≥ 3		
	PVTT radiotherapy group (n=47)	Control group (n=47)	*P* value	PVTT radiotherapy group (n=47)	Control group (n=47)	*P* value
Nausea	9 (19.15)	10 (21.28)	0.797	0 (0.00)	0 (0.00)	–
Anemia	8 (17.02)	7 (14.89)	0.778	0 (0.00)	1 (21.3)	0.315
Increased TBi	7 (14.89)	7 (14.89)	1.000	0 (0.00)	1 (2.13)	0.315
Arthralgia	6 (12.77)	8 (17.02)	0.562	0 (0.00)	0 (0.00)	–
Diarrhea	5 (10.64)	8(17.02)	0.370	1 (2.13)	0 (0.00)	0.315
Vomiting	5 (10.64)	6 (12.77)	0.748	0 (0.00)	0 (0.00)	–
Edema	5 (10.64)	3 (6.38)	0.460	0 (0.00)	0 (0.00)	–
Thrombocytopenia	4 (8.51)	3 (6.38)	0.694	1 (2.13)	1 (2.13)	1.000
Leukopenia	3 (6.38)	8 (17.02)	0.109	0 (0.00)	1 (2.13)	0.315
Gingival bleeding	3 (6.38)	4 (8.51.)	0.694	0 (0.00)	0 (0.00)	–
Elevated uric acid	2 (4.26)	2 (4.26)	1.000	0 (0.00)	0 (0.00)	–
Neutropenia	2 (4.26)	6 (12.77)	0.139	0 (0.00)	1 (2.13)	0.315
Dysphonia	2 (4.26)	1 (2.13)	0.557	0 (0.00)	0 (0.00)	–
Hyperglycemia	1 (2.13)	2 (4.26)	0.557	0 (0.00)	0 (0.00)	–
Pneumonitis	1 (2.13)	0 (0.00)	0.315	0 (0.00)	0 (0.00)	–

PVTT radiotherapy group: Radiotherapy+ICIs+ Bevacizumab; Control group: ICIs+ Bevacizumab. Data were presented as n (%). ICIs, immuno-checkpoint inhibitors; ALT, alanine aminotransferase; AST, Aspartate aminotransferase; TBi, total bilirubin.

with weight loss ($P = 0.765$), 11 cases *vs.* 9 cases with hypertension ($P = 0.614$), 3 cases *vs.* 6 cases with decreased appetite ($P = 0.293$), and 5 cases *vs.* 6 cases with proteinuria ($P = 0.748$) in both groups, 5 cases *vs.* 6 cases of hand-foot syndrome ($P = 0.748$), and 4 cases *vs.* 4 cases of pruritus ($P = 1.000$), respectively for grade ≥ 3 AEs (Table 5).

4 Discussion

The systemic therapy progress of advanced HCC is slow. As sorafenib became the first approved system treatment in 2007, breakthroughs in HCC treatment over the next 10 years have been rare and long-term drugs are lacking. The efficiency of sorafenib is low and limited to improving survival. Additionally, notable adverse effects indicated the need to acquire more effective therapies with lower toxicity against advanced HCC. In recent years, ICIs have become a hot area of clinical research in advanced HCC. Checkmate040 (4) (phase I/II) is a landmark study in the history of HCC immunotherapy, and its results have established nivolumab as a second-line therapy for advanced HCC. The Checkmate-459 (11) study enrolled patients with advanced HCC who were ineligible for surgery or local treatment and patients who progressed after surgery or local treatment. The results have shown clinically meaningful improvements in OS, ORR, and CR rates, but they did not meet the primary endpoint of OS. This study suggests that although monotherapy with ICIs has improved OS and ORR compared to sorafenib, it does not have absolute advantages, and ICIs combined therapy with other methods may be a better choice. Several studies conducted in the last 5 years have reported that ICIs combined with anti-angiogenic therapy have a good effect and can further improve the survival rate of patients. GO30140 (12) and Imbrave150 (8) showed that atezolizumab combined with bevacizumab as the first-line treatment in patients with advanced HCC can improve the ORR and significantly prolong the OS of patients to 17.1 and 19.2 months, respectively. The subgroup data of 194 Chinese patients in the Imbrave150 study showed that the median OS was 24 months (13), which has advanced past the bottleneck of HCC treatment in the past decade. The studies mentioned above indicate that ICIs are feasible and safe for the treatment of advanced HCC; however, these results also showed that the ORR of single-agent ICIs was low, and the combination treatment of ICIs with other methods, such as anti-angiogenic therapy, is promising for future HCC treatment.

Radiotherapy can change the microenvironment of tumour cells, promote the production of T cells and immune infiltration, and stimulate the body to produce anti-tumour immune effects. Radiotherapy can induce immunogenicity of death in tumour cells, release inflammatory factors and cytokines, and generate new tumour antigens. Antigen-presenting cells (APCs) can enter the tumour cells and access the tumour antigen, causing a systemic anti-tumour effect mediated by the immune system, resulting in "remote effects" (14). Abulimiti et al. confirmed that radiotherapy combined with sorafenib improved the survival of patients with HCC, with a median OS of 11.4 months and a median PFS of 6 months (15). Furthermore, another study (16) indicated that the mPFS of patients with advanced HCC treated with IMRT combined

with apatinib was 7.8 months and the ORR was 15%. All the studies mentioned above indicate that radiotherapy has a synergistic effect on systemic anti-tumour therapy. Anti-angiogenic therapy can normalise the blood vessels of tumours and enhance the infiltration of T cells simultaneously (17), providing a theoretical basis for radiotherapy combined with immunotherapy and anti-angiogenic therapy. HCC is a typical inflammation-related tumour (18), and its microenvironment is primarily composed of cellular components, such as tumour-associated macrophages, tumour-associated neutrophils, tumour-infiltrating lymphocytes, tumour-associated fibroblasts, non-cellular components, and extracellular stromal cytokines. The immune-related microenvironment plays an important role in HCC progression, immune escape, and treatment resistance. As an evaluation index of the systemic inflammatory response, the NLR is an independent prognostic factor for various malignant tumours, such as gastric, lung, and colorectal cancers, and studies have also confirmed that NLR can be used as an indicator to evaluate the prognosis of patients with HCC (19). Our study showed that the NLR of the peripheral venous blood increased after radiotherapy in the PVTT radiotherapy group, reflecting an obvious inflammatory reaction in the body after radiotherapy. Moreover, although the CD4 and CD8 counts decreased to a certain degree after radiotherapy for PVTT, the CD4-to-CD8 ratio showed a statistically significant decrease, indicating an increase in the proportion of cytotoxic T cells with killing function and the enhancement of body immunity. ICIs and anti-angiogenic therapies are theoretically feasible based on inflammatory reactions and immune enhancement (20).

Tumour antigen release is a key link in immunotherapy, and therapies that can increase tumour neoantigens should enhance the effects of immunotherapy (11). In our study, radiotherapy with PVTT caused necrosis of the tumour tissue, and the exposure to tumour antigens promoted the inflammatory response of the body, which changed some immune-related indicators of the body, thereby improving the efficacy of ICIs treatment. The median PFS of the PVTT radiotherapy group was 4.2 months longer than that of the control group; the ORR was 48.94% *vs.* 27.66%, and the DCR was 97.87% *vs.* 82.98%, indicating the advantages of radiotherapy for PVTT in the treatment of HCC. Subgroup analysis suggested that the therapeutic effect was directly related to staging. The IMbrave150 study indicated that the main factors affecting the long-term survival of patients with PFS and OS after treatment with atezolizumab plus bevacizumab included viral infection and AFP levels. In this retrospective study, multivariate Cox analysis showed that AFP expression, PVTT type, liver tumour size, and PVTT radiotherapy were independent prognostic factors affecting PFS. Our retrospective study also indicated that the highest incidences of AEs were weight loss, hypertension, and decreased appetite, most of which were grade 1-2. Common immune-related AEs (irAEs) were pruritus, rash, and hypothyroidism, and no serious irAEs were observed in patients in either group.

5 Conclusion

Radiotherapy for PVTT in HCC can quickly eliminate the tumour tissue and induce large quantities of neoplastic *de novo* antigens which activate immunity for the immunotherapy response. Combined ICIs and anti-angiogenic therapy after radiotherapy for PVTT can improve survival and is well-tolerated. Data from prospective clinical studies with higher levels of evidence are required to guide clinical applications, and relevant clinical studies should be conducted in the future.

Data availability statement

The raw data supporting the conclusions of this article will be made available by the authors, without undue reservation.

Ethics statement

The studies involving humans were approved by The Second Affiliated Hospital of Chongqing Medical University Research Ethics Committee. The studies were conducted in accordance with the local legislation and institutional requirements. The human samples used in this study were acquired from primarily isolated as part of your previous study for which ethical approval was obtained. Written informed consent for participation was not required from the participants or the participants' legal guardians/next of kin in accordance with the national legislation and institutional requirements.

Author contributions

CT: Conceptualization, Data curation, Formal Analysis, Investigation, Methodology, Software, Writing – original draft, Writing – review & editing. QH: Data curation, Methodology, Writing – review & editing. JF: Data curation, Methodology, Writing – review & editing. ZL: Data curation, Methodology, Writing – review & editing. YP: Data curation, Methodology, Writing – review & editing. JG: Formal Analysis, Funding acquisition, Project administration, Resources, Supervision, Validation, Visualization, Writing – review & editing.

Funding

The author(s) declare financial support was received for the research, authorship, and/or publication of this article. This work was supported by the National Natural Science Foundation of China (Grant 82173359), Basic Research and Frontier Exploration Project of Chongqing and Technology Commission (cstc2018jcyjAX0181), and Kuanren Talents Program of the Second affiliatedhospital of Chongqing Medical University.

Conflict of interest

The authors declare that the research was conducted in the absence of any commercial or financial relationships that could be construed as a potential conflict of interest.

Publisher's note

References

1. Sung H, Ferlay J, Siegel RL, Laversanne M, Soerjomataram I, Jemal A, et al. Global cancer statistics 2020: GLOBOCAN estimates of incidence and mortality worldwide for 36 cancers in 185 countries. *CA: Cancer J Clin* (2021) 71(3):209–49. doi: 10.3322/caac.21660

2. Liu PH, Huo TI, Miksad RA. Hepatocellular carcinoma with portal vein tumor involvement: Best management strategies. *Semin Liver Dis* (2018) 38:242–51. doi: 10.1055/s-0038-1666805

3. Liu PH, Lee YH, Hsia CY, Hsu CY, Huang YH, Chiou YY, et al. Surgical resection versus transarterial chemoembolization for hepatocellular carcinoma with portal vein tumor thrombosis: a propensity score analysis. *Ann Surg Oncol* (2014) 21(6):1825–33. doi: 10.1245/s10434-014-3510-3

4. El-Khoueiry AB, Sangro B, Yau T, Crocenzi TS, Kudo M, Hsu C, et al. Nivolumab in patients with advanced hepatocellular carcinoma (CheckMate 040): an open-label, non-comparative, phase 1/2 dose escalation and expansion trial. *Lancet* (2017) 389 (10088):2492–502. doi: 10.1016/S0140-6736(17)31046-2

5. Finn RS, Ryoo BY, Merle P, Kudo M, Bouattour M, Lim HY, et al. Pembrolizumab as second-line therapy in patients with advanced hepatocellular carcinoma in KEYNOTE-240: A randomized, double-blind, phase III trial. *J Clin Oncol* (2020) 38 (3):193–202. doi: 10.1200/JCO.19.01307

6. Xu J, Zhang Y, Jia R, Yue C, Chang L, Liu R, et al. Anti-PD-1 antibody SHR-1210 combined with apatinib for advanced hepatocellular carcinoma, gastric, or esophagogastric junction cancer: an open-label, dose escalation and expansion study. *Clin Cancer Res* (2019) 25(2):515–23. doi: 10.1158/1078-0432.CCR-18-2484

7. Zhu AX, Finn RS, Edeline J, Cattan S, Ogasawara S, Palmer D, et al. Pembrolizumab in patients with advanced hepatocellular carcinoma previously treated with sorafenib (KEYNOTE-224): a non-randomised, open-label phase 2 trial. *Lancet Oncol* (2018) 19(7):940–52. doi: 10.1016/S1470-2045(18)30351-6

8. Finn RS, Qin S, Ikeda M, Galle PR, Ducreux M, Kim TY, et al. Atezolizumab plus bevacizumab in unresectable hepatocellular carcinoma. *N Engl J Med* (2020) 382 (20):1894–905. doi: 10.1056/NEJMoa1915745

9. Ren Z, Xu J, Bai Y, Xu A, Cang S, Du C, et al. Sintilimab plus a bevacizumab biosimilar (IBI305) versus sorafenib in unresectable hepatocellular carcinoma (ORIENT-32): a randomised, open-label, phase 2-3 study. *Lancet Oncol* (2021) 22 (7):977–90. doi: 10.1016/S1470-2045(21)00252-7

10. Valero C, Lee M, Hoen D, Wang J, Nadeem Z, Patel N, et al. The association between tumor mutational burden and prognosis is dependent on treatment context. *Nat Genet* (2021) 53(1):11–5. doi: 10.1038/s41588-020-00752-4

11. Yau T, Park JW, Finn RS, Cheng AL, Mathurin P, Edeline J, et al. Nivolumab versus sorafenib in advanced hepatocellular carcinoma (CheckMate 459): A randomised, multicentre, open-label, phase 3 trial. *Lancet Oncol* (2022) 23:77–90. doi: 10.1016/S1470-2045(21)00604-5

12. Lee MS, Ryoo BY, Hsu CH, Numata K, Stein S, Verret W, et al. Atezolizumab with or without bevacizumab in unresectable hepatocellular carcinoma (GO30140): an open-label, multicentre, phase 1b study. *Lancet Oncol* (2020) 21(6):808–20. doi: 10.1016/S1470-2045(20)30156-X

13. Finn RS, Qin SK, Ikeda M, Galle PR, Ducreux M, Kim TY, et al. IMbrave150: updated overall survival (OS) data from a global, randomized, open-label phase III study of atezolizumab (Atezo) plus bevacizumab (Bev) versus sorafenib (Sor) in patients (Pts) with unresectable hepatocellular carcinoma (HCC). *J Clin Oncol* (2021) 39(3):267. doi: 10.1200/JCO.2021.39.3_suppl.267

14. Herrera F, Bourhis J, Coukos GJ. Radiotherapy combination opportunities leveraging immunity for the next oncology practice. *CA Cancer J Clin* (2017) 67 (1):65–85. doi: 10.3322/caac.21358

15. Abulimiti M, Li Z, Wang H, Apiziaji P, Abulimiti Y, Tan YJ. Combination intensity-modulated radiotherapy and sorafenib improves outcomes in hepatocellular carcinoma with portal vein tumor thrombosis. *J Oncol* (2021) 2021:1–10. doi: 10.1155/2021/9943683

16. Qiu H, Ke S, Cai G, Wu Y, Wang J, Shi W, et al. An exploratory clinical trial of apatinib combined with intensity-modulated radiation therapy for patients with unresectable hepatocellular carcinoma. *Cancer Med* (2023) 12(1):213–22. doi: 10.1002/cam4.4900

17. Missiaen R, Mazzone M, Bergers GJ. The reciprocal function and regulation of tumor vessels and immune cells offers new therapeutic opportunities in cancer. *Semin Cancer Biol* (2018) 52:107–16. doi: 10.1016/j.semcancer.2018.06.002

18. Melin BS, Nordfjäll K, Andersson U, Roos G. hTERT cancer risk genotypes are associated with telomere length[J]. *Genet Epidemiol* (2012) 36(4):368–72. doi: 10.1002/gepi.21630

19. Yang T, Zhu J, Zhao L, Mai K, Ye J, Huang S, et al. Lymphocyte to monocyte ratio and neutrophil to lymphocyte ratio are superior inflammation-based predictors of recurrence in patients with hepatocellular carcinoma after hepatic resection. *J Surg Oncol* (2017) 115(6):718–28. doi: 10.1002/jso.24549

20. Guo J, Wang S, Han Y, Jia Z, Wang R. Effects of transarterial chemoembolization on the immunological function of patients with hepatocellular carcinoma. *Oncol Lett* (2021) 22(1):554. doi: 10.3892/ol.2021.12815

Frontiers in Oncology

Advances knowledge of carcinogenesis and tumor progression for better treatment and management

The third most-cited oncology journal, which highlights research in carcinogenesis and tumor progression, bridging the gap between basic research and applications to imrpove diagnosis, therapeutics and management strategies.

Discover the latest Research Topics

See more →

Frontiers

Avenue du Tribunal-Fédéral 34
1005 Lausanne, Switzerland
frontiersin.org

Contact us

+41 (0)21 510 17 00
frontiersin.org/about/contact